Proceedings Book

6th Conference on Sustainability in Civil Engineering

1st August 2024

ISBN: 978-969-23344-5-7

Editors

Dr. Majid Ali
Engr. M. Waqas Malik
Engr. Minhas Shah

Department of Civil Engineering
Capital University of Science and Technology, Islamabad

Publication Note

Published By

Department of Civil Engineering
Capital University of Science and Technology, Islamabad, Pakistan
www.csce.cust.edu.pk
www.cust.edu.pk

Foreword

Welcome to the CSCE 2024, 6th Conference on Sustainability in Civil Engineering (CSCE'24) is held by Department of Civil Engineering, Capital University of Science and Technology, Islamabad, Pakistan. The main focus of CSCE'24 is to highlight sustainability related to the field of civil engineering. It aims to provide a platform for civil engineers from academia as well as industry to share their practical experiences and different research findings in their relevant specializations. We hope all the participants experience a remarkable opportunity for the academic and industrial communities to address new challenges, share solutions and discuss future research directions. The conference accommodates several parallel sessions of different specialties, where the researchers and engineers interact and enhance their understanding of sustainability in the civil engineering dynamics.

This year, we have eight wonderful and renowned keynote speakers for this edition of CSCE. We have received 160 manuscripts from different countries around the world including UK, Ireland, Canada, New Zealand, Italy, Estonia, Thailand, China, Hong Kong, Malaysia, UAE, KSA, and Pakistan. All papers have under gone a comprehensive and critical double-blind review process. The review committee is comprised of 78 PhDs serving in industry and academia of UK, USA, Australia, New Zealand, Thailand, China, Hong Kong, France, Poland, Malaysia, Oman, Bahrain, Morocco, UAE, KSA, and Pakistan. After the screening and review process, 50 papers are to be presented in conference.

We are grateful to all the reviewers and keynote speakers who have dedicated their precious time to share their expertise and experience. With this opportunity, we would also like to express our gratitude to

everyone, especially all the faculty and staff at the Capital University of Science and Technology for their great support and participation. In this regard, the participation and cooperation of all authors, presenters and participants are also acknowledged, without whom this conference would not have been possible. Last but not least, an appreciation to our advising and organizing committees whose hard work and dedication has made this day possible.

Dr. Majid Ali
Capital University of Science and Technology,
Islamabad, Pakistan

Conference Tracks

Track - 01: Green Construction Materials and Structures

- Construction Materials
- Composite Materials
- Modern Materials
- Structural Material Behavior
- Structural Analysis
- Structural Design
- Earthquake Engineering
- Engineering Dynamics

Track- 02: Construction and Project Management for Sustainable Developments

- Building Information Modelling (BIM)
- Project Management for Sustainable Development
- Sustainability in Construction Projects
- Construction Safety
- Construction Contracts
- Smart and Sustainable Construction
- Construction Waste Management
- IT applications in Construction

Track- 03: Resilient Infrastructure and Environment

- Environmental Engineering
- Environmental Sciences
- Irrigation Engineering
- Water Resource Engineering. & Management
- Highway & Traffic Engineering
- Urban & Transportation Planning
- Geotechnical Engineering
- Geological Engineering

Contribution from World

(Papers Received)

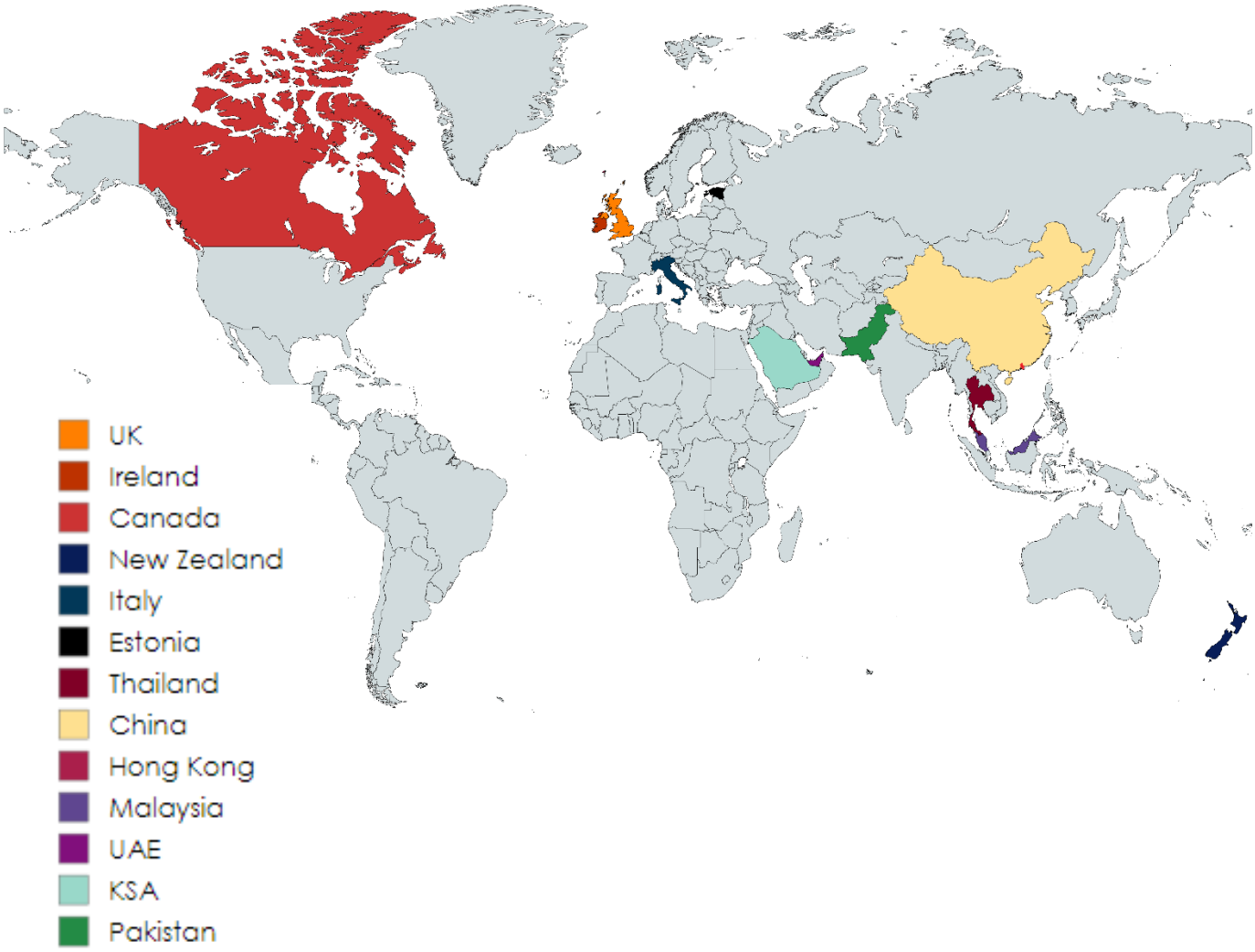

Technical Committee

Dr. Shunde Qin	Jacobs Sutton Coldfield, UK
Dr. Furqan Qamar	WSP, UK
Dr. Mohsin Shehzad	WSP, New Zealand
Dr. Inam Khan	BCRC, Australia
Dr. Munir Ahmed	DAR, KSA
Dr. Robert Evans	Nottingham Trent University, UK
Dr. Akinniyi Damilola Bashir	Coventry University, UK
Dr. Salman Azhar	Auburn University, USA
Dr. Sajjad Ahmad	University of Nevada, Las Vegas, USA
Dr. Afaq Ahmed	University of Memphis, USA
Dr. Arfan Arshad	Oklahoma State University, USA
Dr. Mizan Ahmed	Curtin University, Australia
Dr. Wajiha Shehzad	Massey University, New Zealand
Dr. An Le	Massey University, New Zealand
Dr. Chandana Siriwardana	Massey University, New Zealand
Dr. George Wardeh	IUT de Cergy-Pontoise, France
Dr. Piotr Smarzewski	Military University of Technology, Poland
Dr. Ghazanfar Ali Anwar	The Hong Kong Polytechnic University, Hong Kong
Dr. Numan Malik	The Hong Kong Polytechnic University, Hong Kong
Dr. Muhammad Zeshan Akber	The Hong Kong Uni. of Sci. and Tech., Hong Kong
Dr. Anas Bin Ibrahim	MARA University of Technology, Malaysia

Dr. Khairunisa Binti Muthusamy	Universiti Malaysia Pahang, Malaysia
Dr. Saffuan Wan Ahmad	Universiti Malaysia Pahang, Malaysia
Dr. Faridah Hanim Khairuddin	Uni. Pertahanan Nasional, Malaysia
Dr. Naveed Anwar	Asian Institute of Technology, Thailand
Dr. Ali Ejaz	Chulalongkorn University, Bangkok, Thailand
Dr. Li Li	Northwest A&F University, China
Dr. Wenjie Wang	Southeast University, China
Dr. Hammad Salahuddin	Shenzhen University, China
Dr. Mohsin Usman Qureshi	Sohar University, Oman
Dr. Tahir Mehmood	Sultan Qaboos University, Oman
Dr. Umar Farooq	Islamic University of Madinah, KSA
Dr. Khwaja Mateen Mazhar	King Fahad Uni. of Petroleum and Minerals, KSA
Dr. Mubashir Aziz	King Fahad Uni. of Petroleum and Minerals, KSA
Dr. Tayyab Naqash	Islamic University of Madinah, KSA
Dr. Aref A. Abadel	King Saud University, KSA
Dr. Uneb Gazder	University of Bahrain, Bahrain
Dr. Waris Ali Khan	The British University in Dubai, UAE
Dr. Ramy I. Shahin	Higher Inst. of Engineering and Technology, Egypt
Dr. Ahsen Maqsoom	Mohammed VI Polytechnic University, Morocco
Dr. Irfan Yousuf	World Bank Group, Islamabad, Pakistan
Dr. Hassan Nasir	WSSP, Peshawar, Pakistan
Dr. Muhammad Jamil Ahmad	SPD, Pakistan

Dr. Rao Arsalan Khushnood	Tunnelling Inst. of Pak. (TIP), Islamabad, Pakistan
Dr. Hamza Farooq Gabriel	NUST, Islamabad, Pakistan
Dr. Imran Hashmi	NUST, Islamabad, Pakistan
Dr. Nasir khan	NUST, Risalpur, Pakistan
Dr. Habib Ur Rehman	UET, Lahore, Pakistan
Dr. Ammad Hassan	UET, Lahore, Pakistan
Dr. Khurram Rashid	UET, Lahore, Pakistan
Dr. Izza Anwer	UET, Lahore, Pakistan
Dr. Ayub Elahi	UET, Taxila, Pakistan
Dr. Faisal Shabbir	UET, Taxila, Pakistan
Dr. Naveed Ahmad (Transportation)	UET, Taxila, Pakistan
Dr. Naveed Ahmad (Geotech)	UET, Taxila, Pakistan
Dr. Muhammad Irfan Ul Hassan	UET, Taxila, Pakistan
Dr. Usman Ali Naeem	UET, Taxila, Pakistan
Dr. Jawad Hussain	UET, Taxila, Pakistan
Dr. Faheem Butt	UET, Taxila, Pakistan
Dr. Irshad Qureshi	UET, Taxila, Pakistan
Dr. Muhammad Usman Arshid	UET, Taxila, Pakistan
Dr. Naeem Ijaz	UET, Taxila, Pakistan
Dr. Amjad Naseer	UET, Peshawar, Pakistan
Dr. Farrukh Arif	NED, Karachi, Pakistan
Dr. Shiraz Ahmad	GIKI, Swabi, Pakistan

Dr. Muhammad Faisal Javed	GIKI, Swabi, Pakistan
Dr. Adnan Nawaz	COMSATS, Wah, Pakistan
Dr. Zeeshan Alam	IIU, Islamabad, Pakistan
Dr. Mudasser Muneer Khan	BZU, Multan, Pakistan
Dr. M. Shoaib	BZU, Multan, Pakistan
Dr. Anwar Khitab	MUST, AJK, Pakistan
Dr. Arshad Ali	Sarhad University Peshawar, Pakistan
Dr. Salman Ali Suhail	University of Lahore, Pakistan
Dr. Shoukat Ali Khan	Muslim Youth University, Pakistan
Dr. Sabahat Hassan	HITEC University, Taxila, Pakistan
Dr. Asim Farooq	PAF IAST, Haripur, Pakistan
Dr. Tariq Ali	Swedish College of Engg. and Tech, Wah, Pakistan
Dr. Khursheed Ahmed	KIU, Gilgit, Pakistan

Contribution from World

(Technical Committee Members)

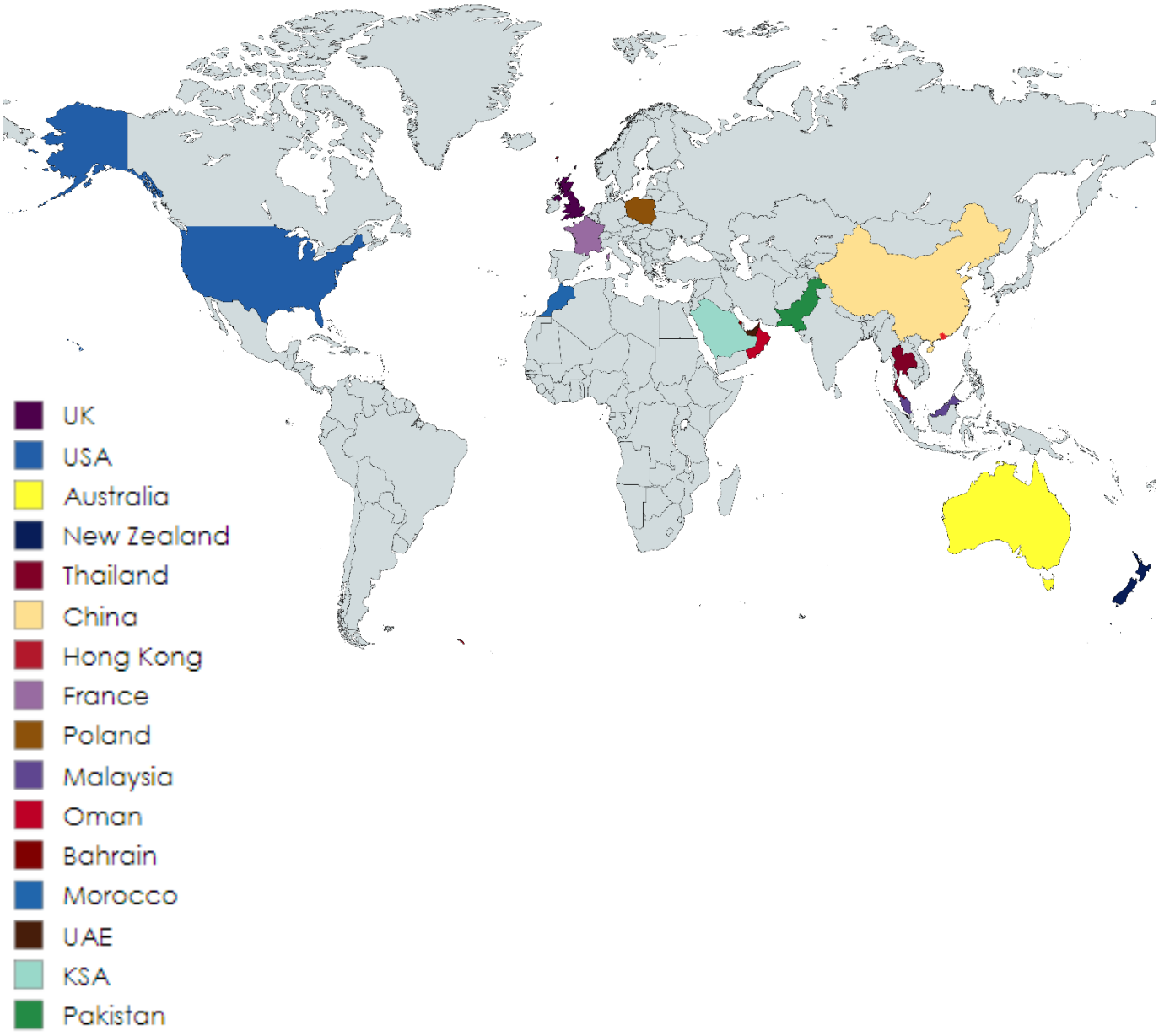

Keynote Speakers

Dr. George Wardeh *IUT de Cergy-Pontoise, France*	*Effect of Mortar Type on The Static and Dynamic Behaviour of Masonry Arches*
Dr. Hammad Anis Khan *University of Sydney, Australia*	*Penetrability in concrete - A perspective to develop durable concrete for sewer environment*
Dr. Mehran Khan *University College Dublin, Ireland*	*3D Printing Concrete: Transforming Construction through Innovative Technology.*
Dr. Jin Cheng Liu *Aurecon, Hong Kong*	*Machine Learning Assisted Iterative Design of Geopolymer Concrete and High Performance Concrete*
Dr. Muhammad Shakeel *AECOM, Hong Kong*	*Applications of Centrifuge Modelling in Geotechnical Engineering and Research*
Dr. Noor Aina *Uni. Pertahanan Nasional, Malaysia*	*Building a Sustainable Future: The Role of Textile Waste Composites in Civil Engineering*
Dr. Khan Shahzada *UET Peshawar, Pakistan*	*Alternative Materials for Buildings Construction in Pakistan*
Dr. Khan Zaib Jadoon *IIU, Islamabad, Pakistan*	*Challenges and Solutions for the Sustainable Groundwater Management in Pakistan*

Contribution from World

(Keynote Speakers)

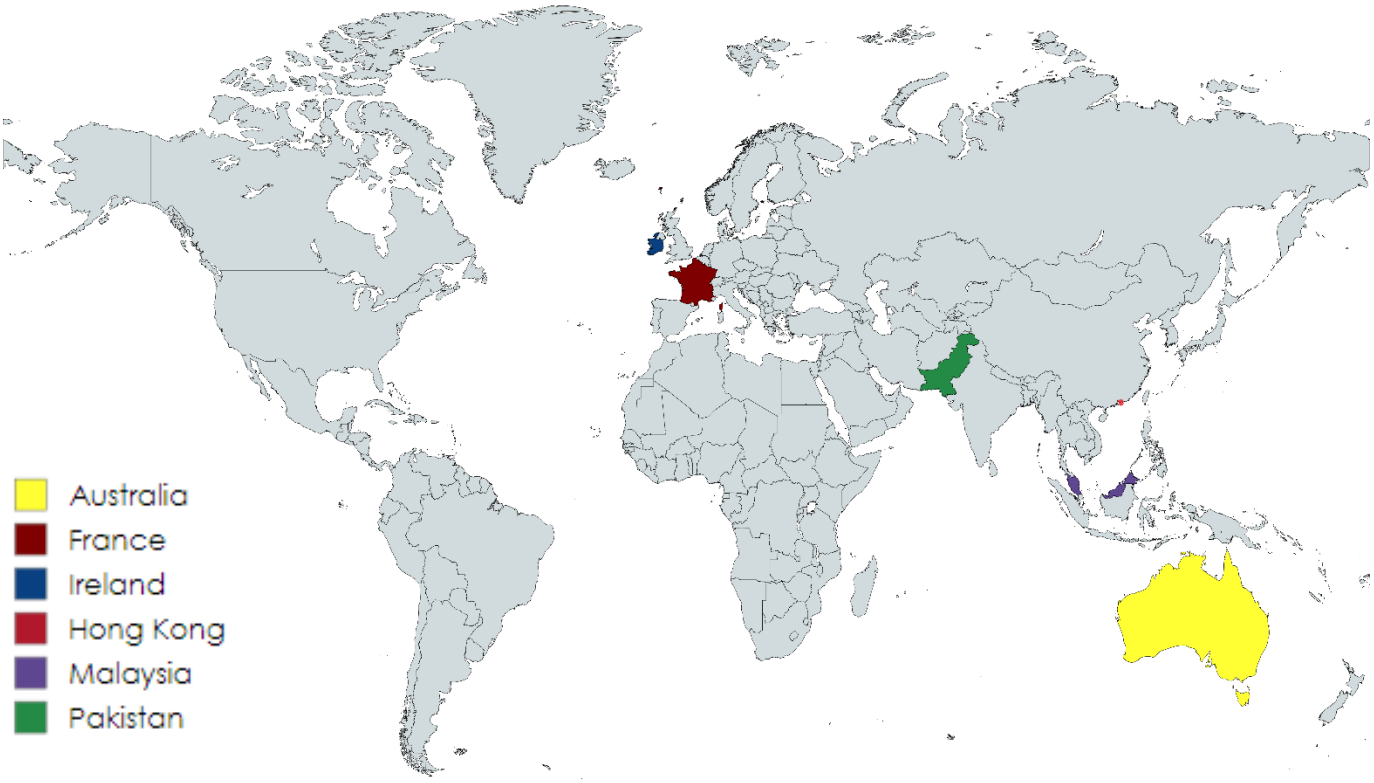

George Wardeh

(IUT de Cergy-Pontoise, France)

Dr. George Wardeh has expertise on concrete materials. He is currently associated with IUT de Cergy-Pontoise, France His research interests include frost behavior of concrete, recycled aggregate concrete, and post-cracking behavior of concrete. He did his Ph.D. from Université Paul Sabatier Toulouse III. George Wardeh is an associate professor at CY Cergy Paris University in the department of Civil Engineering (IUT) and a member of Laboratory of Materials and Mechanics of Civil Engineering (L2MGC) since 2007. He was the head of the civil engineering department between 2016-2019 and he is currently a member of the academic council of CY Cergy-Paris University. He participated in many research projects and he is a member of the editorial board of Journal of Building physics. The research that Dr Wardeh leads is structured into three converging axes. The first axis concerns the frost behavior of construction materials and concrete more particularly. The main aim is to explain the behavior of construction materials within the framework of poromechanics. The second axis is dedicated to the activities on recycled aggregate concrete which are extended from the mix design of these special concretes until the behavior analysis of reinforced recycled concrete beams. The third axis is related to the post-cracking behavior of concrete. The objective is to study the effect of freezing–thawing cycles and recycled aggregates on the fracture energy and the softening behavior of concrete using inverse analysis methods. George WARDEH published 20 research papers, three book's chapter and more than 40 national and international conferences.

Hammad Anis Khan

(University of Sydney, Australia)

Dr. Hammad Anis Khan has expertise on concrete materials. He is currently associated with University of Sydney, Australia. His research interests include RCCP, self-healing concrete, fine recycled concrete aggregate, and cement chemistry. He did his Ph.D. from University of New South Wales, Australia. Dr. Hammad Anis Khan has over 10 years of experience in the field of structural engineering, with a focus on utilizing sustainable construction practices. He has worked on developing green low-carbon concretes like geopolymer, alkali-activated blends, and blended cement-based concrete. He has a strong background in building design, serviceability assessments, infrastructure service life evaluation, durability design, and forensics assessments of damaged structures. He has investigated concrete problems ranging from high-temperature to freeze-thaw damages, chemical attacks like (ASR, ACR, DEF, Thaumasite Sulfate Attack--TSA) to salt efflorescence, and physical disintegrations to mechanical performance reductions. He has also published multiple research papers in peer-reviewed journals with high citations and h-index. He was also awarded the A.C. Kennett special award for the best paper on the corrosion or degradation of non-metallic materials at the Australasian Corrosion and Prevention Conference in 201. He is currently working on the development of sustainable fit-for-purpose concrete for sewer purposes. This project aligns with his passion for creating low-carbon and durable concrete structures that can withstand severely corrosive environments and reduce greenhouse gas emissions.

Mehran Khan

(University College Dublin, Ireland)

Dr. Mehran Khan is a materials expert and is currently associated with the school of civil engineering, University College Dublin, Ireland. His research interest include low carbon 3D printed concrete, HPC, fire resistant composites, and ACMs. He did his PhD from Dalian University of Technology, China. Dr. Mehran Khan specializes in the development of low carbon 3D printed concretes. His innovative research aims to advance sustainable construction practices by exploring the potential of 3D printing technology in reducing carbon emissions associated with traditional concrete production. Dr. Mehran Khan has made significant contributions to his field, authoring over 50 peer-reviewed publications that have collectively garnered more than 2,300 citations, reflecting the impact and relevance of his work. His scholarly achievements are underscored by an h-index of 32 and an i10-index of 36, indicating a robust engagement with the academic community and a strong influence on contemporary research in civil engineering. In addition to his research activities, Dr. Khan has demonstrated a commitment to academic excellence through various editorial roles, including serving as an Associate Editor and Academic Editor for multiple academic journals, as well as participating as a Guest Editor for special issues and a member of topical advisory panels at international conferences. His extensive involvement in these capacities highlights his dedication to advancing knowledge and fostering collaboration within the scientific community. Dr. Khan's expertise and leadership in the field position him as a key contributor to ongoing discussions about sustainable materials and construction technologies, making him a valuable asset to both academia and industry.

Jin Cheng Liu

(Aurecon, Hong Kong)

Dr. Jin Cheng Liu has expertise on both concrete materials and structures. He is currently associated with Aurecon, Hong Kong. His research interests include ECC, UHPC, fire-induced explosive spalling of concrete, green concrete, and AI for civil engineering. He did his Ph.D. from Nanyang Technological University, Singapore. Following his PhD, Dr. Liu worked as a research staff member at both Nanyang Technological University and The University of Hong Kong. Over the years, Dr. Liu has participated in numerous research projects and real-world projects, honing his expertise in various domains such as structural engineering, concrete materials, earthquake engineering, fire safety engineering, and artificial intelligence. His significant research contributions include a) Propounded unified fire-induced concrete spalling theory, and introduced a design concept of "three defense lines against fire-induced concrete spalling", which can be applied in (1) Ultra-high Performance Concrete (UHPC) structural system, (2) vital underground/submerged infrastructure, and (3) nuclear infrastructure. b) Proposed knowledge-enhanced machine learning models to assess explosive spalling risk of concrete, which can be applied in (1) design of explosive spalling-free concrete, (2) assessment of explosive spalling risk of existing concrete, and (3) provide valuable input to Code/Standard/Guideline. c) Improved fire resistance of normal strength Strain Hardening Cementitious composite (SHCC) or Engineered Cementitious Composite (ECC), overcame explosive spalling tendency of Ultra-High Performance Strain Hardening Cementitious Composite (UHP-SHCC).

Muhammad Shakeel

(AECOM, Hong Kong)

Dr. Muhammad Shakeel is a geotechnical expert and is currently associated with AECOM, Hong Kong. His research interests include centrifuge modelling, static liquefaction, slope stability, and numerical modelling. He did his PhD from The Hong Kong University of Science and Technology, Hong Kong. Muhammad Shakeel brings experience from previous roles at The Hong Kong University of Science and Technology, SA BAYTUR CONSTRUCTION CO and Ammico International Contracting Co. Ltd. He possesses robust skill set that includes Deep Foundations, Geotechnical Engineering, High Rise, Highways, SAP2000 and more. Dr. Muhammad Shakeel is a distinguished researcher whose impressive accolades underscore his commitment to excellence in his field. He was honored with the HKPFS Award from the Research Grant Council in Hong Kong in 2015, recognizing his outstanding research contributions. Prior to this, he received the HM King Scholarship in Thailand in 2013, highlighting his academic prowess and dedication to advancing knowledge. In 2012, he was part of the team that earned the Hydro Asia Best Group Award from Kwater in Korea, showcasing his collaborative efforts in addressing water-related challenges. Additionally, Dr. Shakeel received the Honor Award from UET Lahore, Pakistan, in 2010, further affirming his reputation as a leading figure in engineering and sustainability.

Noor Aina

(Universiti Pertahanan Nasional, Malaysia)

Dr. Noor Aina is a construction materials specialist and is currently associated with the department of civil engineering, Universiti Pertahanan Nasional, Malaysia. Her research interests include green steel, green technology, unreinforced masonry building, and building retrofitting. She did her PhD from University of Auckland, New Zealand. Her work primarily focuses on sustainable materials in civil engineering, with a particular interest in concrete technology, including the use of agricultural waste, textile waste, and recycled glass for construction materials. She has contributed to research on the optimization of materials such as bottom ash, limestone, and other industrial by-products in asphalt and concrete mixes, with a focus on enhancing the sustainability and performance of construction materials. Her involvement in studies relating to the soil-water retention properties of materials used for subgrade improvements using agriculture wastes showcasing her commitment to environmental sustainability and infrastructure resilience. Additionally, Noor Aina has been involved in studies relating to unreinforced masonry (URM) retrofitting works as one of the efforts to preserve the heritage.

Khan Shahzada

(UET Peshawar, Pakistan)

Dr. Khan Shahzada is a materials expert and is currently associated with the department of civil engineering, University of Engineering and Technology, Peshawar, Pakistan. His research interests include ECC, waste marble powder, fly ash, and SRA. He did his PhD from University of Engineering and Technology, Peshawar, Pakistan. Dr. Khan Shahzada is a distinguished member of the Provincial Housing Taskforce for the Government of Khyber Pakhtunkhwa, actively contributing to the Prime Minister's Initiative for 5 million affordable homes. He holds a lifetime membership with the Pakistan Engineering Council and is a key member of its national program evaluation committee. His expertise in geotechnical and structural engineering has provided invaluable consultancy services to various government departments, significantly enhancing the financial resources of the University of Engineering and Technology (UET) Peshawar.Dr. Shahzada's robust international research collaborations extend across the USA, Italy, Canada, Turkey, and Hong Kong, reflecting his commitment to advancing engineering practices globally. As an active member of several engineering organizations, including the American Society of Civil Engineers (ASCE), he continues to promote innovation and excellence in the field. His insights and extensive experience position him as an inspiring keynote speaker, poised to share transformative ideas on sustainable housing solutions and engineering advancements at the conference.

Khan Zaib Jadoon

(International Islamic University, Islamabad, Pakistan)

Dr. Khan Zaib Jadoon is a water resource expert and is currently associated with the department of civil engineering, International Islamic University, Islamabad, Pakistan. His research interests include ground water recharge, dam seepage, spatiotemporal monitoring, and WT-ANN. He did his PhD from Universite Catholique de Louvain, Belgium. He is a highly accomplished academic and researcher specializing in the application of ground penetrating radar (GPR) to address hydrological and environmental challenges. Dr. Jadoon has an extensive background in research, having participated in significant projects such as TERENO and CROP.SENSe.net at the Forschungszentrum Jülich in Germany from 2007 to 2011. Following his postdoctoral work at the Water Desalination and Reuse Center at KAUST, he transitioned to academia in Pakistan, where he currently serves as a Professor and Dean of the Faculty of Engineering and Technology at the International Islamic University, Islamabad. His career reflects a commitment to advancing knowledge in civil engineering and hydrology. Dr. Jadoon's research interests are centered on the coupled inversion of geophysical and hydrological data, with a particular emphasis on hydro geophysics and electromagnetic modeling techniques for GPR and electromagnetic induction. His current projects focus on integrated hydro geophysical inversion of time-lapse geophysical data to characterize aquifers and vadose zones effectively. Notably, he is actively developing joint inversion methods for multi-component electromagnetic measurements to optimize drip irrigation systems, which are crucial for sustainable agricultural water management. Additionally, Dr. Jadoon is engaged in monitoring the long-term impacts of climate change on terrestrial hydrology, utilizing precise weighing lysimeters to assess water balance, evapotranspiration, and water retention capacity. His work significantly contributes to understanding and managing water resources in the context of environmental change.

Advisory Committee

Dr. M. Mansoor Ahmed
(Vice-Chancellor CUST Islamabad)
Patron

Dr. Imtiaz Ahmed Taj
(Dean Faculty of Engineering)
General Advisor

Dr. Ishtiaq Hassan
(Head of Civil Engineering Department)
Principal Advisor

CSCE Industrial Partners for its 6th Edition

JS Architectural & Engineering Consultants

Engineering & Design Consultants

City Engineering Consultants

MKAI Climate Consulting

ZAC Engineers

MARK Associates

Design and Consultancy Services

Organizing Committee

Dr. Majid Ali
Convener

Dr. Muazzam Ghous Sohail
Member

Engr. Iqbal Ahmad
Member

Engr. M. Waqas Malik
Member

Engr. Minhas Shah
Secretary

TABLE OF CONTENTS

Extended Abstract 1:	Effect of Mortar Type on the Static and Dynamic Behaviour of Masonry Arches .. George Wardeh	2
Extended Abstract 2:	Penetrability in Concrete: A Perspective to Develop Durable Concrete for Sewer Environment ……. Hammad Anis Khan	5
Extended Abstract 3:	3D Printing Concrete: Transforming Construction through Innovative Technology Mehran Khan	8
Extended Abstract 4:	Machine Learning Assisted Iterative Design of Geopolymer Concrete and High Performance Concrete …….. Jin-Cheng Liu	11
Extended Abstract 5:	Application of Centrifuge Modelling in Geotechnical Engineering and Research ... Muhammad Shakeel	14
Extended Abstract 6:	Building a Sustainable Future: The Role of Textile Waste Composites in Civil Engineering …… Noor Aina Misnon	17
Extended Abstract 7:	Sustainable Alternative Materials in Building Construction ……. Khan Shahzada	19
Extended Abstract 8:	Challenges and Solutions for the Sustainable Groundwater Management in Pakistan …… Khan Zaib Jadoon	22
PAPER ID. 24-101:	Performance of Concrete Containing Steel Waste Fibers ……. Muhammad Fiaz Tahir, Mehar Ali	26
PAPER ID. 24-103:	Mechanical and Permeation Properties of Concrete Using Indigenous Volcanic Ash as Partial Replacement of Cement ……. Munawar Hussain, Ayub Elahi	30
PAPER ID. 24-104:	Physical and Durability Properties of Steel Slag Particles for Use in Road and Concrete Works …… Ahmad Faraz, Anwar Khitab	34
PAPER ID. 24-107:	Performance Evaluation of Sustainable Compressed Stabilized Earth Bricks …….. Shafi Ullah Anjum, Saif Ur Rehman	38
PAPER ID. 24-111:	An Experimental Investigation into the Compressive Strength Behavior of Ultra High Performance Concrete ……. Muhammad Ubair Javed, Muhammad Akbar Malik	42
PAPER ID. 24-112:	Assessment of Flow and Mechanical Properties of Geopolymer Composite Foam Ceramic Fillers ……. Hammad Shaukat, Ali Raza	46
PAPER ID. 24-115:	Enhancing Load-Carrying Capacity of Damaged Geopolymer Concrete Columns by Retrofitting with CFRP Wraps ……. Muhammad Ahsan Sami, Zawar Ahmed	50
PAPER ID. 24-117:	Enhancing Concrete Mechanical Properties Through Graphite Nano-Micro Platelets …… Hassan Tahir, Muhammad Numan	54
PAPER ID. 24-118:	Utilization of Industrial Wastes in Bricks and Tuff Tiles …….. Khawaja Adeel Tariq, Zeshan Ahmad	58
PAPER ID. 24-119:	Performance Evaluation of Self-Cured Bio Geo-Polymer Concrete Regarding Mechanical Strength and Durability ……. Ahmad Ali Sial, Faisal Shabbir	62

PAPER ID. 24-121:	Tensile Strength of Textile Waste Composite ……...	66
	Noor Aina Misnon, Faridah Hanim Khairuddin	
PAPER ID. 24-122:	Bond Behavior of Deformed Steel Rebar Embedded in a Recycled Brick Aggregate Concrete ……..	70
	Muhammad Subhan, Huzaifa Nadeem	
PAPER ID. 24-124:	Optimized Prediction Modeling for Chlorinated Marine Concrete Using Decision Tree ……..	74
	Muhammad Luqman, Majid Khan	
PAPER ID. 24-125:	Rubberized Concrete: Optimum Duration of Pretreatment of Rubber Particles with Alkaline Solutions ……	78
	Raja Bilal Nasar Khan, Anwar Khitab	
PAPER ID. 24-126:	Sustainable Concrete Production: Utilizing Waste and Green Technologies ……...	82
	Usman Ilyas, Fatima Ashfaq	
PAPER ID. 24-128:	Conventional Empirical and Machine Learning Models: A Review of Chloride Concentration in Marine Concrete ……	86
	Muhammad Arif, Muhammad Luqman	
PAPER ID. 24-129:	Retrofitting of Confined Masonry Structure with Fiber Reinforced Polymer ……...	90
	Ajmal Khan, Qazi Sami Ullah	
PAPER ID. 24-212:	A Case Study on Remedial Measures for Fire-Damaged Structure ……..	94
	Muhammad Dawood Ali, Ali Ejaz	
PAPER ID. 24-220:	Sustainable Rehabilitation of Fire-Damaged Low-Rise RC Structures: Assessment, Retrofitting, and Bamboo Fiber Solutions ……...	98
	Faheem Ahmad Gul, Arshad Ullah	
PAPER ID. 24-223:	A Simplified Numerical Model for Reinforced Concrete Beam-Column Joints …..	102
	Muhammad Azeem, Muhammad Fahim	
PAPER ID. 24-224:	Plastic Strength of Externally Welded CHS-Transverse Plate T-Joints ……	106
	Ali Ajwad, Massimo Latour	
PAPER ID. 24-225:	Predicting the Initial Stiffness of Externally Welded CHS-Transverse Plate Joints at Vertical and Horizontal Connections ……	110
	Ali Ajwad, Massimo Latour	
PAPER ID. 24-226:	The Development of Fragility Curves for Masonry Building- State of Art Review	114
	Saif Ur Rehman, Mohammad Ashraf	
PAPER ID. 24-228:	Strengthening of Unreinforced Masonry Structure with Fiber-Reinforced Polymer	118
	Ahmad Suboor, Samiullah Qazi	
PAPER ID. 24-229:	Experimental Investigation of Bridge Pier Scouring with Rip Rap Enclosed in Mesh …….	122
	Fardeen Javaid, Muhammad Bilal	
PAPER ID. 24-230:	Assessing Structural Behaviour of FRP-Confined CFST Columns Through Finite Element Methods …….	126
	Muhammad Azan Iqbal, Ali Raza	
PAPER ID. 24-238:	Enhancing Structural Integrity and Resilience: A Systematic Approach for Retrofitting Design of a Two-Story Hospital Building in Karachi ……	130
	Hassan Tahir, Muhammad Numan	
PAPER ID. 24-239:	A Review on Fire Damage Assessment of Reinforced Concrete Structures of a Building ……	134
	Ghazanfar Ali Anwar, Yousef Khan	
PAPER ID. 24-242:	Bridge Bearings Replacement Challenges – A Review ……	138
	Mustafa Zwain, Furqan Qamar	

PAPER ID. 24-245:	Design and Analysis of Green High-Rise Building Using Recycled Materials ……. Muhammad Bilal Subhani, Minahal Azad	142
PAPER ID. 24-246:	Enhancing Structural Design Efficiency in Pakistan: A Case Study on the Impact of BIM Integration …… Hassan Tahir, Muhammad Umair	146
PAPER ID. 24-247:	Sustainable Design of a Multi-Story Building Using Waste Marble and Ceramic ... Muhammad Haroon Kabir, Anwar Khitab	150
PAPER ID. 24-248:	An Overview on Fire Damage Quantification and Retrofitting of Low-Rise Reinforced Concrete Structures …… Javaria Mehwish, Waseem Akram	154
PAPER ID. 24-303:	Operation and Maintenance of Green Buildings: A Case Study ……... Muhammad Fahad, Hafiz Aiman Jamshaid	158
PAPER ID. 24-304:	Optimizing Energy Performance of Buildings in Pakistan Using BIM ……. Said Haseebullah, Fahad Aslam	162
PAPER ID. 24-308:	Factors Effecting Stakeholder Engagement in Design Bid Built …….. Mehar Ali, Abdul Qadeer	166
PAPER ID. 24-319:	An Insight into Prospects and Challenges of 3D Printing in Developing Countries Sadia Sajid Khan	170
PAPER ID. 24-320:	Optimizing Energy Efficiency in Green Buildings Using BIM-Integrated Energy Analysis Tools …….. Muhammad Sohaib	174
PAPER ID. 24-402:	Assessment of Ablution Waste Water Quality for Various Mosques in Peshawar City ……... Hamad Khan, Abdullah Khan Jadoon	178
PAPER ID. 24-503:	Enhancing Asphalt Pavement Performance with Phase Change Materials ……... Muhammad Usman, Affaq Arif Gill	182
PAPER ID. 24-504:	To Assess the Impact of Organophilic Nanoclay on Marshall Properties of Asphalt Material …… Abu Bakar, Zimran Nasir	186
PAPER ID. 24-507:	Assessing the Combined Effects of Steel Speed Humps and Road Studs on Speed Reduction ……. Ali Hassan Waraich, Jamal Ahmed Khan	190
PAPER ID. 24-513:	A Coss-Sectional Analysis of Sustainable Mobility for Female University Students in Karachi ……. Ashar Ahmed, Bakir Rehman	194
PAPER ID. 24-514:	Examination of the Effect of Illegal Parking on Capacity Reduction of Urban Roads …… Ashar Ahmed, Muhammad Shair	198
PAPER ID. 24-602:	The Impact of Gypsum on the Stabilization of Peat Soil ……... Affaq Arif Gill, Muhammad Waleed	202
PAPER ID. 24-614:	Effect of Aspect Ratio on Bending Moment and Shear Force Distribution of Axially Loaded Piles …… Moeez Saqib, Salman Ali Suhail	206
PAPER ID. 24-615:	Examining Impact of Group Configuration on Pile Response Using Numerical Method ……. Muhammad Awais Yaseen, Salman Ali Suhail	210
PAPER ID. 24-616:	Investigating Load Transfer Behaviour of Bored Piles in Layered Soil …… Muhammad Ammar, Salman Ali Suhail	214

PAPER ID. 24-708: Optimized Prediction Modeling for TiO_2-Catalyzed Photo-Degradation Rate Constants of Water Contaminants Using Machine Learning …… 218
Ayesha Noreen, Majid Khan

PAPER ID. 24-711: Evaluation of Energy Content in Municipal Solid Waste of Low-Income Area Tehkal and High-Income Area Hayatabad of Peshawar K.P.K Pakistan …….. 222
Muhammad Shahid Khan, Saeed Hijab

Annexure-A Photogallery ……. 226

Keynote Speakers' Extended Abstracts

EFFECT OF MORTAR TYPE ON THE STATIC AND DYNAMIC BEHAVIOR OF MASONRY ARCHES

[a] George Wardeh

a: L2MGC, CY Cergy-Paris University, 95031 Neuville-sur-Oise, France, george.wardeh@cyu.fr

Masonry arches have been widely used since antiquity. Many ancient arched bridges are still an important part of transport networks in various countries. Masonry arch structures are ageing and suffering from increased loads. The main difficulties in the requalification of masonry structures lie in the lack of key information needed to identify the material's behavior. To accurately simulate masonry arch failure and serviceability, a numerical and in-situ monitoring approach must be employed. This requires understanding the mechanical properties of the materials and the masonry's behavior under stress and load. Masonry is composed of brick units and mortar, usually with stiffer bricks embedded in an inelastic mortar joint, although code specifications and structural design often consider masonry to be a homogeneous material. Masonry's true characteristics result from the interaction between the brick, mortar and stress. To predict masonry behavior, it is necessary to understand the brick, mortar and masonry properties. While most research has focused on masonry arch bridges' vertical performance, recent studies have begun to investigate their seismic behavior. Seismic evaluation of existing masonry arch bridges is a priority in earthquake-prone areas to ensure safe road and rail infrastructure operating conditions.

This work, which is a part of I. Bello's Ph.D thesis, aims to characterize masonry at the material and structural scale, study the behavior of curved masonry structures, and create models accounting for material nonlinearities. The focus is on the effect of the properties of the mortar on the static and dynamic behavior of the arches. The experimental program was divided into two parts. First, prisms were constructed to study the full stress-strain behavior during cyclic compression. The static and pseudo-dynamic behavior of the arches was studied in a second step. For the construction of the masonry prisms, two non-hollow masonry bricks, B1 and B2, were used with five different mortar mixes developed in the laboratory. The two types of brick are different in terms of their physical properties and their compressive strength, which is 90 MPa for B1 and 37.4 MPa for B2 (table 1). Five different types of mortar were produced, varying in cement and lime content. The sand grain size ranged from 0 to 2 mm. The water to binder ratio had values of 0.55, 0.65 and 0.7. Mortar M1 was formulated entirely from cement, while M5 was formulated entirely from lime. For mortars M2, M3 and M4 the cement/lime ratios were 0.25, 0.5 and 0.75.

Eight masonry arches were prepared using the brick B1 and mortars M1 and M5 only. Each structure has 25 bricks and 24 mortar joints. The intrados and extrados have a radius of 0.5 m and 0.61 m. 2-coulum frame Schenck machine regulated at the rate of 0.5 mm/min and having capability of applying a maximum load of 3000 kN was used to conduct tests on the masonry prisms'. Strains were measured using classical strain gauges and Digital Image Correlations Technique (DIC). The static protocol for arches testing involves instrumentation of masonry arches with 8 LVDT at predicted failure locations and two load cells at springing. The structures intended for dynamic testing were mounted on a steel base and rollers to allow horizontal displacement in one direction. The base was later attached to the hydraulic machine for pseudo-dynamic tests. Two main series of tests were conducted, both under displacement control. In the first series a monotonic compression testing was conducted with a servo-hydraulic testing machine having load cell of 50 kN. A monotonic compressive load is applied on the crown until the complete failure of the arches. The second series involves first applying 50% of the maximum compressive load at the crown. Later, the arches are induced to a pseudo-dynamic test having a constant displacement of ±2mm and a frequency intensity at 1, 3, 5, 7, and 10Hz, while ±1.5mm was applied at 13Hz. (7D Canon digital camera having a pixel resolution of 5184 x 3456) was used to capture images for the 2D digital image correlation (DIC) analysis. (Camera having fixed focal length of 45mm (EF f/2.8L USM) was mounted on a tripod and the masonary arches were position 2.8 m away from the camera.

The results obtained from the compressive testing revealed that the failure pattern of the prism is influenced by the joint mortar composition. Prisms having a higher cement content were characterized by spalling and lateral tensile splitting, leading to a brittle failure mode. (Moreover, prisms with a having higher lime content showed a more ductile

failure mode, characterized by localized strains at the mortar joints. The lime content in the mortar showed a direct relation with its ductility, with an increase in lime dosage more ductile response is observed. Digital Image Correlation proved to be a valuable tool for observing strains up to failure, as traditional strain gauges became unreliable at later stages of the test.

Table 1. Types of bricks and their properties

Specimen	Porosity (%)	Water absorption (%)	Density (g/cm^3)
Brick 1 (B1)	19.37	9.54 ± 0.13	2.00
Brick 2 (B2)	14.58	7.77 ± 1.63	1.88

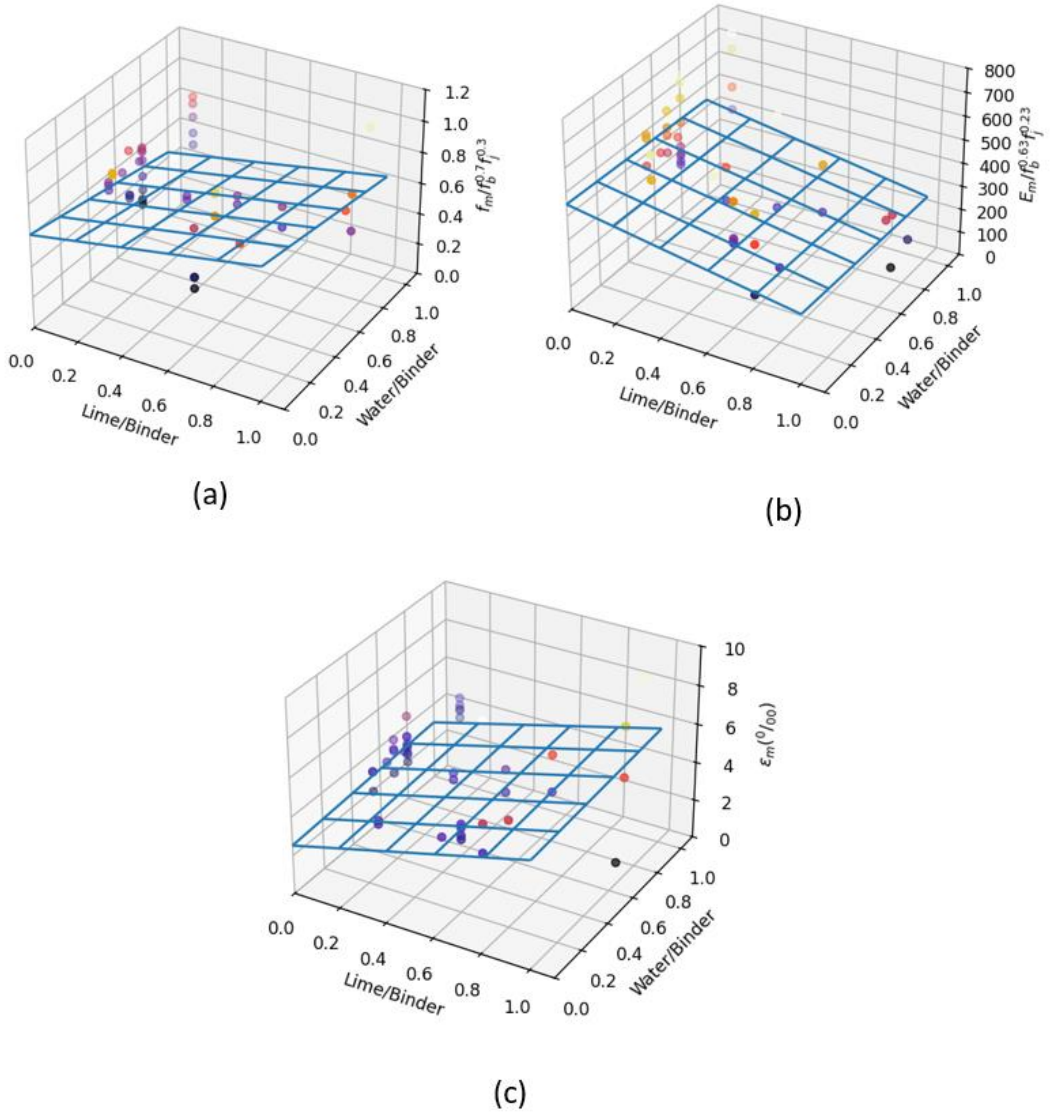

Figure 1. Effect of mortar composition on the mechanical properties of masonry.

The obtained results were added to those available in the literature and illustrated in Figure 1 where it can show that as the water/binder ratio is increased the compressive strength decreases (Figure 1.a). Furthermore, by increasing the lime content, the modulus of elasticity decreases (Figure 1.b) while the strain at peak stress increases (Figure 1.c). It was also found that the decrease in the elastic modulus induces a decrease in the joint tensile strength and its fracture energy.

For the static behavior of masonry arches, it was found that masonry arches using cement as a binder exhibited compressive strengths three times higher than arches built using lime mortar while their deformability is lower. Both structures experienced a decrease in strength, indicating the occurrence of hinge openings on either the extrados (upper surface) or intrados (lower surface) of the arches. Upon pseudo dynamic tests, it was observed that the failure mode is generally attributed to the opening of hinges at the extrados and intrados of the masonry arches. For tender joint mortars the loading-unloading bearing capacity is lower that stiff mortar while the ductility is higher. The arches were numerically studied using ABAQUS and a simplified micro modelling approach to better understand the failure mechanism and a good agreement was found between experimental and numerical results. For all tested elements a good agreement was also found between the displacements obtained using DIC and those obtained by means of classical measurement tools.

Based on the findings of this study the following concluding remarks can be withdrawn:

- The composition of joint mortar influences the behavior of the masonry
- Lime content and Water/Binder ratio are the two key parameters
- Flexible mortars have a more ductile behavior but a lower resistance

PENETRABILITY IN CONCRETE: A PERSPECTIVE TO DEVELOP DURABLE CONCRETE FOR SEWER ENVIRONMENT

Hammad Anis Khan

University of Sydney, Australia. hammadanis.khan@sydney.edu.au

This keynote lecture focuses on Microbially Induced Concrete Corrosion (MICC), a process wherein sulfuric acid produced by microorganisms leads to the degradation of concrete structures like sewer pipes. These pipes subjected to MICC were occupied by *Desulfovibrio* which can use sulfate or sulfur compounds to produce H_2S in the absence of oxygen. The presence of H_2S can initiate the formation of sulfuric acid in the presence of oxygen which leads to the destruction of the concrete. This process is further aggravated by other factors like moisture, air flow and temperatures.

The steps of MICC includes abiotic neutralization with carbonation, the acidification by H_2S through bacterial activity and formation of sulphuric acid formation due to sulphur oxidation. It involves a coordinated combination of chemical and biological agents in a sequential manner to enhance the destruction of concrete particularly in sewer systems. These microorganisms thrive in aerobic conditions, making the surface of concrete highly susceptible to corrosion.

Penetrability and permeability of concrete are one of the most significant properties which define the durability of concrete in this aggressive environment. Penetrability is defined as the ease with which substances like water and harmful chemicals can infiltrate the concrete. Capillary porosity, which is influenced by the water-to-cement (w/c) ratio and the degree of hydration, plays a significant role in determining a concrete's resistance to degradation. Concrete with higher permeability is more vulnerable to deterioration in harsh environments. The lecture emphasizes the importance of understanding these properties to enhance the durability of concrete, especially in sewer systems.

The experimental testing plan was carried out to investigate the performance of two types of concrete mortars: Low Calcium Fly Ash Based Geopolymer Mortar (FA-GPm) and Sulphate Resistant Portland Cement Mortar (SRm). These materials were subjected to long-term exposure in a highly corrosive sewer environment at the North Head Wastewater Treatment Plant in Sydney. Throughout the study, samples were exposed to varying levels of humidity and H_2S concentration. Observations made after 12 months revealed significant surface degradation, scaling, and the formation of white efflorescence, particularly in SRm samples (figure 1).

Table.1 Variation in Porosit, Mass and Strength

Physical Property	**FA-GPm**		**SRm**	
	Control	Digester	Control	Digester
Porosity (%)	18.4 ± 0.1	22.9 ± 0.4	17.7 ± 1.2	20.5 ± 0.8
Compressive Strength (MPa)	46.3 ± 1.6	37.2 ± 2.6	50.7 ± 1.7	35.7 ± 0.9
Strength Loss (%)	-	19.6 ± 2.1	-	29.6 ± 1.6
Mass Loss (%)	-	2.06 ± 0.7	-	2.8 ± 0.5

The results of the study showed that both FA-GPm and SRm experienced reductions in mass and compressive strength after one year of exposure. FA-GPm exhibited a mass loss of 2.06%, while SRm lost 2.8% (table 1). Water-induced porosimetry tests revealed that both mixes became more porous over time, increasing their susceptibility to corrosion. The analysis of neutralization depth indicated that FA-GPm underwent greater loss of alkalinity, highlighting its more porous structure compared to SRm (figure 2). The loss in alkalinity suggests that FA-GPm has a shorter service life when exposed to a sewer environment.

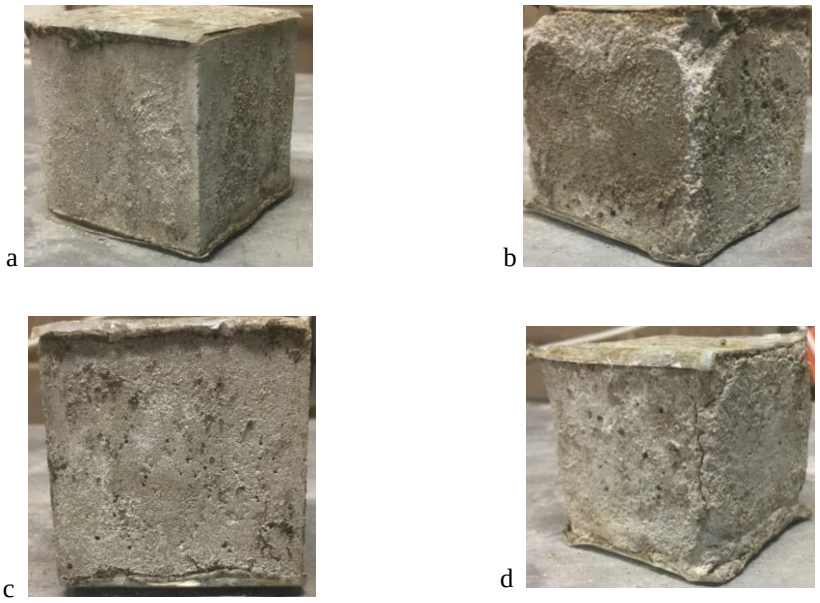

Figure 1. Visual observation after 12 months (a) FA-GPm (b) SRm

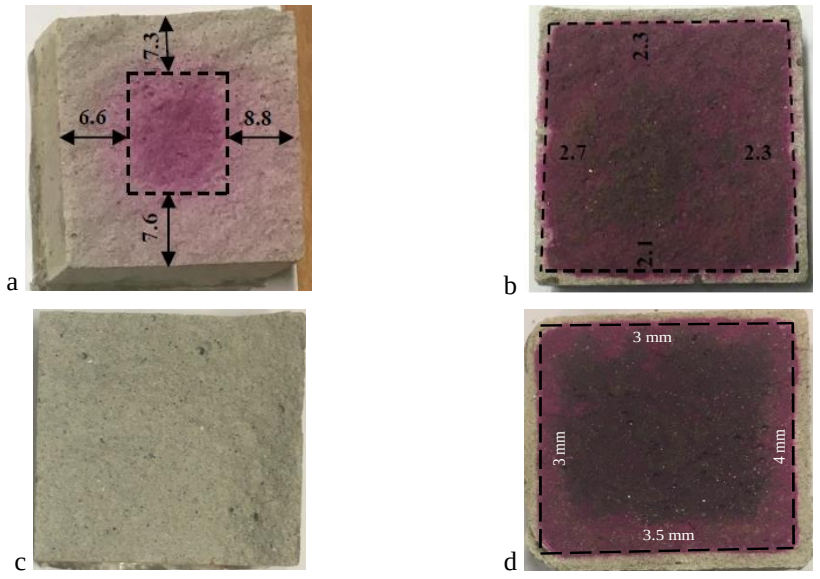

Figure 2. Neutralization depths (a) FA-GPm after 6 months (b) SRm after 6 months (c) FA-GPm after 12 months (d) SRm after 12 months

Finally, XRD and SEM analyses provided insights into the microstructural changes occurring in the mortar samples. These analyses showed the formation of carbonation products such as calcite in SRm and natron in FA GPm, as well as the presence of sulfate products like gypsum and thenardite. These findings suggest that both carbonation and hydrogen sulfide acidification occurred simultaneously in the sewer environment. The microstructural deterioration, particularly the crystallization of sulfur compounds at the aggregate matrix interface, contributed to the reduction in durability. In conclusion, both mixes showed signs of degradation, however, SRm demonstrated slightly better resistance to infield corrosion than FA GPm.

3D PRINTING CONCRETE: TRANSFORMING CONSTRUCTION THROUGH INNOVATIVE TECHNOLOGY

Mehran Khan

School of Civil Engineering, University College Dublin, Ireland. drmehrankhan@outlook.com

Sustainable development is the primary focus today in addressing the negative impacts of climate change. Consequently, modern construction emphasizes technological and material advancements to reduce their adverse impacts on the environment. In the past decade, advancements in robotic technologies and material science have led to the development of full-scale 3D-printed concrete structures. 3D printing concrete technology has come out with significant applications. Its ability to efficiently and accurately construct complex structures has transformed traditional construction methods. The layer-by-layer process of 3D concrete printing addresses several challenges associated with traditional construction methods by allowing the creation of entire structures or specific components directly from digital models. 3D printing technology was initially used to create small-scale prototypes, but it has subsequently advanced to include large-scale construction projects. Europe is primarily at the forefront of this technical growth, along with many other countries (table 1). This is one approach for achieving efficient, sustainable construction with minimal carbon emissions through less waste, limited material consumption, and optimal design. The incorporation of low-carbon, sustainable materials, such as supplementary cementitious materials and recycled components, in 3D printing technology significantly enhances the sustainability of 3D-printed concrete projects. The use of customized materials and localized production of 3D-printed concrete, tailored to specific environmental conditions, reduces material waste and minimizes transportation needs, thereby contributing to sustainability. The 3D concrete printing process involves multiple stages, with the first being the design phase, where a digital model is created using specialized software. The second stage involves preparing the material by optimizing the concrete mix to achieve the required setting time and viscosity for optimal printability. Subsequently, the layer-by-layer concrete extrusion is made during the layering phase, that enables accurate control over its structure and shape. This step is followed by the curing and finishing of the structure to attain strength and durability.

Various European countries are leading the adoption of innovative 3D concrete printing technology. Particularly in Germany, multiple commercial and residential buildings have been constructed using 3D printing concrete technology in order to minimize the material consumption. The sustainable artistic 3D printing concrete projects are a specialty of Italy. Whereas, in Spain, the 3D printing concrete bridges and urban furniture is constructed. The initiative for 3D-printed concrete houses is spearheaded by the Eindhoven, Netherlands. France and Ireland emphasize energy-efficient 3D concrete printing designs as a pathway toward sustainable development. Hence, it can be said that 3D printing concrete technology offers several benefits, including a significant reduction in construction time, bringing completion timelines down to weeks instead of months. In addition, material efficiency is improved by using only the required amount, which minimizes waste and cost. Further, the flexibility of design is also a considerable attribute of 3D printing concrete technology, particularly in the case of complex structures which are very difficult to execute through conventional methods.

However, the implementation of 3D printing concrete technology also poses some challenges. For example, material limitations restrict its application due to the inability to achieve sufficient strength, printability, and sustainability. Similarly, the 3D printing setup demands a higher initial cost when it comes to large-scale projects. Moreover, the lack of standardization and building codes for 3D-printed concrete structures in many countries presents significant regulatory challenges.

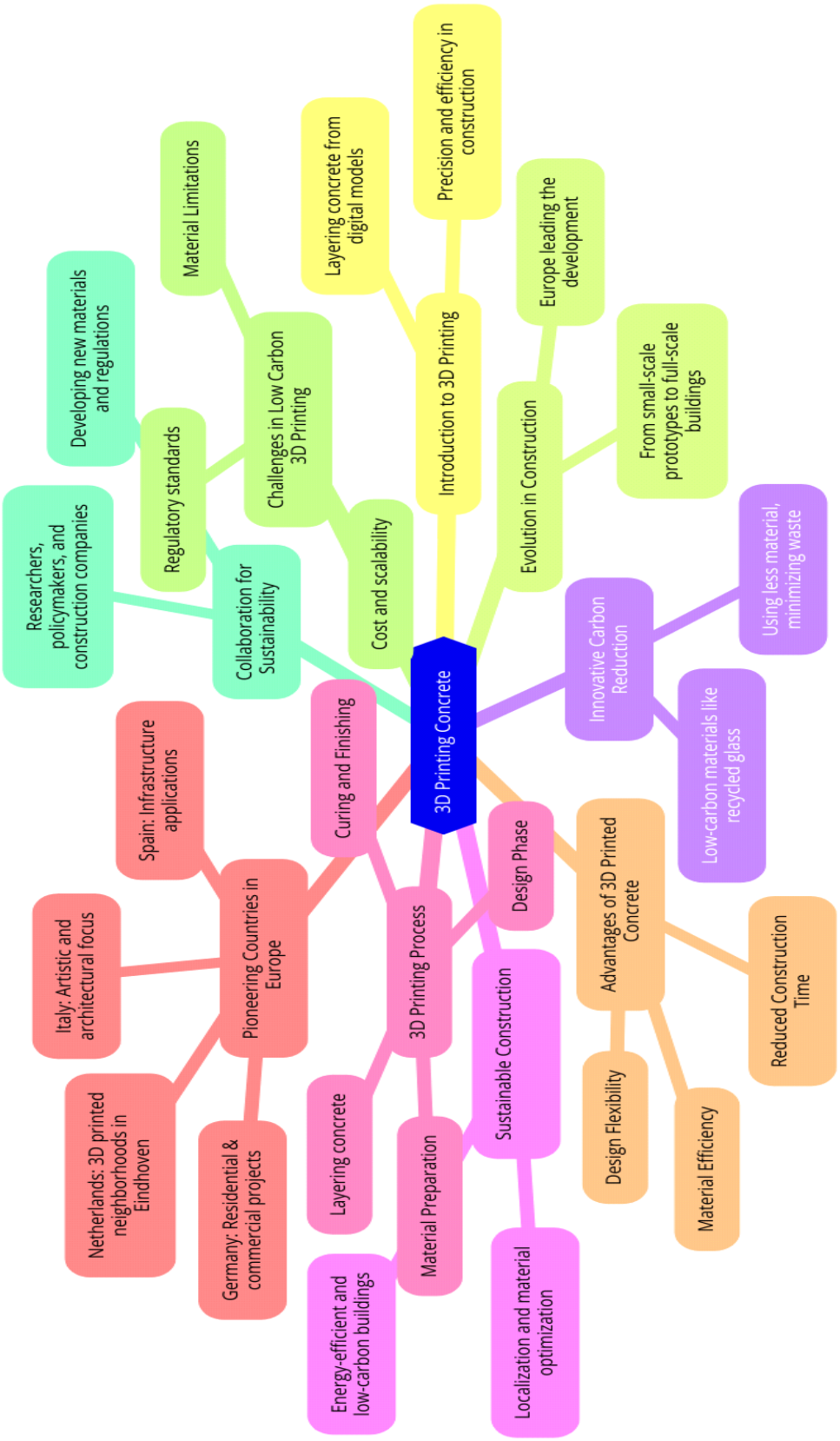

Figure 1. Sustainable Construction through 3D Printing Concrete.

Table 1. 3D Printed Concrete Structures in Europe

Project	Location	Sustainability Features
Striatus Bridge	Venice, Italy	3D printed concrete with recycled materials, solar powered lighting
Kamp Horst Pavilion	Horst, Netherlands	3D printed concrete with bio based admixtures, energy efficient design
Mile Stone Demonstrator	Eindhoven, Netherlands	3D printed concrete with reduced cement content, circular design

Effective collaboration among stakeholders, including the construction industry, researchers, and policymakers, is essential to address these challenges. Likewise, research into the development of novel materials and improved printing techniques is essential. The establishment of policies and regulations is also necessary for promoting sustainable construction practices. In a nutshell, it can be concluded that low carbon 3D printing concrete technology is an emerging revolution in the construction sector. As a result of continuous advancement in sustainable designs through innovations in materials science and robotics, 3D printed concrete is becoming the standard construction technique, contributing to resolve the environmental issues and economic challenges. Therefore, 3D printing concrete technology can be concluded with advancement in sustainable development in the construction sector. The overview of sustainable construction through 3D printing concrete is shown in Figure 1. The achievement of innovative design with reduced material waste and lesser carbon emissions through this technology is heading the built environment toward a greener future.

MACHINE LEARNING ASSISTED ITERATIVE DESIGN OF GEOPOLYMER CONCRETE AND HIGH PERFORMANCE CONCRETE

Jin-Cheng Liu

Aurecon Hong Kong Limited, Hong Kong, China. c130019@e.ntu.edu.sg

Concrete mix design is a technical process used to select and determine the appropriate proportions of concrete ingredients needed to achieve the desired strength and performance, i.e. workability, strength, and durability, etc. Current commonly used concrete mix design methods in Code of Practice (CoP), such as American Concrete Institute (ACI) method, British DoE method, and Indian Standard method, etc., are based on empirical relationships, in the form of charts and graphs developed from extensive experimental investigations. The basic assumptions underlying all these methods are that the compressive strength of workable concretes is primarily determined by water/cement ratio and the slump of concretes is primarily determined by maximum aggregate size and water content. However, various other factors affect slump and compressive strength of modern concrete, for examples, supplementary cementitious materials (SCMs), chemical compositions of cement and SCMs, fineness modulus of fine aggregate, fibers, and curing, etc. Therefore, these deem-to-satisfy methods should be considered only as a basis for concrete mix trial, further adjustments may still be needed to arrive at the desired concrete mix. Moreover, these concrete mix design methods in CoPs primarily focus on achieving the desired compressive strength and slump, often overlooking the detailed considerations on durability properties, such as chloride diffusion coefficient, necessary for ensuring long-term safety of concrete structures under severe complex environment.

As machine learning technique is growing mature and more concrete mix data is produced in laboratory and real-world projects, it becomes possible to leverage machine learning to assist in design of concrete mix that meet multiple objectives. A tentative machine learning framework for assisting high-performance concrete (HPC) mix design is illustrated in Figure 2. The first step is building prediction models, where datasets are developed by collecting and preprocessing data for compressive strength, slump, and chloride diffusion coefficient of concrete, respectively. These datasets form the foundation for the next phase, hyperparameter optimization, where Bayes search cross-validation tunes machine learning model hyperparameters. Subsequently, machine learning models for compressive strength, slump, and chloride diffusion coefficient of HPC are established. In the mix design phase, an objective function is defined along with constraints targeting the same three properties of concrete. The target compressive strength can be specified as a numerical value, while target slump and target chloride diffusion coefficient are recommended to be categorical value defined based on rationality. The mix design model, on basis of the established machine learning models, employs particle swarm optimization (PSO) to minimize the target function to identify the optimal HPC mix. Finally, experiment verification is conducted to ensure the results meet the desired criteria. If the results are unsatisfactory, the process iterates until the desired outcomes are achieved.

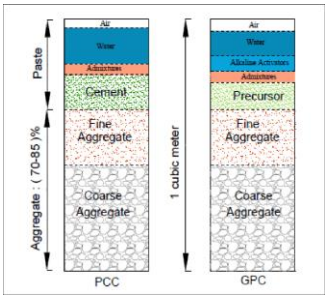

Figure 1. Composition of Plain Concrete vs Geopolymer Concrete

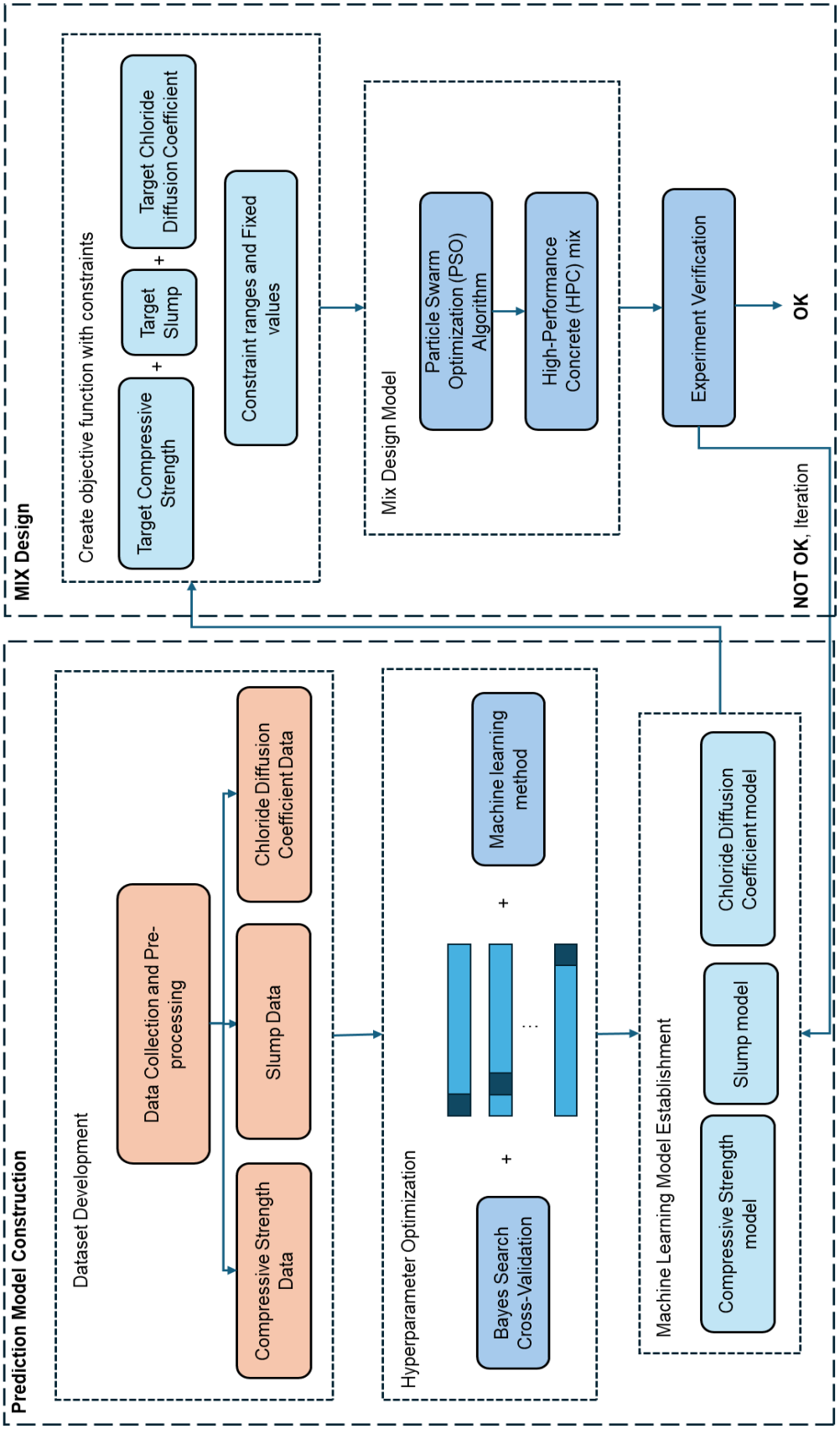

Figure 2. Procedure for machine learning assisted HPC mix design

This proposed machine learning framework is not only applicable for the design of high performance concrete considering chloride diffusion resistance, but can also be applied to other types of concrete or for optimizing other aspects of concrete. For example, it can be used for developing low-carbon concrete, such as fly ash blended concrete, natural pozzolana blended concrete, ground granulated blast furnace slag blended concrete, geopolymer concrete, alkali-activated slag concrete, or alkali-activated fly ash and slag concrete, etc. Additionally, it can be used to develop special concretes, such as ultra-high-performance concrete, water-tight concrete, pervious concrete, lightweight concrete, self-compacting concrete, fire-resistant concrete, etc. In brief, the proposed machine learning assisted concrete design method presents itself as a potentially powerful alternative tool to the traditional concrete mix proportioning method in CoPs.

APPLICATION OF CENTRIFUGE MODELLING IN GEOTECHNICAL ENGINEERING AND RESEARCH

Muhammad Shakeel

AECOM Asia Hong Kong Ltd. mshakeel@ust.hk

Centrifuge testing is commonly used for various geotechnical and geo-environmental applications. Geotechnical modeling has emerged as an alternative tool to complement numerical analyses and field tests. *Ng et al., 2007*, explores the interrelationship among different approaches that complement each other. This paper introduces the major application along with the basic principles of geotechnical centrifuge modeling. All these studies were conducted at the centrifuge modeling facility at the Hong Kong University of Science and Technology (*Ng et al., 2001*) as shown in Figure 1. The major difference between soil and other engineering materials (steel, concrete) is the stress dependent behaviour of soil. The fundamental principle of centrifuge modelling is to recreate the actual stress conditions on a reduced scale model by increasing the gravitational acceleration to ng, where n is the multiplier and g is the acceleration due to gravity of earth. Various scaling laws are formulated through dimensionless analysis (table 1).

Centrifuge modelling can be used as modelling of prototype, to carry out parametric study, investigation of new phenomenon and validation of numerical methods (*Ko, 1988*). Modelling of prototype are used to understand actual engineering problems i.e. slopes, piles, tunnels, excavation, geo environment, consolidation, earthquake and offshore structures. Under controlled settings, parametric studies using centrifuge modeling allow for sensitivity analyses, such as assessing the bearing capacity of footings on slopes, lateral loading of piles, and interactions among multiple tunnels. Centrifuge modelling can be effectively used to understand the new and complex problems such as explosion, plate tectonics, liquefaction, climate change, energy exploration and contaminant transport. Lastly, the reliability of any numerical method can be verified by comparing the results of the centrifuge testing with the adopted numerical approach.

Wang et. al., (2019) conducted a forensic investigation of a high rise building having 13-stories in Shanghai soft clay using centrifuge modelling. Prior to building collapse, an excavation having shallow depth was performed in front of the building and the excavated material was filled on the back of the building. In the centrifuge model, in-situ strength of the soft clay is similar to the undrained shear strength of the model soil. The surcharge loading of the fill on the back of the building was simulated by applying the loading using bearing plate and hydraulic jack. The failure mechanism of the piles in the centrifuge modelling was consistent with what was observed in the field.

To investigate the response of pile group and piled raft adjacent to deep excavation, *Ng et. al., (2021)* conducted a series of centrifuge tests in sandy soil to study the serviceability performance of 2x2 pile group and piled raft. The pile load increased by the amount of 3% and 21%, due to the soil movement and stress release caused by deep excavation of 8m, for the piles that were closer to the excavation for pile group and piled raft, respectively. To further mobilize end bearing and shaft resistance to maintain the vertical equilibrium, the settlement in the piled raft foundation was found to be 20% more than the settlement in the pile group. Furthermore, due to the excavation 30% additional pile bending moment was induced.

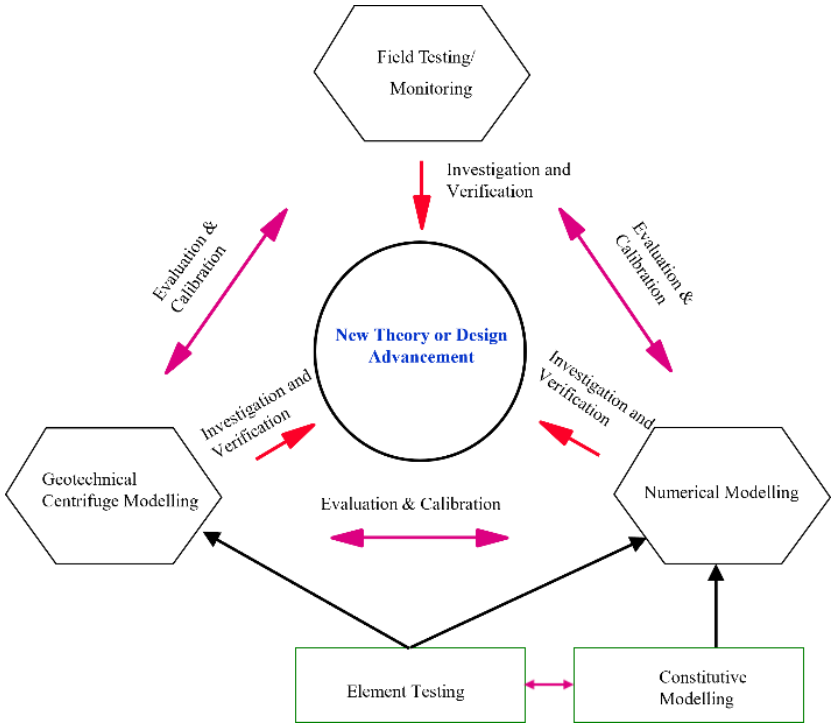

Figure 1 Relationship between field monitoring, centrifuge modelling and numerical modelling (modified from Ng et. al., 2007)

Table 1. Geotechnical Scaling Laws

Parameter	Scale (model/prototype)
Time (Creep, temperature)	1
Time (diffusion)/ Consolidation	$1/n^2$
Time (Dynamic)	1/n
Stress	1
Strain	1
Volume Dimension	$1/n^3$
Area Dimension	$1/n^2$
Linear Dimension	1/n
Acceleration	n
Unit Weight	n
Density	1
Mass	$1/n^3$
Force	$1/n^2$
Bending Moment	$1/n^3$
Pore fluid velocity / rainfall	n
Heat flux	n
Frequency	n
Concentration	1
Velocity	1

Ng et al., (Under review) conducted centrifuge model tests to study the time dependent response of DCM columns in soft marine clay and load transfer mechanism between DCM and sot clay subjected to reclamation fill. It was found that due to development of arching in the fill material, a critical height of 2.2 times the clear spacing between the DCM columns are required to limit the differential settlement. Due to arching mechanism, about 70-90% fill load is transferred to DCM which is transferred to competent stratum through DCM.

Ng et. al., (2022) conducted a series of three dimensional centrifuge tests to investigate the influence of different skew angles between new tunnel under the existing tunnel. Tunneling induces stress relief and arching in the ground which results different stress distribution pattern due to different angles. The existing tunnel experienced maximum settlement and tunnel strain when the skew angle is 30^{o}. The invert settlement at 30^{o} is 1.4 times larger than 90^{o} tunneling.

BUILDING A SUSTAINABLE FUTURE: THE ROLE OF TEXTILE WASTE COMPOSITES IN CIVIL ENGINEERING

Noor Aina Misnon

Department of Civil Engineering, Universiti Pertahanan Nasional Malaysia, Kuala Lumpur, Malaysia.
nooraina@upnm.edu.my

Textile waste is a major concern of environmental issues when millions of tons of textile waste was dumped in landfills each year [1]. The textile waste takes up to 200 years to decompose. This research was carried out to produce composite material namely textile waste composite (TWC). The TWC is a combination of textile waste with epoxy that has the potential to be implemented as a structural strengthening material. Laboratory performance testing revealed that samples strengthened with TWC perform better than plain concrete beamlets. This innovation aligns with the Sustainable Development Goals and has commercial potential as structural strengthening materials.

Cotton textile and nylon textile were used to produce the TWC. Three different configurations of TWC were applied as reinforcement on plain concrete beamlets (100 mm x 100 mm x 500 mm), i.e., full wrapping (FW), diagonal wrapping (DW), and mesh wrapping (MW) and the details are as shown in Table 1. A two point loading test was conducted on the samples to determine the flexural strength of the beamlet samples in accordance with BS EN 12390-5 [2].

Table 1: Details of TWC configurations

Type of reinforcing	Details		
	% reinforcement	Spacing between TWC (mm)	Angle of TWC (°)
FW	100		
DW	25	50	45
MW	75	25	-

Fabric Concrete beam

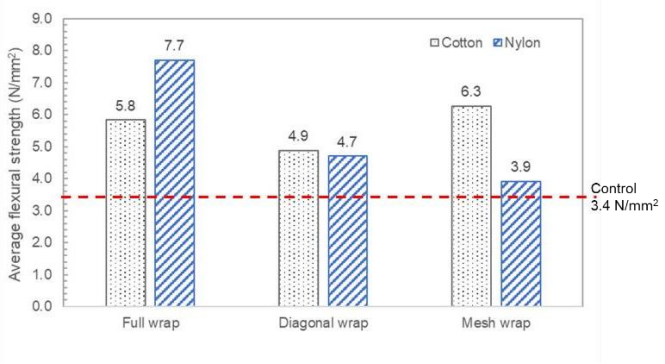

(a)

(b)

Figure 1: Beamlet samples reinforced with TWC (a) flexural strength (b) crack growth resistance

The result shows that all reinforced samples with TWC showed flexural strength increment compared to the control sample as shown in Figure 1a. The optimum configuration for TWC nylon was full wrapping with increments up to 126% followed by diagonal wrapping (38%) and mesh wrapping (14%). For the TWC cotton, mesh wrapping configuration improved approximately 85% of the flexural strength followed by full wrapping (70%) and diagonal wrapping (44%). The installation of TWC also resists the crack growth within the concrete beamlets (see Figure 1b).

Plain concrete beamlets reinforced with TWC showed promising results with significant improvement in flexural strength and has a good ability to resist crack growth of the samples. Further investigation is required on the development of good bonds between the TWC material and concrete substrates.

SUSTAINABLE ALTERNATIVE MATERIALS IN BUILDING CONSTRUCTION

Khan Shahzada

Department of Civil Engineering, University of Engineering and Technology Peshawar, Pakistan.
khanshahzada@uetpeshawar.edu.pk

The construction industry faces immense challenges as it seeks to balance sustainability, cost-effectiveness, and the need for seismic resilience in building structures. This study discusses alternate building materials, focusing most on the context of Dry Stacked Block Masonry (DSBM), Fly Ash Brick Masonry, Rammed Earth Construction and Marble wastes as sustainable options. Such materials not only improve the structural efficiency but also help in environmental sustainability by low carbon footprints and resource conservation.

This abstract presents an overview of research findings and practical applications related to these construction methods.

DSBM is an interlocking mortarless masonry technique using concrete blocks or Stabilized Earth Blocks (SEB). The absence of mortar in construction provides various benefits such as.
Water Savings: The process requires much less water to make, with negligible curing (*Bardhan, 2015).*
Reduced Carbon Emissions: SEB eliminates burning blocks and saves up to 89% of carbon dioxide emissions compared to conventional clay bricks *(Riza et al., 2010).*
.
Speed and Cost Efficiency: DSBM construction can be accomplished in around 30% less time and is over 25% cheaper than the general masonry *(Ramamurthy and Nambiar, 2004), (Ngowi, 2005).*
Three full-scale DSBM specimens, unconfined, confined, and retrofitted, were subjected to tests to demonstrate their seismic behavior. The confined and retrofitted DSBM specimens showed significant improvements in load-bearing capacities and displacement limits, making them viable for regions prone to seismic activity. Table 1 summarizes results of the DSBM structures (Gul et al, 2022).

Fly Ash Brick Masonry is an eco-friendly substitute to the regular clay bricks (figure 1). Fly ash, being a by-product of the coal combustion process, is used to make environment-friendly bricks. The advantages of this material are:

Waste Utilization: Fly ash bricks utilize fly ash formed in an industrial process by reducing its landfilling.
Energy Efficiency: Such bricks are built using lesser amounts of energy than usual bricks. In other words, the entire process is eco-friendly.

Rammed Earth and Mud Structures are one of the eco-friendly as well as low-cost building resources, particularly for rural or developing areas. These structures are constructed using locally sourced materials, reducing transportation costs and environmental impact. Mud buildings have notable advantages including excellent moisture and noise control, along with being naturally fireproof. Furthermore, research shows that bamboo strips and dried jute threads can be used as reinforcing elements in these structures (Aizaz et al., 2024).

Marble waste is the by-product of marble processing industries, creating severe environmental problems. The collection of slurry and waste material hampers the ecology of the area. However, the research conducted in UET Peshawar has used marble waste in the production of bricks (figure 2). Marble waste bricks properly mixed and sun dried can offer a sustainable alternative to conventional construction materials while solving the problems of waste management (Zeeshan et al, 2021 and Adeel et al., 2023).

Table 1: Summary of Quasi-Static Test Results for DSBM Structures (Gul et al., 2022)

Structure Type	Maximum Load (kN)	Displacement (mm)	Drift (%)	Ductility	R-factor
Unconfined DSBM	96.17	16.43	0.49	2.02	1.75
Confined DSBM	148.63	62.00	1.85	7.57	3.76
Retrofitted DSBM	210.81	34.00	1.03	18.59	6.01

Figure 1. Fly ash brick masonry

Figure 2. Marble waste bricks

Development of materials such as DSBM, Fly Ash Bricks, Rammed Earth/Mud structures, and recycled Marble Wastes shows a very bright future for the construction sector. These materials are enhancing the

seismic resistances of structures besides reducing costs, and they are adding greatly to the reduction of overall environmental impacts. Rammed Earth and Mud structures embedded with bamboo or jute provide very robust cost-effective solutions for rural and earthquake-prone areas. Research on marble waste utilization highlights the potential for turning industrial by-products into viable construction materials. As the industry progresses towards more sustainable practices, the integration of these materials can significantly reduce carbon emissions, water usage, and energy demands, providing a path towards environmentally responsible and affordable construction. However, research and innovation are needed for better optimization of these technologies and wide application.

CHALLENGES AND SOLUTIONS FOR THE SUSTAINABLE GROUNDWATER MANAGEMENT IN PAKISTAN

Khan Zaib Jadoon

Department of Civil Engineering, International Islamic University, Islamabad 44000, Pakistan.
khanzaibjadoon@gmail.com

Groundwater has provided a reliable source of high-quality water for human use. Rapid population and economic growth, urbanization, and unsustainable consumption of groundwater in domestic, industrial, and agricultural sectors have aggravated water scarcity in different regions of the World. After India, China and USA, Pakistan is the fourth largest groundwater user in the world and around $60x10^9$ m^3 volume of groundwater is extracted annually. However, in Pakistan the annual rate of groundwater recharge is around $40\text{-}55x10^9$ m^3, which is less than the extracted water and results in continuous groundwater depletion. Such prolonged overexploitation of groundwater has raised concerns about the sustainability of groundwater resources in the region. In Pakistan, 80% of groundwater exploitation is by the private sector and there is no control or restriction on its abstraction. Landowners can install tube wells at any location in their land and extract unspecified amount of water at any time without considering its impact on the groundwater resources. As a result, water table depletes, and wells are getting out of production or groundwater pumping gets more expensive from deeper wells.

In agriculture, traditionally rotation base approach is used in Pakistan to provide share of irrigation water to the farmers and homogeneous irrigation is applied over the entire field. Homogeneous irrigation of the entire field might not be resource efficient at all, because some parts might be irrigated which do not necessarily need irrigation water, while others might not be irrigated enough for optimal crop growth. As a consequence, too many resources might be used in terms of irrigation water and energy for pumping. The challenges in sustainable and resource efficient irrigation system are manifold. First, the underlying heterogeneity of the field has to be known. Second, the influence of these subsurface heterogeneities on the water balance and crop growth has to be known, and third, the irrigation system has to be adapted in a way that only those areas are irrigated which do need additional water.

Domestically maintaining a perfect equilibrium between the society water demands and water supplies is of vital importance for sustainable water resources management. Due to rapidly increasing water demand in urban and rural areas, the easy solution is to increase water supply, which have largely elapsed. However, domestically water usage by the people is taken almost for granted. Only when there is an acute shortage, is the true value of water and efficient management realized. Furthermore, flat rate water billing is applied in urban areas, which provokes waste of water as no incentive is given to those households which save water. On the one hand, in terms of future service expansion the policy of flat rate does not generate enough revenues and on the other hand in long-run this results in poor level of service for the entire community.

Over the last few decades, Pakistan has tried several strategies to manage the overexploitation of groundwater; however, finding a workable and viable solution remains a challenge. The overuse of groundwater in irrigation and domestic use is of major concern. Moreover, the key challenge in groundwater management for irrigation and domestic use is developing capacity to manage and monitor intensive groundwater use in our agricultural fields and urban centers. Pakistan's first National Water Policy has been approved in April 2018, stating that a new organization "Groundwater Authority" will be established in each province to design a regulatory framework and enforce standards for the development and utilization of groundwater resources (table 1).

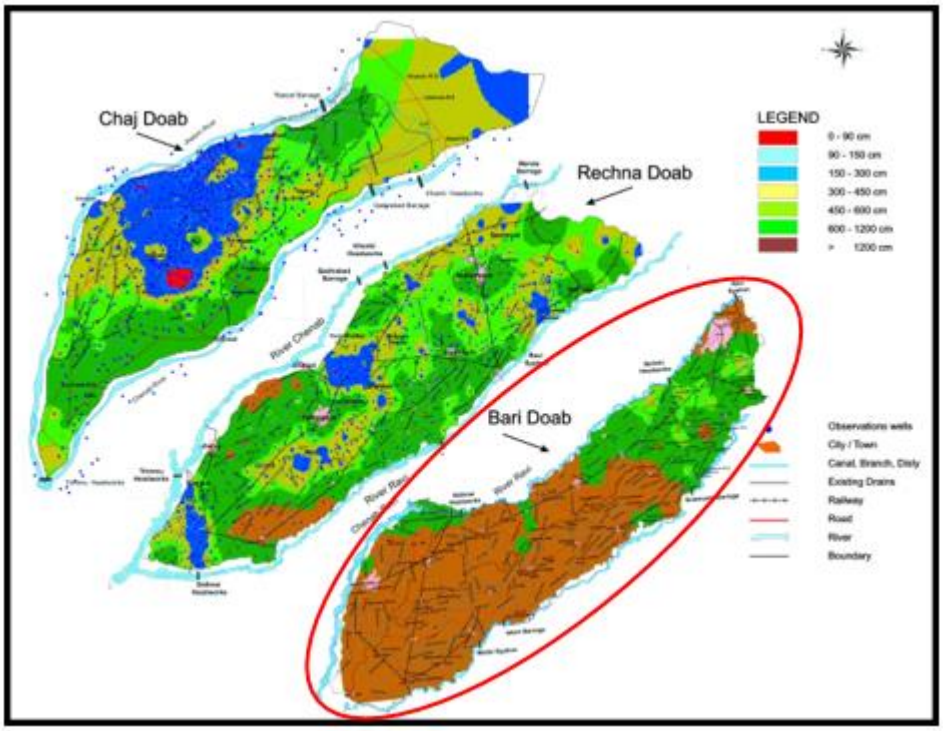

Figure 1. Smart Ground Water Monitoring Field Deployment and Measurements

Table 1. Strategic Priorities of National Water Policy 2018

Priority	Strategy
Groundwater Authorities	Provincial governments shall establish groundwater authority to enforce legislation and take regulatory measures.
Groundwater Management	Groundwater management to determine sustainable groundwater potential and prepare groundwater budgets for sub-basins
Groundwater recharge	Artificial groundwater recharge shall be promoted wherever technically and economically feasible.
Groundwater Table	Groundwater table shall be so managed that it does not impede crop growth or causes land salinity or underground saltwater intrusion.
Capacity Building	Capacity building of Water Sector Institutions at the Federal and Provincial level.

To overcome aforementioned challenges in the sustainable groundwater management in agriculture and domestic sectors of Pakistan, there is dire need of capacity building of stakeholders (groundwater users, water management authorities and research institutions) to develop a better understanding of demands and utilization of the groundwater resources. Workshops and training sessions with the farmers and communities can be arranged, which can be focus on the techniques used for water conservation and methods used for artificial groundwater recharge. There is dire need to provide professional development opportunities for the experts of water management authorities (Irrigation Department, Public Health Engineering Department, and Water Management Department etc.,) that should be targeted to improve the basic understanding of surface and groundwater hydrology, conceptual models for prediction of water flows, and enforcement of the developed regulations for groundwater management. Training can be arranged pertaining to the use of remote sensing, Geographic Information Systems (GIS), and data analytics to improve the understanding, monitoring and management of groundwater. Research institutions have to come forward to build low-cost indigenous

solutions and technologies to monitor the real-time groundwater usage, storage, recharge and depletion for sustainable groundwater management. Moreover, research institutions can develop applied interdisciplinary courses and tutorial modules related to sustainable groundwater management, which will help to fill the gap between the academia and practitioners.

Digital platforms have to be developed where stakeholders can share data for sustainable groundwater management. The end users can share the data pertaining to the groundwater utilized and current status of groundwater quality and levels in the area. Water management authorities can provide access to the real-time groundwater data to the other stakeholders to improve interpretation and decision-making. Research institutions have to provide open access to their latest research related to groundwater trends in the region, future predictions, innovation in technology and policy recommendations pertaining to the sustainable groundwater management. Digital platforms can be help to improve the stakeholder networking and collaborations to get social benefits (promote equity among groundwater users), economic benefits (optimize pumping, which reduces energy cost) and technical benefits (better estimates of water abstraction) for sustainable groundwater management. Digital platforms will help the water management authorities to strengthen regulatory frameworks by enforcing policies related to water rights, prior permission to install wells in specific locations, limits of groundwater withdrawal for sustainability of the aquifer. Research institutions and water management authorities can utilize the data shared on digital platform for climate-resilient water and drought management plan that prioritize groundwater conservation during periods of water scarcity.

In an attempt to address the aforementioned challenges in groundwater management, an innovative approach has been undertaken in collaboration with SCARP Monitoring Organization (SMO) of Water and Power Development Authority (WAPDA), to develop a low-cost smart groundwater monitoring system (SGMS), to monitor real-time groundwater depletion and couple measured data with Gravity Recovery and Climate Experiment (GRACE) satellite mission data to precisely estimate groundwater storage depletion at regional scale. The newly developed SGMS is tested and calibrated in the Department of Civil Engineering, International Islamic University, Islamabad, before deployment in the Bari Doab. The collected in-situ observations and GRACE data was downscale both spatially (from 0.25° × 0.25° to 0.01° × 0.01°) and temporally (from monthly to daily time scale) by using the two-stage machine learning algorithm (Boosted Regression Tree, BRT). The smart groundwater monitoring system provided in-situ real-time groundwater measurement at high special and temporal resolution (figure 1). Furthermore, in-situ and remote sensing data was used as an input data for groundwater simulator MODFLOW (i.e., GMS) to infer groundwater flow dynamics for at a local scale with daily temporal resolution. The proposed solution enables groundwater researchers and decision makers to have real-time access to the groundwater data and models with less cost and effort for sustainable groundwater management. Furthermore, the SGMS was installed in the aquifer recharge wells to access the impact of surface water recharge on the water levels in the recharge wells in real-time. The newly developed and tested smart groundwater monitoring system can be easily adapted to other locations of Pakistan for sustainable groundwater management to save water for the generations to come.

Authors' Papers

PERFORMANCE OF CONCRETE CONTAINING STEEL WASTE FIBERS

[a] Muhammad Fiaz Tahir*, [b] Mehar Ali

a: Department of Civil Engineering, University of Engineering and Technology, Taxila, Pakistan, fiaz.tahir@uettaxila.edu.pk
b: Department of Civil Engineering, University of Engineering and Technology, Taxila, Pakistan, meharaliali25@gmail.com
* Corresponding author.

Abstract- Concrete's mechanical properties are significantly influenced by the addition of steel waste fibers. This study investigates the impact of varying dosages of steel waste fibers on the performance of concrete cube specimens. Compression strength tests on cubes reveal a 39% increase in maximum strength when 1% steel waste is added, attributed to improved bonding between steel waste and the concrete matrix. However, it was concluded that higher dosages lead to fiber clustering and inadequate bonding, causing non-uniform distribution and localized stress concentrations, resulting in a modest loss in compressive strength. This study provides valuable insights into how different dosages of steel waste affect the mechanical properties of concrete, informing sustainable building practices and waste management strategies.

Keywords- Concrete, Mechanical Properties, Steel Waste, Sustainable Construction.

1 Introduction

This research explores the mechanical properties of high-strength concrete reinforced with fibers, aiming to mitigate crack formation and enhance overall mechanical performance for practical applications. The introduction of steel fibers significantly improves concrete's ability to withstand tension, leading to the development of steel fiber reinforced concrete (SFRC) [1]. Studies have shown that incorporating steel waste fibers into concrete enhances its mechanical properties, contributing to more durable and structurally robust constructions [2, 3]. Sustainable construction methods have increased interest in utilizing industrial waste materials in concrete. Steel waste fibers have shown promising results in improving concrete's mechanical properties, but further investigation is needed to determine their optimal concentration and impact on different concrete components [4].

During a past study program, it was concluded that the concrete's ductility and stiffness improved with the inclusion of steel scrap [5]. However, the study observed that with the increasing amount of metal scrap, the workability of the concrete decreased. This finding suggests that there is a trade-off between the improvement in strength properties and the ease of working with concrete. Despite the reduction in workability, the results highlight the potential benefits of incorporating steel scrap waste into concrete mixes to enhance its overall mechanical properties [1]. The authors used various percentages of steel scrap ranging from 0% to 1.5% by volume. A total of twelve cubic specimens and twelve-cylinder specimens were prepared and subjected to laboratory testing after 28 days of curing. The test results demonstrated that the addition of scrap steel had a positive impact on the concrete's compressive and split tensile strengths. Notably, the inclusion of 1.5% scrap steel by volume increased the compressive strength by 5.3%, 0.75% by volume led to a substantial increase of 30.7%, and 0.5% by volume resulted in a notable rise of 26.8%. Similarly, the splitting tensile strength of the concrete also showed improvement with the addition of scrap steel. At 0.5% by volume, the splitting tensile strength increased by 11.2%, at 0.75% by volume it rose by 5.8%, and at 1.5% by volume, there was a 2.5% increase in splitting tensile strength. Additionally, as the amount of scrap steel incorporated into the concrete increased, the peak strain and elasticity modulus of the material also noticeably rose. [1].

Aiello et al. conducted a study with the aim of exploring the mechanical behavior of concrete reinforced with recycled steel fibers (RSF) derived from used tire rubber through a mechanical process [6]. The researchers performed pull-out tests to evaluate the bonding characteristics between the concrete and RSF, enabling them to determine the optimal fiber length for reinforcement. Additionally, flexural tests were conducted to investigate the post-cracking behavior of the RSF-reinforced concrete (RSFRC). The study also examined the compressive strength of the concrete for different volume ratios of RSF and included samples reinforced with industrial steel fibers (ISF) for comparison. The findings revealed that the

bond between the recycled steel fibers and the concrete was satisfactory [7]. However, despite the uneven geometrical characteristics of the fibers, they did not seem to have a significant impact on the compressive strength of the concrete. Overall, the study demonstrates the potential viability of utilizing recycled steel fibers from used tire rubber as an alternative reinforcement in concrete. While the bonding characteristics were satisfactory and the compressive strength was not significantly affected, the post-cracking behavior may differ from that of concrete reinforced with industrial steel fibers. These findings provide valuable insights into the mechanical performance of RSF-reinforced concrete and open new avenues for sustainable and eco-friendly practices in the construction industry. In this study program experiments were planned to evaluate the enhancement in mechanical properties of concrete and its cracking behavior. This study aims at exploring the mechanical properties of concrete through (a) Preparation of control mix for cubes, (b) Varying the dosages of steel waste fibers in the mix, (c) Performing strength tests on cubes.

Fiber reinforced concrete has various applications in civil infrastructure projects, offering greater durability and reduced maintenance [2, 8, 9]. The study reveals that fibers improve the strength and durability however, achieving uniform distribution of fibers throughout the concrete mix is crucial for its effectiveness[10, 11].This study investigates optimal dosages of steel waste fibers and their impact on concrete. Unlike previous studies, it compares varying fiber concentrations with industrial steel fibers, offering insights into sustainable construction. The findings demonstrate how specific dosages enhance concrete performance, supporting eco-friendly construction practices.

2 Research Methodology

In this study twelve specimens were tested. The specimen nomenclature was decided according to percentage of fibers and is elaborated in Table 1.

Table 1: Nomenclature of cube specimen

Sr. No.	Specimen ID	Mix Proportion	W/C Ratio	Steel Fibers Percentage (w.r.t binder)
1	CN (1)	1:1:2	0.45	0 %
2	CN (2)	1:1:2	0.45	0 %
3	CN (3)	1:1:2	0.45	0 %
4	C1 (1)	1:1:2	0.45	1%
5	C1 (2)	1:1:2	0.45	1%
6	C1 (3)	1:1:2	0.45	1%
7	C2 (1)	1:1:2	0.45	2%
8	C2 (2)	1:1:2	0.45	2 %
9	C2 (3)	1:1:2	0.45	2 %
10	C3 (1)	1:1:2	0.45	3 %
11	C3 (2)	1:1:2	0.45	3 %
12	C3 (3)	1:1:2	0.45	3 %

2.1 Material and Methods

In this study it was ensured that well graded coarse aggregate was used. The gradation curve of the coarse aggregates is s shown in Figure 1. The sand used in the mix was the Lawrencepur sand. The gradation curve of fine aggregates is shown in Figure 2.

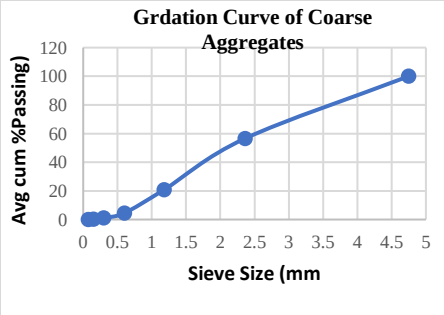

Figure 1: Gradation Curve of coarse aggregate.

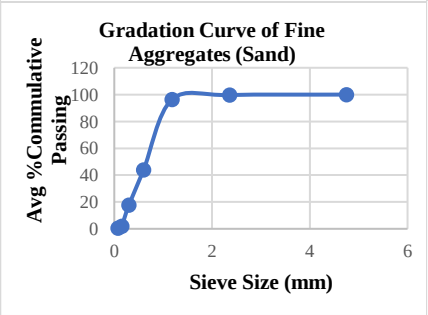

Figure 2: Gradation curve of fine aggregate

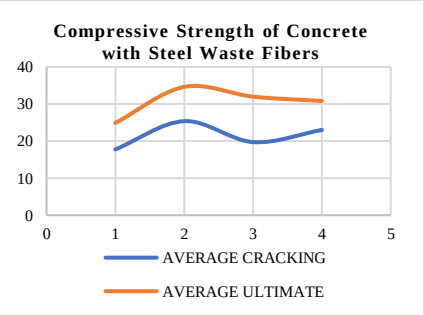

Figure 3: Compressive Strength of Concrete with steel waste fibers

The steel chips (SC) or fibers (SF) Utilized in this study was obtained by the process of recycling old and waste steel found in the local market of Taxila at cheap rates. Results show the gradation curve of steel waste fiber is well graded. The mixer has capacity greater than one cubic yard and set according to ASTM C94/C94 M-21 [12] minimum revolution of 100 and mixing time range 1-5 minutes after putting water, cubes having size of 70 x 70 x 70 mm are used. The twelve cubes were cast having three cubes of normal mix, three containing 1%, three containing 2% and three containing 3% steel waste of binder material respectively. We used the mixed ratio of cement, sand, and coarse aggregate as 1:1:2. The water cement ratio used is 0.45. The water used during the casting process is drinkable water.

2.2 Procedure of Testing

One of concrete's most important qualities is its compressive strength because it reflects the material's overall effectiveness. On cube specimens of 70 mm x 70 mm x 70 mm, a compressive test was performed in a CTM machine with a 5000 kN capacity. As per ASTM C39, the machine's loading rate is between 20 and 50 psi, or 2.5 and 6.5 kN in our Specimens. The test was carried out on a cube containing three specimens of the control mixture, three specimens of 1% steel waste, three specimens of 2% steel waste, and three specimens of 3% steel waste. The 12 cubes were tested in the on the Compression Testing Machine in the concrete laboratory of UET Taxila. All specimens of control mix and specimens of waste were tested. The first cracking and ultimate cracking load on the cube is noted.

3 Results & Discussion

During the test cracking strength, ultimate strength, average cracking, and average ultimate strength of cube specimens were recorded and is presented in Table 2.

Table 2: Compressive strength test results

Cube	Cracking Load (Kn)	Ultimate Load (Kn)	Area (Mm2)	Cracking Strength (Mpa)	Ultimate Strength (Mpa)	Average Cracking	Average Ultimate
CN (1)	125	143	4900	25.51	29.18	17.75	24.89
CN (2)	82	112	4900	16.73	22.85		
CN (3)	54	111	4900	11.020	22.65		
C1 (1)	98	158	4899	20.004	32.25	25.37	34.62
C1 (2)	164	164	4900	33.469	33.46		
C1 (3)	111	187	4900	22.653	38.16		
C2(1)	99	135	4863.5	20.35	27.75	19.71	31.97
C2 (2)	83	227	4900	16.93	46.32		
C2 (3)	107	107	4900	21.83	21.83		
C3 (1)	128	154	4900	26.122	31.42	22.99	30.81
C3 (2)	92	144	4900	18.775	29.38		
C3 (3)	118	155	4900	24.081	31.63		

The compressive strength of cube having control mix is obtained almost 25 MPa which is the ultimate compressive strength of concrete having mix ratio of 1:1:2 after 28 days. The ultimate compressive strength of cube containing 1% waste is increased by 39% and is increased by 28% by adding 2% steel waste and is increased by 23% by adding 3% steel waste as compared to the control mix. The Cubes show a maximum strength at 1% dosage of steel waste. However, by further adding of steel waste dosage (beyond 1%) the compressive strength is slightly decreased. The maximum compressive strength achieved at 1% dosage which is 39% greater than the control mix. The experimental results of Akhtar Gul [13] also point to the concrete losing compressive strength when steel waste is added in large quantities. One percent waste has a compressive strength that is higher than the control mix, whereas two percent waste has a compressive strength that is slightly lower than one percent waste's and higher than the control mix. The higher dosage of waste reduced the strength of concrete due to the loss in the workability and balling effect. The strength up to a certain limit is increased due to the bridging action of the fibers with the concrete matrix. Individually the minimum compressive strength shown by specimen C2 (3) and maximum is achieved by C2 (2) which is 46.32 MPa. The 3 specimens of each dose are tested and then taken the average of these. The overall maximum strength is achieved by the sample containing 1% steel waste. The maximum

cracking strength is shown by specimen C1(2) which is 33.469 MPa that is mentioned above in table no.1. The minimum cracking strength is shown by the specimen CN (3) which is almost 11 MPa. The average cracking strength is also increased up to the dosage of 1% and decreased by adding more dosage of the waste in the specimens due to the same reason that is mentioned above. Figure 3 shows that both the average cracking and ultimate compressive strengths of concrete initially increase with the addition of steel waste fibers, peaking at 1% fiber content. Beyond this point, the strengths decrease, indicating a diminishing return as fiber content increases. Specifically, the highest ultimate compressive strength is achieved at 1%, with subsequent additions leading to a decline, suggesting that 1% steel waste fiber is optimal for enhancing concrete strength.

4 Conclusion

In conclusion, the addition of steel scrap fibers significantly improves the compressive strength of concrete. The concrete cubes with 1% steel waste showed a 39% increase in strength, those with 2% showed a 28% increase, and those with 3% showed a 24% increase. The optimal strength was achieved with 1% steel waste, but higher dosages decreased workability and strength. These findings highlight the importance of precise dosage optimization for enhancing mechanical properties and support sustainable construction practices.

Acknowledgment

The authors would like to extend their gratitude to Engr. Arslan Akbar, Engr. M. Safeer, Engr. Allah Wasaya and Civil Engineering Department UET Taxila.

References

[1] Y. W. Shewalul, "Experimental study of the effect of waste steel scrap as reinforcing material on the mechanical properties of concrete," *Case Studies in Construction Materials*, vol. 14, p. e00490, 2021.

[2] F. Althoey and M. A. Hosen, "Physical and mechanical characteristics of sustainable concrete comprising industrial waste materials as a replacement of conventional aggregate," *Sustainability*, vol. 13, no. 8, p. 4306, 2021.

[3] C. Wu, Y. Shi, J. Xu, M. Luo, Y. Lu, and D. Zhu, "Experimental Study of Mechanical Properties and Theoretical Models for Recycled Fine and Coarse Aggregate Concrete with Steel Fibers," *Materials*, vol. 17, p. 2933, 06/15 2024, doi: 10.3390/ma17122933.

[4] A. Caggiano, P. Folino, C. Lima, E. Martinelli, and M. Pepe, "On the mechanical response of hybrid fiber reinforced concrete with recycled and industrial steel fibers," *Construction and Building Materials*, vol. 147, pp. 286-295, 2017.

[5] S. H. L. S. H. Song, and J. H. Bae, "Effect of steel fiber reinforcement on the mechanical properties of high-strength concrete," *Construction and Building Materials*, vol. vol. 93, 2015.

[6] M. A. Aiello, F. Leuzzi, G. Centonze, and A. Maffezzoli, "Use of steel fibres recovered from waste tyres as reinforcement in concrete: Pull-out behaviour, compressive and flexural strength," *Waste management*, vol. 29, no. 6, pp. 1960-1970 Page 11, 2009.

[7] A. K. S. K. Singh, and S. Sharma, "Experimental investigation of compressive strength of concrete containing recycled steel fibers," *Journal of Materials in Civil Engineering, ,* vol. vol. 32, no. 6, p. 04020100,, 2020.

[8] A. E. Naaman, "Engineered steel fibers with optimal properties for reinforcement of cement composites," *Journal of advanced concrete technology*, vol. 1, no. 3, pp. 241-252, 2003.

[9] A. A.-D. a. S. Mahmood, "Impact of steel fiber reinforcement on the mechanical properties of concrete," *International Journal of Civil Engineering*, vol. vol. 9, no. 3, pp. 243-252, 2011.

[10] M. N. a. N. Khan, "Effect of fiber distribution on the mechanical properties of fiber reinforced concrete,," *Construction and Building Materials*, vol. vol. 23, no. 8, pp. 2873-2883, , 2009.

[11] H. W. H. Zhang, and W. Zhang, "Experimental study on the mechanical properties of concrete with waste steel fibers," *Advances in Civil Engineering,*, vol. vol. 2021, 2021, Art no. 8853657, 2021.

[12] *ASTM C94/C94M − 21*, ASTM.

[13] A. Gul *et al.*, "Impact of length and percent dosage of recycled steel fibers on the mechanical properties of concrete," *Civil Engineering Journal (Iran)*, vol. 7, no. 10, pp. 1650-1666, 2021.

MECHANICAL AND PERMEATION PROPERTIES OF CONCRETE USING INDIGENOUS VOLCANIC ASH AS PARTIAL REPLACEMENT OF CEMENT

[a] Munawar Hussain*, [b] Ayub Elahi

a: Department of Civil Engineering, University of Engineering and Technology, Taxila, Pakistan. sm65rb@gmail.com
b: Department of Civil Engineering, University of Engineering and Technology, Taxila, Pakistan. ayub.elahi@uettaxila.edu.pk
* Corresponding author.

Abstract- The current study aims to examine the effects of indigenous Volcanic Ash (VA) on mechanical and permeation properties of concrete upon partial substitution of Ordinary Portland Cement (OPC). The study further aims to search out the most probable benefits and the constraints of use of VA in concrete mixes as partial replacement of cement. The VA has been used as partial replacement as percentage of Binder (with ratios as 0% (the Control Mix), 5%, 10%, 15%, 20%, 25%, 30%, 35% and 40% of Binder) to examine the impacts on mechanical and permeation properties of concrete. The W/B ratio (0.5) was kept the same for all the mixes. Slump Test was also performed to determine the workability of concrete for each above-mentioned ratio of VA. It was found that increasing the ratio of VA content in concrete reduced workability. The ideal concrete mix is known to have a 10% VA component in place of cement since it meets the requirements for both the Control Mix's mechanical and permeation qualities.

Keywords- Indigenous Volcanic Ash, Workability, Compressive Strength, Splitting Tensile Strength, Water Absorption, Permeability.

1. Introduction

Over the past few decades, the construction industry has significantly contributed to urbanization and industrialization. Construction activities produce approximately 30% of waste and 40% of CO_2 emissions. The manufacture of hydraulic cement alone contributes to roughly 7-9% of the total global carbon dioxide emissions [1]. Cement factories account for approximately five percent of the world's carbon dioxide emissions. We can reduce CO_2 emissions in construction by using alternative cementitious materials instead of traditional cement. To protect the environment, regulate waste, enhance air quality, and preserve ecological integrity, the construction sector needs to incorporate sustainability. Several scholars have examined the use of volcanic ash (VA) in mixed cement [2]. Across the globe, over 50 nations yield volcanic ash (VA) and its associated products, such as pumice, in significant quantities. Italy stands out as one of the foremost producers of volcanic ash materials [3][4]. Other notable producers include Chile, Canada, Spain, Turkey, and the United States. Volcanic ash has been extensively researched as a potential substitute for cement, tested at varying proportions ranging from 0% to 20% [5][6]. The findings indicate that incorporating volcanic ash as a cement alternative enhances compressive strength [7]. Volcanic Ash (VA), a natural pozzolanic material abundant in Pakistan, is a potential candidate. This research aims to assess the impact of using VA as a partial replacement for cement on the mechanical and permeability properties of concrete, while also considering the potential cost benefits. This research aims to develop an eco-friendly and cost-effective concrete by partially replacing cement with a natural pozzolanic material, Volcanic Ash (VA), readily available in Pakistan. The primary goal is to investigate the influence of VA on the mechanical properties and durability properties of the concrete.

2. Research Methodology

2.1 Materials

In the study under consideration, locally manufactured Ordinary Portland Cement has been used that met the required ASTM C-150 Type-1 (Normal) [8]. The indigenous VA has been used obtained from the source situated in Chilas (Gilgit Baltistan), Pakistan. This investigation utilized naturally sourced coarse sand from the Lawrancepur quarry as the fine

aggregate (FA) in the concrete blends. Moreover, well-graded granite crushed aggregate from Margalla Hills served as the coarse aggregate. Various tests were conducted to assess different properties of the concrete. Workability was evaluated following ASTM C-143 standards [9], compressive strength was measured in accordance with ASTM C-39 [10], splitting tensile strength was assessed per ASTM C-496 guidelines [11], permeability testing followed IS-3085 standards, and water absorption testing was conducted as per ASTM C-642 [13].

2.2. Mix Proportioning

The mix proportioning for the various concrete mixes is given below in Table 1. The samples were cured for 28 days under ambient temperature.

Table 1: Concrete Mix Proportions

Mixes	OPC (Kg/m^3)	VA (Kg/m^3)	Water (L/m^3)	FA (Kg/m^3)	CA (Kg/m^3)
Control Mix i.e. VA-00	320	0	160	640	1280
VA-05	304	16	160	640	1280
VA-10	288	32	160	640	1280
VA-15	272	48	160	640	1280
VA-20	256	64	160	640	1280
VA-25	240	80	160	640	1280
VA-30	224	96	160	640	1280
VA-35	208	112	160	640	1280
VA-40	192	128	160	640	1280

3. Results and Discussions

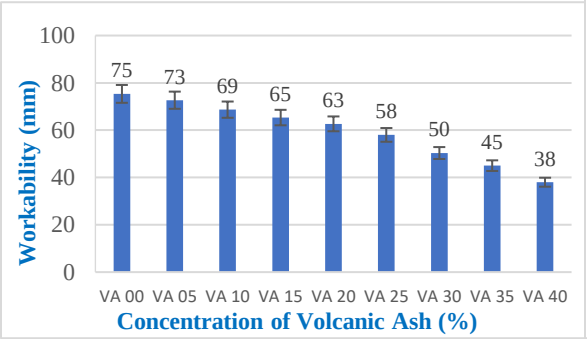

Figure 1: Workability Results of Concrete Mixes

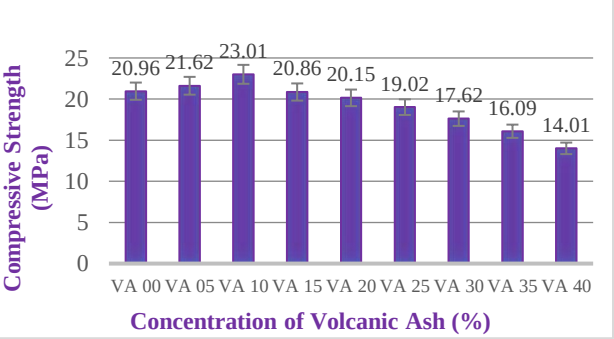

Figure 2: Compressive Strength Results of Concrete Mixes

3.1. Workability Test

It is clear from the graphical representation workability results in Figure 1 that it has decreased with the increased concentrations of the VA in the concrete. VA-40 has slump as 38 mm which is nearly 49% less than that of control mix concrete. It may be said that workability of fresh concrete decreases by increasing the concentration of the VA in the same that is most likely due to that the VA had smaller particle size and higher value of fineness making it more absorbable upon addition of water.

3.2. Compressive Strength Test

The compressive strength results have been represented in the Figure 2. Upon addition of VA, at first the compressive strength increases but then tends to decrease. The maximum compressive strength of concrete is with VA-10 (nearly 9.8% more than that of VA-00). Exothermic chemical reaction beween cement and water produces C-S-H gel, a cemetious compound and C-H, a non-cementious one. When VA is added, it reacts with C-H resulting into production of cemetious compounds in addition which ipmroves the strength upto VA-10 as compare to VA-00. Further increase in concentration of VA, will result in decrease in the strength as excessive quantity of VA beyound requirements of produced C-H will act

as only a non cemetious fine agrregates like sand. It may also be because of enhanced substitution of cement with VA, lowering the cementious proportions in the mix [14].

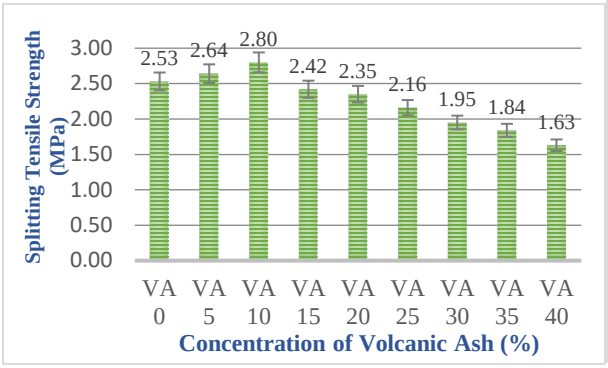

Figure 3: Spilitting Tensile Strength Results of Concrete Mixes

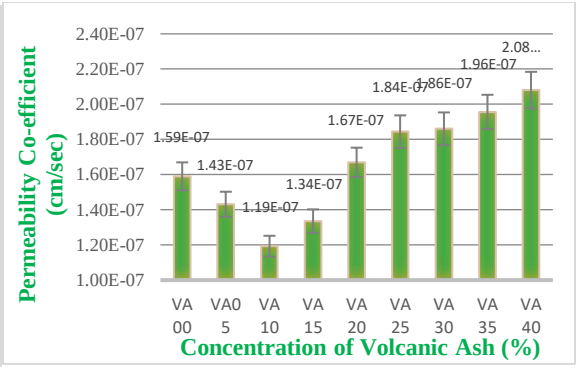

Figure 4: Permeability Test Results of Concrete Mixes

3.3 Splitting Tensile Strength Test

The obtained results for splitting tensile strength have been represented in the Figure 3. Once the VA is added to the concrete, at first the spilitting tensile strength of the concrete increases but then tends to fall down. The maximum value was obtained for the Mix VA-10 (nearly 9.6% more than that of VA-00). The values of tensile strength of concrete are more than that of VA-00 with the concentrations of VA-05 and VA-10 whereas the values of tensile strength are less than that of control mix having concentrations of VA-15 or higher. It could be due to the chemical reaction of SiO_2 in VA with C-H. As a result, the amount of C-H reduced while C-S-H increased, improving the splitting tensile strength of concrete. As IVA increases from 15% to 40%, the splitting tensile strength of concrete decreases. It could be because replacing cement with IVA decreases the cement content of the mix [15].

3.4 Permeability of Concrete

The obtained results for permeability of concrete have been represented in the Figure 4. When VA is added to the concrete, at first the permeability of the concrete decreases but then tends to rise after having the lowest value at VA-10. The minimum said preamability of concrete is with the concentration of VA-10 (nearly 25% more than that of Control Mix). However, due to further increased concentration beyond VA-15, high porosity of VA due to its fine particles results in overall porosity of the Concrete i.e., resulting into increased Permeability as compare to that of VA 10.

3.5 Water Absorption Test

Figure 5 illustrates the water absorption outcomes for various concrete blends. Upon the addition of volcanic ash to the concrete mixtures, there is initially a decline in water absorption. However, this trend shifts after reaching its minimum at VA-10, with water absorption tending to increase thereafter.The minium said water absorption is with the concentration of VA-10. However, due to further increased concentration beyond VA-15, high porosity of VA due to its fine particles results in overall porosity of the concrete.

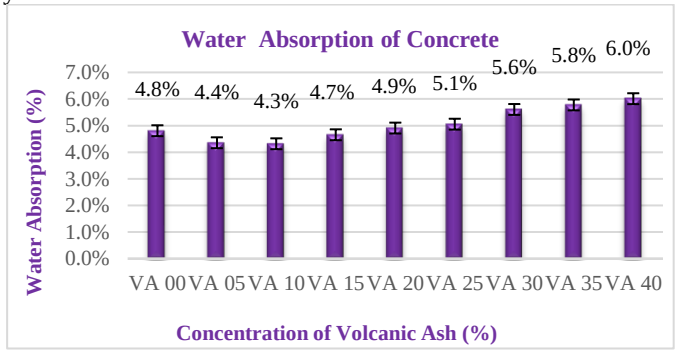

Figure 5: Water Absorption Results of Various Concrete Mixes

4. Conclusions and Recommendations

This comprehensive study on cement replacement in concrete yields several key findings:

- The slump value of Concrete VA-40 is approximately 50% lower than that of the Control Mix Concrete (VA-00).
- The compressive strength of Concrete VA-10 at 28 days exhibits the highest value, with an increase of nearly 9.8% compared to the Control Mix (VA-00).
- Similarly, the splitting tensile strength of Concrete VA-10 at 28 days achieves the maximum value, showing an improvement of approximately 10.7% over the Control Mix Concrete (VA-00).
- Concrete VA-10 demonstrates the lowest coefficient of permeability at 28 days.
- Moreover, the water absorption of Concrete VA-10 at 28 days records the lowest value among the studied mixes.

A few recommendations based on the same, are stated as under:

- It is advisable to work on other properties like Shrinkage Analysis and Toughness Testing of Concrete using VA as SCM would provide valuable insights.
- Study on Bricks made from the Concrete using VA as SCM as well as partial use of VA in making Bricks conventionally.

5. Acknowledgements

I am very much thankful to Mr. Hassan Akhtar and Chaudhary Hassan Nisar for their kind support in this research work at the Concrete Technology Lab in the Department of Civil Engineering, University of Engineering and Technology, Taxila.

References

[1] Worrell, E., et al., Carbon dioxide emissions from the global cement industry. Annual review of energy and the environment, 2001. 26(1): p. 303- 329.
[2] Mehta, P.K., Greening of the concrete industry for sustainable development. Concrete international, 2002. 24(7): p. 23-28.
[3] Kupwade-Patil, K., et al., Use of silica fume and natural volcanic ash as a replacement to Portland cement: Micro and pore structural investigation using NMR, XRD, FTIR and X-ray microtomography. Construction and Building Materials, 2018. 158: p. 574-590. 16.
[4] Kupwade-Patil, K., et al., Impact of Embodied Energy on materials/buildings with partial replacement of ordinary Portland Cement (OPC) by natural Pozzolanic Volcanic Ash. Journal of cleaner production, 2018. 177: p. 547-554.
[5] Zeyad, A.M., B.A. Tayeh, and M.O. Yusuf, Strength and transport characteristics of volcanic pumice powder based high strength concrete. Construction and Building Materials, 2019. 216: p. 314-324. 47.
[6] Presa, L., et al., Volcanic Ash from the Island of La Palma, Spain: An Experimental Study to Establish Their Properties as Pozzolans. Processes, 2023. 11(3): p. 657.
[7] Liu, J.-C., et al., High-performance green concrete with high-volume natural pozzolan: Mechanical, carbon emission and cost analysis. Journal of Building Engineering, 2023. 68: p. 106087.
[8] Anon. 2019. Standard Specification for Portland Cement C150/C150M.
[9] "ASTM C143 Standard Test Method for Slump of Hydraulic-Cement Concrete".
[10] "ASTM C39 Standard Test Method for Compressive Strength of Cylindrical Concrete Specimens"
[11] "ASTM C496 Standard Test Method for Splitting Tensile Strength of Cylindrical Concrete Specimens".
[12] "ASTM C642-06 Standard Test Method for Density, Absorption, and Voids in Hardened Concrete".
[13] "IS 3085: Method of test for permeability of cement mortar and concrete"
[14] Mohamad, Safaa A., Rwayda Kh S. Al-Hamd, and Teba Tariq Khaled. 2020. "Investigating the Effect of Elevated Temperatures on the Properties of Mortar Produced with Volcanic Ash." Innovative Infrastructure Solutions 5 (1): 1–11.
[15] Anwar Hossain, Khandaker M. 2006. "High Strength Blended Cement Concrete Incorporating Volcanic Ash: Performance at High Temperatures." Cement and Concrete Composites 28 (6): 535–45.

PHYSICAL AND DURABILITY PROPERTIES OF STEEL SLAG PARTICLES FOR USE IN ROAD AND CONCRETE WORKS

[a]Ahmad Faraz, [b]Anwar Khitab*

a: Civil Engineering Department, Mirpur University of Science & Technology, Mirpur (AJK) Pakistan. ahmadujaas444@gmail.com
b: Civil Engineering Department, Mirpur University of Science & Technology, Mirpur (AJK) Pakistan. anwar.ce@must.edu.pk
*Corresponding author.

Abstract- This study aimed to assess the viability of steel slag as a substitute for natural coarse aggregates for road and concrete works. The slag aggregates underwent evaluation based on impact value, crushing strength, bulk density, abrasion value, and flakiness index. Concrete samples incorporating steel slag aggregates were then prepared and compared against those containing natural coarse aggregates in terms of physical and durability performance. For this investigation, a 1:2:4 (M15) concrete mix design was targeted. Results indicated that the slag aggregates exhibited an impact value of 29.5%, a bulk density of 1208 kg/m³, an elongation index of 10.8%, a crushing value of 31.3%, and a flakiness index of 10.95%. The prepared concrete samples demonstrated a water absorption rate of 4%, a Rebound number of 22, and a wet surface skid resistance of 56 on the British Pendulum scale. The findings suggest that steel slag aggregates hold promise as a viable alternative to natural aggregates in concrete production. This substitution offers several advantages, including the environmentally sound disposal of slag waste, the promotion of green concrete and road practices, and potential cost reductions in construction projects. These benefits align with the sustainable development goals outlined by the United Nations.

Keywords- Concrete, Performance, Road, Slag Aggregates.

1 Introduction

About 12 million tons of concrete are being used world widely every year for construction purposes. Natural aggregates for concrete are acquired from rocks and mountains. Excessive use of natural rock in construction is disrupting the naturally balanced environment of the world by introducing air pollution, earthquakes, and landslides due to bombarding, volcanic eruptions, and non-recoverable resources loss. Using steel slag instead of traditional coarse aggregate for construction would reduce pollution, unbalanced environment, cost of construction and ensure safe disposal of steel slag. Several studies are available on the use of steel slag for use in cementitious materials. Some important and recent studies are mentioned here. Sezer et al. used steel slag as a partial replacement for natural fine, and coarse aggregates. The slag had a higher density than the natural aggregates. This not only enhanced the density of concrete, but also decreased the strength. The strength loss was more prominent where, fine aggregates were replaced with the slag particles [1]. Lai et al. used steel slag in percentages from 0-80% as a partial replacement of natural coarse aggregates. The authors revealed that the optimum value for strength enhancement of concrete is 50% [2]. Nguyen et al. investigated the effect of steel slag as a full replacement of natural coarse aggregates on the compressive strength of concrete. The main objective of the research was to examine the effect of age on compressive strength of slag concrete. Three types of concrete samples were prepared. The effect of higher cement content and lower sand and steel slag contents were studied. The results demonstrated an increase in strength of slag concrete up to an age of one year [3]. Jalil et al. used steel slag as a partial replacement of cement for making green concrete. The results showed that the slag has little pozzolanic value and the strength drastically reduced with the increasing slag content [4]. This work is an extension of our previous research. The previous study showed that slag has no cementing or pozzolanic value. Therefore, in this study the slag was used as a 100% replacement of coarse aggregates for making an eco-friendly concrete. The novelty of the work lies in the fact that a complete chemical, physical and mechanical analysis of the slag was performed before deciding its suitability for concrete work. The previous studies while address the physical and chemical analysis did not focus of the mechanical properties of the slag. The prepared

samples were evaluated in terms of water absorption for durability, rebound number for strength and skid resistance for safety in concrete pavements.

2 Research Methodology

2.1 Materials

For this study, steel slag was sourced from a local steel factory and subsequently converted into aggregates through a crushing process. The waste slag and resulting aggregates are depicted in Figure 1. Specifically, aggregates passing through a 37.5 mm sieve and retained on a 9.5 mm sieve were selected for use as coarse aggregates in the experimentation. The concrete samples were prepared as per ASTM C31 specifications [5]. Two types of specimens were prepared for testing purposes, cylindrical and rectangular slabs. Rectangular slabs were specifically used for performing skid resistance test while the other tests were performed using concrete cylinders such as hardened density test, water absorption, acidic attack and Schmidt hammer test.

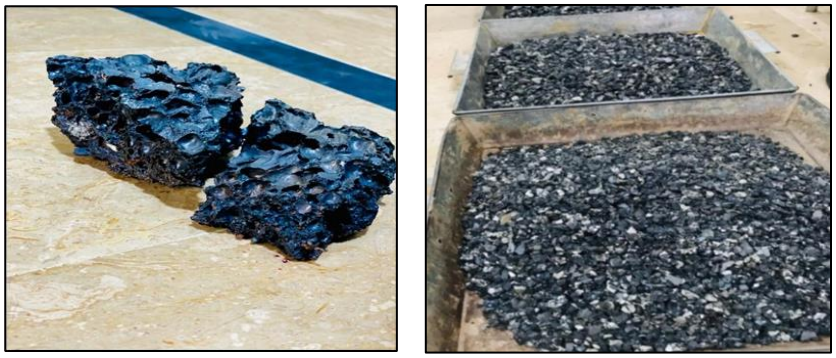

(a) (b)

Figure 1: Waste steel slag (a) raw form, (b) coarse aggregates.

2.2 Testing

The impact value of the aggregates was determined through D5874-16 method [6]. The elongation and flakiness indices were worked out through ASTM D4791-19 standards [7]. The crushing value was determined by ASTM D5821 standard method [8]. The abrasion value was determined by ASTM C131/C13M-14 [9]. The bulk density was determined by ASTM C29/C29-17 method [10]. Once the aggregate properties have been determined, the aggregates were mixed in a concrete mix 1:2:4 (M15). This is a common mix used for ordinary concrete works. Grade 53 OPC cement, Mangla reservoir sand, and tap water were used for making concrete. The hardened density, and water absorption were determined by ASTM C642-21 method [11]. The resistance to acid attack was measured through ASTM C1898-20 method [12], while the skid resistance and Schmidt rebound number were determined through ASTM E2340 2021[13] and ASTM C805/C805M-18 [14] respectively.

3 Results

3.1 Characterization of Slag Aggregates

The characteristics of the slag aggregates are compared with the natural limestone aggregates and the comparison is presented in Table 1.

Table 1: Comparison of characteristics of slag and natural aggregates

Sr. No.	Test on Aggregate	Natural Limestone Aggregate	Slag Aggregate
1	Impact value	13.20%	29.50%
2	Crushing strength	28.20%	31.35%
3	Bulk density	1601 kg/m^3	1369.8kg/m^3

Sr. No.	Test on Aggregate	Natural Limestone Aggregate	Slag Aggregate
4	Abrasion value	30%	34.28%
5	Flakiness Index	Less than 15%	10.95%
6	Elongation Index	Less than 15%	10.81%

The impact value of 10-20% designate the aggregates strong enough for all concrete works, whereas an impact value of 10-30% is designated as satisfactory for road works. This indicates that the impact value is a bit inferior to that of the natural aggregates. According to ASTM D5821, the crushing value of the aggregate shall not exceed 30% [8]. Here, the crushing value of steel slag material turns out to be 31.35%. Materials with lower crushing values are suitable for roads and pavements, as well for dense carpeting and bituminous dressing. According to ASTM C29 standard, the ideal Bulk Density range of aggregate is 1200-1750 kg/m³[15]. However, the bulk density of steel slag aggregate comes out approximately 1370 kg/m³. The obtained density value represents that the concrete mixture can provide good structural support and durability along with light weight structures. The abrasion value of steel slag turned out 34.28%; this value makes the aggregates suitable for a variety of works concrete and road works except the bituminous concrete surface coarse [9]. According to ASTM 4791-10 Standard, the flakiness index for road construction should remain in the limit of 15%, normally and should not exceed 25% [8]. The flakiness index of steel slag aggregate came out 10.95% which is quite within the limits for road construction. The elongation index is approximately 11%. According to ASTM D4791-19 standards, the elongation index should remain within the limit of 15% when it comes to aggregate and construction of roads. For pavements with bitumen included in the mixture, the value can go beyond 20 to 25 percent.

3.2 Concrete Containing Slag Aggregates

The Fresh and Hardened Density value obtained by performing the test is approximately 2292kg/m^3 and 2333kg/m^3 respectively. The density of ordinary concrete ranges from 2200 to 2400 kg/m^3 [16]. The experimental density shows that the material can provide high performance where integrity of structure and protection is concerned. The skid resistance results are shown in Figure 2. According to ASTM E303, the obtained skid resistance value of 56 for wet surface represents an extremely low chances of slipping [17]. The dry surface skid resistance value represents that the concrete is appropriate for heavy duty [18].

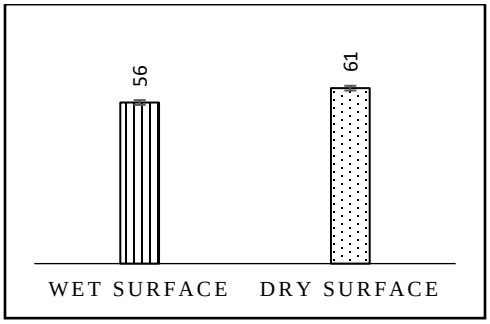

Figure 2: Skid resistance of slag concrete.

For acid attack test, the concrete cylinders containing natural and slag aggregates were dipped in 5% concentrated sulfuric acid. The compressive strength of the mixes cured for 28 days was measured before and after the test. The strength of concrete reduced by 18% and 22% respectively for natural and slag aggregates. The strength factor calculated before dipping into the acid, came out to be approximately 20% for the cylindrical steel slag concrete sample. On average, upon keeping the sample into the 5% H_2SO_4 mixed with water, the compressive strength value came out to be approximately 18%. The reduction in strength is an indication of lower resistance of slag against the acidic attack. The rebound number for concrete came out to be 30 and 22 for natural and slag aggregates respectively. Although Rebound number test is not considered to be a true measure of the quality, yet the lower number for slag is an indication of a lower strength for slag concrete.

4 Practical Implementation

The characteristics of the slag aggregates given in this work can guide the designers to adapt them in road and concrete structures. This will ensure a sustainable construction. The cost of the project will also reduce. The use of steel slag will

result in lightweight structures, which are much beneficial in many practical situations like lightweight concrete, nonstructural concrete, subbase and base layers in roads, and more specifically in blended form, where these aggregates can be combined with the natural aggregates.

5 Conclusion

From this experimental work, the following conclusions are derived

1 The slag aggregates have an impact value of less than 30, which make them suitable for road works. The slag aggregates are light in weight (only 1370 kg/m^3) and thus shall reduce the dead weight of the structure. This makes them suitable for works, where lightweight members are required like subbase and base Layers in Road Construction, Precast concrete products, and pavement bedding etc.

2 The slag aggregates have adequate elongation (10.9%) and flakiness (10.8%) indices, whereas the crushing strength is 31%, which is a slightly lower than that of the natural aggregates.

3 The slag concrete offers suitable skid resistance in both dry (61 on British Pendulum scale) and wet conditions (56 on British Pendulum scale)however their resistance to chemical attack is lower than that of the concrete containing natural aggregates. The concrete containing slag concrete exhibits adequate water absorption characteristics and therefore can be considered as durable against moisture transport.

References

[1] G. İ. Sezer and M. Gülderen, "Usage of steel slag in concrete as fine and/or coarse aggregate," *Indian J. Eng. Mater. Sci.*, vol. 22, pp. 339–344, 2015.

[2] M. H. Lai, J. Zou, B. Yao, J. C. M. Ho, X. Zhuang, and Q. Wang, "Improving mechanical behavior and microstructure of concrete by using BOF steel slag aggregate," *Constr. Build. Mater.*, vol. 277, p. 122269, Mar. 2021, doi: 10.1016/j.conbuildmat.2021.122269.

[3] T.-T.-H. Nguyen, D.-H. Phan, H.-H. Mai, and D.-L. Nguyen, "Investigation on Compressive Characteristics of Steel-Slag Concrete," *Materials (Basel).*, vol. 13, no. 8, p. 1928, Apr. 2020, doi: 10.3390/ma13081928.

[4] A. Jalil, A. Khitab, H. Ishtiaq, S. H. Bukhari, M. T. Arshad, and W. Anwar, "Evaluation of Steel Industrial Slag as Partial Replacement of Cement in Concrete," *Civ. Eng. J.*, vol. 5, no. 1, p. 181, Jan. 2019, doi: 10.28991/cej-2019-03091236.

[5] ASTM C31, "Standard Practice for Making and Curing Concrete Test Specimens in the Laboratory," *ASTM Int.*, pp. 1–8, 2013, doi: 10.1520/C0192.

[6] ASTM D-5874-16, "Standard Test Methods for Determination of the Impact Value (IV) of a Soil," West Conshohocken, PA, 19428-2959 USA, 2016.

[7] ASTM D4791−19, "Standard Test Method for Flat Particles, Elongated Particles, or Flat and Elongated Particles in Coarse Aggregate," West Conshohocken, PA, 19428-2959 USA, 2019.

[8] ASTM D5821−13, "Determining the Percentage of Fractured Particles in Coarse Aggregate," West Conshohocken, PA, 19428-2959 USA, 2013.

[9] ASTM C131/C13M-14, "Standard Test Method for Resistance to Degradation of Small-Size Coarse Aggregate by Abrasion and Impact in the Los Angeles Machine," West Conshohocken, PA, 19428-2959 USA, 2014.

[10] ASTM C29 / C29M-17a, "Standard Test Method for Bulk Density ('Unit Weight') and Voids in Aggregate, ASTM International, West Conshohocken, PA," *Annu. B. ASTM Stand.*, no. C, pp. 1–7, 2017.

[11] ASTM C642-21, "Standard Test Method for Density, Absorption, and Voids in Hardened Concrete," West Conshohocken, PA, 19428-2959 USA, 2021. doi: 10.1520/C0642-21.

[12] ASTM C1898-20, "tandard Test Methods for Determining the Chemical Resistance of Concrete Products to Acid Attack," West Conshohocken, PA, 19428-2959 USA, 2020.

[13] ASTM E2340, "Standard Test Method for Measuring the Skid Resistance of Pavements and Other Trafficked Surfaces Using a Continuous Reading, Fixed-Slip Technique," West Conshohocken, PA, 19428-2959 USA, 2021.

[14] ASTM C805/C805M-18, "Standard Test Method for Rebound Number of Hardened Concrete," 2018, doi: 10.1520/C0805_C0805M-18.

[15] ASTM C29/C29M-17, "Standard Test Method for Bulk Density ('Unit Weight') and Voids in Aggregate," West Conshohocken, PA, 19428-2959 USA, 2017.

[16] A. Khitab, *Materials of Construction*. Allied Books, 2012.

[17] ASTM E303-22, "Standard Test Method for Measuring Surface Frictional Properties Using the British Pendulum Tester," West Conshohocken, PA, 19428-2959 USA, 2022.

[18] M. R. Anwar, N. Ahmad, A. Khitab, and R. B. N. Khan, "Development of Pervious Concrete with Enhanced Skid Resistance using Waste Tires Particles," *Proc. Pakistan Acad. Sci. A. Phys. Comput. Sci.*, vol. 61, no. 1, Mar. 2024, doi: 10.53560/PPASA(60-1)830.

PERFORMANCE EVALUATION OF SUSTAINABLE COMPRESSED STABILIZED EARTH BRICKS

[a] Shafi Ullah Anjum*, [b] Saif Ur Rehman

a: Civil Engineering, University of Engineering & Technology, Peshawar, Pakistan. 17pwciv4766@uetpeshawar.edu.pk
b: Civil Engineering, University of Engineering & Technology, Peshawar, Pakistan. saifgandapur@uetpeshawar.edu.pk
* Corresponding author.

Abstract- Manufacturing of bricks with compression and stabilization is an ancient technique used from the decades. In this technique, mainly locally available soil is used as raw material along with certain stabilizer. Cement and lime are mostly used as stabilizers in the previous researches. Soil along with stabilizer is molded in the compression machine which applies a pre-defined amount of pressure to cast a brick sample. Cement is used as stabilizer in this study and due to adverse environmental effects of cement production process, the amount of cement used as stabilizer was kept minimum 5%. Comparison is done between controlled samples (CS) of 0% cement stabilizer and 5% cement stabilizer used for the preparation of compressed stabilized earth bricks (CSEBs). Water absorption test is a durability test done on CSEBs resulting 12.23% water absorption of CSEBs while CS units completely deteriorated during 24-hour submersion in water. Compression test was done on the brick samples in the universal testing machine and 28 days average compressive strength was found 416.4 psi for stabilized brick unit and 212.4 psi for controlled samples. This 96% increase in the compressive strength of stabilized units depicts the strengthening behavior of minimum (5%) cement content. Masonry prisms of 18"x18" was fabricated using the designed stabilized brick unit and mortar used was mud mortar with the compressive strength of 291.5 psi. The compressive strength and modulus of elasticity of masonry prism was found to be 171.27 psi and 41.4 ksi which indicates that the designed brick unit can be used as a construction material for single storey building.

Keywords- CSEB, stabilized, cement, masonry, brick unit, compression test

1 Introduction

Residential building are made of walls built with brick units and combined with the help of mortar [1]. Bricks commonly used are fired clay bricks which releases a large amount of energy and carbon dioxide CO_2 [2]. To be more specific, CO_2 emission from conventionally used fired clay bricks is 200 kg/t which is very alarming for the environment [3]. An alternative measure of these fired clay bricks is unfired clay bricks for construction [4]. Compressed stabilized earth bricks (CSEB) is also a type of unfired clay brick. CSEB are made by using soil as raw material, stabilizing the soil with certain stabilizer and compressing the mixture in a compressing machine [5]. These stabilized blocks are very efficient for low cost housing [6]. These CSEBs are cheap, affordable, easy to use, sustainable, fire resistant and environmentally friendly to be used as construction material in the industry [7]. Different materials are used for the stabilization in CSEBs and each material have its own effect on the properties of CSEB. Cement stabilization is very effective and it enhances all the properties such as strength, water resistant, erosion resistance, and reduces shrinkage of bricks [8]. Compression of brick sample while molding also has great effect on the properties of CSEB units. As dry density of brick is increases with compression so it can be stated that compressive strength also increases with compression [9].

In a study 8% cement, 46% quarry dust and 46% granite sludge were used in varying proportions and concluded that stabilized block have greater strength than ordinary adobe block [10]. Achievement of low cost housing is possible practically is stabilizing materials are used properly in proper proportions [11]. Cement increases the strength of units [12].

2 Research Methodology

2.1 General

In this study, soil was first tested for the basic properties. After that cement was tested for finess which was passing the criteria specified by ASTM C184-94. CSEB sample moulding was done in the compression machine by pouring the soil in the mould and then mechanical compression and vibration is applied to fabricate the brick unit. Compression test was done on brick sample according to ASTM C67 to find the compressive strength of units. After that water absorption test (ASTM D570) was done to find the durability behaviour of CSEB units. Two types of samples, controlled and stabilized, were prepared for the compression testing of brick unit to compare the stabilized sample with controlled sample. Masonry prism fabrication was done using the pre-designed clay mortar of compressive strength 291.5 psi. Lastly, compressive test on the masonry prism according to ASTM C1314 concluded the study.

2.2 Compressive Test on Brick Unit

Brick unit of standard size having area A (in^2) is placed in the universal testing machine (UTM). Two rigid plates are placed above and below the brick unit for the uniform distribution of load as shown in the figure (1). Load is applied up to the rupture of brick. The value of this load is noted as P (lb).

Figure 1: Experimental setup for CSEB unit compressive strength

2.3 Compressive Test on Masonry Prism

Masonry prisms were tested for compression in the universal testing machine (UTM). The load capacity of UTM is 50 tons. Size of masonry sample used for testing was 18"x18". Linear variable digital transformer (LVDT) were attached on both sides of masonry prisms as shown in figure (2) to detect the linear shortening of masonry sample under compressive loads. The LVDTs were connected with data logger to obtain stress strain data.

Figure 2 Experimental setup for masonry compressive strength

3 Results

3.1 Soil Test Results

The results of all the basic tests done on soil are given in table 1.

Table 1: Soil test results

Test	Results	Test	Results	Test	Results	Test	Results
Moisture Content	7.30%	Liquid Limit	39%	Plasticity Limit	15%	Specific gravity	2.53

3.2 Water Absorption Test Results

Water absorption test is done according to ASTM C67-94. Results of this test are given in table 2.

Table 2: Water absorption test results

Dry weight (kg)	Wet Weight (kg)	Water Absorption (kg)	% WA	Average % WA	COV (%)
3.541	4.012	0.471	13.301	12.232	9.72
3.601	3.994	0.393	10.914		
3.518	3.953	0.435	12.365		
3.598	3.998	0.4	11.117		
3.61	4.096	0.486	13.463		

3.3 Brick Unit Compressive Test Results

Compressive strength is an important parameter to be found for CSEB units. Five samples of each CSEB units with 5% cement and controlled sample (CS) with 0% cement were tested for compressive strength at the ages of 3 days, 14 days and 28 days. The results are given in table 3.

Table 3: Compressive test results for CSEB and CS

Sample Name	Compressive strength (P/A) in psi (CSEB samples 5 % cement)			Compressive strength (P/A) in psi (Controlled samples 0% cement)		
	3 day	7 day	28 day	3 day	7 day	28 day
Sample 1	150	271	416	78	132	201
Sample 2	157	265	408	63	121	214
Sample 3	147	289	412	72	125	209
Sample 4	141	280	425	81	118	217
Sample 5	159	276	421	85	135	221
Average	**150.8**	**276.2**	**416.4**	**75.8**	**126.2**	**212.4**

3.4 Masonry Prism Compressive Test Results

In this study three samples of single wall of size 18" x 18" were tested and stress strain response was detected with data logger connected to testing machine. Properties of masonry prisms and results are given in table (4) and stress strain behavior of masonry is shown in figure 3.

Table 4: Masonry prism compressive test results

Sample Name	Size of specimen (in)			Maximum Load (Ton)	Maximum Stress (psi)	Modulus of elasticity (ksi)
	Length	Width	Thickness			
Prism 1	18.3	18	9.1	14.4	193.8	40.76
Prism 2	18	18.5	8.8	12.1	163.4	44.1
Prism 3	18.5	18.2	9.3	12	156.6	39.2
Average Values				12.8	171.3	41.4

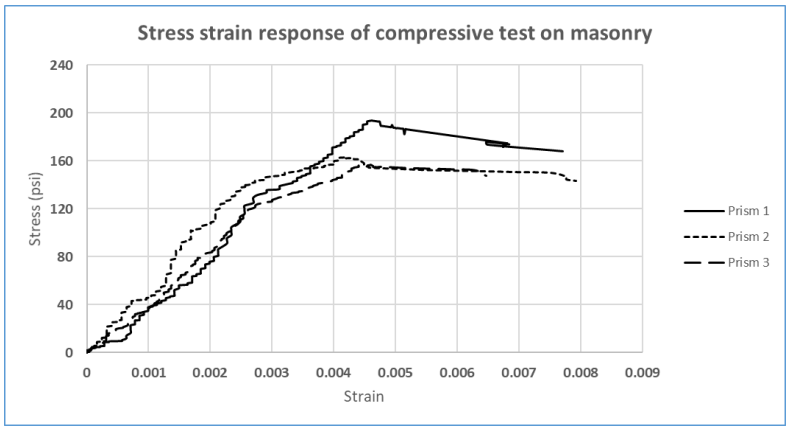

Figure 3: Stress strain curve for masonry compressive test

4 Conclusion

Following are the conclusions that can be drawn from the study conducted:

1 Water absorption of CSEB is 12.23% which is less than water absorption of 1st class brick. This depicts durable behavior of CSEB unit to be used in rainy season.
2 The compressive strength of CSEB units (5% cement) increased by 96% to that of CS with no cement content.
3 Average compressive strength of masonry is found to be 171.3 psi which is 41% of brick unit strength and average modulus of elasticity is 41.4 ksi. Compressive strength and modulus of elasticity of masonry prisms yield satisfactory results to be used in single storey low cost housing in the developing countries.

References

[1] T. Morton, *Earth Masonry: Design and Construction Guidelines (EP 80)*. IHS bre press, 2008.
[2] S. N. Monteiro and C. M. F. Vieira, "On the production of fired clay bricks from waste materials: A critical update," *Constr. Build. Mater.*, vol. 68, pp. 599–610, 2014.
[3] M. S. Islam, Tausif-E-Elahi, A. R. Shahriar, K. Nahar, and T. R. Hossain, "Strength and durability characteristics of cement-sand stabilized earth blocks," *J. Mater. Civ. Eng.*, vol. 32, no. 5, p. 04020087, 2020.
[4] A. S. Muntohar, "Engineering characteristics of the compressed-stabilized earth brick," *Constr. Build. Mater.*, vol. 25, no. 11, pp. 4215–4220, 2011.
[5] S. Nagapan, A. Antonyova, K. Rasiah, R. Yunus, and S. Sohu, "Strength and absorption rate of compressed stabilized earth bricks (CSEBs) due to different mixture ratios and degree of compaction," presented at the MATEC Web of Conferences, EDP Sciences, 2017, p. 01028.
[6] A. Veena, P. S. Kumar, and E. Sakaria, "Experimental investigation on cement stabilized soil blocks," *Int J Struct Civ. Eng Res*, vol. 3, no. 1, pp. 44–53, 2014.
[7] S. Deboucha and R. Hashim, "A review on bricks and stabilized compressed earth blocks," *Sci. Res. Essays*, vol. 6, no. 3, pp. 499–506, 2011.
[8] M. A. Bahobail, "The mud additives and their effect on thermal conductivity of adobe bricks," *JES J. Eng. Sci.*, vol. 40, no. 1, pp. 21–34, 2012.
[9] R. Bahar, M. Benazzoug, and S. Kenai, "Performance of compacted cement-stabilised soil," *Cem. Concr. Compos.*, vol. 26, no. 7, pp. 811–820, 2004.
[10] M. Lokeshwari and K. Jagadish, "Eco-friendly use of granite fines waste in building blocks," *Procedia Environ. Sci.*, vol. 35, pp. 618–623, 2016.
[11] R. Baliga, C. Prathibha, B. C. Nayak, and V. Sumanth, "Examination of Compressive Strength and Water Absorption of Adobe Blocks prepared using Black Cotton Soil and Granite Sludge," *Int. J. Appl. Eng. Res.*, vol. 13, no. 7, pp. 110–113, 2018.
[12] A. Raheem, O. Bello, and O. Makinde, "A comparative study of cement and lime stabilized lateritic interlocking blocks," *Pac. J. Sci. Technol.*, vol. 11, no. 2, pp. 27–34, 2010.

AN EXPERIMENTAL INVESTIGATION INTO THE COMPRESSIVE STRENGTH BEHAVIOR OF ULTRA HIGH PERFORMANCE CONCRETE

[a] Muhammad Ubair Javed*, [b] Muhammad Akbar Malik

a: Department of Civil Engineering, The Islamia University, Bahawalpur, Pakistan. ubairce2024@gmail.com.
b: Department of Civil Engineering, The Islamia University, Bahawalpur, Pakistan. m.akbarmalik@iub.edu.pk
* Corresponding author.

Abstract- This study investigates the behavior of Ultra High-Performance Concrete (UHPC), a material renowned for its exceptional strength and durability. UHPC has garnered global attention for its potential to enhance sustainability and prolong the lifespan of buildings and infrastructure. Despite its growing prominence, challenges such as limited knowledge, the absence of standardized design codes, and high production costs hinder its universal acceptance. To address these challenges, research initiatives have been undertaken globally, including substantial programs in Germany, South Korea, and Malaysia. This research work encompasses comprehensive mix design, sample preparation, and compressive strength testing. Notably, UHPC specimens achieved an average compressive strength of 80 MPa at 7 days and 121 MPa at 28 days, significantly outperforming conventional concrete. The factors contributing to this exceptional strength include high-performance cement, low water-to-cement ratio, silica fume and class F flyash. These findings underscore the potential of UHPC to revolutionize the construction industry, and ongoing research efforts aim to develop sustainable formulations that reduce environmental impact and production costs.

Keywords Ultra High Performance Concrete (UHPC), Compressive Strength, Sustainable Construction, Mix Design Optimization

1 Introduction

Ultra-High Performance Concrete has made significant progress in construction materials, known for its exceptional strength and durability. Over the last twenty years, UHPC has been acknowledged as a possible method for enhancing sustainability and extending the lifespan of global buildings and infrastructure [1]. It has demonstrated versatility across diverse sectors, being employed in building elements, bridges, offshore structures, and other applications. These advancements have been made possible due to extensive research and development efforts aimed at understanding the behavior, properties, and potential applications of UHPC [2].

Despite its widespread adoption in certain regions like Europe and parts of Asia, challenges persist in achieving universal acceptance and implementation due to limited knowledge, absence of standardized design codes, and high production costs[3-6].

Recognizing its transformative potential globally led to research initiatives aimed at addressing key challenges while promoting innovation such as Germany's multimillion-dollar program focused on expanding awareness about UHPB making it economically feasible for widespread use along with similar endeavors in South Korea and Malaysia focusing on specific applications such as cable-stayed bridges or rural infrastructure development projects[7-9].

The journey witnessed demonstrable progress marking transformational progression within the built environment industry. While persevering through persistent obstacles ongoing research aims at pushing boundaries hence paving the way forward toward more progressive, sustainable variants opening new opportunities.

2 Material

2.1 Cement

52.5 R CEM cement is employed for its outstanding early strength and durability characteristics, and it is added to UHPC mixtures to improve mechanical properties and overall effectiveness.

2.2 Superplasticizer

A polycarboxylic acid based superplasticizer is added to concrete mixes to enhance workability and fluidity while maintaining strength. This chemical is recognized for its efficient dispersion of cement particles, leading to improved flow and decreased water content in the mix.[10].

2.3 Supplementary Cementitious Materials

Class F fly ash and silica fume are used as alternatives to cement in concrete blends. They improve the ease of handling, longevity, and robustness of the material, while also lessening ecological ramifications by repurposing industrial by-products[11-14].

2.4 Aggregates

Fine aggregates that have been sieved through a 1.18 mm sieve are applied in concrete mixes to fill spaces and enhance manageability. Fine aggregates significantly contribute to maximizing the density of concrete packing and improving its mechanical properties.[15].

2.5 Water-to-Cement Ratio

A 0.2 water-to-cement ratio is employed in UHPC formulas to attain high strength and reduce permeability while retaining suitable workability. This reduced water-to-cement ratio decreases porosity and guarantees effective hydration of cement particles, leading to compact and long-lasting concrete with excellent mechanical attributes.[16].

3 Methodology

The research methodology for Ultra-High Performance Concrete starts with a detailed mix design process according to specific specifications shown in table 1. This involves determining the proportions of essential components such as cement, silica fume, fine aggregates, water, high-range water reducer, and fibers.

Table 1: Composition of UHPC

Material	Conventional Concrete kg/m3	UHPC Proportion kg/m3
Cement	300	600
Fly ash	-	120
Silica Fume	-	153.5
Sand	1000	630
HRWR	10	17
Water	180	131

Sample preparation is carried out precisely to weigh each component accurately. The dry ingredients are combined in a mixing container and thoroughly blended for a homogeneous mixture for 5 minutes. Then, the mixing water and high-range water reducer are gradually added while continuously blending to create a uniform UHPC slurry for 3-4 minutes.

The casting procedure follows a systematic approach where the UHPC mixture is poured into prepared molds ensuring complete filling. After casting, specimens undergo curing covered with plastic sheets during the initial curing period lasting 24 hours then transferring them to a curing tank for 7 days and 28 days. For comparison the conventional control cube specimens of 50x50x50 mm sizes were also prepared.

Following the requisite curing period, the compressive strength of the UHPC specimens is determined using a compressive testing machine. This machine measures the maximum load withstood by the cube until failure, which is then recorded as the compressive strength. The material casting and testing procedure is illustrated in Figure [1], which provides a visual representation of the process.

Figure:1 Casting and Testing of specimens

4 Discussion and Results

The section discusses the results of testing the compressive strength of UHPC specimens at 7 days and 28 days using ASTM C109/C109M. The average compressive strength, recorded as 80 MPa and 121 MPa at 7 and 28 days respectively, is accompanied by the standard deviation to illustrate data variability as shown in figure 2.

A 0.2 W/B ratio indicates a very low amount of water, resulting in a dense microstructure and reduced porosity, leading to higher strength. Silica fume's high pozzolanic reactivity enhances the binding properties, contributing to increased strength. Class F fly ash's low calcium content and high silica content promote a slow and steady pozzolanic reaction, improving strength over time. The use of 1.18 mm fine aggregate allows for a dense packing, reducing voids and increasing strength. The HRWR admixture enables the achievement of a low W/B ratio while maintaining workability, ensuring a dense and strong microstructure.

The significant strength gain between 7 and 28 days (from 80 MPa to 121 MPa) can be attributed due to Continued pozzolanic reactions between silica fume and Class F fly ash. Ongoing hydration of cement and fly ash. Increased bonding between aggregate and paste due to continued cement hydration. The mix design probably involved high-performance cement and a low water-to-cement ratio, both promoting rapid early-age strength development [17].

In comparison with conventional concrete typical 35 MPa compressive strength at 28 days Figure [2], these results underscore substantial advantage offered by UHPC. While impressive, further exploration into long-term strength development as well as other mechanical properties would offer a more comprehensive assessment of the UHPC mixture's performance.

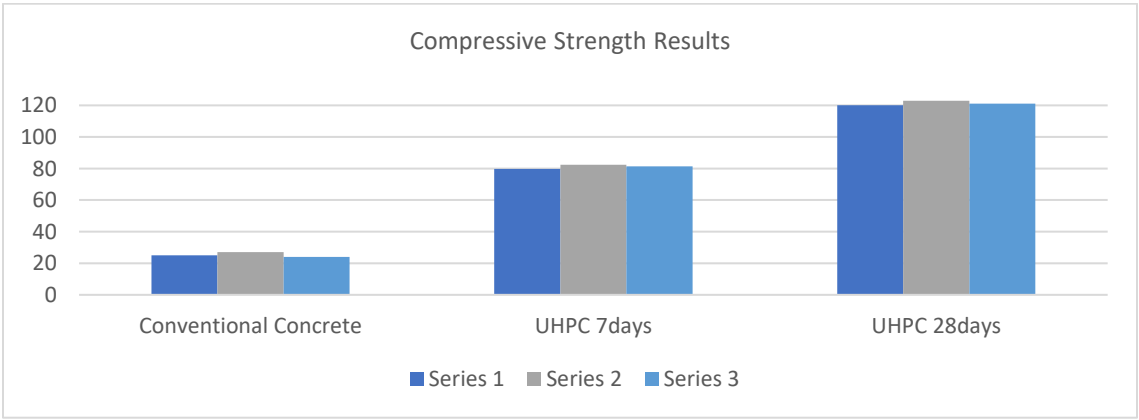

Figure 2: Comparison of UHPC and Conventional Concrete

Possible future testing includes assessing later-stage (56 days) strengths to track evolution; evaluating additional mechanical properties like tensile and flexural strengths; or exploring influences from different mix design parameters on UHPC's mechanical behavior.

5 Conclusion

In conclusion, the Ultra High Performance Concrete (UHPC) specimens demonstrated exceptional compressive strength, reaching 80 MPa at merely 7 days and further increasing to 121 MPa at 28 days. This investigation into the properties and behavior of UHPC has yielded significant findings. Notably, UHPC exhibits outstanding compressive strength, surpassing traditional concrete by a substantial margin. The use of high-quality materials and a low water-to-cement ratio confers enhanced durability and resistance to environmental degradation. Ongoing research endeavors aim to develop sustainable UHPC formulations, mitigating environmental impact and production costs. Despite its favorable attributes, the widespread adoption of UHPC is hindered by the absence of standardized design codes, limited understanding of its properties, and higher initial costs relative to conventional concrete.

Future areas for study involve improving mixture designs to boost sustainability and cost-effectiveness, evaluating long-term resilience in different conditions, advocating for standardization initiatives, and performing thorough life-cycle cost evaluations to showcase its financial advantages.

Acknowledgment

I extend my sincere gratitude to my academic advisors, colleagues, family, and friends for their unwavering support and encouragement throughout this research journey. Their guidance, feedback, and understanding have been invaluable.

Reference

1. Bajaber, M. and I. Hakeem, *UHPC evolution, development, and utilization in construction: A review.* Journal of Materials Research and Technology, 2021. **10**: p. 1058-1074.
2. Zhou, M., et al., *Application of ultra-high performance concrete in bridge engineering.* Construction and Building Materials, 2018. **186**: p. 1256-1267.
3. Azmee, N.M. and N. Shafiq, *Ultra-high performance concrete: From fundamental to applications.* Case Studies in Construction Materials, 2018. **9**: p. e00197.
4. Randl, N., et al., *Development of UHPC mixtures from an ecological point of view.* Construction and Building Materials, 2014. **67**: p. 373-378.
5. Křížová, K. and R. Hela, *Options of UHPC in the Czech Republic.* Key Engineering Materials, 2017. **722**: p. 292-297.
6. Abbas, S., M. Nehdi, and M. Saleem, *Ultra-high performance concrete: Mechanical performance, durability, sustainability and implementation challenges.* International Journal of Concrete Structures and Materials, 2016. **10**: p. 271-295.
7. Phillips, P.S., et al., *A UK county sustainable waste management programme.* International Journal of Environment and Sustainable Development, 2002. **1**(1): p. 2-19.
8. Quitoras, M.C.L. and J.E. Abuso, *Best Practices of Higher Education Institutions (HEIs) for the Development of Research Culture in the Philippines.* Pedagogical Research, 2021. **6**(1).
9. Alsulami, S., et al., *Perception of academic stress among health science preparatory program students in two Saudi universities.* Advances in medical education and practice, 2018: p. 159-164.
10. Macijauskas, M. and G. Skripkiūnas. *The influence of superplasticizers based on modified acrylic polymer and polycarboxylate ester on the plasticizing effect of cement paste*. in *Materials Science Forum*. 2017. Trans Tech Publ.
11. Bajpai, R., et al., *Environmental impact assessment of fly ash and silica fume based geopolymer concrete.* Journal of Cleaner Production, 2020. **254**: p. 120147.
12. Mustapha, F., et al., *The effect of fly ash and silica fume on self-compacting high-performance concrete.* Materials Today: Proceedings, 2021. **39**: p. 965-969.
13. Gil, D.M. and G.L. Golewski. *Potential of siliceous fly ash and silica fume as a substitute for binder in cementitious concretes*. in *E3S Web of Conferences*. 2018. EDP Sciences.
14. Sankar, L.P., et al., *Investigation on binder and concrete with fine grinded fly ash and silica fume as pozzolanic combined replacement.* Materials Today: Proceedings, 2020. **27**: p. 1157-1162.
15. Zhao, Y., et al., *Characterization of coarse aggregate morphology and its effect on rheological and mechanical properties of fresh concrete.* Construction and Building Materials, 2021. **286**: p. 122940.
16. Kim, S., et al., *Experimental and theoretical studies of hydration of ultra-high performance concrete cured under various curing conditions.* Construction and Building Materials, 2021. **278**: p. 122352.
17. Ullah, R., et al., *Ultra-high-performance concrete (UHPC): A state-of-the-art review.* Materials, 2022. **15**(12): p. 4131.

ASSESSMENT OF FLOW AND MECHANICAL PROPERTIES OF GEOPOLYMER COMPOSITE FOAM CERAMIC FILLERS

[a] Hammad Shaukat*, [b] Ali Raza

a: Department of Civil Engineering, University of Engineering and Technology, Taxila, Pakistan. hammadshaukat47@gmail.com
b: Department of Civil Engineering, University of Engineering and Technology, Taxila, Pakistan. ali.raza@uettaxila.edu.pk
* Corresponding author.

Abstract- While creating cellular geopolymer mortar with geopolymers (GPL) has attracted a lot of attention, little study has been done to determine how particle fillers affect the final porosity. The goal of this research is to thoroughly examine the necessary elements for producing composite cellular geopolymer mortar. Analyzing the viscosity of the GPL slurry, which contains small particles derived from fireclay and ceramic dichroite, is one of the main goals. For GPL with fireclay and dichroite fillers, the viscosity values at 100 s^{-1} were 4.99 Pa. s and 4.23 Pa. s, respectively. Due to a significant distribution of linked porosity and big pores in the matrix, composite cellular geopolymer mortar reinforced with ceramic fillers has compressive strengths ranging from 1.51 to 10.1 MPa.

Keywords- Cellular Geopolymer Mortar, Compressive Strength, Fireclay Ceramics, Flow Properties.

1 Introduction

A novel family of inorganic polymers known as geopolymers (GPL) are produced when aluminosilicate materials are activated with an alkali-activated solution. Growing interest in GPL materials because of economic expansion and urbanization has centered attention on learning about the creation of GPL composites and their properties [1, 2]. The scientific community has emphasized the GPL system's potential to lower carbon emissions in addition to aluminosilicates' capacity to give desired features such durability, thermal stability, and resistance to acid attack [3, 4]. Numerous studies have investigated the parametrization of GPL to obtain the necessary porosity and microstructural stability [5, 6]. More uses for GPL cellular geopolymer mortar have surfaced recently, including concrete cellular geopolymer mortar [7], heavy metal adsorbents [9], fire-resistant panels [8], acoustic and thermal insulations [10], monolithic adsorbents for wastewater treatment [11], and ion exchangers [12]. The appropriate chemical cellular geopolymer mortar can be used to provide the necessary porosity, regardless of variations in development protocols and techniques [13]. Furthermore, a thorough analysis of variables is necessary for the synthesis of a porous composite to track changes in the test slurries' in-situ flow properties when different fillers or additives are added [5]. The goal of this research is to thoroughly examine the most essential factors to create composite cellular geopolymer mortar. Examining the viscosity of the GPL slurry with tiny particles sourced from fireclay and ceramic cordierite is one of the main goals. The research explores a novel blend of geopolymer and foam ceramic fillers, aiming to enhance sustainability through reduced carbon emissions and improved mechanical properties. This innovative approach holds promise for diverse engineering applications, offering lightweight, durable materials with enhanced thermal insulation capabilities.

2 Experimental Program

2.1 Materials

The GPL slurries were made using fireclay ceramics (FC), dichroite ceramics (DC), and metakaolin (MKL) powder as the main ingredients and ceramic fillers, respectively. The utilization of an alkaline potassium silicate solution resulted in a SiO_2/K_2O ratio of 1.65. A 30% concentration of H_2O_2 was utilized to provide the foaming properties. In addition, $Cl \leq 5$

ppm, retention ≤ 5 ppm, Pb ≤ 0.02 ppm, N ≤ 20 ppm, and Fe ≤ 0.5 ppm are specified by the manufacturer. The pore size distribution of the utilized components is shown in Table 1.

Table 1: Grain sizes of MKL, FC, and DC particles

Size distribution	Mean size (µm)	Dv10 (µm)	Median size D50 (µm)	Dv90 (µm)	Density (g/cm^3)
DC	288.28	32.76	253.95	591.47	2.77
FC	302.07	85.34	247.85	539.11	2.81
MKL	6.12	2.55	5.33	10.39	0.72

2.2 Preparation of Samples and Testing

The GPL slurry was made in accordance with a weight ratio of 1:1 for MKL and potassium silica solution at a room temperature of 23 °C. A 30% relative humidity was kept constant. Previous data reports served as the foundation for mix design [14]. The chemical formations of the porous GPL, GPL_DC, and GPL_FC solid specimens are shown in Table 2.

Table 2: Chemical formation of GPL, GPL_FC, and GPL_DC solid specimens

Mix	SiO_2	Al_2O_3	CaO	Fe_2O_3	TiO_2	K_2O	MgO	Na_2O
GPL	50.167	28.754	0.201	0.732	1.275	17.933	0.815	0.123
GPL_FC	51.506	32.82	0.151	2.939	2.333	10.048	0.158	0.045
GPL_DC	48.565	30.783	0.409	1.646	2.322	11.021	5.143	0.111

3 Results and Discussion

3.1 Mechanical Properties

To examine the specimen cylinders measuring 15 by 30 mm for compression strength, the average strength results were computed, and the discrepancies were depicted using error bars. The impact of ceramic fillers on measurements of compression strength and relative compression strength of samples is depicted in Figure 1. There is a paucity of important research contrasting the porosity microstructure at elevated temperatures. However, bulk GPL exhibits a comparable mechanism [15]. Higher temperatures, such as those between 70°C and 90°C, are known to improve the alkaline solution's interaction with the aluminosilicate source during GPL formation [16]. This generally increases the mechanical strength, although the GPL systems' chemical makeup has a big impact on it [17].

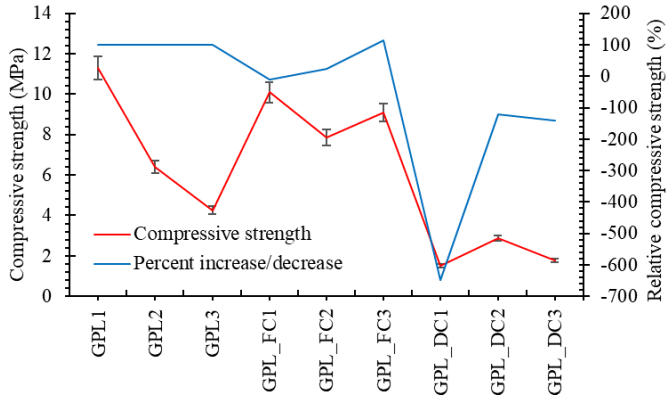

Figure 1: Results for compression strength and relative compressive strength of samples.

3.2 Viscosity and Flow Properties

The dynamic viscosity of the fresh GPL mixtures was tested around two minutes after mixing. After measuring the viscosity, H_2O_2 was added as the blowing material. In the rising regime of shear rate, testing of the unreinforced GPL slurry revealed that the material behaved as a non-Newtonian fluid, with viscosity fluctuating with induced stress [18]. For the GPL mix at 100 s^{-1}, the green circle plot in Figure 2 validates a shear thinning response of 0.58 Pa.s. Furthermore, in the quasi-plateau plot zone, the viscosity of the GPL decreased beyond 50 s^{-1}. The curve displayed a linear increase up to 50.1 Pa. s at 100 s^{-1}, as shown in Figure 2.

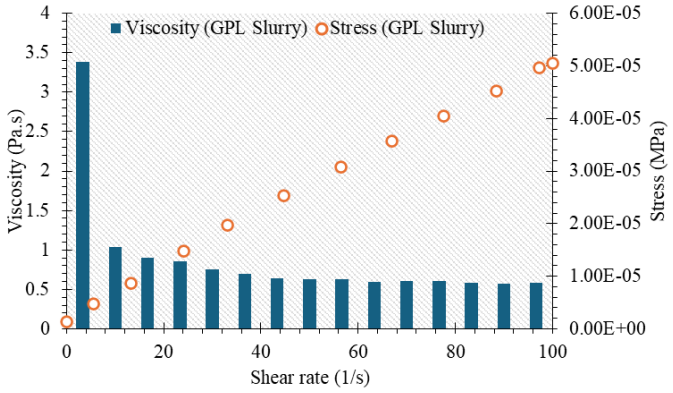

Figure 2: Flow and viscosity plots as a function of the shear rate of GPL slurry.

At a shear rate of 100 s^{-1}, the GPL_DC mixture's viscosity was determined to be 4.99 Pa. s, while the GPL_FC mixtures was 4.23 Pa. s (Figure 3). The viscosity of the GPL_DC particles increased during shear deformation. Similar trends in pycnometer results, which displayed equivalent bulk density values, can be linked to this tendency. The flow properties of GPL slurries were greatly impacted by the presence of ceramic fillers, which resulted in decreased workability during the initial mixing stage. System densification is the main cause of this decline [19]. The apparent viscosity of the slurry increased by more than eight times when ceramic fillers were added. It went from 10 s^{-1} to 100 s^{-1}. The system continued to behave in a pseudoplastic manner, as seen by the viscosity decreasing as the shear rate increased [20]. To find the dynamic yield stress and plastic viscosity of the matrices under study, curve fitting with the Bingham model was utilized.

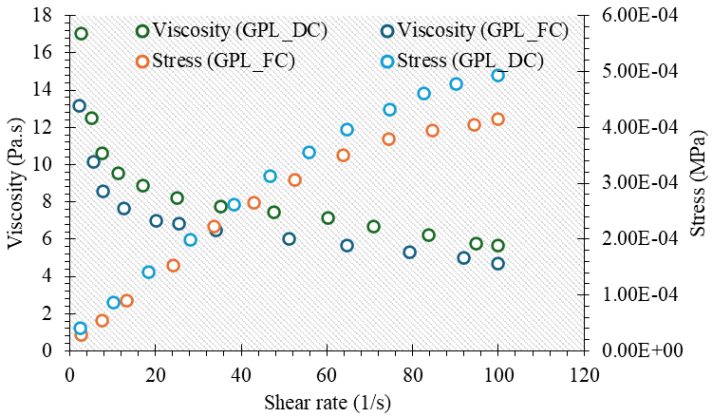

Figure 3: Flow and viscosity plots versus shear rate of GPL_FC and GPL_DC mixes.

4 Conclusion

The geopolymer slurry's apparent viscosity was enhanced by adding ceramic filler while preserving a pseudoplastic reaction. For instance, the plastic viscosity increased to over 5.89 Pa. s with a yielding stress surpassing 24.98 Pa. with the addition of dichroite fillers. The FC particles preserved the mechanical integrity of the composite cellular geopolymer mortar, exhibiting a compression strength of approximately 11.29 MPa. The slurry's apparent viscosity grew dramatically

from 10 s^{-1} to 100 s^{-1}, frequently by more than eight times, with the addition of ceramic fillers, while the system's pseudoplastic behavior stayed the same. This innovative approach holds promise for diverse engineering applications, offering lightweight, durable materials with enhanced thermal insulation capabilities

Acknowledgment

The careful review and constructive suggestions by the anonymous reviewers are gratefully acknowledged. The effort and help by Muhammad Abdullah (email: abdullah.aby11@gmail.com) for this research paper is greatly acknowledged.

References

[1] Lemougna, P.N., et al., Recent developments on inorganic polymers synthesis and applications. Ceramics International, 2016. 42(14): p. 15142-15159..
[2] Pacheco-Torgal, F., J. Castro-Gomes, and S. Jalali, Alkali-activated binders: A review. Part 2. About materials and binders manufacture. Construction and building materials, 2008. 22(7): p. 1315-1322
[3] Raza, A., S. Abdellatif, and M.H. El Ouni, A GMDH model and parametric investigation of geopolymeric recycled concrete FRP-spiral-confined members. Engineering Applications of Artificial Intelligence, 2023. 125: p. 106769.
[4] Elhag, A.B., et al., A critical review on mechanical, durability, and microstructural properties of industrial by-product-based geopolymer composites. Reviews on Advanced Materials Science, 2023. 62(1): p. 20220306.
[5] Farhan, K.Z., M.A.M. Johari, and R. Demirboğa, Assessment of important parameters involved in the synthesis of geopolymer composites: A review. Construction and Building Materials, 2020. 264: p. 120276.
[6] Zhang, Z., et al., Geopolymer foam concrete: An emerging material for sustainable construction. Construction and Building Materials, 2014. 56: p. 113-127.
[7] Rickard, W.D. and A. Van Riessen, Performance of solid and cellular structured fly ash geopolymers exposed to a simulated fire. Cement and Concrete Composites, 2014. 48: p. 75-82.
[8] M. U. Farooqi and M. Ali, "Effect of pre-treatment and content of wheat straw on energy absorption capability of concrete," *Construction and Building Materials*, vol. 224, pp. 572-583, 2023.
[9] Rasaki, S.A., et al., Geopolymer for use in heavy metals adsorption, and advanced oxidative processes: A critical review. Journal of Cleaner Production, 2019. 213: p. 42-58.
[10] Zhang, Z., et al., Mechanical, thermal insulation, thermal resistance and acoustic absorption properties of geopolymer foam concrete. Cement and Concrete Composites, 2015. 62: p. 97-105.
[11] Roviello, G., et al., Hybrid geopolymeric foams for the removal of metallic ions from aqueous waste solutions. Materials, 2019. 12(24): p. 4091.
[12] Luukkonen, T., et al., Removal of ammonium from municipal wastewater with powdered and granulated metakaolin geopolymer. Environmental technology, 2018. 39(4): p. 414-423.
[13] Henon, J., et al., Porosity control of cold consolidated geomaterial foam: temperature effect. Ceramics International, 2012. 38(1): p. 77-84.
[14] Kovářík, T., et al., Thermomechanical properties of particle-reinforced geopolymer composite with various aggregate gradation of fine ceramic filler. Construction and Building Materials, 2017. 143: p. 599-606.
[15] Li, Q., et al., Effect of curing temperature on high-strength metakaolin-based geopolymer composite (HMGC) with quartz powder and steel fibers. Materials, 2022. 15(11): p. 3958.
[16] Heah, C., et al., Effect of curing profile on kaolin-based geopolymers. Physics Procedia, 2011. 22: p. 305-311.
[17] Bournonville, B. and A. Nzihou, Rheology of non-Newtonian suspensions of fly ash: effect of concentration, yield stress and hydrodynamic interactions. Powder technology, 2002. 128(2-3): p. 148-158.
[18] Rovnaník, P., et al., Rheological properties and microstructure of binary waste red brick powder/metakaolin geopolymer. Construction and Building Materials, 2018. 188: p. 924-933.
[19] Güllü, H., et al., On the rheology of using geopolymer for grouting: A comparative study with cement-based grout included fly ash and cold bonded fly ash. Construction and Building Materials, 2019. 196: p. 594-610.
[20] Roussel, N., et al., Steady state flow of cement suspensions: A micromechanical state of the art. Cement and Concrete Research, 2010. 40(1): p. 77-84.

ENHANCING LOAD-CARRYING CAPACITY OF DAMAGED GEOPOLYMER CONCRETE COLUMNS BY RETROFITTING WITH CFRP WRAPS

[a] Muhammad Ahsan Sami*, [b] Zawar Ahmed

a: Civil Engineering Department, University of Engineering and Technology Taxila, Pakistan. ahsansami0045@gmail.com
b: Civil Engineering Department, University of Engineering and Technology Taxila, Pakistan. zawarahmad110@gmail.com
*Corresponding author.

Abstract- An environmentally friendly substitute for conventional concrete is geopolymer concrete, which are created from by-products of industry such as fly ash, slag, quarry rock dust (QRD) and other aluminosilicate minerals. This test study includes eight specimens of 200mm x 200mm x 1000mm which were already tested to the Ultimate load carrying capacity. The specimens include four GCD columns with 0% fiber and four GCD columns with 0.75% fiber. The damaged specimens were first repaired by GCD (Geopolymer concrete with QRD), and then retrofit with CFRP sheets by wrapping around the column using epoxy adhesives and tested under the compression testing machine (5000 KN) at concentric and eccentric loading (at 15E, 35E, 50E) with a 20 mm magnetic LVDT. As a result, the column's load-bearing capacity, flexural strength, ductility, is improved by retrofitting columns with CFRP sheets, which is a minimally invasive, high strength-to-weight ratio, and low thermal expansion.

Keywords- Geopolymer Concrete, Strengthening, Retrofitting, Carbon Fiber Reinforced Polymer.

1 Introduction

Geopolymer concrete encourages resource efficiency, protects natural resources, and helps to reduce carbon emissions[1]. A further benefit of geopolymer concrete is its exceptional resilience, which lowers the frequency of repairs and replacements while increasing the life of buildings[2]. A geopolymer binder is combined with aggregates like sand, gravel, and crushed stone to create geopolymer concrete, as opposed to conventional concrete, which is manufactured using Portland cement[3]. An alumina and silica source, such as fly ash, crushed granulated blast furnace slag, or quarry rock dust is combined with an alkali activator solution, such as sodium silicate solution (12M) to create the geopolymer binder. With the passage of time, environmental factors like, temperature changes, chemical reactions, and moisture comes in contact with all the constructions including reinforced concrete columns which can cause deterioration of concrete and corrosion of reinforcing steel[4]. Mechanical stress poses a threat, to the columns potentially causing cracks, deformities and structural failure when subjected to vibrations and impacts[5].

One effective method to enhance the strength and durability of columns is through the use of Carbon Fiber Reinforced Polymer (CFRP) strengthening [6]. CFRP is resistant to corrosion reinforces structures significantly without adding weight and can be easily attached to column surfaces. Its flexibility allows it to absorb energy during earthquakes reducing the risk of failure [7]. Moreover CFRP sheets offer lasting toughness and protection to the elements. This strengthening technique enhances load bearing capacity, stiffness and resilience, under different loading conditions including sesmic stresses.

2 Research Methodology

The columns were 200 mm x 200 mm in cross-sectional dimension and had a height of 1000 mm. Eight of the columns were examined, repaired, and their tensile strengths have been compared with those of formerly examined columns without

CFRP. The columns were reinforced with six 12 mm Dia bars having yield strength of 450 MPa as the main reinforcement and 6 millimeters Dia @100mm center to center having yield strength of 300 MPa as the transverse reinforcement. For repair, firstly remove the loose or broken material from the columns. Apply the repair material, whose composition is specified in section 2 of [8], after removing. After repairs, give the seven-day curing time- to columns, and smoothen the column's surface using a grinder once it has gained enough strength.

After smoothening the surface, apply the binding material to the columns and wrap the CFRP strips (20 mm) at a 20-degree angle. Apply pressure while applying to ensure that the CFRP strips are free of air bubbles and wrinkles. Use a compression testing machine (5000 KN) with a 20 mm magnetic LVDT (Linear Variable Differential Transformer) to test the columns to see how they perform structurally. The LVDT is properly placed to measure the deflection exactly. Apply force to columns until they reach their yielding point with the deflection rate set to 1 mm per minute. Take the deflection values that the LVDT computer has produced to check the column behavior.

2.1 Preparation of Specimens

To prepare the samples, the GCD surface was cleaned and made ready. Loose or damaged material, dust, filth, or other pollutants were removed by hammering them out of the specimens. After removing any loose debris, surface cracks were filled with GCD mortar (50% FA + 30% Slag + 20% QRD) using NaOH and Na2SiO3 as alkali activators. The same GCD mix design used which was already used in the preparation of the specimen, taken from table 1 of [8]. The exterior of the column was ground rough to strengthen the bond between its surface as well as the CFRP. After grinding, the holes were filled with epoxy to create an equal surface and prevent air pockets. Chemdur-300 (components A and B) were combined and applied in a 2:1 ratio to the GCD surface as a bonding agent to create a strong connection between the concrete and the CFRP (Figure 1c). The CFRP was cut into an appropriate strip size of 82 mm wide, and 10 ft (3048 mm) long based, and wrapped it on columns at 20^0 angle (Figure 1b). The GCD columns surface was coated with CFRP using the bonding agent Chemdur 31(Figure 1a), and to get rid of any air pockets between the concrete surface and CFRP, then the CFRP should be pressed firmly against the surface to create solid contact.

a)  b)  c) 

Figure 1: Preparation of specimen, a. CHEMDUR 300 (component A and B), b. Covered column by CFRP strips at 20^0, and c. Applying bonding agent on column.

2.2 Testing

The test subjects were subjected to axial unidirectional force until total failure, and a schematic sketch of concentric loading is shown in (Figure 2a). The load was delivered in periodic intervals of 1 KN/s. Before testing, a pair of 76mm wide by a thickness of 3.2 mm thick steel collars were wrapped around both ends of a column to avoid overstressed premature failure A layer of plaster of Paris with a sufficient thickness was applied to each of the upper and lower faces of the column to ensure a uniform transfer of load (Figure 2b). The axial displacement of columns under 5000KN CTM and at a deflection rate of 1mm/minute was measured using a 20 mm magnetic LVDT device (Figure 2c).

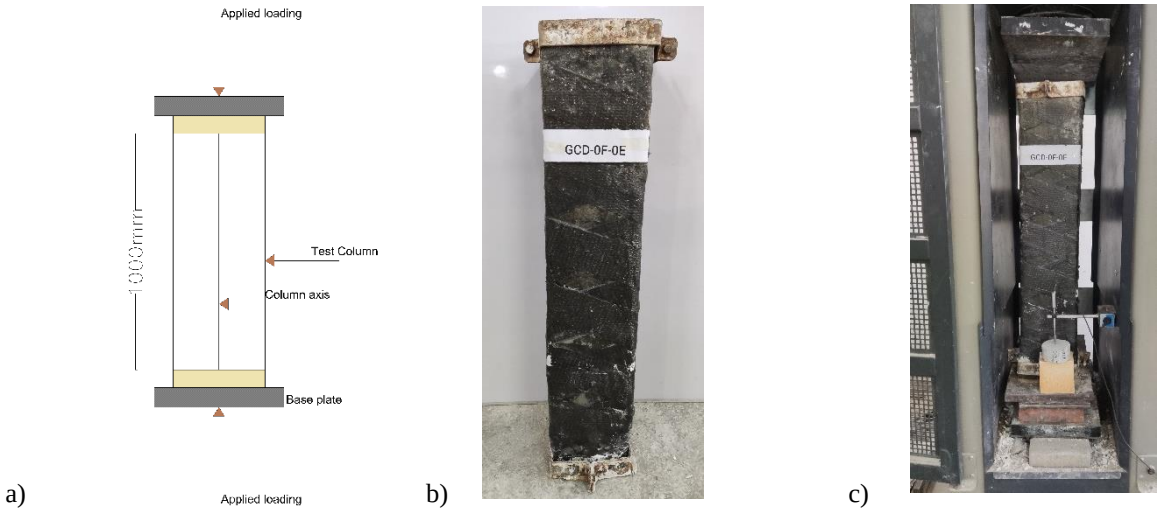

Figure 2: Testing of specimen, a. Schematic sketch of concentric loading, b. Specimen before testing, and c. Specimen placed in CTM with magnetic LVDT

3 Results

Table 1 shows that the GCD columns without fiber follows the trend, as the eccentricity (E) increases load bearing capacity of the columns is decreased from 0E to 50E. But the ultimate load of these columns was improved from previous results. On the other hand, GCD columns with fiber did not follow any trend. Firstly, at 0E ultimate load goes down by 19.9%, at 15E it increases but at 35E it again decreases and shows its maximum at 50E. The reason for showing lower value at concentric loading is due to the rusting of fibers and reinforcement in the column which affects the ultimate load of the columns. After strengthening columns results are compared with, without CFRP columns results [8]. The graph is drawn between the Ultimate load carrying capacity (Pmax) in KN and Displacement (mm) from the data obtained from the LVDT computer (Figure 3).

Table 1: Post-strengthening performance of structural elements

Gr. no.	Gr. ID	Col. ID	Fiber Fraction	E (mm)	Pmax (KN)	Percentage Improvement %	Axial displacement at Pmax (mm)	Ductility Index (DI)
1	GCD	GCD-0F-0E	--	0	1105	39.8	13.5	1.13
2		GCD-0F-15E	--	15	697	35.3	14.6	1.08
3		GCD-0F-35E	--	35	570	95.2	10.3	1.06
4		GCD-0F-50E	--	50	451	124.3	7.8	1.01
5	GCD	GCD-0.75F-0E	0.75%	0	759	-19.9	13.9	1.15
6		GCD-0.75F-15E	0.75%	15	782	19.6	11.1	1.07
7		GCD-0.75F-35E	0.75%	35	654	68.6	16.3	1.02
8		GCD-0.75F-50E	0.75%	50	861	224.9	18.4	1.04

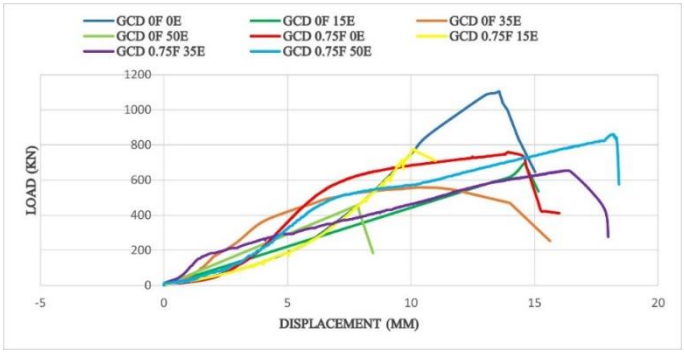

Figure 3: Columns ultimate load graph of strengthened geopolymer concrete

4 Practical Implementation

CFRP sheets or strips can be externally bonded to the tension face of beams and columns to increase their load-carrying capacity and flexural strength. For concrete slabs with inadequate shear strength, CFRP can be applied to the slab's underside to enhance its shear resistance. Furthermore, where steel structures have suffered from corrosion, CFRP can be employed as a seismic and durable external reinforcement.

5 Conclusion

Eight columns, whose dimensions were 200 x 200 x 1000 mm were used in this research. For strengthening, CFRP technique is used to increase the structure durability and strength. From the results it is demonstrated that the strength of geopolymer concrete column without fiber follows a trend and showed its maximum at 0E (1105 KN) followed by 15E (697 KN), 35E (570 KN), and (451 KN) at 50E by wrapping 20mm CFRP strips at 20^{o}. Other the other hand, GCD columns with fiber showed a different behavior due to the rusting of fibers and showed a maximum at 50E (861 KN), followed by 15E (782 KN), 0E (759 KN), and (654 KN) at 35E. It is concluded from the above discussion that, as the eccentricity of GCD columns increases the ultimate load bearing capacity of the columns is decreased. Secondly, strength of destructed columns is increased by CFRP sheet by wrapping at 20^{0} angles from the horizontal and by this method the need to destroy and rebuild the structural elements is eliminated.

Acknowledgment

We are grateful to our supervisor, Dr. Faheem Butt, for overseeing and supporting our research, as well as Rana Waqas for his guidance.

Reference

[1] M. A. Ansari, M. Shariq, and F. Mahdi, "Geopolymer concrete for clean and sustainable construction–A state-of-the-art review on the mix design approaches," in *Structures*, 2023, vol. 55: Elsevier, pp. 1045-1070.

[2] T. Stengel, J. Reger, and D. Heinz, "Life cycle assessment of geopolymer concrete–what is the environmental benefit," *Concrete Solutions*, vol. 9, 2009.

[3] B. Al Muhit, K. Foong, U. Alengaram, and M. Z. JUMAAT, "Geopolymer concrete: A building material for the future," *Electronic Journal of Structural Engineering*, vol. 13, no. 2, pp. 11-15, 2013.

[4] C.-K. Ma, A. Z. Awang, and W. Omar, "Structural and material performance of geopolymer concrete: A review," *Construction and Building Materials*, vol. 186, pp. 90-102, 2018.

[5] A. Hassan, M. Arif, and M. Shariq, "Use of geopolymer concrete for a cleaner and sustainable environment–A review of mechanical properties and microstructure," *Journal of cleaner production*, vol. 223, pp. 704-728, 2019.

[6] G. T. Truong, J.-C. Kim, and K.-K. Choi, "Seismic performance of reinforced concrete columns retrofitted by various methods," *Engineering Structures*, vol. 134, pp. 217-235, 2017.

[7] R. D. Iacobucci, S. A. Sheikh, and O. Bayrak, "Retrofit of square concrete columns with carbon fiber-reinforced polymer for seismic resistance," *Structural Journal*, vol. 100, no. 6, pp. 785-794, 2003.

[8] R. M. Waqas and F. Butt, "Behavior of Quarry Rock Dust, Fly Ash and Slag Based Geopolymer Concrete Columns Reinforced with Steel Fibers under Eccentric Loading," *Applied Sciences*, vol. 11, no. 15, p. 6740, 2021.

ENHANCING CONCRETE MECHANICAL PROPERTIES THROUGH GRAPHITE NANO-MICRO PLATELETS

[a] Hassan Tahir*, [b] Muhammad Numan

a: Structure Engineering Department, Designmen Consulting Engineers, Islamabad, Pakistan. hassantahir275@gmail.com
b: Infrastructure Engineering Department, Designmen Consulting Engineers, Islamabad, Pakistan. engr.numans@gmail.com
*Corresponding author.

Abstract- This research explores the enhancement of conventional concrete properties through the incorporation of graphite nano-micro platelets (GNMPs). The experiment involved the addition of GNMPs in varying concentrations of 0.1%, 0.3%, and 0.5% with a testing period of 28 days. The findings revealed a significant improvement in both compressive and tensile strength with the inclusion of 0.3% GNMPs. The research concludes the potential advantages of using GNMPs as an additive in concrete, especially for enhancing strength and increasing the durability and efficiency of conventional concrete. These findings are particularly promising for the construction sector, which is constantly seeking to develop concrete materials that are stronger and more durable.

Keywords- Nano Micro Graphite, Strength Improvement, Durability, Material Testing.

1 Introduction

Concrete, having versatile properties compared to other materials such as strong durability, low maintenance, ease of use, fire resistance, water resistance, and fitting to any shape, is one of the most widely used construction materials in the construction industry globally. As the construction industry grows day by day, it poses more demands, for which conventional concrete alone is not enough to meet the required demands. Because of the low elastic and flexural strength of cementitious materials exposed to breaking, this breaking cycle begins with nanocracks, and with the progression of time, it transforms into microcracks and, afterward, large microcracks inside the grid of concrete. In the beginning, researchers tried to restrict these cracks with the addition of microfibers, although these microfibers do not hold out against the crack at the macro level but slow their transfer to the micro level. It provides a good opportunity for the researchers to increase the mechanical properties of conventional concrete by adding cementitious composites. Little consideration has been shown to investigate the helpful effects of GNMPs in concrete. Incorporating glass powder GP in concrete increases workability and decreases density, absorption, and porosity, with 20% GP being optimal for compressive strength when using conventional mixing methods [1]. Recycled aggregate concrete showed 90% of the compressive and shear strengths of natural aggregate concrete, with a 3% lower modulus of elasticity and 5.5% higher strain at peak stress [2]. This paper describes the effect of the addition of nano-graphite when added to the concrete with different percentages in comparison to the control specimen to investigate the enhancement of mechanical properties such as compressive, tensile, and flexural strengths of conventional concrete.

2 Literature Review

A. Dinesh et al (2023) in his study investigated the effect of nano graphite powder (NGP) and nano silica (NS) on the mechanical properties of concrete. Adding NGP and NS, especially at optimal dosages of 0.3% and 1.5% respectively, significantly improves compressive, flexural, and splitting tensile strength. This enhancement is due to the nano-powder filling gaps and pores within the concrete matrix, resulting in a dense and stronger material [3]. Saha (2017) determined that the compressive strength of concrete-decreases sharply with the addition of fly ash after curing for 28 days [4]. Fly ash decreases the rate of hydration and drying shrinkage of concrete with fly ash is lower than control mix concrete. The absorptivity and chloride permeability are also lower in fly ash concrete [5,6]. The compressive strength, split tensile

strength, and flexural strength are maximum when glass powder is replaced by 10% of cement. 20% cement replaced by glass powder gives satisfactory strength. At 28 days the strength of the control mix, the result of compressive strength, split tensile strength, and flexural strength is 45.5 MPa, 7 MPa, and 8.65 MPa respectively. The feasible replacement of cement by glass powder is 20%. [7]

Nakhi et al (2019) found that the density and air content both decrease with an increase in recycled aggregate as recycled has lower bulk density. The slump of concrete is between 60 to 92 mm. When the content of recycled concrete aggregate is increased, the compressive strength of concrete is decreased. 40% replacement of recycled aggregate with natural aggregate shows satisfactory compressive strength. After 28 days of saturation in chloride, the diffusion of chloride increases with an increase in the content of recycled concrete aggregate. [8]. Another study showed that adding 5% nano-graphite platelets by cement weight to concrete with recycled coarse aggregate improves compressive strength by 3.86% [9].

3 Physical Properties

Physical properties, elemental details, and chemical composition of raw graphite and Acacia gum have been shown in Table 1 respectively [10].

Table 1: Raw graphite and Acacia gum properties

Property	Raw graphite	Acacia gum
Density g/cm^3	2.23	1.4
specific gravity	1.9	1.35
Surface area m^2/g	24	-
Color	Steel grey to black	-
Luster	Metallic	-

4 Workability

As per ASTM C-143, a slump test was performed to check the workability. To attain a slump in between 75-100 mm, several trails were performed. It was observed that a drop of 8.89 %, 21.26%, and 29.82% occurred as the percentage of GNMPs increased from 0 % to 0.1%, 0.3%, and 0.5% respectively as shown in Table 2. The reason for the drop in slump was that GNMPs have more tendency to absorb water and have a greater surface-to-volume ratio.

Table 2: Workability

WORKABILITY		
	Slump (mm)	% Reduction
0% (Control)	98	-
0.10%	90	8.89
0.30%	74	21.62
0.50%	57	29.82

5 Flexural Strength

Table 3 below shows the flexural strength with respect to percentages of GNMPs. It shows the maximum value of 4.76 MPa when 0.3% GNMPs were added to the mix.

Table 3: Results

Control	Flexural Strength MPa
0%	3.85
0.10%	4.31
0.30%	4.76
0.50%	4.48

6 Compressive Strength

As per ASTM C-39. After curing concrete cylinders for 28 days, in Fig 1. compression testing was performed on the Concrete cylinders having size of 100mm x 200mm. For the compression test, the specimen was removed from curing tank after complete curing time. For 24 hours, the specimen was placed in the lab to dry in the air. Afterward, the specimen was placed in a compression testing machine. The load was applied to the cylindrical specimen. The load was applied in a controlled manner so that the loading rate was the same during the whole test. The loading rate applied on the cylindrical specimen was 0.25 MPa/sec. The result in Table 4 shows an increase in the compressive strength of concrete with the addition of GNMP'S.

Table 4: Compressive Strength Test Results

Control	Max Load (KN)	Max Strength (KN)	Max Load (KN)	Max Strength (KN)	Max Load (KN)	Max Strength (KN)	Avg	
							Load (KN)	Strength (MPa)
0%	158.0405	20.1224	155.9228	19.8527	158.2235	20.1457	157.396	20.04
0.10%	222.655	28.3493	133.524	17.0008	172.354	21.9447	176.178	22.432
0.30%	191.45	24.3792	203.2007	25.8724	183.8808	23.4125	192.844	24.555
0.50%	181.4327	23.1008	181.263	23.0791	182.5637	23.2448	181.753	23.142

Figure 1: Compression test assembly

From the results it is concluded that the compressive strength of concrete cylinders after 28 days of curing is 20.04 MPa at 0%. It can be seen in Table 4 that a gradual increase in compressive strength occurs by the addition of GNMPs in concrete cylinders. The compressive strength of graphene concrete cylinders is 22.43 MPa, 24.55 MPa, and 23.14 MPa by the addition of 0.1 %, 0.3 %, and 0.5% GNMP respectively. Optimum compressive strength occurs at 0.3 % of GNMP's; which is 24.55 MPa.

7 Tensile Strength

As per ASTM-C496, a tensile strength test was performed on the concrete beams. The results are shown in Table 5 respectively against the concrete cylinders having no GNMPs.

Table 5: Splitting Tensile Test Results

Control	Max Load (KN)	Max Strength (KN)	Max Load (KN)	Max Strength (KN)	Max Load (KN)	Max Strength (KN)	Avg	
							Load (KN)	Strength (MPa)
0%	141.07	4.491	134.605	4.285	103.7265	3.302	126.467	4.026
0.10%	141.98	4.52	142.61	4.54	143.24	4.56	142.61	4.54
0.30%	150.15	4.78	151.09	4.81	148.58	4.73	149.94	4.773
0.50%	144.81	4.61	144.18	4.59	142.93	4.55	143.973	4.583

From the results it is concluded that the tensile strength of concrete cylinders after 28 days of curing is 4.026 MPa at 0%. It can be seen in Table 6 that a gradual increase in tensile strength occurs by the addition of GNMPs in concrete cylinders. Tensile strength of graphene concrete cylinders is 4.54 MPa, 4.773 MPa, 4.58 MPa by the addition of 0.1 %, 0.3 % and 0.5% GNMP's respectively. The highest tensile strength occurs at 0.3 % of GNMPs; which is 4.773 MPa.

8 Results and Discussion

Adding GNMPs to concrete increases the packing density of the concrete, which leads to a stronger and more durable material. GNMPs also improve the adhesion between the cement and the aggregate, which further strengthens the concrete. Additionally, GNMP's can help to prevent cracks from forming in the concrete. Significantly, the results show that the compressive strength of the concrete cylinders increased from 20.04 MPa to 24.55 MPa when 0.3% GNMPs were added. The tensile strength of the concrete beams also increased from 2.9 MPa to 4.2 MPa when 0.3% GNMPs were added.

9 Conclusion

A comprehensive investigation into the impact of incorporating Graphite Nano-Micro Platelets (GNMPs) on the properties of concrete. The primary objective of the research is to assess how the addition of different percentages of GNMPs influenced the mechanical and durable properties of conventional concrete in comparison to a control specimen. The experimental study involved the use of 0.1%, 0.3%, and 0.5% GNMPs, with a testing duration of 28 days. Adding Nano Graphite to the concrete mixture increased the flexural strength of concrete cylinder by 4.76 MPa at 0.3%

Compressive strength and tensile strength of the concrete cylinders also showed an improvement with the addition of GNMPs, the strength at 0.3% GNMPs reached 24.55 MPa while the control sample achieved 20.04 MPa. The highest tensile strength was observed at 0.3% of GNMPs with a value of 4.773 MPa, compared to the control sample at 4.026 MPa. It is important to note that these research findings provided valuable insights into the potential benefits of GNMPs as a concrete additive, particularly in terms of strength enhancement and improved resistance to water penetration. These findings hold promising implications for the construction industry, where the development of more durable and resilient concrete materials is of utmost importance.

References

[1] H. A. Elaqra, M. a. A. Haloub, R. N. Rustom, and F. K. Alqahtani, "Effect of curing temperature on mechanical behaviour of green concrete containing glass powder as cement replacement," Advances in Cement Research, vol. 33, no. 10, pp. 458–468, Oct. 2021, doi: 10.1680/jadcr.20.00095

[2] K. N. Rahal, "Mechanical properties of concrete with recycled coarse aggregate," Building and Environment, vol. 42, no. 1, pp. 407–415, Jan. 2007, doi: 10.1016/j.buildenv.2005.07.033.

[3] A. Dinesh, S. Yuvaraj, S. Abinaya, and S. Bhanushri, "Nanopowders as an additive for strength and durability enhancement of cement composite: Review and prospects," Materials Today: Proceedings, Apr. 2023, doi: 10.1016/j.matpr.2023.03.651.

[4] S. K. Patel and A. N. Nayak, "Study on Specific Compressive Strength of Concrete with Fly Ash Cenosphere," in Lecture notes in civil engineering, 2020, pp. 561–572. doi: 10.1007/978-981-15-4577-1_47.

[5] Mr. Aditya Agrawal, Mr. Jayesh Shrivastav, Mr. Aditya Lange, and Mr. Sumit Chourasia, "Analysis for Compressive Strength with Fly Ash in Concrete," Journal of civil and construction engineering, vol. 3, no. 3, pp. 1–4, Nov. 2017

[6] M. Kosior-Kazberuk and M. Lelusz, "STRENGTH DEVELOPMENT OF CONCRETE WITH FLY ASH ADDITION," Journal of Civil Engineering and Management, vol. 13, no. 2, pp. 115–122, Jun. 2007, doi: 10.3846/13923730.2007.9636427.

[7] P. Jagadesh, A. Juan-Valdés, M. I. Guerra-Romero, J. M. M.-D. Pozo, J. García-González, and R. Martínez-García, "Effect of Design Parameters on Compressive and Split Tensile Strength of Self-Compacting Concrete with Recycled Aggregate: An Overview," Applied Sciences, vol. 11, no. 13, p. 6028, Jun. 2021, doi: 10.3390/app11136028.

[8] A. B. Nakhi and J. M. Alhumoud, "Effects of recycled aggregate on concrete mix and exposure to chloride," Advances in Materials Science and Engineering, vol. 2019, pp. 1–7, Jun. 2019, doi: 10.1155/2019/7605098.

[9] S. M. Bukhari, M. Ahsan, M. Farhan, and M. Khan, "Enhancement of Concrete Compressive Strength by Introducing NGPs in a Mix with Partially Substituted Recycled Coarse Aggregate for Natural Coarse Aggregate", *TJ*, vol. 3, no. ICACEE, pp. 102-107, Apr. 2024.

[10] H. W. Iqbal, R. A. Khushnood, W. L. Baloch, A. Nawaz, and R. F. Tufail, "Influence of graphite nano/micro platelets on the residual performance of high strength concrete exposed to elevated temperature," Construction & Building Materials, vol. 253, p. 119029, Aug. 2020, doi: 10.1016/j.conbuildmat.2020.119029.

UTILIZATION OF INDUSTRIAL WASTES IN BRICKS AND TUFF TILES

[a] Khawaja Adeel Tariq*, [b] Zeshan Ahmad

a: Civil Engineering Department, University of Engineering and Technology, Narowal, Pakistan. khawaja.adeel@uet.edu.pk
b: Civil Engineering Department, University of Engineering and Technology, Narowal, Pakistan. zeshanashraf464@gmail.com
*Corresponding author.

Abstract- This study aims to address the problem of pollution caused by carbon dioxide emissions from cement production in Pakistan by investigating the feasibility of using waste to produce tuff tiles. The utilization of industrial wastes in clay bricks is also explored. A variety of organic and inorganic wastes are considered potential substitutes for traditional building materials. This study explored different ways to integrate these waste materials into the manufacturing process while maintaining a strong and durable design. The resulting product are carefully evaluated for their overall mechanical performance. The results show that replacing part of the cement in the tuff tiles with waste materials, especially glass powder and marble powder, up to 5%, can achieve good results. Optimum replacement percentage of clay with rice rusk ash in brick is found as 6%.

Keywords- Sustainable Construction Materials, Tuff Tiles, Wastes, Bricks.

1 Introduction

In Pakistan, clay bricks and tuff tiles are fundamental components of construction. However, the burning of clay bricks uses coal, and tuff tiles have a component which is cement; both are linked to considerable negative effects on the surrounding ecosystem, including carbon dioxide (CO_2) emissions, which is also one of the major causes of ozone depletion, affecting human health and the environment for other living beings.

Researchers have investigated the use of waste materials on the mechanical properties, energy efficiency, and environmental impact of the bricks. Results indicate that incorporating these waste materials into clay bricks can lead to a reduction in energy consumption during firing, improved mechanical strength, and decreased environmental footprint, making them eco-friendly and economical alternatives to conventional clay bricks [1].

Over the past decade, several researchers have explored novel construction techniques to develop efficient and affordable solutions for sustainable tuff tiles. Mortar with waste rice husk ash showed improved strength activity index and reduced bulk density with waste Rice hush ask (RHA). RHA because of its fine size can be used in improving the mechanical behavior of soil. Researchers have found beneficial usage of rice husk ash for the purpose of ground improvement. is also used as a soil improvement agent with cement. The experiment on use of rice husk ash as a partial replacement of cement to be used in deep soil mixing has shown promising results [2].

Ceramic Wastes Powder (CWP) is also used in brick kiln industries as a partial replacement of clay in bricks. The findings indicated that incorporating CWP led to enhanced durability of the bricks. It's used is found beneficial in improving the efflorescence and also resistance against acid attacks. Moreover, the bricks displayed reduced porosity and a compact microstructure [3]. Plastic paver blocks were created from plastic bag waste. The results are compared with concrete paver block. It was concluded that plastic paver block is not only sustainable but also exhibit similar strength properties [4].

Dust waste generated during the sizing of volcanic tuff stones are used as an alternative raw material for industrial floor tile manufacturing. Comparing the properties of tiles before and after firing, it was found that incorporating 5 wt. % tuff waste into the industrial formulation yielded the highest green strength (9.83 MPa) and fired strength (26.77 MPa) values,

along with the lowest water absorption rate (5.77) [5]. Glass powder and marble powder have been used by the researchers in enhancing the durability and mechanical behavior of concrete and bricks. Optimum usage of marble powder and glass powder was observed as 10% [6] and 15% [7] respectively.

The issue of producing various unutilized byproducts from industries and agriculture sectors, such as inorganic wastes of plastic, glass, marble, stones, etc. are causing environmental concerns in Pakistan as shown in following Figure 1 [8]. The major sources of waste generation in Pakistan are from food, yard, and construction. Waste from Waste generation estimates of Urban and Rural areas of Punjab are shown in Table 1 [9]. The efficiency of our mechanism for controlling waste generation and disposal is minimal.

Table 1: Waste Generation Estimates (reproduced)

Typology	Waste Generated (kg per capita)	Waste Generated (Metric Ton per year)	Collection (% of generated)	Disposal (% of collected)
Large Cities	0.55	9.44	80	0
Mid and small sized cites	0.42	4.44	50-70	0
Rural communities	0.33	13.72	<20	0

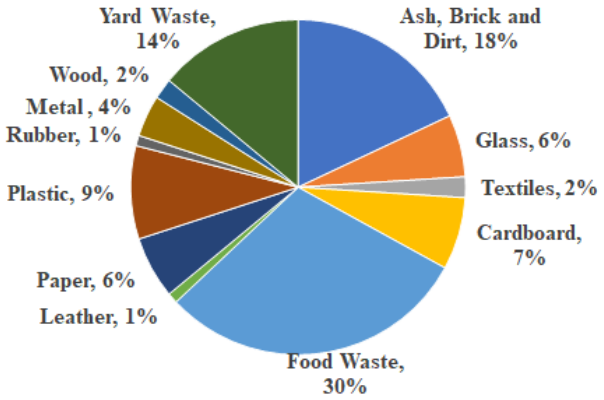

Figure 1: Composition of waste generation in Pakistan (reproduced)

Most of the industries are using conventional techniques in the production of tuff tiles i.e. without employing any compaction pressure. Whereas, some industries are now shifted to automated process of manufacturing with compaction to ensure durable tuff tiles.

The purpose of this research study is to explore the possibilities of utilization of industrial wastes in bricks and tuff tiles. Eco-friendly tuff tiles and bricks are more than just construction materials; they represent our commitment towards a better sustainable future. It will offers a durable, aesthetically pleasing solutions that seamlessly blend into our surroundings, making our cities more livable and eco-conscious.

2 Materials and Methods

2.1 Materials

Cement, sand, aggregate are used in conventional tuff tiles. Waste materials (plastic, marble powder and glass powder) were used as a partial replacement of cement and clay in bricks. Sargodha crush and Chenab sand was used in the production of tuff tiles. Tuff tiles are available in market in numerous designs with commonly used thickness of 60 mm. The dimension of casted tuff tiles was 200(L) x 100(W) x 60(T) mm. The strength of control specimen of tuff tiles and brick was 28 MPa and 3.0 MPa respectively. After preliminary investigation, marble powder, glass and plastic was decided to be used as partial replacement of cement in the tuff tiles, and rice husk ash and baggase ash as partial replacement of clay in the bricks.

2.2 Methods

In order to access the actual situation of the tuff tiles and brick industries of Gujranwala Division, industries were visited. Samples from various industries were collected and tested in laboratory for density, water absorption and compression test. It is observed that compressive strength of some of the collected specimens are below the target strength as advertised by the manufactures. The ratios of replacement of cement and clay is selected as 5%, 10% and 15% by weight. These ratios are decided based on previous studies in similar research areas [6,7].

3 Results and Discussions

Water absorption and compression tests were performed on the collected and casted specimens.

3.1 Density

It was observed that the average density of the collected brick and tuff tiles specimens was about 2.0 g/cm^3 and 2.25 g/cm^3 respectively. The casted bricks and tuff tiles optimum density with replacement of selected wastes was about 1.7 and 2.0 g/cm^3 respectively. Figure 2(a), shows the effect on density of tuff tiles for various wastes replacement levels. It was observed that effect on density was minimum for various replacement levels. The lower density was likely due to non-compaction/vibration of casted tuff tiles specimens.

3.2 Water Absorption Test

It was observed that the average water absorption of the collected tuff tiles and bricks was about 6 to 8% and 8 to 12% for bricks respectively. The casted bricks and tuff tiles optimum water absorption with replacement of selected waste was about 16 to 18 % and 4 to 6% respectively. Figure 2(b), shows the effect on water absorption of tuff tiles for various wastes replacement levels. It was observed that water absorption increases with the increase in replacement level of wastes. The lower values were observed in marble and glass powder. It was due to its fine content that results in a better interlocking of the fine aggregates and thereby improving the composite matrix.

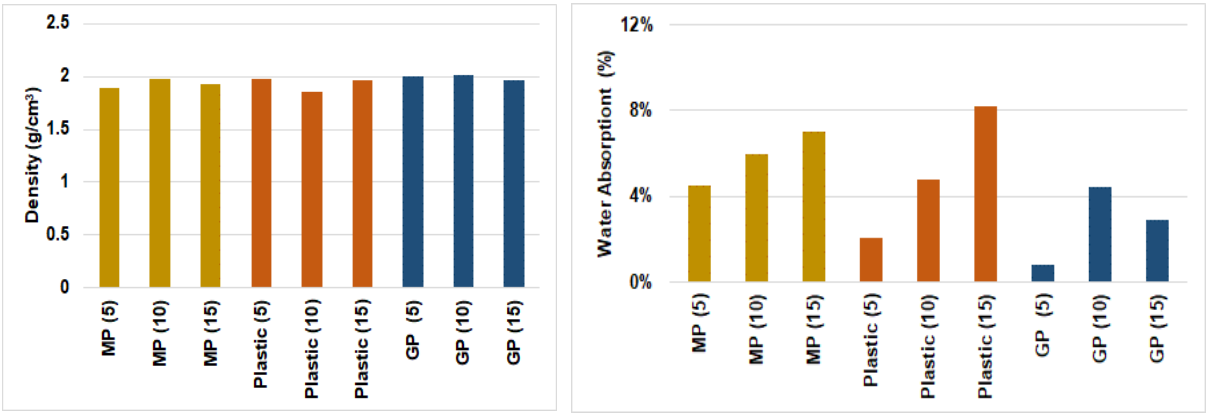

a) *b)*

Figure 2: Variations with addition of Marble powder (MP), Plastic and Glass powder (GP) in a. density and, b. water absorption (Replacement percentages are mentioned in brackets).

3.3 Unconfined Compression Test

Uniaxial compression test was performed on controlled (5.0 MPa and 28 MPa for bricks and tuff tiles respectively) and tuff tiles and brick specimens prepared from various wastes. Optimum result in compressive strength was observed for tuff tiles having Plastic and Glass powder as partial replacement of cement, and rice rusk ash for bricks as shown in Figure 3. Glass powder is finer as compared with plastic used for tuff tiles preparation, whereas rice husk ash imparts pozzolanic effect in the bricks.

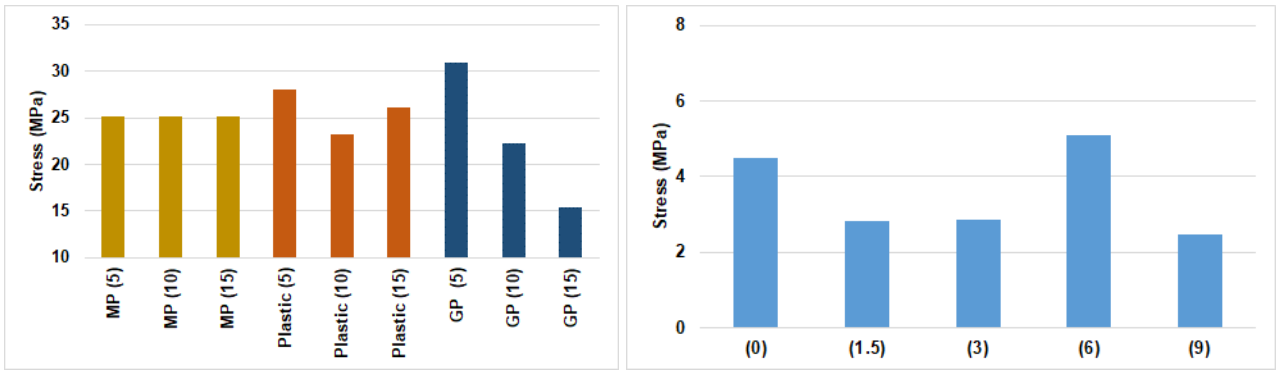

a) *b)*

Figure 3: Variations in unconfined compressive strength with addition of a. Marble powder (MP), Plastic and Glass powder (GP) in tuff tiles and, b. Rice husk ash in brick (Replacement percentages are mentioned in brackets).

4 Practical Implementation

Brick and Tuff tiles are most commonly used building material. Millions of tons of solid waste is generated in Pakistan. By utilizing the waste in bricks and tuff tiles, can results not only economically friendly bricks but also a sustainable solution for developing countries like Pakistan.

5 Conclusion

It is observed from experimentation that the waste used is beneficial in producing sustainable bricks and tuff tiles. However, with increase of replacement percentage effects the durability of the products. The optimum percentage of replacement was found as 5 to 10% for bricks and tuff tiles using rice husk ash and glass powder; marble powder respectively.

Acknowledgment

The research is financially supported by Higher Education Commission Pakistan through National Research Grant Program for Universities (NRPU-16783) and by Pakistan Engineering Council Award for Final Year Design Projects.

References

[1] R.D.A. Hafez, B. A. Tayeh and R.O. Al Ftah, "Development and evaluation of green fired clay bricks using industrial and agricultural wastes," Case Studies in Construction Materials, vol. 17, pp. 1-20, 2022.
[2] S.S. Hossain, L. Mathur and P.K. Roy, "Rice husk/rice husk ash as an alternative source of silica in ceramics: A review," Journal of Asian Ceramic Societies, vol. 6, pp. 299-313, 2018.
[3] M.H. Riaz, A. Khitab, S. Ahmad, W. Anwar and M.T. Arshad, "Use of ceramic waste powder for manufacturing durable," Asian Journal of Civil Engineering, vol. 21, pp. 243-252, 2019.
[4] J. Ghuge, S. Surale, B.M. Patil and S.B. Bhutekar, "Utilization of waste plastic in manufacturing of paver blocks," International research journal of engineering and technology, vol. 6(4), pp.1967-1970, 2019.
[5] S. Akpınar and S. T. Anli, "Using volcanic tuff wastes instead of feldspar in ceramic tile production," Journal of Material Cycles and Waste Management, vol. 25, pp. 2159-2170, 2023.
[6] K. Khan, W. Ahmad, M.N. Amin, A. Ahamd, S. Nazar, A.A. Alabdullah and A.M.A. Arab, "Exploring the use of waste marble powder in concrete and predicting its strength with different advanced algorithms," Materials, vol. 15(12), pp. 1-28.
[7] K.L. Jain, G. Sancheti and L.K. Gupta, "Durability performance of waste granite and glass powder added concrete," Construction and Building Materials, vol. 252, pp. 1-11, 2020.
[8] United Nations Environment Programme, report on waste management in Pakistan (https://www.trade.gov/country-commercial-guides/pakistan-waste-management#).
[9] Center for peace and development intitaives, "Punjab's waste woes: a look at solid waste management, sanitation, and water supply", 2022.

PERFORMANCE EVALUATION OF SELF-CURED BIO GEO-POLYMER CONCRETE REGARDING MECHANICAL STRENGTH AND DURABILITY

[a] Ahmad Ali Sial*, [b] Faisal Shabbir

a: Civil Engineering Department, University of Engineering and Technology Taxila, engineerahmadali122@gmail.com
b: Civil Engineering Department, University of Engineering and Technology Taxila, faisal.shabbir@uettaxila.edu.pk
* Corresponding author.

Abstract- The process of geo-polymerization widely occurs by heat or steam curing of geopolymer concrete (GPC) to improve its mechanical properties. Heat curing is the usual method for the development of its strength, which poses a challenge for in-field applications. This study emphasizes preparing fly ash based geopolymers under ambient settings without an external heat source. Using low calcium fly ash and 20% ordinary Portland cement (OPC) accelerates the curing of geopolymer concrete, eliminating the requirements for enhanced heat applications. During the experimental phase, samples were cured at room temperature (25 oC) and relative humidity of 65 ± 10%. Additionally, self-curing of geopolymers has been investigated in ambient curing conditions by utilizing bio additives including Terminalia chebula and natural sugar (honey). To achieve desired mechanical properties, such as compressive strength, optimized percentages of these bio additives have been determined. Moreover, durability properties of the GPC have been analyzed by conducting sorptivity test on the specimen. Both bio-additives were incorporated in different percentages by the weight of aluminosilicate minerals and prepared mixes of geopolymer concrete i.e. GPC1 and GPC2 respectively. Experimental results showed that GPC2 prepared by adding 1.5 % Terminalia chebula and 0% honey has improved the compressive strength by 3.10% as compared to controlled specimen (GPC0) cured at ambient conditions for 28 days. Durability analysis showed that with these percentages of Terminalia chebula and honey, the sorptivity coefficient (S) obtained for GPC2 is 1.88% less in comparison to controlled specimen GPC0, indicating the improved durability properties of prepared geopolymer concrete.

Keywords: Bio Additives, Geo-polymerization, Geopolymer Concrete, Mechanical Properties, Sorptivity Coefficient.

1. Introduction

The production of ordinary Portland cement, also known as OPC, uses a significant amount of thermal energy and accounts for 5-8 percent of global greenhouse gas emissions. An analysis of the emissions showed an alarming ratio of 1 - emissions of carbon dioxide and cement output. [1]. Based on a 5% annual growth rate, the forecasts indicated that global production would reach 4.38 billion tons by 2050[2]. For regular Portland cement concrete, there is an alternate low ecological footprint option called "Geo polymers."[3]. Waste aluminosilicate was used as the foundation material to create geopolymers[4]. Rich in silica (Si) and alumina (Al), minerals can be utilized as an initial source for polymerization reactions when they encounter alkaline solutions like hydroxides and silicates of alkalis.[5]

The procedure is generating polymeric chains of the three-dimensional.[6] It was discovered that the inclusion of calcium to a geopolymer material structure (OPC) improved its properties both when specimens were cured at room temperature and when they were cured at a temperature [7][2]A few research used room-temperature geopolymer

concrete that had OPC added to it. Instead of using additional heat, geopolymer concrete dried quicker when less calcium-rich fly ash was used in place of part of the OPC in the entire binder [8]. The current study significantly focuses on the effects of partially substituting fly ash with OPC, a rate of 20% in a temperature-cured system of low-calcium fly ash-based geopolymer concrete [9]. Moreover, incorporation of bio additives in the GPC mixes is an important consideration for studying mechanical strength under ambient curing conditions.

2. Materials and the Methods

The materials used in this study include: Fly ash (Class F, low calcium) from a thermal power station in Muzaffargarh, Punjab, Pakistan; Ordinary Portland Cement (OPC) from Best Way Cement Factory, added up to 20% as a source of calcium; aggregates (fine and coarse) from Margalla crush, tested in UET Taxila concrete laboratory; alkaline liquid (sodium silicate and sodium hydroxide flakes, 98% pure) mixed to create 8M NaOH solutions; superplasticizer (naphthalene sulphonate-based, available from local traders); and bio-additives (honey, and Terminalia chebula, purchased from local vendors and added in various proportions).

3. Methodology

3.1. Manufacturing Procedure of Geopolymer Concrete

Details on the mix design for the geopolymer concrete were provided in Table 1. The geopolymer concrete mix design consisted of 80% fly ash and 20% OPC. The silicate ratio was adjusted to 2.5, and the alkaline liquid to aluminosilicate ratio was fixed at 0.45. Honey and Terminalia chebula were added as bio-additives, and additional water and superplasticizer. The mixes were cured at 25 ± 3°C and 65 ± 5% humidity after demolding at one day. In

Table 2, GPC0 is the control mix which includes the standard GPC components without any additives such as Terminalia Chebula or honey. GPC1 contains the base GPC components along with 1.5% honey. GPC2 incorporates 1.5% Terminalia Chebula into the base GPC components, without honey.

Table 1: Ingredients for geopolymer concrete

Mix ID	Fly Ash: (kg/m³)	Cement (kg/m³)	Fine Aggregate (kg/m³)	Coarse Aggregate (kg/m³)			(NaOH) solution (kg/m³)	(Na_2SiO_3) solution (kg/m³)	Super-plasticizer (kg/m³)
				20 mm	12 mm	6mm			
GPC	320	80	546	382	528	364	51	129	7.9

Table 2: Various proportions of Bio-additives used for the preparation of geopolymer concrete mixes.

MIX ID	Geopolymer (GPC)	Terminalia Chebula	Honey
GPC0	Alkaline liquids, superplasticizer, fly ash and cement, fine and coarse aggregate.	0%	0%
GPC1		0%	1.5%
GPC2		1.5%	0%

4. Results and Discussions

4.1. Compressive Strength Test

Three cubic samples of geopolymer concrete of size 150 mm X 150 mm X 150 mm were subjected to a compressive strength test in accordance with ASTM C109/C109M – 12 after a curing period of 28 days. The compressive strength

outcomes of tests are displayed below in figure 1. The compressive strength values obtained for geopolymer concrete specimen is of the following order from maximum to minimum: GPC2>GPC0>GPC1

In GPC1 there is only a percentage of Honey. The compressive strength decreases by 3.10% as compared to controlled specimen GPC0. This is because honey is a humectant, and its presence has introduced excess moisture resulting in an increased water-to-geopolymer binder ratio, leading to a weaker concrete structure. Additionally, honey contains sugars that can react with the alkaline properties of the geopolymer binder, forming expansive compounds that cause internal stresses and reduce compressive strength. In **GPC2,** there is only percentage of Terminalia chebula (TC) resulting in increase in the compressive strength by 2.99% as compared to controlled specimen GPC0. The possible reasons include TC promotes the formation of calcium silicate hydrates (CSH), a key component of geopolymer concrete that contributes to its strength and durability.

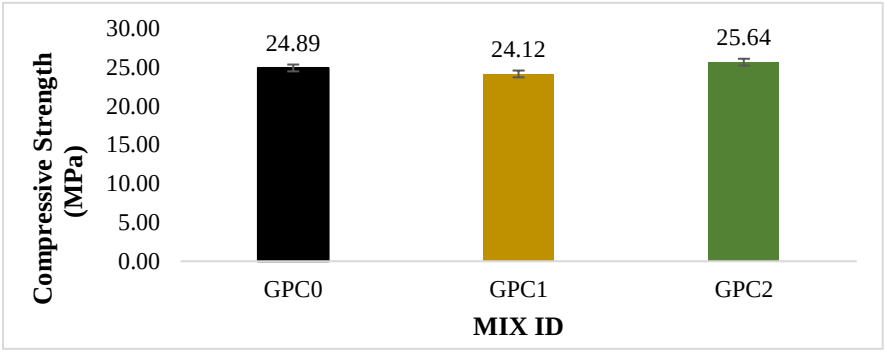

Figure 1: Compressive strength of various mixes of GPC.

4.2. Sorptivity Test

For the sorptivity test, three cylindrical specimen of 200 mm diameter and 100 mm height of geopolymer concrete have been casted and tested as per ASTM C 1585.The present research provides guidance about the geo polymer's ability to resist water penetration, which is crucial for assessing its durability. The outcomes obtained from the sorptivity test are presented in figure 2. The sorptivity coefficient is a measure of the capacity of a porous material to absorb fluids, such as water. It is typically measured in units of mm/√min or cm/√sec. Here's the mathematical representation ((**1**) used for calculating the sorptivity coefficient:

$$\textbf{Sorptivity Coefficient (S)} = \left(\frac{I}{\sqrt{t}}\right) \quad (1)$$

Where, **S** is the sorptivity coefficient in mm/√min or cm/√sec, *I* represent the cumulative absorption (mm or cm) and t is the time in minutes or seconds observed for evaluating the cumulative absorption values of specimen [7].

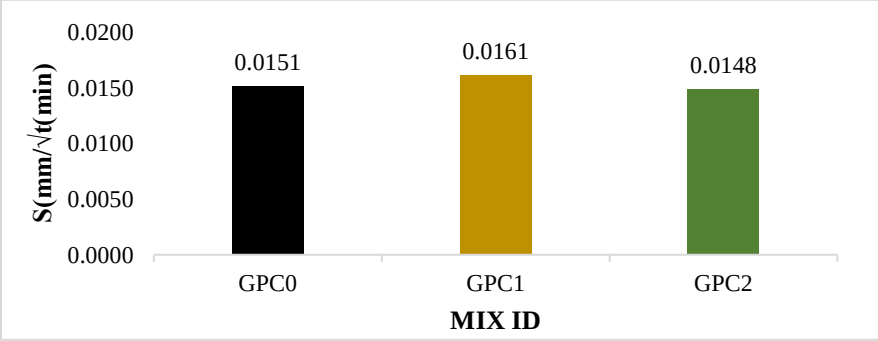

Figure 2: Sorptivity coefficient of various mixes of GPC.

In GPC1, there is only 1.5% honey, as a result the sorptivity coefficient increases by 6.42% as compared to controlled specimen GPC0. Honey is a humectant, which means it attracts and retains water. This increases the water content in the geopolymer concrete, leading to higher sorptivity. Similarly, GPC2 contains only 1.5% Terminalia chebula (TC) in geopolymer concrete, the sorptivity coefficient decreases 1.88% as compared to controlled specimen GPC0. Terminalia chebula (TC) contains corilagin which is known for their water-repelling properties, reducing water absorption and sorptivity.

5. Conclusion

Experimental results demonstrated that adding 1.5% Terminalia chebula to geopolymer concrete significantly improved its mechanical properties by enhancing the formation of calcium silicate hydrates, a key component of geopolymer concrete. This resulted in a 2.99% increase in compressive strength, indicating a notable improvement in the material's ability to withstand axial loads. Additionally, the inclusion of Terminalia chebula reduced the sorptivity coefficient by 1.88% due to its water-repelling properties. The increases and decreases in strength and durability obtained in the study are much smaller and fall within the limits of statistical errors. This study highlights the potential of Terminalia chebula as a natural additive for improving strength and durability, contributing significantly to the field of civil engineering.

Acknowledgment

I owe immense gratitude to Engr. Muhammad Arsalan, my colleague, for providing the opportunity and guidance throughout the research. His technical and moral support during the study was invaluable.

References

[1] R. Manjunath and R. V. Ranganath, "Performance Evaluation of Fly-ash based Self-compacting geopolymer concrete mixes," in *IOP Conference Series: Materials Science and Engineering*, 2019. doi: 10.1088/1757-899X/561/1/012006.

[2] R. Pantawane and P. K. Sharma, "Evaluation of Mechanical Properties of Metakaolin Geo-Polymer Concrete," in *Lecture Notes in Civil Engineering*, 2023. doi: 10.1007/978-981-19-4731-5_25.

[3] R. Andalib *et al.*, "Geo-polymer Bacterial Concrete Using Microorganism," *Journal of Environmental Treatment Techniques*, vol. 3, no. 4, 2015.

[4] I. Patel and S. Thakkar, "Geo-polymer Mortar as Retrofitting Material for R.C. Element," *Mater Today Proc*, 2023, doi: 10.1016/j.matpr.2023.09.130.

[5] UU Republik Indonesia *et al.*, "PENENTUAN ALTERNATIF LOKASI TEMPAT PEMBUANGAN AKHIR (TPA) SAMPAH DI KABUPATEN SIDOARJO," *Energies (Basel)*, vol. 15, no. 1, 2022.

[6] R. Andalib *et al.*, "Geo-polymer Bacterial Concrete Using Microorganism," *Journal of Environmental Treatment Techniques*, vol. 3, no. 4, 2015.

[7] M. A. Memon, Bashir Ahmed Memon, Shahzeb Khan Jamali, Ali Arsalan Memon, and M Umair Bhatti, "Effect of Recycled Coarse Aggregates (RCA) on Geo-Polymer-Based Concrete," *Sir Syed University Research Journal of Engineering & Technology*, vol. 13, no. 2, 2024, doi: 10.33317/ssurj.542.

[8] K. M. Haneefa, M. Santhanam, and F. C. Parida, "Performance characterization of geopolymer composites for hot sodium exposed sacrificial layer in fast breeder reactors," *Nuclear Engineering and Design*, vol. 265, 2013, doi: 10.1016/j.nucengdes.2013.09.004.

[9] I. M. Aashaq and M. Z. Ul Haq, "A Sustainable Approach to Geopolymer Concrete Utilizing Waste Materials Including Plastic Waste," in *AIP Conference Proceedings*, 2024. doi: 10.1063/5.0196296.

TENSILE STRENGTH OF TEXTILE WASTE COMPOSITE

[a] Noor Aina Misnon*, [b] Faridah Hanim Khairuddin

a: Faculty of Engineering, Universiti Pertahanan Nasional Malaysia, Kuala Lumpur, Malaysia. nooraina@upnm.edu.my
b: Faculty of Engineering, Universiti Pertahanan Nasional Malaysia, Kuala Lumpur, Malaysia. hanim@upnm.edu.my
* Corresponding author.

Abstract- The increasing numbers of textile waste in Malaysia are alarming when in 2018 approximately 195300 tonnes of textile waste were dumped and occupied about 6.3% of the landfills. Textiles made of synthetic fibers such as nylon, lycra, polyvinyl chloride, polyurethane, and spandex could be detrimental to the environment and take up to 200 years to decompose in landfills. The tensile strength of the textile could achieve up to 800 MPa and potentially be used as retrofitting materials. This study aims to utilize textile waste as one of the structural retrofitting materials with specific objective to determine the tensile strength of two types of textile waste (cotton and nylon) layered with epoxy namely textile waste composite (TWC). The tensile strength of TWC of with different layers (1 layer, 2 layers, and 3 layers) was determined by conducting a tensile test. The TWC of nylon textile showed better strength than cotton textile with tensile stress value up to 17.9 MPa. This material is possible for low-cost concrete retrofitting materials options in improving or restoring the capacity of structures.

Keywords- Cotton, Nylon, Sustainability, Textile Waste Composite, Tensile Strength.

1 Introduction

In 2018, Malaysia recorded 195,300 tonnes of textile waste that constituted about 6.3% of the total waste in landfills [1]. Over 60% of the dumped textile was composed of synthetic materials which take decades up to 200 years to decompose. Synthetic textiles like polyester, nylon, and acrylic are derived from petrochemicals and are known for their durability and resistance to wrinkles and moisture. However, the non-biodegradable nature of the synthetic textiles poses environmental challenges due to difficulty to breaking down the fibers [2]. On the other hand, the hydrophobic feature of synthetic fibers and could achieve up to 830 MPa of tensile strength makes this material a promising candidate to be incorporated into building construction materials [3].

Utilization of textile waste in engineering field has been explored and showed promising outcomes [4], [5], [6], [7]. Combination of cotton, polyester mixed waste and natural rubber successfully developed sustainable sound insulation material where the acoustic performance was comparable to commercially sound insulation panels [4]. It was reported that the addition of waste woven polypropylene fiber and textile mesh in the production of gypsum board showed post-peak behavior improvement and lead to a more ductile material which can be used for sustainable finishes in construction [5]. Kamble and Behera [6] employed cotton fibres to produce hybrid composite with significant improvement of tensile, flexural and impact strength which can be replaced the low and medium-cost timber in building materials.

A common building material for most infrastructure and building construction is concrete. Concrete is a strong and durable, yet long service might cause concrete deterioration that can affect the ultimate capacity of the concrete elements. Thus, concrete retrofitting is necessary to at least restore the structural capacity. Concrete retrofitting refers to the process of enhancing or upgrading existing concrete structures to improve their performance, durability, safety, or functionality using various techniques such as fiber reinforcement, external post tensioning, and base isolation. Typical structural retrofitting work is using steel due to its high tensile strength. However, the drawback of steel is the risk of rust when exposed to water. This could lead to poor strength and appearance. Fiber reinforced polymers are other options due to excellent performance and easy installation for the retrofitting work, yet the cost has become a concern [8].

Thus, this study was carried out by utilizing textile waste and epoxy as retrofitting materials which were later known as textile waste composite (TWC). This paper presents a part of the study that provides information on tensile strength of two types of textiles.

2 Research Methodology

2.1 Sample Preparation and Testing

Two types of textiles were used to prepare the samples, i.e., cotton (T) and nylon (N) for tensile testing. A total number of 24 samples consisting of control sample (C), one layer (1-L), two layers (2-L) and three layers (3-L). For the 1-L, 2-L and 3-L samples, the textiles were layered with epoxy. Figure 1 shows the arrangement of the TWC samples. All the sample were cut into dog-bone shape (see Figure 2) as recommended by ASTM E8 [9]. The TWC samples were air cured up to 72 hours prior to the testing. The tensile test was conducted according to the ASTM E8 [9] using universal testing machine (UTM). The displacement of the samples was measured using linear variable displacement transducer (LVDT).

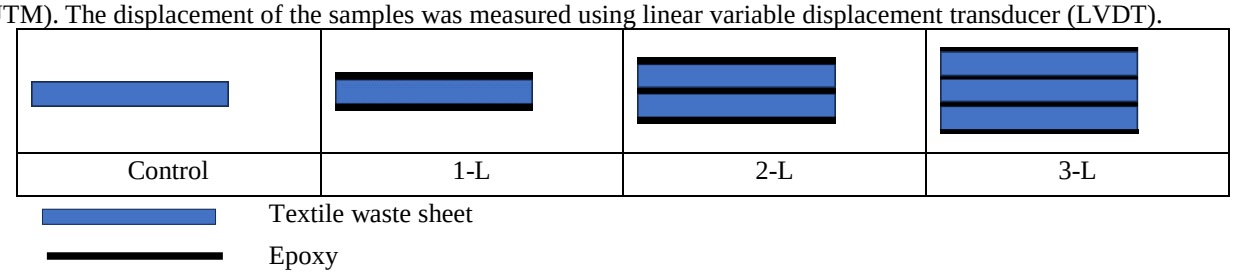

Figure 1: TWC sample arrangement

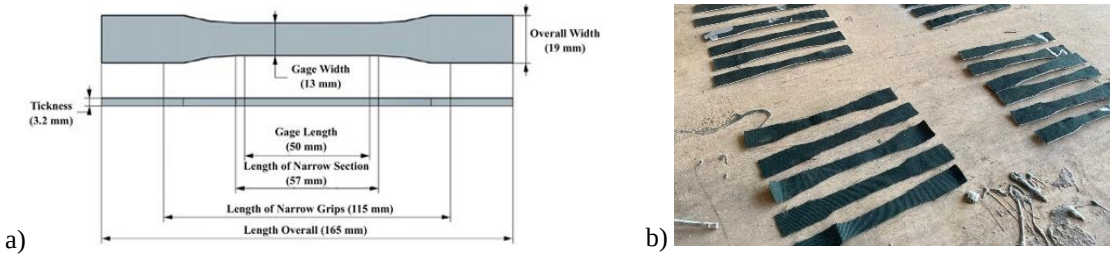

Figure 2: Dog-bone shape, a. dimension, and b. TWC sample

3 Results

3.1 Mode of Failure of TWC Samples

From the observation, the samples showed three different failure mode which can be classified as textile failure (TXF), epoxy failure (EXF) or total failure (AF) (see Figure 3). The TXF failure occurred on TWC sample when the textile tears into two parts due to gradual loss of load carrying capacity. The control sample for both types of textiles (CT and CN) and 2-LT sample exhibit the TXF failure. The EXF failure was observed on 1-LT sample when the layer of epoxy failed first. The remaining samples for both cotton and nylon (coated and uncoated) showed AF failure when both textile and epoxy break together.

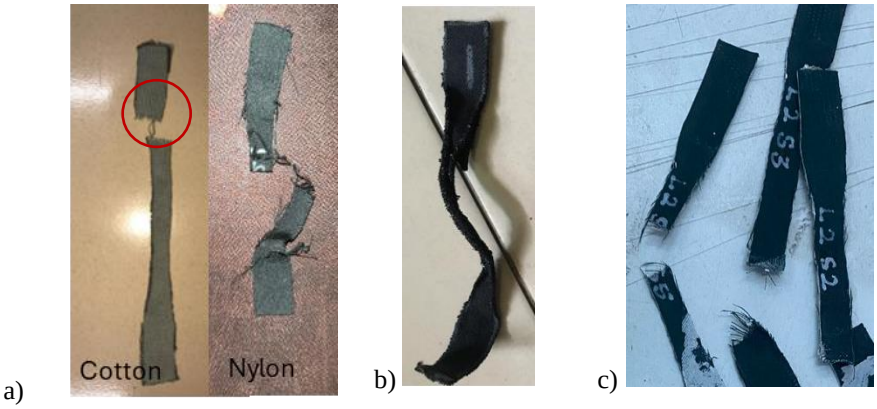

Figure 3: Mode of failure of TWC samples, a. textile failure (TXF), b. epoxy failure (EXF), c. total failure (AF)

3.2 Load-Displacement Curve

Figure 4 shows load-displacement curve of TWC samples. In general, all the TWC samples show ductility pattern with elongation before failure. The strength of TWC samples increased with increment of textile layer for both cotton and nylon samples. It can be observed that uncoated nylon has higher tensile strength with maximum loading of 240.7 N while uncoated cotton sample only achieved about 54.6 N. All the nylon samples show higher maximum load when compared to the cotton samples with the highest maximum tensile load of approximately 1100 N for the 3-LN sample. This suggest that the 3-LN sample has better ductility and might be used for application that requires high strength and flexibility. All the cotton samples experienced large elongation more than 60 mm when compared to the nylon samples.

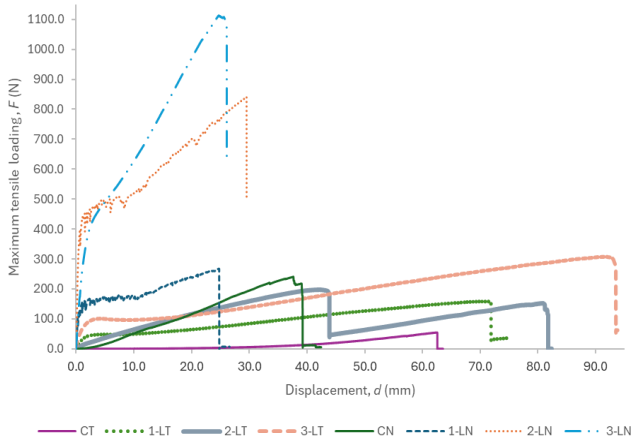

Figure 4: Load-displacement curve of TWC samples

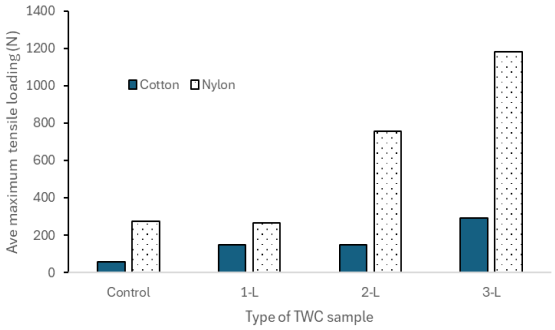

Figure 5: Maximum tensile loading of the TWC samples

3.3 Tensile Strength of TWC Samples

Tensile test results of the TWC samples are summarized in Table 1. All nylon textile samples showed higher tensile strength value when compared to cotton textile samples (see Figure 5). It was predicted since the nylon textile is categorized as synthetic fibre which has long strands and hydrogen bonds with strong intermolecular forces while cotton textile composed of cellulose which has a weaker bond [10]. For both cotton and nylon textile samples, 3-L samples exhibit the highest maximum tensile loading with value of 291.5 N and 1183.3 N, respectively. The presence of epoxy assists in strength and stress improvement of the TWC with a positive linear pattern can be observed for both types of TWC textile. For the cotton textile, the strength of 2-LT sample slightly reduces to 30% that might be resulted from inadequate bond intact between the textile and epoxy.

Table 1: Summary of tensile test of TWC samples

Sample	Uncoated/ Coated	n	Types of failure	Average maximum tensile loading (N)	COV (%)	Average Tensile stress at break (MPa)	COV (%)
CT	uncoated	3	TXF	55.9	15	0.5	20
1-LT	coated		EXF	148.8	10	6.4	9
2-LT			TXF	147.5	23	3.8	11
3-LT			AF	291.5	11	7.4	6
CN	uncoated		TXF	273.3	34	0.1	23
1-LN	coated		AF	263.3	13	0.2	30
2-LN			AF	756.7	10	12.4	10
3-LN			AF	1183.3	4	17.9	8

Note: **n** = number of tested samples; **COV** = Coefficient of variation

4 Application

The retrofitting procedure is performed on deteriorated structures with the aim of restoring the load-carrying capacity of the structural elements. Fibre-reinforced polymer is currently a favorable material to be used for retrofitting since it does not only restore the capacity but also improves the performance of the structures, yet the cost becomes a concern. This study was carried out as a pilot to utilize textile waste as a potential material for non-structural or/and structural retrofitting purposes. Further research on the application of the TWC is suggested on small scale beam or panel with various methods of retrofitting installation such as TWC wrapping or near surface mounted.

5 Conclusion

A pilot study was carried out to unleash the potential of textile waste to be utilized as structural retrofitting materials. Cotton and nylon textile waste were layered with epoxy resin to produce TWC retrofitting materials and undergo tensile strength tests. It can be inferred that:

1. The use of epoxy assists in tensile strength improvement for both cotton and nylon TWC samples.
2. TWC of nylon showed better performance when compared to cotton due to strong bond molecules formation of the nylon textile.
3. The highest tensile strength for both cotton and nylon textile were obtained from 3-L TWC samples with maximum load increments up to 400% compared to the control sample.

Further investigation on the development of the TWC material using different textiles and epoxy is required.

Acknowledgment

This research was funded under grant SF0133 – UPNM/2023/SF/TK/2. The careful review and constructive suggestions by the anonymous reviewers are gratefully acknowledged.

References

[1] S. N. H. Syed Abdul Khalid, "Reducing textile waste is everyone ' s responsibility," *New Straits time*, 2021. [Online]. Available: https://www.nst.com.my/opinion/letters/2021/12/752229/reducing-textile-waste-everyones-responsibility#:~:text=In 2018%2C Malaysians dumped a,the second most polluting industry.

[2] A. Patti and D. Acierno, "Fibers Waste in Textiles , Their Recycling and Applications in Composites," *Trends Textile Eng Fashion Technol.*, vol. 6, no. 1, pp. 704–706, 2020, doi: 10.31031/TTEFT.2020.06.000628.

[3] S. S. Rahman, S. Siddiqua, and C. Cherian, "Sustainable applications of textile waste fiber in the construction and geotechnical industries: A retrospect," *Clean Eng Technol*, vol. 6, no. January, p. 100420, 2022, doi: 10.1016/j.clet.2022.100420.

[4] D. G. K. Dissanayake, D. U. Weerasinghe, L. M. Thebuwanage, and U. A. A. N. Bandara, "An environmentally friendly sound insulation material from post-industrial textile waste and natural rubber," *Journal of Building Engineering*, vol. 33, Jan. 2021, doi: 10.1016/j.jobe.2020.101606.

[5] R. Alyousef, W. Abbass, F. Aslam, and M. I. Shah, "Potential of waste woven polypropylene fiber and textile mesh for production of gypsum-based composite," *Case Studies in Construction Materials*, vol. 18, Jul. 2023, doi: 10.1016/j.cscm.2023.e02099.

[6] Z. Kamble and B. K. Behera, "Sustainable hybrid composites reinforced with textile waste for construction and building applications," *Constr Build Mater*, vol. 284, p. 122800, 2021, doi: 10.1016/j.conbuildmat.2021.122800.

[7] R. Yadav and Z. Kamble, "Textile waste-based cellulose composites: a review," May 01, 2024, *Springer*. doi: 10.1007/s10853-024-09585-6.

[8] C. Del Vecchio, M. Di Ludovico, and A. Prota, "Cost and effectiveness of fiber-reinforced polymer solutions for the large-scale mitigation of seismic risk in reinforced concrete buildings," *Polymers (Basel)*, vol. 13, no. 17, 2021, doi: 10.3390/polym13172962.

[9] ASTM E8/E8M (2013). Standard test methods for tension testing of metallic materials, *American society for testing and material*.

[10] D. Pogue, "Breaking Point : Testing Tensile Strength," 2010

BOND BEHAVIOR OF DEFORMED STEEL REBAR EMBEDDED IN A RECYCLED BRICK AGGREGATE CONCRETE

[a] Muhammad Subhan*, [b] Huzaifa Nadeem

a: Civil Engineering Department, University of Engineering & Technology, Lahore, Pakistan. mughalsubhan919@gmail.com
b: Civil Engineering Department, University of Engineering & Technology, Lahore, Pakistan. huzaifacivil34@gmail.com
* Corresponding author.

Abstract The demolition of old structures creates a lot of waste, particularly in Asian countries, producing brick waste as most of the old structures are made of brick, which needs to be tackled. Researchers have tried to use it as aggregate in concrete and study its effect on different concrete properties. In this study, the bond behavior of steel rebar with recycled brick aggregate concrete (RBC) has been studied and compared with natural aggregate concrete (NAC) and recycled aggregate concrete (RAC). For this purpose, a number of cubes were cast along with cylinders to relate the effect of compressive strength with bond strength. Two types of ratios were chosen: one is R50%-50%, containing 50% coarse and 50% fine aggregate, and the second is R33%-67%, containing 33% coarse aggregate and 67% fine aggregate. A cement content of 20% by weight of aggregate was used. It was found that for the ratios R33%-67% and R50%-50%, the bond strength of RBC is 24% and 13% more than that of RAC, respectively. For the ratios R33%-67% and R50%-50%, the bond strength of RBC is 9% and 60% less than that of NAC, respectively. The practical results were then compared with the equation proposed by Md. Mozammel Haque to find the bond strength of RBC using compressive strength, and the difference was found to range from 0.4 to 0.9 for all the different ratios used. Further, the study showed the direct relation of compressive strength with bond strength: the greater the compressive strength, the greater the bond strength

Keywords- Bond Strength, Concrete, Compressive Strength, Recycled Aggregate

1 Introduction

Concrete is the second most consumed material, by mankind, on earth after water. Global annual production of concrete is around 33 billion tons (ISO, 2016). That's why the construction industry is one of the largest consumers of raw materials. And the demand for building materials, particularly concrete, has risen exponentially. Since the world is moving towards modernization and using modern materials like concrete rather than bricks, although in most Asian countries brick is still used in construction, the demolition of old structures produces a lot of brick waste which needs to be tackled. One of the best ways is to use it as a recycled aggregate, both as fine and coarse aggregate, in concrete. Many researchers have used brick as a recycled aggregate in concrete and found its effect on different properties of concrete.

Paulo B. Cachim [1] in his studies found out that up to 15% crushed bricks can be used as natural aggregates substitutes without strength reduction. And there is a reduction of concrete properties (up to 20%, depending on the type of brick), for 30% of natural aggregate substitution. Mounir M. Kamal et al. [2] have studied the effect of using different ratios of recycled brick aggregate in concrete mix and found that as the amount of recycled aggregate increases, the compressive strength and bond strength decrease. And he summarizes that bond strength of recycled brick aggregate concrete is 8% of its compressive strength. Yang et al. [4] found out that the failure pattern of specimen is "Splitting Failure" without lateral

pressure (confinement), while failure pattern of specimen with different biaxial lateral pressure can be classified as "splitting pullout failure".

The most concerning thing while using recycled brick aggregate in concrete is its bond strength with rebar, because if the concrete does not make a good bond, then under the application of load, the bar will slip or pull out and cause the whole structure to collapse. The bond strength of concrete with rebar plays a pivotal role in every element of structure i.e. beam, column, slab etc. Because of this importance of bond behavior this study will discuss the effect on bond strength by replacing natural aggregate with recycled aggregate (both recycled brick and recycled concrete). and compares with bond strength of natural aggregate concrete.

Further compressive strength of concrete has a great influence on its bond strength. So, this study also finds a relationship between bond strength and compressive strength of concrete. Additionally, it analyzes the equation proposed by M.M. Hoque et al. [5] for the evaluation of bond strength in BAC. The following equation developed by M.M. Hoque et al.

$$U = 0.525\sqrt{f'_c}\left(\frac{c}{d_b}\right)^{0.42}$$

2 Research Methodology

2.1 Material and Concrete mixes

Recycled Aggregate Concrete (RAC), Recycled Brick Aggregate Concrete (RBC), and Natural Aggregate Concrete (NAC) were investigated. Concrete mixes were prepared by replacing 100% of natural aggregates with either recycled concrete (RCA) or brick aggregates (RBA) in equal or different ratios, while third mix used 100% natural aggregates for comparison. Meanwhile, to get RBAs & RCAs old bricks and concrete cylinders were manually broken down and then crushed using a roller crusher. The resulting aggregates were sieved to separate coarse and fine aggregates, as shown in *fig 1*.

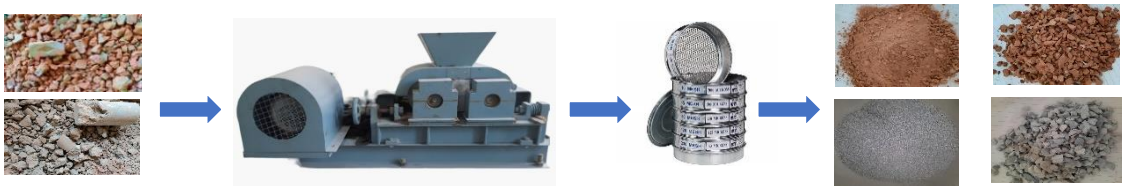

Figure 1: Schematic diagram of producing RBA & RCA

The *table 1* illustrates that the 12 concrete mixes were prepared with weights of coarse and fine aggregates used and on which the direct pull-out and compressive strength test was then performed [5]. RBC-1, RAC-1 represent coarse recycle brick and concrete aggregate, each of them having a ratio of R(33%-67%). Also, RBC-2, RAC-2 represent fine recycle brick and concrete aggregate, each of them having a ratio of R(50%-50%). NAC-1 & NAC-2 represents natural aggregate concrete 33-67% & 50-50% of coarse and fine aggregate, respectively. Also, all coarse aggregate used in saturated surface dry (SSD) condition because of high water absorption capacity of recycled brick aggregate. For this purpose, aggregates were soaked in water for 24 hours before casting and water cement ratio of 0.5 was used.

Table 1: Mix Proportions

Name	Recycled Aggregate Type	Weight in kg/m^3			No. of Sample	
		Cement	Coarse Aggregate	Fine Aggregate	Cube	Cylinder
RBC-1	Coarse: Brick	317	523	1061	2	2
RBC-2	Fine: Brick	317	792	792	2	2
RAC-1	Coarse: Concrete	400	660	1340	2	2
RAC-2	Fine: Concrete	400	1000	1000	2	2
NAC-1	Natural Aggregate Concrete	400	660	1340	2	2
NAC-2		400	1000	1000	2	2

3 Specimen & Testing

3.1 Pull-out & Compressive Strength Test

The pull-out test was preferred to directly assess the force required to pull out the rebar. For this test, cube specimens (200mm³) having a 19mm diameter rebar centrally embedded with a bonded length of $5d_b$ [6] were prepared, with the ends unbonded using PVC pipes and silicone tape. A 1000KN Universal testing machine applied load at 0.5 min/mm, recording slip value and peak force automatically. This test was conducted as per ASTM C900-19 [7] for all concrete mixes. Moreover, to assess concrete quality, 75mm x 150mm cylindrical specimens were prepared. Using a 2000KN testing machine per ASTM C39 [8], the compressive strength test recorded the maximum load each cylinder sustained. Two samples from each mix were tested, and their average compressive strength is reported. Casting and testing of samples are shown in *fig 2*.

a) b) c)

Figure 2: a. Bar Placement b. Cast Specimens c. Pull-out Test Arrangement

4 Results

4.1 Bond Strength & Compressive Strength

The average peak force obtained was used in the following formula to get the ultimate bond strength values $\sigma_{ult} = \frac{P_{Peak}}{\pi * d * L}$. *fig 4*(a) shows that for 33% coarse and 67% fine aggregate ratio NAC had the highest bond strength among the other mixes having RBC value relatively less. *fig 4(b)* indicates that when coarse aggregate ratio was increased from 33% to 50% more higher value of NAC 12.2MPa was obtained among other mixes. Compressive strength tests were conducted 28 days after casting. *fig 4(c)* shows that for 33%-67% ratio NAC had the highest compressive strength among the other mixes as well and also having RBC value relatively less. *fig 4(d* indicates that when coarse aggregate ratio was increased from 33% to 50% more higher compressive strength value for NAC 28.2MPa was obtained. This shows that bond strength has a direct relationship with compressive strength.

a)

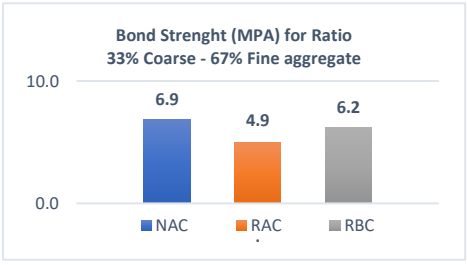

b)

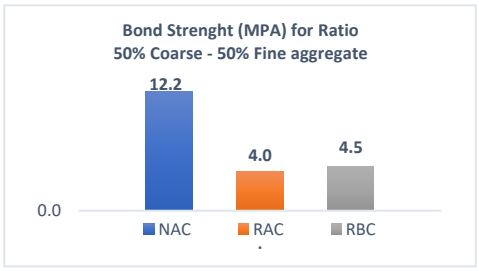

Figure 3: Bond strength for a. Ratio 33%-67% & b. Ratio 50%-50%

a)

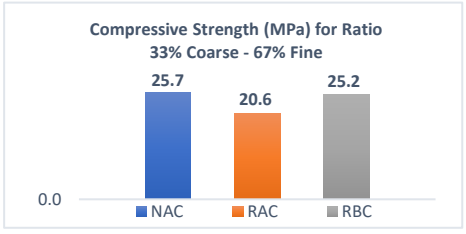

b)

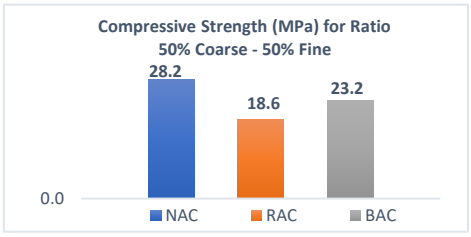

Figure 4: Compressive strength for a. Ratio 33%-67% & b. Ratio 50%-50%

4.2 Relation Between Bond Strength and Compressive Strength

It is clear from the above results that the bond strength is directly related to compressive strength show in *fig 5.* Also, the increased ratio of coarse aggregate influenced negatively on the both the strengths of RAB & RAC. Moreover, the Practical results were also compared with the equation proposed by Md. Mozammel Haque to find bond strength using compressive strength and the difference is found to be range from 0.4-0.9 for all different ratios tested.

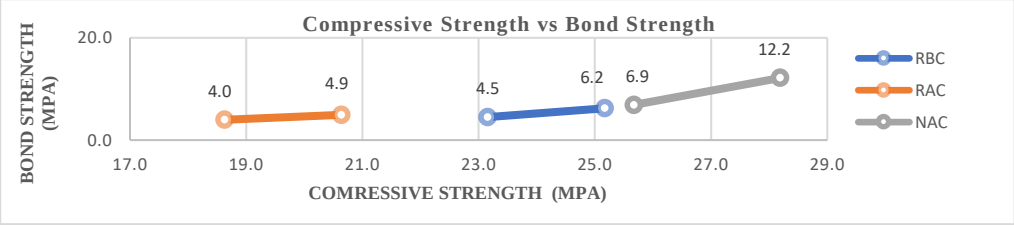

Figure 5: Graphical comparison of the relation b/w bond and compressive strength

5 Modes of Failure

Two modes of failure were observed during pull-out tests. In specimen having strong bond with bar splitting mode of failure was observed (*fig 6b*) due to radial outward forces caused by ribs on the rebar. While in specimen having weak bond with bar, slippage of bar (*fig 6a*) occurred that could be due to various factors, including poor surface preparation, improper bar placement, or inadequate adhesive properties of the bonding material.

a)  b) 

Figure 6: Splitting failure in a) RBC & b) RAC

6 Conclusion & Recommendations

In conclusion compressive strength of a specimen has direct influence on its bond strength Increasing the recycled coarse aggregate content in the ratio influences the bond strength due to reduction in strength of recycled aggregate. Mozammel Haque equation found useful for measuring bond strength of recycled brick aggregate concrete directly from its compressive strength. Lastly, it is recommended to study the different RBA ratios, bar diameters, and recycled aggregates effects on concrete properties.

7 Acknowledgement

The authors would humbly like to thank dept. and advisors who helped in research execution, particularly Prof. Dr. Rashid Hameed and Dr. Syed Asad Ali Gillani.

8 References

[1] Cachim, Paulo. "Mechanical properties of brick aggregate concrete," *Construction and Building Materials*, vol. 23, pp 1292-1297, 2009.
[2] Kamal, Mounir M., Zeinab A. Etman, Mohamed R. Afify, and Mahmoud M. Salem. "Bond Strength of concrete containing different recycled coarse aggregate," *Concrete Research Letters 6*, no. 2, 2015.
[3] Yang, Haifeng, Youdong Huang, and Liangsheng Lv. "Bond behavior between recycled aggregate concrete and steel rebar subjected to biaxial lateral pressure," *Elsevier, Structures, vol. 41, pp. 139-146, 2022.*.
[4] Hoque, M.M., Islam, M.N., Islam, M. and Kader, M.A. "Bond behavior of reinforcing bars embedded in concrete made with crushed clay bricks as coarse aggregates," *Construction and Building Materials*, vol. 244, p.118364, 2020.
[5] ACI PRC-211.1-91 standard practice for selecting proportion and setting time.
[6] M. John Robert Prince, Bhupinder Singh. "Bond behaviour of deformed steel bars embedded in recycled aggregate concrete", *Construction and Building Materials*, vol 49, pp 852-862, 2013.
[7] ASTM C900-19 Standard Test Method for Pullout Strength of Hardened Concrete.
[8] ASTM C39 Concrete cylinder standered testing.

OPTIMIZED PREDICTION MODELING FOR CHLORINATED MARINE CONCRETE USING DECISION TREE

[a] Muhammad Luqman*, [b] Majid Khan

a: Barrick Gold Corporation, Pakistan.18pwciv5026@uetpeshawar.edu.pk
b: Department of Civil Engineering, COMSATS University, Abbottabad, Pakistan. 18pwciv4988@uetpeshawar.edu.pk
* Corresponding author.

Abstract- Chloride concentration (Cs) at the surface of concrete is an essential metric for designing resilience and estimating the lifespan of concrete structures in aquatic settings. Consequently, due to chlorine action, many reinforced concrete constructions cannot reach their intended or planned lifespan and experience early degradation. This study utilizes the independent machine learning technique Decision Tree (DT) to forecast concrete's surface chloride concentration (Cs). A comprehensive database consisting of 642 observations of Cs exposure data in the marine field, including the applicable mixture quantity of constraints, conditions of the environment, and exposure time, has been created through a thorough investigation of relevant literature. Diverse statistical criteria evaluated the model's accuracy and suitability. During the validation process, the DT model demonstrated enhanced accuracy with correlation coefficients (R) of 0.95 for training and 0.96 for validation and mean absolute errors (MAE) of 0.009. The results indicate that by including more diverse datasets and considering new variables, the predicted accuracy of standard models may be improved. The DT machine learning model, trained on a vast database, can effectively include 13 key characteristics that pose challenges for conventional models. However, to lessen the problem of overfitting, it is advisable to use a more extensive dataset, including synthetic or genuine experimental data.

Keywords- Regression, K-Fold Method, Semi exponential Model, Particle Swarm Optimizer (PSO).

1 Introduction

The erection of sea-crossing bridges, dock piers, coastal highways, and buildings is among the many applications of reinforced concrete (RC) structures in marine and coastal environments. Broadly, a passive oxide deposit can protect reinforcing steel in RC structures from rusting, as it is resilient in the high pH micro-environment that results from the concrete pore solution [1], [2]. Chloride ions present in saltwater and airborne aerosols may adhere to and infiltrate the exterior of reinforced concrete structures in coastal and aquatic settings. Suppose the chloride ions infiltrate and capture inside the matrix of concrete encasing the steel reinforcement. In that case, they have the potential to destabilize the protective layer and commence and expedite corrosion of the steel, resulting in the formation of cracks and spalling of the concrete, as well as a reduction of the load-bearing capacity of reinforced concrete structures [3]. Researchers recently developed mathematical frameworks in laboratory settings that generate chloride profiles from the underlying structure of wet concrete [4]. In 2023, Reichert et al. [5] proposed a semiempirical double exponential model designed explicitly for the penetration of chlorine in diffusion and convection zones, which does not encompass different practical conditions.

Corrosion in RC structures may cause crashes, safety hazards, and significant economic losses, affecting the normal functioning of the engineered environment. Consequently, many reinforced concrete constructions cannot reach their intended or planned lifespan and experience early degradation [6]. Hence, the problem of designing concrete buildings with longevity or accurately predicting their lifespan has become a significant undertaking in current design practices. This effort requires using solid models that can effectively include several influencing elements and provide a more precise description of the processes responsible for degradation [7]. Marine ecosystems are often categorized into four zones based

on the types of chloride exposure they experience: atmospheric, tidal, splash, and submerged zones. Fick's second law of diffusion describes chloride infiltration into concrete regardless of the zone [8]. Eq (1) provides the mathematical solution for Fick's second law, often used in maritime service life design of RC structures.

$$C(x,T) = C_S.\,ERF * \left(\frac{x}{2 * (D_e * T)^{0.5}}\right) \quad (1)$$

The function *C(x, T)* represents the concentration of chloride ions, [Cl-], at a certain distance *x* into the concrete, measured from the exposed surface, after a certain amount of time *T*. The term D_e refers to the effective diffusion coefficient. If Eq (1) is written with the assumption that De is independent of *x* and T, then the concentration of chloride ions ([Cl-]) at the surface of the concrete is supposed to be constant throughout time. The Gaussian error function (ERF) is used in this context. Additionally, at the onset of corrosion, *C(x, T)* is $C_{T,}$ and *x* represents the thickness of the rebar cover. Unlike D_e, *Cs* is a multidimensional characteristic that includes material characteristics, time, and external factors. Additional study is required to enhance the accuracy of predicting the advancement of Cs and chloride influx.

The work aims to predict Cs, accounting for all critical parameters that previous research lacks, to help design durable RC structures in maritime conditions. Using nonlinear independent variables, ML has been employed in Material Engineering and corrosion prediction [9], [10]. In order to address the shortcomings of traditional approaches, this study employs ML models (Supervised) to construct an accurate and practical model for concrete chloride intrusion prediction. This ML model will solve the material's complex composition degrees of flexibility and the multivariate link between the mixture in dependent variables and attributes.

2 Research Methodology

2.1 Theoretical Background of Decision Tree

Decision trees are adequate for both regression and classification tasks in machine learning. Resembling flowcharts, decision trees can make repeated practical decisions and handle unstructured information for predictions. One challenge in machine learning is communicating model results, but decision trees make this more straightforward due to their clear decision paths [11]. A decision tree starts with a root node and branches out, with each node representing a decision based on a specific attribute and each leaf node representing an outcome. Decision nodes lead to further branches, while leaf nodes provide the final decision. The k-fold cross-validation (CV) method, specifically the 12-fold CV, helps find the best hyper-parameters. The training data is split into 12 equal parts. Nine folds (482 observations) train the model, while three folds (160 observations) are used for testing. This process repeats nine times with different fold combinations to train and test the model. CV errors are calculated at each cycle, and model parameters are adjusted accordingly [12].

2.2 Data Collection

To develop reliable machine learning models to forecast the Cs (Surface Chloride Concentration as Wt. of Concrete) relationship to changes in concrete mix designs, environmental variables, and exposure duration, 642 experimental and fitted analytical data points were gathered from recently published research. The developed model utilizes evident exterior chloride concentration in marine concrete from field measurements on RC structures exposed to sea splash conditions tidal, and submerged zones. The mix design of concrete has ten variables. The environmental settings are also characterized by T (mean annual temperature, °C) and Cl^{-} (seawater chloride concentration, g/L). Exposure time (ETM) is a single variable representing the duration of exposure. A supplementary input was included to account for the environmental conditions exposed to the concrete. This input was assigned values of 0 for the tide zone, 1 for the splash zone, and 2 for the submerged zone. All these data attributes are concise in Table 1. This demonstrates a minimal likelihood of multicollinearity, as the correlation values are lower than the indicated threshold. Table 1 presents the dataset's statistical characteristics, including indicators such as the mean, standard deviation, skewness, and kurtosis. The variables demonstrate skewness and kurtosis values within the prescribed ranges of ±3 and ±10, respectively. Moreover, it is crucial to note that CSB has the strongest positive correlation (+0.97) with Cs compared to all other input parameters (Cs). The following variable is the ET, with a correlation value of +0.50. We have the FA and W, with a correlation coefficient of + 0.38 and + 0.48, respectively. Lastly, the exposure time has the lowest correlation coefficient of -0.01.

2.3 Model Development

Thoroughly analyzing various DT setup configurations is essential for creating a robust model in the field of ML modeling. These generated parameters are recommended based on several trial runs since they consider the essential population size

parameter directly affecting the number of programs produced. While the convergence process may be time-consuming, a more intricate and precise model benefits from a larger population. Overfitting may occur when the size of the population surpasses a particular range. The fundamental operations in the paradigm are addition, division, multiplication, and subtraction. Prior to the completion of the method, the generation numeral establishes the desired degree of precision for the model. Multiple iterations of algorithms have contributed to developing a simulation model with minimal imperfections. The present technique experimented with several combinations of parameters to identify the optimal model and successfully created one with the lowest error levels. An inherent challenge in machine learning modeling is overfitting, which occurs when the model demonstrates high accuracy on the original dataset but fails to generalize effectively to new, concealed data. To address this issue and get insight into the model's ability to generalize, evaluating its performance on data that has not been previously examined is recommended. In order to mitigate the issue of overfitting, the data is divided into two groups, allocating 75% for training purposes and 25% for validation. The algorithm's performance is evaluated using an independent validation set that was not used during the construction of the model.

Table 1: Statistical description of input variables in the database for CS

Parameter	Unit	Mean	SD[1]	Min	Max	Kurtosis	SKS[2]	OPN[3]
OPC	Kg/m^3	370.70	75.60	110.00	519.00	0.60	-0.65	Input
FAH	Kg/m^3	33.97	59.88	0.00	239.00	3.46	1.99	Input
GGBS	Kg/m^3	11.41	45.45	0.00	292.50	15.49	4.03	Input
SF	Kg/m^3	5.41	12.85	0.00	50.00	4.11	2.29	Input
S	Kg/m^3	1.47	1.99	0.00	10.20	4.67	2.09	Input
W	Kg/m^3	187.54	44.08	38.50	311.00	2.80	0.82	Input
FA	Kg/m^3	765.77	116.46	552.00	1232.00	4.74	1.46	Input
CA	Kg/m^3	993.81	135.44	410.00	1305.00	7.56	-1.85	Input
w/b	-	0.46	0.08	0.30	0.75	1.04	0.96	Input
ETM	Years	4.24	6.28	0.08	48.65	24.71	4.45	Input
T	°C	17.78	9.38	7.00	50.00	-0.85	0.42	Input
CSB	%	3.67	2.09	0.14	13.58	1.89	1.02	Input
Cl^{--}	g/L	18.99	2.79	13.00	27.37	0.72	0.52	Input
ET	0,1,2	N/A	N/A	N/A	N/A	N/A	N/A	Input
C_s	%	0.66	0.39	0.02	1.95	-0.18	0.68	Output

[1]Standard Deviation, [2]Skewness, [3]Operation

3 Results - Model Performance

The correctness of the created model is assessed by examining the gradient of the regression line derived from concrete values shown on the x-axis against projected values on the y-axis, as shown in Figure 1.

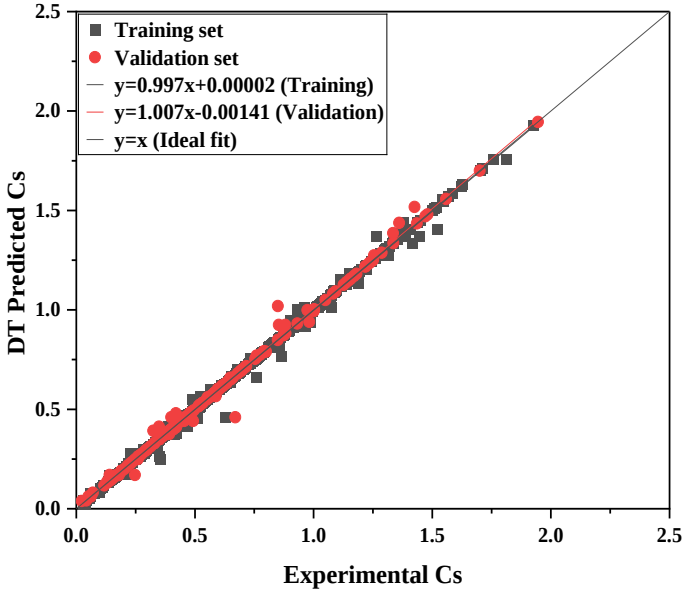

Figure 1: Regression Slope Analysis of Model

Table 2: Performance Assessment of the ML Models

Subset	RMSE	MAE	R	a_{10} Index	a_{20} Index
Training	0.020	0.007	0.95	0.120	0.230
Validation	0.028	0.009	0.96	0.081	0.144

Researchers often use this methodology to evaluate the precision of machine learning models [13], [14], [15]. Predictions were then compared for both training and testing datasets to assess the predictive capabilities of the models. Figure 1 and Table 2 display the statistical assessment of the model with five statistical parameters and their corresponding findings for this specific objective. The DT model exhibits slopes of 0.997 and 1.007 for the training and validation datasets. Moreover, the DT model showed R-values of 0.95 for training and 0.96 for validation. The MAE values for the DT model are shallow: 0.007 for training and 0.009 for validation. Predictions were then compared for both training and testing datasets to assess the predictive capabilities of the models.

4 Conclusions

This study employs a machine learning technique, the Decision Tree (DT), to forecast concrete's surface chloride concentration (Cs). A comprehensive database of 642 observations of Cs exposure data in the marine field—including mixture quantities, environmental conditions, and exposure times—was compiled from relevant literature. The model's accuracy and suitability were evaluated using diverse statistical criteria. The DT model demonstrated high accuracy during validation, with correlation coefficients (R) of 0.95 for training and 0.96 for validation and mean absolute errors (MAE) of 0.009. For future studies, hybrid ML models might be established, which may increase predicted accuracy. This study employs Statistical means to comprehend the model, but future investigations may benefit from model-agnostic tools like LIME, PDP, and SHAP. Understanding the study's limitations is crucial. Current literature shows experimental setup discrepancies across research. Further research should focus on controlled experimental testing to increase model robustness and dependability using a single, dependable source in the same context to collect data.

5 References

[1] O. E. Gjørv, Durability design of concrete structures in severe environments, vol. NA, no. NA. 2009. doi: NA.
[2] S. W. Tang, Y. Yao, C. Andrade, and Z. J. Li, "Recent durability studies on concrete structure," Cement and Concrete Research, vol. 78. 2015. doi: 10.1016/j.cemconres.2015.05.021.
[3] C. E. T. R. Balestra Thiago Alessi; Savaris Gustavo, "Contribution for durability studies based on chloride profiles analysis of real marine structures in different marine aggressive zones," Constr Build Mater, vol. 206, no. NA, pp. 140–150, 2019, doi: 10.1016/j.conbuildmat.2019.02.067.
[4] T. A. Reichert, C. E. T. Balestra, D. A. O. Balestra, and R. A. de Medeiros-Junior, "Laboratory procedure for obtaining chloride profiles from concrete structures cores: a mathematical approach," Journal of Building Pathology and Rehabilitation, vol. 8, no. 1, 2023, doi: 10.1007/s41024-023-00286-2.
[5] T. A. Reichert, W. A. Pansera, C. E. T. Balestra, and R. A. Medeiros-Junior, "New semiempirical temporal model to predict chloride profiles considering convection and diffusion zones," Constr Build Mater, vol. 367, 2023, doi: 10.1016/j.conbuildmat.2022.130284.
[6] L. F. C. Yang Rong; Yu Bo, "Investigation of computational model for surface chloride concentration of concrete in marine atmosphere zone," Ocean Engineering, vol. 138, no. NA, pp. 105–111, 2017, doi: 10.1016/j.oceaneng.2017.04.024.
[7] A. F. B. A. Costa Julio, "Chloride penetration into concrete in marine environment-Part II: Prediction of long term chloride penetration," Mater Struct, vol. 32, no. 5, pp. 354–359, 1999, doi: 10.1007/bf02479627.
[8] M. M. Collepardi Aldo; Turriziani Renato, "Penetration of Chloride Ions into Cement Pastes and Concretes," Journal of the American Ceramic Society, vol. 55, no. 10, pp. 534–535, 1972, doi: 10.1111/j.1151-2916.1972.tb13424.x.
[9] J.-S. N. Chou Ngoc-Tri; Chong Wai Kiong, "The use of artificial intelligence combiners for modeling steel pitting risk and corrosion rate," Eng Appl Artif Intell, vol. 65, no. NA, pp. 471–483, 2017, doi: 10.1016/j.engappai.2016.09.008.
[10] W. Z. S. Taffese Esko, "Machine learning for durability and service-life assessment of reinforced concrete structures: Recent advances and future directions," Autom Constr, vol. 77, no. NA, pp. 1–14, 2017, doi: 10.1016/j.autcon.2017.01.016.
[11] H. I. Erdal, "Two-level and hybrid ensembles of decision trees for high performance concrete compressive strength prediction," Eng Appl Artif Intell, vol. 26, no. 7, pp. 1689–1697, Jan. 2013, doi: 10.1016/j.engappai.2013.03.014.
[12] A. Karbassi, B. Mohebi, S. Rezaee, and P. Lestuzzi, "Damage prediction for regular reinforced concrete buildings using the decision tree algorithm," Comput Struct, vol. 130, pp. 46–56, Jan. 2014, doi: 10.1016/j.compstruc.2013.10.006.
[13] M. I. Khan et al., "Effective use of recycled waste PET in cementitious grouts for developing sustainable semi-flexible pavement surfacing using artificial neural network (ANN)," J Clean Prod, vol. 340, p. 130840, Jan. 2022, doi: 10.1016/j.jclepro.2022.130840.
[14] M. Iqbal, Q. Zhao, D. Zhang, F. E. Jalal, and A. Jamal, "Evaluation of tensile strength degradation of GFRP rebars in harsh alkaline conditions using nonlinear genetic-based models," Materials and Structures/Materiaux et Constructions, vol. 54, no. 5, 2021, doi: 10.1617/s11527-021-01783-x.
[15] H. Alabduljabbar, M. Khan, H. H. Awan, S. M. Eldin, R. Alyousef, and A. M. Mohamed, "Predicting ultra-high-performance concrete compressive strength using gene expression programming method," Case Studies in Construction Materials, vol. 18, p. e02074, Jan. 2023, doi: 10.1016/j.cscm.2023.e02074.

RUBBERIZED CONCRETE: OPTIMUM DURATION OF PRETREATMENT OF RUBBER PARTICLES WITH ALKALINE SOLUTIONS

[a] Raja Bilal Nasar Khan, [b]Anwar Khitab*

a: Civil Engineering Department, Mirpur University of Science & Technology, Mirpur (AJK) Pakistan. bilal.ce@must.edu.pk
b: Civil Engineering Department, Mirpur University of Science & Technology, Mirpur (AJK) Pakistan. anwar.ce@must.edu.pk
*Corresponding author.

Abstract- Rubberized concrete incorporates waste rubber particles as a partial replacement for sand, providing an innovative solution for the disposal of waste rubber tires and reducing the demand for natural sand in concrete production. Despite its environmental benefits, untreated rubber particles adversely affect concrete workability, density, and strength. However, pretreatment with alkaline solutions can mitigate these effects. This study investigates the impact of pretreatment with NaOH and bleaching powder solutions on the workability and density of rubberized concrete, focusing on the effect of soaking time. The results indicate that a 2-hour soaking time optimally enhances the workability and reduces the density of the concrete mix. Soaking beyond 2 hours results in a reduction in both slump and density, which could be detrimental to the concrete's strength.

Keywords- Rubberized Concrete, Pre-treatment, Soaking Time, Alkaline Solution.

1 Introduction

Approximately 30billiontons of concrete are produced globally in a year [1]. Natural aggregates for concrete are sourced from rocks and mountains, and the excessive use of natural sand in construction is disrupting the naturally balanced environment of the world [2]. Sand is not only heavily used in construction but also in electronic devices as a source of silicon. On the other hand, waste rubber tires are non-biodegradable and are often dumped in earth pits. In developing countries like Pakistan, people use them as fuel, which emits toxic gases into the environment. This situation necessitates the exploration of alternative materials to replace sand and the safe recycling of rubber tires. In the past, numerous studies have been conducted to recycle rubber tires in building materials. Due to the nature of rubber, many researchers believe that rubber can be used as a partial replacement for sand in cementitious materials. A few relevant past studies are described as follows:

Gerges et al. conducted a study using rubber powder as a partial replacement for sand in concrete. The replacement levels were fixed at 5%, 10%, 15%, and 20%. The results revealed a reduction in compressive strength with an increase in toughness and impact resistance. The reduction in compressive strength was attributed to the lower level of adhesion between the cement paste and the rubber particles. [3]. Khan et al. examined the effect of rubber particles as a partial replacement for sand in concrete. The substitution levels were kept at 0%, 5%, 10%, and 15%. The results demonstrated a decrease in mechanical strength. The rubberized concrete was reported to have lower density and lower thermal conductivity. The decrease in strength was attributed to the lower level of bonding between the cement paste and the rubber particles [4]. Anwar et al. developed a porous concrete with enhanced skid resistance using rubber particles as a fractional substitute for sand. The replacement proportions were fixed at 0%, 5%, 10%, and 15%. The rubberized concrete exhibited lower mechanical strength, lower density, higher thermal insulation, and higher skid resistance in both wet and dry conditions. The reduction in strength was attributed to the elastically deformable and softer nature of the rubber particles, which induced additional pores and resulted in lower adhesion between the cement paste and the rubber particles [5]. For the enhancement of the bonding between the cement paste and the rubber particles, several other researchers have proposed pre-treatment of rubber particles with a compatible chemical before mixing with the concrete ingredients. Roychand et al. pre-treated the rubber particles in tap water and in a 5% dilute sulfuric acid solution for 2 and 24 hours before mixing. The

authors reported an increase in bond strength between the rubber particles and the cement paste and enhanced overall strength with the pre-treated rubber particles soaked for 2 hours. They found that the water molecules present in the rubber particles replaced the air inside the pores, facilitating a higher degree of hydration, which improved the interstitial transition zone (ITZ) [6]. Sattar et al. investigated the effect of the nature of pre-treatment chemicals on the performance of rubberized concrete (1:2:4). The authors used two types of chemicals: caustic soda and bleaching powder. They reported that bleaching powder was more effective in enhancing the bond between the rubber particles and the cement paste. This was attributed to the higher strength, lower water absorption, and reduced porosity of the resulting concrete [7], [8].

This study aims to investigate the impact of pre-treatment and soaking time of rubber particles on the performance of rubberized concrete. Previous research shows that soaking times have explicitly defined. This work aims to explore an optimum soaking time for saving efforts. Building upon previous research, two pre-treatment chemicals were chosen: caustic soda (NaOH) and bleaching powder, also known as Calcium hypochlorite ($Ca(ClO)_2$). The soaking time for pre-treatment was set at 2 hours, 24 hours, and 72 hours. Sand in the concrete was replaced by 0%, 5%, and 10% rubber by mass of sand. The concrete's performance was assessed based on slump, fresh and hardened densities.

2 Research Methodology

2.1 Materials

For this study, a 1:1.5:3 concrete mix ratio was selected, commonly used for residential structures, commercial buildings, and pavements. Ordinary Portland Cement (OPC) from a local brand, Paidaar cement, was used, with its chemical composition detailed in Table 1. Sand was sourced from Lawrencepur, and coarse aggregates were collected from Margalla. The properties of these aggregates are provided in Table 1. Waste rubber was chopped from tires at a local dumping site. The rubber pieces were converted to fine powder of the size of the sand by shredding. The composition of the concrete mix is detailed in Table 2.

Table 1: Properties of cement and aggregates

Cement		Aggregates		
Component	**Percentage**	**Properties**	**Fine**	**Coarse**
SiO_2	21	Specific gravity	2.69	2.48
Al_2O_3	6.2	Fineness modulus	2.6	-
Fe_2O_3	2.4	Bulk density (kg/m^3)	1500	1598
CaO	62	Dry rodded density (kg/m^3)	1850	1610
MgO	1.2	Water absorption (%)	3.88	1.49
SO_3	3.7	Water content (%)	2.01	0.94
LOI	2.4	Impact value (%)	-	28.20
		Crushing value (%)	-	2.48

Table 2: Materials composition per cubic meter of concrete

Concrete Sample	Cement (kg)	Sand (kg)	Crumb Rubber (kg)	Coarse Aggregate (kg)	Water (L)
C0	244	365	0	730	116
RC5	244	346.75	18.25	730	116
RC10	244	328.5	36.5	730	116

The gradation of the fine aggregates with crumb rubber was checked and compared with the natural sand through sieve analysis according to ASTM C136 method [9]. The concrete samples were prepared as per ASTM C31 specifications [10]. Cylindrical specimens were prepared for testing purposes. The crumb rubber particles were soaked in caustic soda and bleaching powder solutions for 2 hours, 24 hours and 72 hours prior to mixing in concreteCaustic soda (NaOH) is frequently used as an industrial cleaning agent. When added to water and applied, it can dissolve grease, oils, fats, and protein-based deposits. Bleaching powder ($Ca(ClO)_2$) is a white color powder and is a cleaning agent like Caustic soda. Dilute solutions containing 5% by mass of caustic soda and bleaching powder were prepared. The rubber particles were immersed and stirred for uniform dispersion. Afterwards the rubber particles were left for soaking for a specific period.

2.2 Testing

The slump of the concrete mix was determined through ASTM C143-20 method [11]. The fresh and hardened densities were determined by ASTM C642-21 method [12].

3 Results

3.1 Workability

The results are presented in Figure 1. In the Figure 1, the "simply modified samples" refer to samples containing rubber content without any pre-treatment. The results demonstrated that pre-treatment significantly enhanced the slump values. Specifically, for 5% rubber content, the slump increased from 40 mm to 49 mm with NaOH pre-treatment and to 46 mm with bleaching powder pre-treatment. For 10% rubber content, the slump increased from 31 mm to 47 mm with caustic soda pre-treatment and to 44 mm with bleaching powder pre-treatment. Additionally, it was observed that a 2-hour soaking time was sufficient to enhance the workability, with longer soaking times (up to 24 hours) showing no further improvement and a decreasing trend in slump values observed at 72 hours. These results suggest that pre-treating rubber with either

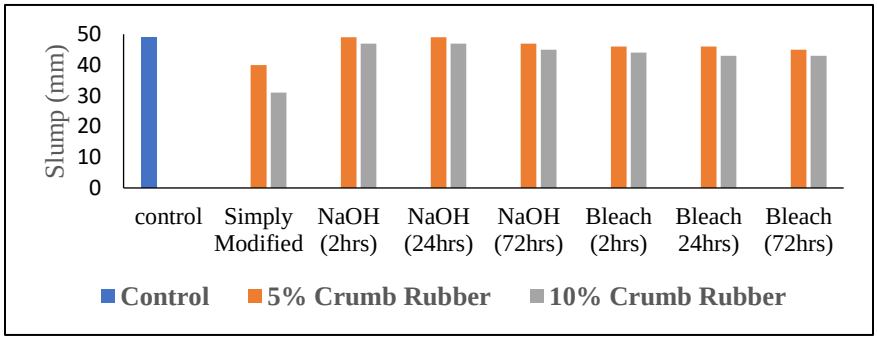

Figure 1: Effect of pre-treatment on workability of concrete

NaOH or bleaching powder significantly enhances the slump, thereby improving workability, with NaOH being slightly more effective. Cleaning agents like caustic soda and bleaching powder removed contaminants, enhanced particle roughness, increased hydrophilicity, and improved integration with the mix, thereby enhancing workability [13], [14].

3.2 Density

The fresh and hardened densities of the rubberized concrete are illustrated in Figure 2 (a) and Figure 2 (b) respectively. From these figures, it was evident that pre-treatment reduced the density of concrete. Additionally, the density decreased with an increase in rubber content. The lowest hardened density was observed in the samples treated with bleaching powder, showing a 12% decrease compared to the control specimen. In Figure 2, N2, N24, and N72 indicate specimens with rubber particles soaked in NaOH for 2, 24, and 72 hours, respectively, while B2, B24, and B72 refer to specimens with rubber particles soaked in bleaching powder for the same durations. The previous literature demonstrates that the cleaning agents owing to the enhanced bonding and surface characteristics, result in a reduction of air voids around the rubber particles, which improves the density [15], [16].

(a)

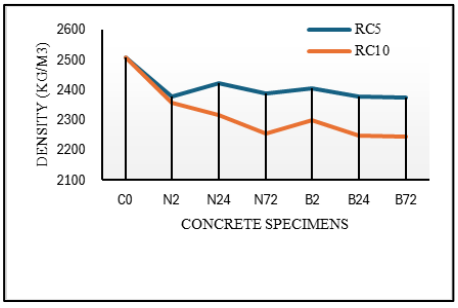

(b)

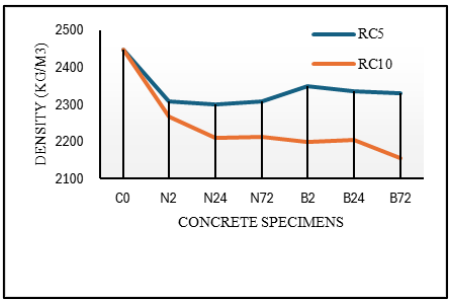

Figure 2: Effect of pre-treatment on (a) Fresh density, (b) Hardened density.

4 Conclusion

Based on the experimental work conducted, the following conclusions can be drawn:

1. The pretreatment of rubber particles with alkaline solutions, specifically caustic soda and bleaching powder, is an effective method for enhancing the workability of rubberized concrete.
2. A 2-hour soaking duration of rubber particles in caustic soda and bleaching powder solutions significantly improves the workability of rubberized concrete, increasing it by up to 22% compared to rubberized concrete with untreated rubber particles.
3. The 2-hour soaking treatment of rubber particles results in a 12% reduction in the density of the concrete compared to control specimens.
4. The study indicates that a 2-hour soaking time is optimal for achieving desirable slump and density values. Prolonged soaking times of 24 and 72 hours lead to a deterioration in workability and a further reduction in density, which negatively impacts the strength of the concrete.

References

[1] M. D. Jackson *et al.*, "Concrete needs to lose its colossal carbon footprint," *Nature*, vol. 597, no. 7878, pp. 593–594, Sep. 2021, doi: 10.1038/d41586-021-02612-5.
[2] M. Syarif *et al.*, "Development and assessment of cement and concrete made of the burning of quinary by-product," *J. Mater. Res. Technol.*, vol. 15, pp. 3708–3721, Nov. 2021, doi: 10.1016/j.jmrt.2021.09.140.
[3] N. N. Gerges, C. A. Issa, and S. A. Fawaz, "Rubber concrete: Mechanical and dynamical properties," *Case Stud. Constr. Mater.*, vol. 9, p. e00184, Dec. 2018, doi: 10.1016/j.cscm.2018.e00184.
[4] R. B. N. Khan and A. Khitab, "Enhancing Physical, Mechanical and Thermal Properties of Rubberized Concrete," *Eng. Technol. Q. Rev.*, vol. 3, no. 1, pp. 33–45, 2020.
[5] M. R. Anwar, N. Ahmad, A. Khitab, and R. B. N. Khan, "Development of Pervious Concrete with Enhanced Skid Resistance using Waste Tires Particles," *Proc. Pakistan Acad. Sci. A. Phys. Comput. Sci.*, vol. 61, no. 1, Mar. 2024, doi: 10.53560/PPASA(60-1)830.
[6] R. Roychand, R. J. Gravina, Y. Zhuge, X. Ma, J. E. Mills, and O. Youssf, "Practical Rubber Pre-Treatment Approch for Concrete Use—An Experimental Study," *J. Compos. Sci.*, vol. 5, no. 6, p. 143, May 2021, doi: 10.3390/jcs5060143.
[7] M. Sattar, R. B. N. Khan, and A. Khitab, "Strength Evaluation of Ordinary Concrete having Crumb Rubber Pre-treated with Caustic Soda and Bleaching Powder Solutions," *Tech. Journal, UET Taxila*, vol. 3, no. ICACEE, pp. 1–7, 2024.
[8] M. Sattar, R. B. N. Khan, and A. Khitab, "Performance Evaluation of Ordinary Concrete having Crumb Rubber Treated with Alkaline Solution," *Tech. Journal, UET Taxila*, vol. 3, no. ICACEE, pp. 8–13, 2024.
[9] ASTM International, "ASTM C 136 Standard Test Method for Sieve Analysis of Fine and Coarse Aggregates," *Annu. B. ASTM Stand.*, vol. 04, no. C, pp. 1–5, 2010, doi: 10.1520/C0136-06.2.
[10] ASTM C31, "Standard Practice for Making and Curing Concrete Test Specimens in the Laboratory," *ASTM Int.*, pp. 1–8, 2013, doi: 10.1520/C0192.
[11] ASTM C143/C143M-20, "Standard Test Method for Slump of Hydraulic-Cement Concrete," West Conshohocken, PA, 19428-2959 USA, 2020.
[12] ASTM C642-21, "Standard Test Method for Density, Absorption, and Voids in Hardened Concrete," West Conshohocken, PA, 19428-2959 USA, 2021. doi: 10.1520/C0642-21.
[13] Z. Jiang *et al.*, "Surface Treatment of Rubberized Waste Reinforced Concrete," *Front. Built Environ.*, vol. 7, May 2021, doi: 10.3389/fbuil.2021.685067.
[14] L. He *et al.*, "Research on the properties of rubber concrete containing surface-modified rubber powders," *J. Build. Eng.*, vol. 35, p. 101991, Mar. 2021, doi: 10.1016/j.jobe.2020.101991.
[15] N. A. M.N., N. A.B., N. A. S., and F. N. A. A.A., "A comparative investigation on mechanical strength of blended concrete with surface modified rubber by chemical and non-chemical approaches," *Case Stud. Constr. Mater.*, vol. 17, p. e01444, Dec. 2022, doi: 10.1016/j.cscm.2022.e01444.
[16] M. Nuzaimah, S. M. Sapuan, R. Nadlene, and M. Jawaid, "Sodium Hydroxide Treatment of Waste Rubber Crumb and Its Effects on Properties of Unsaturated Polyester Composites," *Appl. Sci.*, vol. 10, no. 11, p. 3913, Jun. 2020, doi: 10.3390/app10113913.

SUSTAINABLE CONCRETE PRODUCTION: UTILIZING WASTE AND GREEN TECHNOLOGIES

[a]Usman Ilyas, [b]Fatima Ashfaq*

a: Department of Civil Engineering, University of Management and Technology, Lahore, Pakistan, usman.ilyas@umt.edu.pk
b: Department of Civil Engineering, University of Management and Technology, Lahore, Pakistan, fatima.ashfaq@umt.edu.pk
* Corresponding author.

Abstract- Concrete, the most widely used construction material globally, has a significant environmental impact due to the extraction of virgin materials and high carbon dioxide emissions. This paper specifically investigates methodologies to enhance concrete sustainability, focusing on the incorporation of waste materials and the development of green technologies. Through detailed analysis, trends such as the use of recycled aggregates, industrial by-products like fly ash and slag, and innovative materials like nano-silica were reviewed. Key findings include improved mechanical properties and reduced environmental footprints of these sustainable concretes. The paper also addresses challenges in market adoption, advancements in material processing techniques, and the potential for these practices to significantly support sustainable urban development.

Keywords- Sustainable Concrete, Waste Utilization, Green Building Materials, Environmental Conservation, Recycling.

1 Introduction

Concrete is essential for global construction and infrastructure, but its widespread use causes significant environmental impacts, including habitat disruption and high carbon dioxide emissions. For illustration, traditional concrete production contributes approximately 8% of global carbon emissions, highlighting its environmental impact. Additionally, extracting raw materials for concrete disrupts natural habitats, leading to biodiversity loss. In 2021 alone, the concrete industry consumed 25 billion tons of sand, exacerbating erosion and habitat destruction. Furthermore, land degradation from mining for concrete components affects over 100,000 square kilometers of land annually, showcasing the extensive ecological footprint of this material, highlighting the urgent need for sustainable alternatives in the construction industry [1, 2]. To address these environmental concerns, the construction sector is actively exploring sustainable practices that minimize waste and reduce carbon emissions. A key focus area is the integration of waste materials as partial substitutes for traditional concrete components. Research has demonstrated that materials such as plastic, glass, fly ash, slag, and construction waste can effectively replace virgin substances in concrete mixes. This approach not only reduces reliance on natural resources but also provides a viable solution for managing and repurposing waste materials [3-5]. In addition to waste utilization, advancements in green concrete technologies are reshaping the landscape of sustainable construction. These technologies aim to enhance concrete properties while extending its lifespan, thereby reducing maintenance requirements and early replacement of structural elements. For illustration, the use of reinforcing fibers and recycled aggregates has been shown to improve the compressive and flexural strength of concrete, leading to more durable and environmentally friendly structures [6-9]. The transition to sustainable concrete production is challenged by concerns over cost, availability, and performance. Despite these hurdles, regulatory incentives and certification programs like LEED are crucial in promoting green building practices. These initiatives encourage the use of sustainable materials and technologies, aligning with goals for sustainable urban development and environmental conservation. As a result, the construction industry is increasingly adopting sustainable practices to meet regulatory standards and the demand for eco-friendly solutions.

To accelerate this transition, a comprehensive approach is needed, integrating waste material utilization and green technologies. Innovations such as recycled aggregates, supplementary cementitious materials, and carbon capture technologies can significantly reduce the industry's environmental footprint. This review explores the effectiveness of these strategies in enhancing concrete sustainability, focusing on resource conservation, emission reduction, and overall environmental impact, along with their acceptability and implementation in the industry. This paper is structured into two main sections. The first section explores current strategies for utilizing waste and implementing green technologies in the construction industry. The second section assesses the industry's reception and current implementation of these sustainable practices, providing insights into their practical application and acceptance followed by conclusions and recommendations.

1.1 Recycled Aggregate Concrete

Recycled aggregate concrete (RAC) offers a sustainable alternative to traditional concrete by reducing the consumption of non-renewable resources, utilizing construction waste, conserving land, and lowering CO_2 emissions through reduced cement use. Consequently, RAC preserves natural aggregates, reduces waste disposal, and effectively conserves the environment while mitigating climate change, as described in Figure 1. Studies have shown that RAC can achieve mechanical properties comparable to conventional concrete, especially when high-quality recycled aggregates are used. This makes RAC suitable for a wide range of construction applications, including pavements and structural elements. Its adoption is increasing globally, supported by infrastructural law relaxations in several countries to promote its use [10, 11].

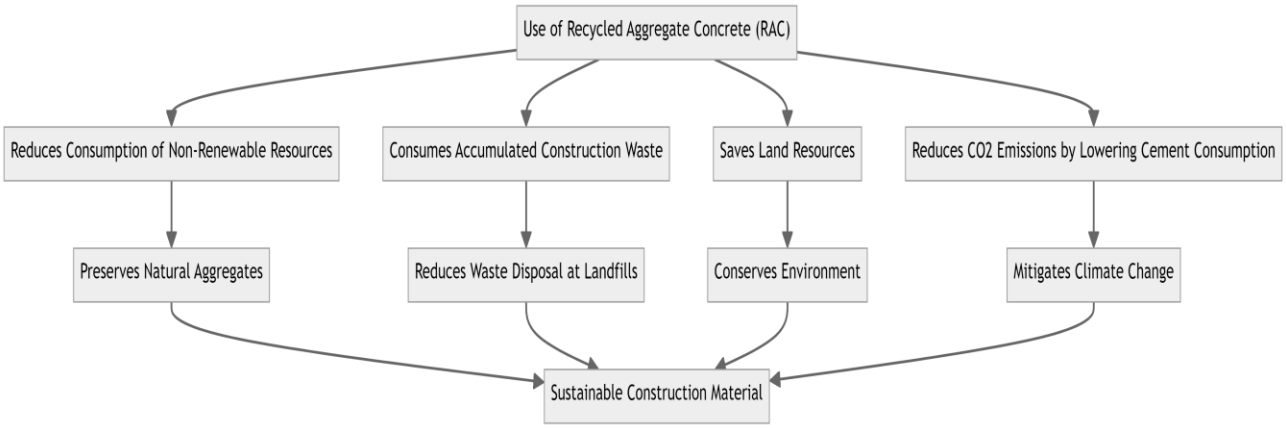

Figure 1: Environmental Benefits of using Recycled Aggregate Concrete

1.2 Incorporation of Waste Materials

Incorporating waste materials like recycled plastics, glass, industrial by-products and agricultural wastes into concrete enhances sustainability and specific properties [12, 13]. However, challenges include potential reductions in mechanical properties, compatibility issues with cementitious binders, and ensuring long-term durability [14, 15]. Addressing these challenges through innovative research is crucial which may involve usage of waste materials like waste polypropylene [16] and steel fibers recovered from old tires [17]. Even though much of it is recyclable, lots of waste polypropylene sadly ends up in landfill. Researchers are tackling the compatibility issues of incorporating waste materials into concrete through several innovative approaches. Surface treatments like carbonation are being used to enhance the bond between recycled aggregates and cement paste. The use of supplementary cementitious materials (SCMs) such as fly ash, slag, and silica fume is also improving performance and compatibility. Advanced characterization techniques, including scanning electron microscopy (SEM) and X-ray diffraction (XRD), are helping optimize mix designs. Additionally, nano-materials like nano-silica and carbon nanotubes are being integrated to improve mechanical properties and durability. New chemical admixtures specifically designed for recycled aggregate concrete (RAC) are enhancing workability and performance, making the incorporation of waste materials more feasible and effective. Despite this, A significant barrier to practical implementation is the lack of comprehensive guidelines and standards for safe and effective use of waste materials in concrete.

1.3 Geopolymer Concrete

Geopolymer concrete offers environmental benefits and durability over traditional cement-based materials [18]. It reduces CO_2 emissions and demonstrates superior resistance to various environmental factors. Produced through aluminosilicate polymerization, its properties can be optimized by adjusting activator-to-binder ratios. Adding fibers enhances its mechanical properties. However, challenges like property variability and material availability persist. Standardizing production, implementing quality controls, and establishing guidelines are vital for wider adoption. Incorporating waste materials as binders further boosts sustainability, making geopolymer concrete a viable alternative to conventional cement. One prominent example is the construction of the Brisbane West Wellcamp Airport in Toowoomba, Queensland, Australia. This airport, completed in 2014, is the world's first greenfield airport built using geopolymer concrete. The project utilized geopolymer concrete for various structural elements, demonstrating its feasibility and effectiveness as a sustainable construction material. This application not only showcased the material's environmental benefits but also highlighted its practical performance in large-scale infrastructure projects.

1.4 Use of Supplementary Cementitious Materials (SCMs)

The adoption of Supplementary Cementitious Materials (SCMs) like fly ash, slag, and silica fume as substitutes for cement in concrete production has become increasingly popular due to their potential to lower carbon emissions and enhance the durability of concrete structures. Table 1 illustrates the global awareness and utilization levels of various SCMs.

Table 1: Supplementary Cementitious Materials Usage in Construction Industry

Material Name	***Chemistry of SCM***	***Current State of Knowledge***	***References***
Fly Ash (FA)	Contains aluminosilicate materials	Used up to 20% as SCM, improves mechanical and durability properties	[1] [14] [19]
Rice Husk Ash (RHA)	High silica content	Optimal replacement level in concrete is 10%, enhances compressive strength	[2] [20]
Palm Oil Fuel Ash (POFA)	Contains siliceous and aluminous materials	Increased compressive strength	[20]
Silica Fume (SF)	Consists of amorphous silicon dioxide	Enhances concrete strength, workability, and durability	[1] [21]
Ground Granulated Blast Furnace Slag (GGBFS)	By-product of iron and steel making, contains calcium, silicon, magnesium, and aluminum oxides	Used as SCM to reduce cement consumption, improves strength and durability of concrete	[21]
Metakaolin (MK)	Produced by the calcination of kaolin clay	Enhances durability properties of concrete	[1] [21] [22] [23]
Waste Brick Powder (WBP)	Derived from brick waste, contains silicates and aluminates	Usage up to 20% as SCM, improves compressive strength of and concrete	[24]

2 Adoption of Sustainable Practices in Construction Industry

The adoption of sustainable practices in construction is vital for mitigating environmental impacts and promoting ecological balance. Sustainable construction (Figure 2), including the use of green building materials, energy-efficient designs, and waste reduction techniques, offers environmental and economic benefits. However, acceptance varies due to factors like awareness, cost, and regulatory support. Initial implementation costs and lack of standardized guidelines pose significant barriers, along with insufficient training for industry professionals. Despite these challenges, momentum is growing due to increased environmental awareness, regulatory pressures, and consumer demand for green buildings. Governments and industry bodies are supporting this shift with incentives and clear regulatory frameworks. Technological advancements are reducing costs and simplifying sustainable construction methods, making them more accessible. These trends are expected to diminish barriers, enabling more widespread adoption of sustainable practices in the construction industry.

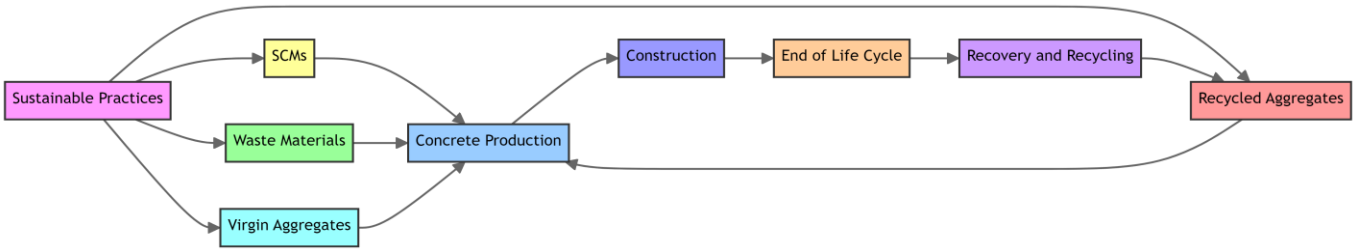

Figure 2: Sustainable Practices in Construction

3 Conclusions and Recommendations

Incorporating waste materials and green technologies in concrete production offers significant potential for enhancing sustainability in construction. Utilizing recycled aggregates, supplementary cementitious materials, and innovative technologies like carbon capture can reduce environmental impact and enhance resource efficiency. Overcoming challenges such as material compatibility, optimizing mechanical properties, and standardizing production methods is critical for widespread adoption. Future research should focus on refining techniques for waste material utilization, conducting thorough durability testing, and establishing guidelines for safe implementation. These efforts will advance sustainable construction practices, ensuring concrete remains a resilient and eco-friendly building material.

References

[1]. Alamri, M., Ali, T., Ahmed, H., Qureshi, M. Z., Elmagarhe, A., Khan, M. A., Ajwad, A., & Mahmood, M. S. (2024). Enhancing the engineering characteristics of sustainable recycled aggregate concrete using fly ash, metakaolin and silica fume. *Heliyon*, *10*(7), e29014. https://doi.org/10.1016/j.heliyon.2024.e29014

[2]. Ajwad, A., Ahmad, S., Abdullah, Jaffar, S. T. A., Ilyas, U., & Adnan, M. A. (2022). Effect of Using Rice Husk Ash as Partial Replacement of Cement on Properties of Fresh and Hardened Concrete. *Architecture Civil Engineering Environment*, *15*(2), 85–94. https://doi.org/10.2478/acee-2022-0017

[3]. Ajwad, A., Khadim, N., Abdullah, Ilyas, U., Rashid, M. U., & Aqdas, A. (2020). Effect of Mixing Steel Dust and Shred-Like Steel Fibres on the Properties of Concrete. *NFC IEFR Journal of Engineering and Scientific Research*, *7*, 16–21.

[4]. Zamora-Castro, S. A., Salgado-Estrada, R., Sandoval-Herazo, L. C., Melendez-Armenta, R. A., Manzano-Huerta, E., Yelmi-Carrillo, E., & Herrera-May, A. L. (2021). Sustainable Development of Concrete through Aggregates and Innovative Materials: A Review. *Applied Sciences*, *11*(2), 629. https://doi.org/10.3390/app11020629

[5]. Ajwad, A. (2023). *Concrete Evolution: An Analysis of Recent Advancements and Innovations*, pp. 1–8, 6th Conference on Sustainability in Civil Engineering, Capital University of Science and Technology, Islamabad, Pakistan.

[6]. Amin, M. N., Iqbal, M., Althoey, F., Khan, K., Faraz, M. I., Qadir, M. G., Alabdullah, A. A., & Ajwad, A. (2022). Investigating the Bond Strength of FRP Rebars in Concrete under High Temperature Using Gene-Expression Programming Model. *Polymers*, *14*(15), 2992. https://doi.org/10.3390/polym14152992

[7]. Ali, T., Ajwad, A., Abbas, A., Khan, M. A., Kashif, M., & Usman, M. (2016). Used Marble Waste Aggregate: Oppurunities For Production Of Eco-Friendly Concrete. *Science International*, 28(2).

[8]. Qureshi, L.A., Ajwad, A., & Ali, B., (2018). Effect of Adding Glass Fibre Reinforced Concrete Topping on Flexural Behaviour of Hollow Core Slab Units, *Engineetring and Technology Journal*, vol. 3(7), pp. 451-455.

[9]. Zajac, M., Skocek, J., Skibsted, J., & Ben Haha, M. (2021). CO_2 mineralization of demolished concrete wastes into a supplementary cementitious material – a new CCU approach for the cement industry. *RILEM Technical Letters*, *6*, 53–60. https://doi.org/10.21809/rilemtechlett.2021.141

[10]. Xu, Z., Huang, Z., Liu, C., Deng, X., Hui, D., & Deng, S. (2021). Research progress on mechanical properties of geopolymer recycled aggregate concrete. *Reviews on Advanced Materials Science*, *60*(1), 158–172. https://doi.org/10.1515/rams-2021-0021

[11]. González-Fonteboa, B., Seara-Paz, S., De Brito, J., González-Taboada, I., Martínez-Abella, F., & Vasco-Silva, R. (2018). Recycled concrete with coarse recycled aggregate. An overview and analysis. *Materiales de Construcción*, *68*(330), 151. https://doi.org/10.3989/mc.2018.13317

[12]. Iqbal, M. J., Zaman, B., & Budihardjo, M. A. (2023). Utilization of recycled and waste material in construction - a review. *IOP Conference Series: Earth and Environmental Science*, *1268*(1), 012046–012046. https://doi.org/10.1088/1755-1315/1268/1/012046

[13]. Gao, X. (2023). Review: Development Trends in the Reuse of Waste Materials in Concrete Production. *Academic Journal of Science and Technology*, *8*(2), 26–30. https://doi.org/10.54097/ajst.v8i2.14714

[14]. Ajwad, A., Ilyas, U., Khadim, N., Usman, A., Ahmad, S., Zahid, B., Waqar, A., Online, A., & Akhtar, A. (2019), Article Assessing the Durability of Concrete with the Addition of Low Quality fly ash, Scientific Inquiry and Review (SIR)

[15]. Ajwad, A., Taseer, S., Jaffar, A., & Ilyas, U., Utilization Of Wastewater For Production Of Sustainable Concrete. *Journal of Natural and Applied Sciences Pakistan*, *4*(1), 2022, pp.876-890.

[16]. Ajwad, A., Ilyas, U., Muzammal, L., Umer, A., & Haider, S. M. (2024). Evaluation of strength parameters of plain and reinforced concrete with the addition of polypropylene fibers. Mehran University Research Journal Of Engineering & Technology, 43(1), 111–118. https://search.informit.org/doi/10.3316/informit.T202404120000770060538705 3.

[17]. Ajwad, A. (2018). Production of Steel Fiber Reinforced Concrete with Different Mix Design Ratios. Scientific Inquiry and Review, 2(4), 23-32. https://doi.org/10.32350/sir.24.03

[18]. Ali, T., Ouni, M.H., Qureshi, M.Z., Mahmood, M.S., Ahmed, H., and A. Ajwad (2024) A Systematic Literature Review of AI-based Prediction Methods for Self-Compacting, Geopolymer, and Other Eco-friendly Concrete Types: Advancing Sustainable Concrete, *Construction and Building Materials*, 137370, In-press.

[19]. Li, G., Zhou, C., Ahmad, W., Usanova, K. I., Karelina, M., Mohamed, A. M., & Khallaf, R. (2022). Fly Ash Application as Supplementary Cementitious Material: A Review. *Materials*, *15*(7), 2664. https://doi.org/10.3390/ma15072664

[20]. Owaid, H., Hamid, R., & Taha, M.R. (2012). A review of sustainable supplementary cementitious materials as an alternative to all-portland cement mortar and concrete. *Australian journal of basic and applied sciences*, *6*, 287-303.

[21]. Nawab, M. S., Ali, T., Qureshi, M. Z., Zaid, O., Kahla, N. B., Sun, Y., Anwar, N., & Ajwad, A. (2023). A study on improving the performance of cement-based mortar with silica fume, metakaolin, and coconut fibers. *Case Studies in Construction Materials*, *19*, e02480. https://doi.org/10.1016/j.cscm.2023.e02480

[22]. Amin, M.N., Raheel, M., Iqbal, M., Khan, K., Qadir, M.G., Jalal, F.E., Alabdullah, A.A., Ajwad, A., Al-Faiad, M.A., Abu-Arab, A.M. Prediction of Rapid Chloride Penetration Resistance to Assess the Influence of Affecting Variables on Metakaolin-Based Concrete Using Gene Expression Programming. *Materials* 2022, *15*, 6959. https://doi.org/10.3390/ma15196959

[23]. Najeeb Al-Hashem, M., Amin, M., Ajwad, A., Afzal, M., Khan, K., Faraz, M. I., Qadir, M. G., & Khan, H. (2022). Mechanical and Durability Evaluation of Metakaolin as Cement Replacement Material in Concrete. *Materials*, *15*(22), 7868.

[24]. Sallı Bideci, Ö., Bideci, A., & Ashour, A. (2024). Utilization of Recycled Brick Powder as Supplementary Cementitious Materials—A Comprehensive Review. *Materials*, *17*(3), 637. https://doi.org/10.3390/ma17030637.

CONVENTIONAL EMPIRICAL AND MACHINE LEARNING MODELS: A REVIEW OF CHLORIDE CONCENTRATION IN MARINE CONCRETE

[a] Muhammad Arif*, [b] Muhammad Luqman

a: Barrick Gold Corporation, Pakistan 18pwciv5179@uetpeshawar.edu.pk
b: Barrick Gold Corporation, Pakistan 18pwciv5026@uetpeshawar.edu.pk
* Corresponding author.

Abstract- The measurement of chloride concentration (Cs) on the surface of the concrete is a crucial parameter for durable design and predicting concrete buildings' longevity in aquatic habitats. As a result of the effects of chloride, numerous reinforced concrete structures cannot achieve their intended or planned lifespan and undergo premature degradation. This study reviews both independent and ensemble machine learning methods applied previously, along with standard empirical provisions now in practice in the design industry. However, the empirical models have some uncertain calculation fallouts in some areas with different onsite constraints, which results in the diversion from experimental onsite measured chloride content. On the other hand, the machine learning model, which utilizes experimental data rather than an empirical calculation foundation, yields much better results but cannot be practiced in design fields due to its reliability on a small set of experimental data. Additionally, the statistical quality of experimental data and onsite experimental and environmental setup constraints are another chapter that needs to be addressed carefully. The overfitting issue is another drawback of machine learning models, though evolutionary models can derive the most superficial and complex empirical equations from surpassing the classical work in this field. The most recent machine learning model, trained on an extensive dataset, successfully incorporated 13 essential features that present a way to confront traditional model limitations. In Swift, all the findings suggest that the predicted accuracy of standard models could be enhanced by incorporating more varied datasets and considering novel variables. It is recommended that a more extensive dataset using applied Physics Informed Neural Networks (PINNs) be employed to reduce overfitting and increase the application of ML models in design disciplines.

Keywords- Conventional Models, Diffusion Constraints, LNEC Model, PINNs.

1 Introduction

Marine concrete's surface chloride content (Cs) is crucial in designing and considering durability. The growing importance of coastal infrastructure is giving rise to an increased focus on studying chloride-induced corrosion in reinforced concrete (RC) structures. Extensive and long-term investigations are currently conducted by researchers on the endurance of concrete when exposed to marine environments, resulting in a significant amount of test data [1]. Ahmad et al. [2] investigated the machine learning (ML) model application for calculating Cs in marine concrete containing waste. The durability design for marine concrete categorizes exposure circumstances into the air, splash, tidal, and submerged zones based on specific standards and recommendations [3], [4]. The benefits and suitability of the ML approach have been confirmed by comparisons with traditional experimental data based quantitative Cs models [5]. The forecast performances of ensemble ML model, standalone ML models, and traditional approaches are compared to determine if, considering domain restriction and applicability while normalizing the experimental data yielding, the best model for predicting

concrete Cs. By comparing traditional and ML methods, this study proposes using a novel method, PINNs, that may help with C_s Prediction and, hence, the durable design of RC structures in coastal settings.

2 Empirical and Conventional Models

Fick's second law of diffusion is often employed to characterize the total entrance of chloride into concrete, regardless of the zone [6]. Eq (1) provides the analytical solution for Fick's second law, commonly used in the service life design of reinforced concrete buildings in marine settings [7].

$$\frac{d\varphi}{dt} = D\ \frac{d_{\varphi}^{2}}{dt^{2}} \tag{1}$$

More specifically, from the perspective of marine concrete, we have simplified this to Eq (2)

$$C(x,T) = C_o + (C_C - C_o)\ [1 -\ \ ERF * \left(\frac{x}{(4 * D_{\ L} * T)^{\frac{1}{2}}}\right)] \tag{2}$$

Where C (x, t) is the chloride concentration after exposure time t, measured at distance x from the surface; C_o represents initial chloride concentration in concrete, C_c represents apparent surface chloride concentration, apparent chloride diffusion coefficient is represented by D_L, and the error function is represented by erf (•). Since C_o is a constant, Cc and D_L define the amount of chloride intrusion. A time-dependent material attribute, the chloride diffusion coefficient D may be calculated or predicted using data related to the microstructure and composition of the material. Cc is a more complex variable than D_L since it varies on time, environmental factors, and material qualities. A convection zone is often seen in many concrete fields. In this scenario, the region of the chloride profile that involves the movement of particles in large quantities is adjusted to determine the value of Cs. Convection zones may not be visible in some laboratory experiments. Hence, the whole profile might be analyzed to determine Cs. Consequently, the vacant applicability space is created while calculating the ingress chloride when compared to the experimental results of the same marine site. Alongside empirical equations, we analyzed many conventional quantitative models of Cs, selecting only a few to substantiate their reliability and applicability compared to other options in the design industry, as represented in Table 1.

Table 1: Ingress Chloride Conventional Models

S.No	Conventional Model (Applicability)	Equation and Description	Ref.
1.	Cai-Yang (Submerged Zone)	$C_{s-ts} = 4.12 * A_c * \left(\frac{w}{b}\right) * C_{sw} * (1 - e^{-0.56*t})$	[8]
2.	DuraCrete (All Zones)	$C_s = A_c \left(\frac{w}{b}\right)$	[9]
3.	Song's (All Zones)	$C_s = 1.52 * ln(3.77t + 1)$	[10]
4.	Chalee's (Tidal Zones)	$C_s = \left[-0.379\ \left(\frac{w}{b}\right) + 2.064\right] \ln(t) + \left[4.078\ \left(\frac{w}{b}\right) + 1.01\right]$	[11]
5.	Petcherdchoo's (Tidal Zones)	$C_s = 10^{(0.814\left(\frac{w}{b}\right)*0.213} + 2.11 * t^{0.5}$	[12]
6.	Costa's (Tidal Zones)	$C_s = 0.38 * t^{0.37}$	[13]
7.	LNEC (All Zones)	$C_s = 2.5\left(w/_b\right)k_T C_b$	[14]
8.	Cai's (Tidal and Splash Zones)	$C_{s-ts} = 10.01 * A_c * \left(\frac{w}{b}\right) * (1 - e^{-0.96*t})$	[15]
***C_{sw}**: Seawater Chloride Concentration (%), ***A_c**: binder type correction factor (%) , ***t**: exposure time (years), ***k_T**: coefficient accounting for the concrete temperature and ***C_b**: Cs in the conditions of the specific coastal (%),			

The Root-Mean Square Error (δ) and the μ (projected to the experimental values mean ratio) are used to assess each model's prediction accuracy and determine their usefulness. Among the eight standard C_s models, the Cai-Yang model possesses the best fitting accuracy, with δ being 1.71% and μ being 1.17 applicable to only submerged zones. The empirical equation of this model relies on the water-to-binder ratio (w/b) and A_c (a correction factor representing the binder type). The performance of the Song's and DuraCrete models is inferior to that of the Yang model. The DuraCrete, like the Cai-Yang model, relies on identical parameters but can be implemented throughout all zones. Furthermore, Song's model [10], unlike the other two models, relies on the duration of exposure and suggests a logarithmic relationship between C_s and t. Costa's, Petcherdchoo's, and Chalee's models provide accurate forecasts but are limited in their applicability to the tidal zone. A thorough comparison of traditional models reveals that a model that incorporates a broader range of data sources and considers more influential elements has the potential to achieve superior performance in forecasting Cs. Costa et al. [13]

demonstrated that the Cs in concrete exposed to all climates except submerged zones consistently rise over time, irrespective of the concrete compositions used. Power functions were used to fit time-dependent models of Cs based on long-term exposure field data for concrete. The LNEC Model suggests that the Cs model is a folded-linear equation, where Cs increases linearly during the initial exposure stage and then reaches and maintains a constant value during the stable stage following prolonged exposure. Petcherdchoo et al. [12] proposed the Cs model as a n^{th} root function. However, the model's projected values were found to overestimate the Cs during the steady period of concrete weathering.

Some investigators also offered exponential time-dependent Cs models. Time-dependent Cs models in the literature contain exponential, logarithmic, linear, folded-linear, and square root functions. These models were not developed entirely from field test data but with several expedited lab tests.

3 Machine Learning Models

While using Eq. (2), recommendations often assume that C_o remains constant in specific surroundings. However, this assumption might result in a substantial margin of error. Several previous studies have shown a wide range of field values for C_o and have also presented quantitative frameworks for this significant parameter [8], [15], [16]. Nevertheless, the models could have performed better in accurately predicting or describing Cs. This is due to the intricate nature of Cs, which is influenced by numerous factors, including environmental conditions (such as chloride levels in seawater, zonation, carbonizing effects, climate, and relative the level of humidity), material properties (such as content of binder, composition of binder, ratio of water and binder(w/b)), and the period of contact. Cia et al. [17] applied the ensemble ML technique to forecast the chloride content in marine concrete with the highest correlation factor up till now in the literature. However, these models fail to adequately capture the pattern of fast initial growth followed by eventual stabilization of Cs levels [11], [18]. In addition, several models failed to include other crucial elements, namely, the composition of materials and the classifications of environmental actions. Previous studies [12], [16], [19] have developed predictive models for Cs concentrations based on the (w/b) and exposure duration (t). However, these models did not include the influence of binder type and environmental conditions. The models presented in [9] and Costa et al. [14] include variables related to materials and environmental action classes in the context of Cs. However, these models fail to include the significant influence of exposure duration. These typical quantitative Cs models are limited in addressing all significant elements due to insufficient experimental data and a robust flow to account for many variables. The empirical equations, conventional models, and ML models had flaws due to reliability, limited applicability, and overfitting. ML experts often recommend an extensive dataset with more reliable parameters. This often leads to synthetic and experimental data in a controlled environment with different site conditions and climate catalysts. However, taking in-depth data trends from such a diverse dataset, Artificial Neural Networks (ANN) is insufficient. This review study recommends that the Physic Informed Neural Networks (PINNs) forecast the marine concrete chloride content. A PINN is a network that integrates physical rules or principles into its structure and training methodology. Incorporating physics into the neural network makes it more adept at accurately representing and following the fundamental equations regulating a given system. Fig. 1 illustrates that data taken by PINNs will result in a prediction later compared with experimental values and onward fed back to the same loop, reinforcing the accuracy and making the loop dynamic.

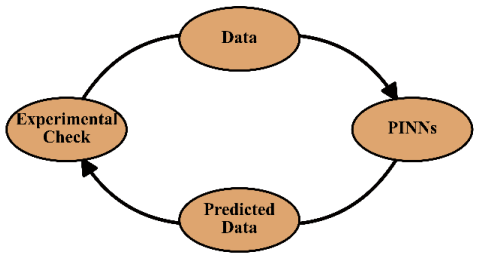

Fig. 1: PINNs Workflow Loop

They are engineered specifically to adhere to and integrate established physical rules or equations that govern a particular system. This is accomplished by integrating words into the neural network design that embodies these fundamental physical laws. PINNs seek to integrate the advantages of data-driven machine learning by explicitly incorporating physics rules. This enables the model to provide precise forecasts using the existing data while staying in line with the underlying rules governing the system. They are significant when a limited amount of data is available or when acquiring data is costly. These networks may provide precise forecasts using the constraints even when training data has low dimensions.

4 Conclusion

This study reviews the employed ensemble and independent ML prediction techniques in contrast with the empirical equations for chloride content in marine space while considering the experimental data as standard. Fick's law is the most practiced empirical equation, but it has flaws due to parameter representations and inclusive relationships. Some conventional quantitative models addressed all zones of the marinated environment but still lag experimental data due to missing critical parameters. In contrast, others are limited to specific zones and yield good results in local environments. ML Models considerably have more accurate results than conventional models and design practical equations. The most diverse dataset considered till now consists of 642 data points from different zones, but due to the data clustering, linearization, and symmetry, the issue of overfitting arises, which suggests that Physics-Informed Neural Networks (PINNs) should be used instead of Artificial Neural networks (ANNs) while tackling the experimental setup discrepancies across laboratory research. To improve proposed model's endurance and dependability, future research should concentrate on controlled experimental testing with PINNs, a reliable source for data collection in the same setting from different environmental conditions with more diverse parameters taken into account.

5 References

[1] C. E. T. Balestra, T. A. Reichert, and G. Savaris, "Contribution for durability studies based on chloride profiles analysis of real marine structures in different marine aggressive zones," *Constr Build Mater*, vol. 206, 2019, doi: 10.1016/j.conbuildmat.2019.02.067.

[2] A. Ahmad, F. Farooq, K. A. Ostrowski, K. Śliwa-Wieczorek, and S. Czarnecki, "Application of novel machine learning techniques for predicting the surface chloride concentration in concrete containing waste material," *Materials*, vol. 14, no. 9, 2021, doi: 10.3390/ma14092297.

[3] T. A. Reichert, C. E. T. Balestra, and R. A. de Medeiros-Junior, "Coupled model on the variation of diffusion coefficient and surface chloride concentration in reinforced concrete structures over time," *Constr Build Mater*, vol. 411, 2024, doi: 10.1016/j.conbuildmat.2023.134715.

[4] V. Q. Tran, V. L. Giap, D. P. Vu, R. C. George, and L. S. Ho, "Application of machine learning technique for predicting and evaluating chloride ingress in concrete," *Frontiers of Structural and Civil Engineering*, vol. 16, no. 9, 2022, doi: 10.1007/s11709-022-0830-4.

[5] D. Chen, G. Mei, and L. Xiao, "Chloride diffusion in marine pipe pile considering time-dependent surface chloride concentration: Experimental analysis and analytical model," *Applied Ocean Research*, vol. 140, 2023, doi: 10.1016/j.apor.2023.103722.

[6] M. COLLEPARDI, A. MARCIALIS, and R. TURRIZIANI, "Penetration of Chloride Ions into Cement Pastes and Concretes," *Journal of the American Ceramic Society*, vol. 55, no. 10, 1972, doi: 10.1111/j.1151-2916.1972.tb13424.x.

[7] I. Stipanovic Oslakovic, D. Bjegovic, and D. Mikulic, "Evaluation of service life design models on concrete structures exposed to marine environment,"*Materials and Structures/Materiaux et Constructions*, vol.43, no.10,2010, doi: 10.1617/s11527-010-9590-z.

[8] L. F. Yang, R. Cai, and B. Yu, "Modeling of environmental action for submerged marine concrete in terms of surface chloride concentration," *Structural Concrete*, vol. 19, no. 5, 2018, doi: 10.1002/suco.201800072.

[9] DuraCrete, "General Guidelines for Durability Design and Redesign," *The European Union-Brite Euram III, Project No. BE95-1347, Probabilistic Performance -based Durability Design of Concrete Structures*, 2000.

[10] H. W. Song, H. B. Shim, A. Petcherdchoo, and S. K. Park, "Service life prediction of repaired concrete structures under chloride environment using finite difference method," *Cem Concr Compos*, vol. 31, no. 2, 2009, doi: 10.1016/j.cemconcomp.2008.11.002.

[11] W. Chalee and C. Jaturapitakkul, "Effects of W/B ratios and fly ash finenesses on chloride diffusion coefficient of concrete in marine environment," *Materials and Structures/Materiaux et Constructions*, vol. 42, no.4,2009, doi: 10.1617/s11527-008-9398-2.

[12] A. Petcherdchoo, "Time dependent models of apparent diffusion coefficient and surface chloride for chloride transport in fly ash concrete," *Constr Build Mater*, vol. 38, 2013, doi: 10.1016/j.conbuildmat.2012.08.041.

[13] A. Costa and J. Appleton, "Chloride penetration into concrete in marine environment - Part I: Main parameters affecting chloride penetration," *Materials and Structures/Materiaux et Constructions*, vol. 32, no. 4, 1999, doi: 10.1007/bf02479594.

[14] P. F. Marques, A. Costa, and F. Lanata, "Service life of RC structures: Chloride induced corrosion: Prescriptive versus performance-based methodologies," *Materials and Structures/Materiaux et Constructions*, vol. 45, no. 1–2, 2012, doi: 10.1617/s11527-011-9765-2.

[15] L. F. Yang, R. Cai, and B. Yu, "Investigation of computational model for surface chloride concentration of concrete in marine atmosphere zone," *Ocean Engineering*, vol. 138, 2017, doi: 10.1016/j.oceaneng.2017.04.024.

[16] W. Chalee, C. Jaturapitakkul, and P. Chindaprasirt, "Predicting the chloride penetration of fly ash concrete in seawater," *Marine Structures*, vol. 22, no. 3. 2009. doi: 10.1016/j.marstruc.2008.12.001.

[17] R. Cai *et al.*, "Prediction of surface chloride concentration of marine concrete using ensemble machine learning," *Cem Concr Res*, vol. 136, 2020, doi: 10.1016/j.cemconres.2020.106164.

[18] A. Jayasuriya and T. Pheeraphan, "Prediction of Time to Crack Reinforced Concrete by Chloride Induced Corrosion," *International Journal of Civil and Environmental Engineering*, vol. 11, no. 9, 2017.

[19] Q. Li, K. Li, X. Zhou, Q. Zhang, and Z. Fan, "Model-based durability design of concrete structures in Hong Kong-Zhuhai-Macau sea link project," *Structural Safety*, vol. 53, 2015, doi: 10.1016/j.strusafe.2014.11.002.

RETROFITTING OF CONFINED MASONRY STRUCTURE WITH FIBER REINFORCED POLYMER (FRP)

[a] Ajmal Khan*, [b] Qazi Sami Ullah

a: Civil Engineering, University of Engineering and Technology, Peshawar, Pakistan. ajmalkhan.civ@uetpeshawar.edu.pk
b: Civil Engineering, University of Engineering and Technology, Peshawar, Pakistan. samiullah.qazi@uetpeshawar.edu.pk
* Corresponding author.

Abstract- The following experiment presents a method for evaluating the earthquake resistance of confined masonry buildings before and after being strengthened using fiber-reinforced polymer (FRP). The results of this research are anticipated to substantially impact future studies' direction and design guidelines' development, contributing to the global understanding of seismic retrofitting in confined masonry structures. A 1:3 scale-down single-story confined masonry structure (CM) constructed by ERRA guidelines was subjected to a novel application of a consistent vertical force and displacement-based reverse cyclic lateral loading up to maximum resistance. The damaged model underwent a retrofit using fiber-reinforced polymer (FRP) and was then tested again until it failed under the same conditions. The efficiency of FRP retrofitting was assessed through a thorough examination of the damage distribution and force-displacement characteristics of the retrofitted confined masonry structure (RCM) compared to the original confined masonry structure (CM). The experimental data, presented as force-deformation parameters, clearly demonstrate the benefits of FRP in improving lateral displacement and deformability.

Keywords- Confined Masonry, Retrofitting, Seismic.

1 Introduction

The most admired type of residential structure is masonry. These structures are economical and have good thermal insulation properties, with aesthetic vistas. Three types of masonry structures exist confined masonry (CM), un-reinforced masonry (URM), and masonry infill RC frame structures. After the Kashmir earthquake in October 2005, which resulted in 73000 fatalities and left 70000 people injured, 3.5 million individuals were also displaced from their homes.[1]. Most damaged structures were unreinforced masonry (URM) buildings[2]. Confined masonry (CM) is now extensively utilized for cost-effective building construction, addressing the issues about unreinforced masonry, and this study aims to validate its effectiveness further. The confined masonry structures have also sustained significant damage in previous earthquakes. Now, buildings that have experienced partial damage can be retrofitted or rebuilt. We often lean towards retrofitting as it is more cost-effective and efficient than reconstruction, providing a sense of reassurance and confidence in our approach. Different researchers have analyzed different retrofitting techniques.[3]

Different researchers have worked on the behavior of FRP-retrofitted masonry walls under seismic forces. Relatively, no study has been seen on an experimental investigation of the influence of FRP on confined masonry structures built according to the ERRA guidelines, which represents the typical building structure found in the northern regions of Pakistan.

In this context, a 1:3 scale-down CM single-story structure was built and placed to a quasi-static lateral load test. The damaged building underwent retrofitting with FRP before being retested to assess the repair approach's effectiveness. The experimental results regarding lateral deformation and deformability were compared and discussed.

2 Research Methodology

2.1 Test Specimen

A typical 1/3 reduced-scale confined masonry structure was built at UET Peshawar. First, the test specimen was constructed on a substantial reinforced concrete raft footing of dimension 72"x64"x6" (length x width x height)), reinforced with 12mm bars placed at 4-inch intervals in both directions, all vertical confinement elements (3"x3") rebar were extended from the foundation to the RCC slab, were cast. The building was erected upon the pad using handmade burnt clay brick units till sill band. Then, the openings (a door and window) were provided, which were confined horizontally and vertically with the seismic band and lintel band, having a cross-section of 2"x3" (depth x width), reinforced with four longitudinal bars of 3/24" diameter and stirrups of 3/24" diameter spaced at 12" c/c. Similarly the construction was continuous up to lintel band. Finally, the construction of specimens was completed by casting 3" thick RC slab. Details of the room are shown in Figure 1.

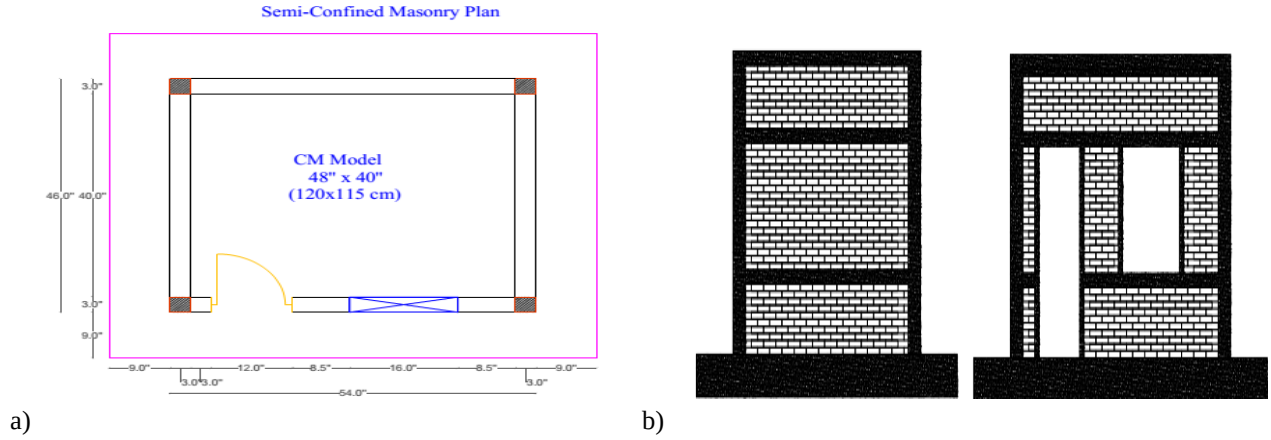

a) b)

Figure 1: Test Specimen, a. Plan view of the Model, and b. Elevation view of the model

2.2 Testing

The upper part of the specimens was clear to enable unrestricted movement in all directions while keeping the lower part immobile. A constant vertical load of 735 kg was imposed by placing steel plates of known weights above the specimen. The structure was subjected to lateral load with the help of a hydraulic jack. Horizontal displacement was recorded by connecting twelve LVDTs. The load cell and LVDTs were connected to the UCAM-70A data logger to record the induced load and resulting displacement and strains at various locations.

The structure was placed to displacement control horizontal loading with a constant vertical load at the roof level. Each cycle of displacement is comprised of two (negative and positive) amplitudes, with similar loading conditions in both directions. Starting from 0.25mm, all displacement cycles were repeated three times. After every cycle, the appeared cracked marked with marker and prepare short note from load and displacement. This load cycle procedure was in progress until the load decreased by 20% of the maximum load because, in this stage, the structure could be retrofitted.

3 Retrofitting Technique

3.1 Retrofitting with FRP

The cracks and overall structure were cleaned with a brush, and loose mortars were replaced with fresh mortar. Then, injection ports or nozzles made of plastic, each with a diameter of 6 mm, were placed into pre-drilled holes located at intervals of about 150 mm along the cracks. The surface cracks were sealed using cement mortar and left to cure for seven days. Before grout injection, the air was directed through nozzles to eliminate any dust inside the cracks and to inspect the connection between the nozzles. Grout was pumped under high pressure of over 0.6 MPa from the lower to the upper nozzles against the force of gravity. The CFRP's woven structure was unidirectional. The FRP strips, which have a width

of 3 inches, were bonded in the vertical direction on the coated surface, and then, The FRP strips received an additional layer of epoxy coating.CHEMDUR-52 LP of components A and B with 2:1 was used as epoxy resin. Anchors were installed to prevent FRP strip detachment and to improve the bond performance between the FRP and masonry substrate. The FRP strips received a final epoxy coat to avoid the detachment of the FRP strips and improve the bonding performance between the FRP and the masonry substrate anchors during testing. The Retrofitted CM structure (CFRP-Retrofitted masonry) was subjected to the same loading condition and test procedure as the control specimen.

4 Results

4.1 Before Retrofitting

A cyclic horizontal load was performed on the model. The damage scheme is shown in Figure 2. A. The primary type of failure observed was a step crack that traversed mortar joints and a diagonal shear crack in the confined vertical column at the joint where the slab corner meets. The experiment was halted when reaching a maximum displacement of 19 millimeters, resulting in moderate damage. Figure 2. b illustrates the envelope curve of the CM structure. The structure reached its high lateral load-resisting capacity (40.50 KN) at 18mm displacement, after which strength degradation started.

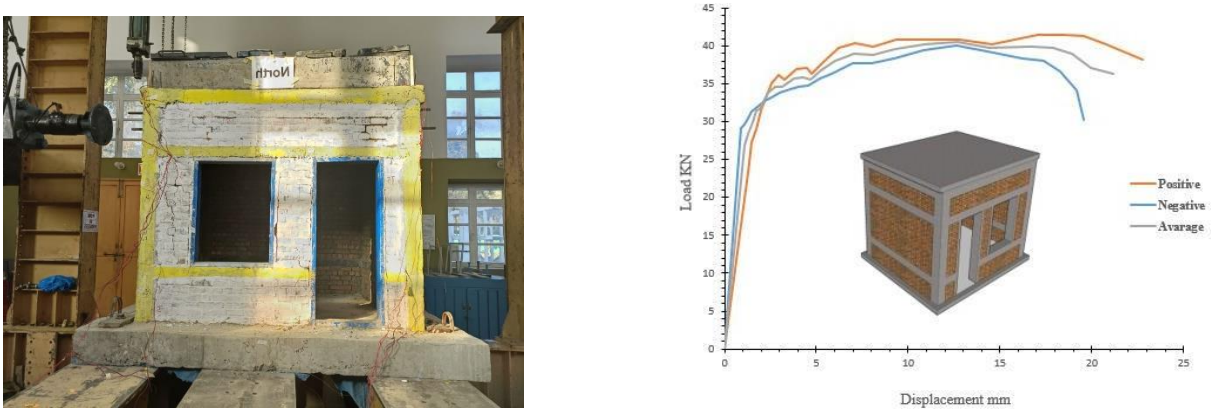

a) b)

Figure 2: CM results, a. Failure of confined vertical column b. Envelope curve

4.2 After Retrofitting

Similar to the CM structure, a shear crack at an angle appeared in the tie column near the corner joint of the slab, which was wide enough to be visible during testing, and the FRP was ruptured at that point, as shown in Figure 3. a. The test was then stopped. Figure 3. b shows hysteresis loops of retrofitted confined masonry structures. The structure's highest resistance was 57KN, reached at a displacement of 28mm, following which there was a gradual decrease in strength.

a) b)

Figure 3: Retrofitted CM results, a. Failure of retrofitted confined tie column b. Envelope curve

4.3 Force-Deformation Parameters Comparison

A comparison of the force deformation parameters is shown in Table 1.

The estimated maximum load, Vu, is calculated using the formula Vu=0.9Vmax. The effective stiffness, Keff, is determined by dividing 0.75Vu by the displacement on the envelope curve that corresponds to it. The displacement at yield is determined by the formula Δy=Vu/Keff. The maximum displacement occurs at a location corresponding to 0.8 times the ultimate shear strength in the envelope curve. Once these values have been calculated, the displacement ductility, represented by μ, is defined as the ultimate displacement divided by the yield displacement, or μD = Δu/Δy[4]. The response modification factor (R) and the displacement amplification factor (Cd) were computed using equations 4.1 and 4.2, respectively.

$$R = \sqrt{2\mu - 1} \quad \text{eq.4.1} \qquad C_d = \frac{\mu}{\sqrt{2\mu - 1}} \quad \text{eq.4.2}$$

Table 1: Force-deformation parameters

Parameters	CM specimen	CFRP-retrofitted Specimen	Ratio (CFRP-retrofitted/CM)
Maximum load Vu (kN)	36.45	51.30	1.40
Elastic Stiffness (kN/mm)	18.22	6.41	0.35
Yield Displacement (Δy) (mm)	2.00	8.00	4.00
Ultimate Displacement (Δu) (mm)	19.00	32.00	1.68
Displacement Ductility μ	9.5	4.00	0.42
Response modification factor (R)	4.24	2.64	0.62
Displacement amplification factor (Cd)	2.23	1.51	0.67

5 Conclusion

The following conclusions can be drawn from the conducted study:

1 Externally bonded CFRP strips are an effective retrofitting system for enhancing the seismic performance of CM buildings.
2 After retrofitting, the structure's lateral load capacity increased from 40.50 kN to 57 kN, 40.7 % higher.
3 Formability experienced a substantial decrease of 0.42.
4 The modification factor R and the displacement-amplification factor Cd were determined based on the idealized bilinear curves for the cases before and after retrofitting. The values for R and Cd were 34.24 and 2.23 for the original buildings and 2.64 and 1.51 for the retrofitted structure, respectively. Values for consideration in the development of seismic design guidelines are recommended.

Acknowledgment

The author would like to thank the staff of the Civil Engineering Department, University of Engineering and Technology, Peshawar, for their support and guidance. The careful review and constructive suggestions by the anonymous reviewers are gratefully acknowledged.

Reference

[1] Asian Development Bank/World Bank (ADB/WB), "Preliminary Damage and Needs Assessment-Pakistan 2005 Earthquake, Report No. ADB-WB 2005." 2005.
[2] M. Javed, "Seismic Risk Assessment of Unreinforced Brick Masonry Buildings System of Northern Pakistan," p. 200, Jan. 2009. [Online]. Available: https://www.researchgate.net/publication/257943495
[3] M. ElGawady, P. Lestuzzi, and M. Badoux, "A REVIEW OF CONVENTIONAL SEISMIC RETROFITTING TECHNIQUES FOR URM". [Online]. Available: https://www.researchgate.net/publication/312341576
[4] Z. Ahmad et al., "Seismic Capacity Assessment of Unreinforced Concrete Block Masonry Buildings in Pakistan Before and After Retrofitting," J. Earthq. Eng., vol. 19, no. 3, pp. 357–382, Apr. 2015, doi: 10.1080/13632469.2014.963744.

A CASE STUDY ON REMEDIAL MEASURES FOR FIRE-DAMAGED STRUCTURE

[a] Muhammad Dawood Ali*, [b] Ali Ejaz

a: Rk Engineering & Consulting Services, Islamabad, Pakistan. kdaud914@gmail.com
b: Center of Excellence in Earthquake Engineering and Vibration, Department of Civil Engineering, Chulalongkorn University, Bangkok 10330, Thailand. enggaliejax@gmail.com
* Corresponding author.

Abstract- This paper addresses solutions for buildings damaged by fire and the measures needed for their future usability. Some buildings suffer severe damage from intense fires, while others can be salvaged with a swift response. The case study focuses on Galaxy Heights, a five-story multipurpose building in Gulberg Greens, Islamabad, which, despite significant fire damage, remained usable. During the site visit, no major structural damage was observed, indicating that the building could be rehabilitated using a proposed solution that includes various strengthening chemicals, fire-resistant paint, and the installation of a proper firefighting system. The implementation of this restoration methodology successfully restored the building to its normal usage.

Keywords- Deterioration, Thermal, Strengthening, Retrofit.

1 Introduction

Gulberg is a major construction project in Islamabad, featuring numerous residential and commercial buildings. Developed by the Intelligence Bureau Residential Housing Society, it is strategically located in the heart of Islamabad, along the Islamabad Highway Express. The project is conveniently situated, a 10-minute drive from G.T. Road and only 6 to 7 minutes from the Capital University of Sciences and Technology. Additionally, it is just 10 to 12 minutes away from the Blue Area of Islamabad [1]. During their lifespan, buildings are exposed to a range of hazards, including natural events such as earthquakes, hurricanes, and tsunamis, as well as man-made incidents like fires and explosions. These hazards pose significant risks, potentially causing partial or total collapse of buildings, rendering them inoperative. To mitigate these risks, buildings in projects like Gulberg are designed with advanced engineering techniques and materials to enhance their resilience. This includes incorporating seismic design principles, fire-resistant materials, and robust structural systems to ensure the safety and longevity of the infrastructure. Additionally, regular maintenance and inspections are conducted to identify and address any potential vulnerabilities, ensuring that the buildings remain safe and functional throughout their intended lifespan [2]. In the event of operational hazards, such damage or failure can pose a significant threat to the safety of residents and result in substantial direct and indirect financial losses. Direct losses include the cost of repairing or rebuilding damaged structures, while indirect losses encompass disruptions to daily life, business operations, and the broader economy. To mitigate these risks, it is crucial to implement comprehensive safety measures and emergency response plans. This includes advanced engineering techniques, rigorous building codes, regular maintenance, and proactive disaster preparedness programs. Ensuring the resilience and safety of buildings not only protects residents but also minimizes financial impacts and enhances community stability and economic resilience.

Therefore, structures are constructed to endure various expected risks [3]. These designs safeguard structural integrity and protection throughout the building's lifespan. Fire is one of the most dangerous hazards, and fire safety encompasses a set of methods aimed at preventing fires and mitigating their effects. Key fire safety measures include the use of fire-resistant materials, installation of smoke detectors and sprinkler systems, and the incorporation of fire escapes and emergency exits. Additionally, buildings are equipped with fire alarms and extinguishers, and regular fire drills are conducted to ensure occupants are prepared in case of an emergency. Proper planning and adherence to fire safety regulations are essential in

minimizing the risk of fire-related incidents and ensuring the safety and well-being of residents and users [4], [5]. When internal stresses surpass the allowable tensile limits of concrete elements, thermal cracks and spalling can initiate within the material. The deformation characteristics under uniaxial stress of the concrete composite are distinctly manifested based on its type [6]. Fire safety also involves managing the development and consequences of accidental or intentional fires. Fire safety in structures is currently ensured by various specifications outlined in the Building Code of Conduct. Active fire protection techniques, such as sprinklers, heat and smoke detectors, are crucial for detecting, controlling, or extinguishing fires at an early stage, which is vital for life safety [7]. Passive fire protection techniques, including both structural and non-structural modules, are designed to guarantee the stability of the structure during a fire and to prevent its spread. Their primary purpose is to provide sufficient time for firefighting and rescue works and to reduce financial costs [8]. Fig. 1 provides some forms of active and passive fire protections.

This paper addresses solutions for buildings damaged by fire and the measures needed for their future usability. The objectives of this work are to evaluate the extent of fire damage, propose effective rehabilitation techniques, and ensure the restored buildings meet safety standards for future use. The case study focuses on Galaxy Heights, a five-story multipurpose building in Gulberg Greens, Islamabad, which, despite significant fire damage, remained structurally sound. During the site visit, no major structural damage was observed, indicating the building could be rehabilitated. The proposed solution includes applying various strengthening chemicals, fire-resistant paint, and installing a proper firefighting system. This restoration methodology not only restored the building to its normal usage but also enhanced its resilience against future fire incidents, ensuring long-term safety and functionality.

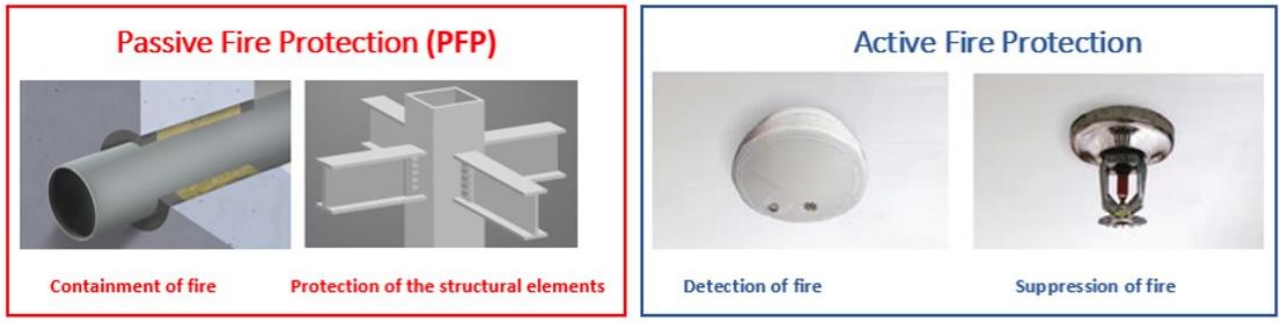

Figure 1: Active vs. passive fire protections (examples) [9]

1.1 Fire Causes/Reason

For the subject building, initial observations indicated that the fire started due to a short circuit in the main distribution board of the generator. Around 7 A.M., when the Water and Power Development Authority (WAPDA) shut down electricity (load shedding), the generator activated automatically. As the generator began supplying power to the board, a short circuit occurred, igniting the fire. The fire then spread to the generator control room and eventually engulfed the entire top floor of the building. These initial observations were later confirmed by the findings of the firefighting team [7].

2 Post-Fire Observed Damages

Heat transfer significantly impacts the mechanical and thermal behavior of both concrete and steel. Thermal propagation causes heat to move from one point to another, affecting the materials. When steel is exposed to high temperatures, it loses its mechanical properties and experiences additional thermal strain [10]. Compared to steel, concrete loses strength at relatively higher temperatures. Unlike steel, concrete does not melt but deteriorates and decomposes. Concrete starts losing its strength around 500-600 degrees Celsius. Upon cooling, it loses strength again, behaving like a brittle material. Exposure to direct fire damages the structural properties of concrete, and the redistribution of forces within the structure increases the probability of failure of structural members [4].

2.1 Concrete Colors at Different Temperatures (Visual Color Change)

After the fire incident, the building owner engaged a company called "RK Engineering & Consulting Services, Islamabad" to assess the damage caused by the fire. The company dispatched a team of senior civil engineers to inspect the condition

of Galaxy Heights and document the damage. The team made the following observations. Table 1 details the changes in concrete color over a range of fire exposure.

- Two columns of the 5th floor were found damaged by fire. (concrete covers were damaged & steel was exposed but remained undamaged)
- Two beams of the 5th floor roof were found damaged by fire. (concrete covers were damaged & steel was exposed but remained undamaged)
- 5th floor roof was burnt up to some extent
- Wooden sealing was found burnt.
- Wooden doors were burnt.
- There was some furniture on the 5th floor of the building that caught fire.

Table 1: Color changes in concrete due to temperature

Temperature Range, ºC	Concrete Color	Visual	State
Smaller than 300	Normal	Normal	Normal
300 to 600	Pink to red	Surface crazing, cracking and aggregate pop outs	Sound but strength may be reduced
600 to 950	Whitish grey	Spalling, exposed of steel reinforcement and powdered existence	Weak
Greater than 950	Buff	Extreme spalling	Extreme/severe

3 Possible Solutions to Make Reusable Building

- Strengthening the columns, beams, and slab of the 5th floor by increasing the size of structural element. (by using strengthening chemicals in concrete + plaster) (Design change)
- Repair structural damage by using different strengthening chemicals and apply fire resistant paint with proper firefighting system installation.
- Provision of steel bracings to weak structural elements (columns, beams)
- Substitute structural element introduce (column, beam)
- Demolish the entire structure and rebuild the whole building.
- Rebuild only 5th floor of Galaxy Heights.
- Repair the damaged portion the same as it was before fire simply by ordinary concrete and plaster. (Without any epoxies, chemical use in it).

3.1 Most Economical Solution/Purposed Solution from Engineering Point of View

As engineering point of view, keeping in experience and technical knowledge of structures and building load transfer mechanism we will go for second point, i.e., "Repair structural damage by using different strengthening chemicals, retrofit new wooden feature parts, and apply fire resistant paint with proper firefighting system installation" The main purpose of this solution is related to the building condition [8]. The structure was not in the worst condition, and it could be repaired with structural strengthening chemicals like Sikawarp-300 (structural strengthening fabrics) & Sikawarp-900C (Stitched carbon fiber fabric). In addition to this, we will go for SBR Chemical (Ressi SBR 5850) & SLR chemical (SLR-L 4601) joints in steel and concrete [8].

3.2 Solution Mechanism Proposed

The recommended rehabilitation measures for the fire-damaged Galaxy Heights building in Gulberg Greens include several crucial steps. First, remove all damaged or weakened concrete and plaster from the affected areas, including columns, beams, and slabs, to ensure a clean and stable base for repairs. Next, replace weakened reinforcement and apply strengthening chemicals to improve the efficiency of bonds between steel and concrete. Use plaster mixed with chemicals containing carbon fibers, such as Sikawarp-900C, to enhance structural strength. Once the structural damage is rectified, apply fire-resistant paints to the repaired columns, beams, and slabs. Install new wooden doors treated with fire-resistant epoxies to further enhance safety. Finally, implement a comprehensive firefighting plan, ensuring that all systems, including fire alarms and sprinklers, are up to date and fully operational. These measures are designed to restore the building's structural integrity, improve fire safety, and ensure the building's future usability.

4 Conclusions

In conclusion, the assessment of the fire damage to Galaxy Heights in Gulberg Greens, Islamabad, reveals both the immediate challenges posed by the fire and the potential for effective remediation. Despite significant damage to elements such as columns, beams, and wooden features, the structural integrity of the building remained largely intact, offering hope for restoration and reuse:

- Despite fire damage, Galaxy Heights presented an opportunity for restoration, ensuring continued utilization of existing infrastructure.
- By employing advanced strengthening chemicals, refurbishing wooden features, and implementing fire-resistant coatings, structural integrity could be regained.
- The proposed solution balances effectiveness with cost-efficiency, offering a practical approach to rehabilitation.

Acknowledgement

The careful review and constructive suggestions by the anonymous reviewers are gratefully acknowledged.

References

[1] A. Bayraktar, A. C. Altunişik, and M. Pehlivan, "Performance and Damages of Reinforced Concrete Buildings During the October 23 and November 9, 2011 Van, Turkey, Earthquakes," *Soil Dynamics and Earthquake Engineering*, vol. 53, pp. 49–72, Oct. 2013, doi: 10.1016/J.SOILDYN.2013.06.004.
[2] "https://policies.wsu.edu/prf/index/manuals/8-00-fire-safety/8-20-reporting-fires-fire-survival/ ".
[3] C. X. Xu, S. Peng, J. Deng, and C. Wan, "Study on Seismic Behavior of Encased Steel Jacket-Strengthened Earthquake-Damaged Composite Steel-Concrete Columns," *Journal of Building Engineering*, vol. 17, pp. 154–166, May 2018, doi: 10.1016/J.JOBE.2018.02.010.
[4] "https://www.amherst.edu/offices/enviro_health_safety/fire/report_fire ".
[5] "https://few.kp.gov.pk/page/forest_fires_analysis_report_2022/page_type/news ".
[6] M. Amran, S. S. Huang, A. M. Onaizi, G. Murali, and H. S. Abdelgader, "Fire spalling behavior of high-strength concrete: A critical review," *Constr Build Mater*, vol. 341, p. 127902, Jul. 2022, doi: 10.1016/J.CONBUILDMAT.2022.127902.
[7] D. Qin, P. K. Gao, F. Aslam, M. Sufian, and H. Alabduljabbar, "A comprehensive review on fire damage assessment of reinforced concrete structures," *Case Studies in Construction Materials*, vol. 16, p. e00843, Jun. 2022, doi: 10.1016/J.CSCM.2021.E00843.
[8] "https://www.concrete.org.uk/fingertips-nuggets.asp?cmd=display&id=895".
[9] "https://www.nullifire.com/en-gb/expert-insights/expert-advice/understanding-passive-fire-protection/".
[10] M. Shahpari, P. Bamonte, and S. Jalali Mosallam, "An experimental study on mechanical and thermal properties of structural lightweight concrete using carbon nanotubes (CNTs) and LECA aggregates after exposure to elevated temperature," *Constr Build Mater*, vol. 346, p. 128376, Sep. 2022, doi: 10.1016/J.CONBUILDMAT.2022.128376.

SUSTAINABLE REHABILITATION OF FIRE-DAMAGED LOW-RISE RC STRUCTURES: ASSESSMENT, RETROFITTING, AND BAMBOO FIBER SOLUTIONS

[a] Faheem Ahmad Gul*, [b] Arshad Ullah

a: School of Civil and Architectural Engineering, Nanchang Institute of Technology, Nanchang 330099, China. faheem@nit.edu.cn
b: M/s Hidayat Ullah Khan & Brothers, Islamabad, Pakistan. hkb.engineers@gmail.com
* Corresponding author.

Abstract- Urban fires pose significant risks to structures, lives, and the environment, necessitating efficient post-fire rehabilitation methods. This paper explores the assessment, retrofitting techniques, and sustainable solutions for fire-damaged low-rise reinforced concrete (RC) structures. Understanding fire behavior and its impact on concrete integrity is crucial, with post-fire assessments playing a pivotal role in determining structural viability. Various parameters, including temperature variations and concrete conditions, are evaluated to quantify fire damage accurately. Retrofitting techniques aim to restore structural integrity, with bamboo fiber reinforcement emerging as a sustainable alternative. Bamboo fibers enhance strength and durability while reducing reliance on non-renewable materials, offering cost-effective solutions for urban infrastructure repair. This research emphasizes the importance of sustainable rehabilitation practices to mitigate the impact of fires on urban infrastructure.

Keywords- Assessment, Bamboo Fibers, Retrofitting Techniques, Sustainable Solutions, Urban Fires.

1 Introduction

Urban fires cause significant property damage and loss of life. Rehabilitating fire-damaged concrete structures must consider structural integrity, safety, and sustainability. Sustainable rehabilitation methods are crucial for mitigating the impact on urban infrastructure, especially in underdeveloped nations where fire disasters are common [1]. To address the sustainability and effectiveness of bamboo fibers in post-fire retrofitting, a summary of research studies and their findings is provided in Table 1. This compilation highlights the benefits and applications of bamboo fibers in enhancing the structural integrity of fire-damaged concrete structures. Fire-damaged RC structures worldwide showcase the resilience of reinforced concrete. Despite intense flames, these buildings often retain their integrity and avoid collapse, demonstrating recovery potential from fire disasters [1]. Studies of rare events like fires triggered by earthquakes highlight various risks to buildings, including natural and human-induced causes such as hurricanes and explosions, which can lead to structural failure [2]. Fires exceeding 1000°C weaken construction materials, threatening stability and increasing the risk of collapse [3-6].

Understanding fire behavior from pre-flashover to post-flashover stages is crucial [7]. During the pre-flashover phase, toxic gases like carbon monoxide, hydrogen cyanide, and phosgene pose severe health risks. Combustion smoke irritates and obstructs escape routes, heightening the risk of toxic gas inhalation and burns. Oxygen depletion during fires escalates these hazards, posing a significant threat to personal safety [8-9]. Fire-related incidents result in billions of dollars in losses globally, emphasizing the need for efficient prevention and mitigation strategies [7]. Combustion, firefighting, and hazardous substance releases contribute to environmental pollution. They worsen air and water contamination and cause significant environmental deterioration [10]. It's vital to engineer structures to withstand various risks, including fire, ensuring human safety and environmental sustainability throughout their lifecycle [2].

Table 1: Research summary on bamboo fibers in post-fire retrofitting of concrete structures

No.	Authors	Focus	Key Findings and Benefits	Ref.
1	Ni & Gernay (2020)	Residual deformations in RC structures post-fire	Bamboo fibers reduce residual deformations, enhancing structural stability.	[1]
2	Kodur et al. (2019)	Fire hazards and safety strategies	Bamboo fibers improve fire resistance and recovery, boosting fire resilience.	[2]
3	Buchanan & Abu (2001)	Structural design for fire safety	Bamboo fibers enhance fire resistance and structural integrity.	[3]
4	Khan et al. (2021)	Mechanical properties of hybrid fiber concrete	Bamboo fibers strengthen concrete, enhancing durability.	[4]
5	Xie et al. (2021a)	Testing methods for fiber-reinforced composites	Bamboo fibers provide superior fracture properties post-fire, leading to enhanced crack resistance.	[5]
6	Xie et al. (2021b)	Structural failure prediction with hybrid fibers	Bamboo fibers delay failure under fire conditions, extending structural lifespan.	[6]
7	Awoyera et al. (2024)	Structural performance of fire-damaged beams	Bamboo fiber laminates increase strength and performance of fire-damaged beams.	[22]
8	Cuce et al. (2024)	Energy efficiency and thermal resistance	Bamboo-reinforced briquettes enhance thermal performance and sustainability.	[23]
9	Bala & Gupta (2023)	Sustainable building materials	Bamboo-reinforced concrete is sustainable building material that support eco-friendly construction.	[24]
10	Awoyera et al. (2024)	Green retrofitting materials	Bamboo fibers offer sustainable repair solutions for fire-damaged RC buildings.	[25]

Fire significantly impacts reinforced concrete (RC) structures, reducing their load-bearing capacity. Assessing post-fire strength is crucial for effective repairs, with research focusing on concrete flexural strength under fire conditions [11]. Although concrete is non-combustible, high temperatures weaken its integrity, necessitating robust assessment frameworks for fire damage. Rehabilitating fire-damaged concrete structures is essential for safety and functionality. Integrating bamboo fibers into concrete offers a sustainable solution, enhancing fire resilience, reducing residual deformations, and improving post-fire strength and durability [1-6, 22-25]. This review highlights the novel use of bamboo fibers in post-fire rehabilitation, promoting eco-friendly practices in mitigating structural damage.

2 Quantification of Fire Damage in Low-Rise RC Structures

Fires pose significant risks to lives, RC structures, and the environment. This article focuses on fire-related issues in RC buildings and low-rise structures, examining fire damage using petrographic techniques. It identifies firefighting system deficiencies and safety measures. Visual inspection is crucial for evaluating RC elements' quality, cracks, and bond condition, while surface examination assesses color change, crazing, and cracking. Table 2 provides data on temperature variations, color changes, appearance alterations, and concrete conditions [18]. For assessing fire damage in low-rise RC structures, various techniques are used based on fire intensity. At early stages (0 to 300°C), visual and surface inspections detect initial cracks and color changes. For moderate exposure (300 to 600°C), petrographic analysis and infrared thermography reveal internal damage. In severe conditions (600 to 950°C), ultrasonic testing and core sampling assess internal and reinforcement damage. For extreme fires (>950°C), carbonation depth and rebound hammer tests evaluate penetration and surface strength. These techniques ensure thorough assessment and effective repair.

Table 2: Color variations in concrete occur across different temperature ranges [18]

Temperature variation	Color modification	RC Structure appearance	Status of concrete
0 to 300°C	Unchanged	Normal	Unaffected
300 to 600°C	Pink to red	Cracking	Stable but with reduced strength
600 to 950°C	Whitish grey	Spalling steel exposed & powder existence	Weak
> 950°C	Buff	Severe Spalling	Intense/Severe

3 Post-Fire Assessment and Retrofitting Techniques

RC buildings generally withstand fires well, but post-fire assessments are essential to evaluate concrete conditions, as fire often affects only the surface layer [12]. Due to their superior fire resistance compared to materials like stainless steel and wood, RC structures are extensively studied [11]. Thicker concrete covers help insulate reinforcement, preserving load capacity, though high-strength concrete is less fire-resistant than lightweight concrete. RC beams and slabs near ceilings are particularly vulnerable to heat currents during fires [13]. While RC structures retain some residual strength post-fire, heat degradation can cause irreversible damage, necessitating thorough evaluations for future use and repair [14]. Figure 1 shows fire-induced water evaporation in cement paste, leading to dehydration and concrete discoloration. Moderate fires can also cause spalling and surface crazing, underscoring the need for comprehensive assessment and rehabilitation to restore integrity.

a) *b)* *c)*

Figure 1: Assessment of RC structures, a. Crazing [26], b. Spalling [27], c. Color changing [27]

Assessing concrete's residual strength post-fire is critical for deciding on future use, repair, or demolition. Both laboratory and on-site tests, emphasizing compressive strength, provide detailed insights into post-fire damage severity [21]. Research on reinforced concrete structures employs various testing approaches, including standard fire tests, parametric variations, and natural fire scenarios, which offer more realistic depictions than conventional methods [15]. Post-fire assessments should determine the thickness of sections where concrete damage is severe enough to be considered destroyed [16]. Heat exposure alters thermal and mechanical properties, affecting structural toughness and resistance, and influencing compression, tension, and strain characteristics [17]. Thermal expansion of reinforcing bars during fires can crack concrete covers, especially at supports and beam bases. Structural fire engineering combines active measures like detectors and sprinklers with fire-resistant materials and design strategies. Rapid assessments of fire-damaged structures ensure safety and identify repair needs for low-rise buildings. Research on natural fibers, particularly bamboo, shows significant strength improvements in reinforced and retrofitted RC beams [19, 20].

4 Sustainable Solutions

Concrete structures degrade in high heat, requiring effective repair methods. Traditional approaches, like replacing damaged sections or using non-renewable materials, are resource-intensive and harmful to the environment. Bamboo fiber reinforcement offers a sustainable alternative, improving strength and durability post-fire. Bamboo, a quickly renewable resource, has minimal environmental impact compared to steel or synthetics. Studies show bamboo fiber composite plates can boost retrofitted concrete beam strength by 10-21%. Affordable and accessible, bamboo fibers are ideal for widespread use, especially in fire-prone regions. Their use reduces reliance on non-renewables and cuts concrete's carbon footprint. Bamboo fiber reinforcement enhances structural integrity. It provides significant environmental benefits. This method offers a sustainable and cost-effective solution for urban infrastructure repair.

5 Conclusion

In conclusion, the research underscores the significance of sustainable rehabilitation methods in mitigating the impact of urban fires on infrastructure. By prioritizing sustainability, researchers can address the following key points:

1. Understanding the resilience of reinforced concrete (RC) structures in fire disasters highlights the possibility of recovery and emphasizes the importance of sustainable rehabilitation approaches.

2. Thorough post-fire assessment techniques are vital for evaluating concrete conditions and determining suitable retrofitting techniques to regain structural integrity.
3. Bamboo fiber reinforcement emerges as a sustainable alternative, offering improved strength and durability post-fire while reducing reliance on non-renewable resources and cutting concrete's carbon footprint.
4. Implementing bamboo fiber reinforcement in concrete repair not only enhances structural integrity but also provides significant environmental benefits, offering a cost-effective solution for fire-prone regions.

References

[1] S. Ni and T. Gernay, "Predicting residual deformations in a reinforced concrete building structure after a fire event," Engineering Structures, vol. 202, p. 109853, Jan. 2020, doi: https://doi.org/10.1016/j.engstruct.2019.109853.
[2] V. Kodur, P. Kumar, and M. M. Rafi, "Fire hazard in buildings: review, assessment and strategies for improving fire safety," PSU Research Review, vol. 4, no. 1, pp. 1–23, Sep. 2019, doi: https://doi.org/10.1108/prr-12-2018-0033. https://doi.org/10.1155/2014/468510.
[3] A.H. Buchanan, A.K. Abu, "Structural Design for Fire Safety", second ed., John Wiley & Sons, Inc., 2001.
[4] M. Khan, M. Cao, C. Xie, and M. Ali, "Efficiency of basalt fiber length and content on mechanical and microstructural properties of hybrid fiber concrete," Fatigue Fract. Eng. Mater. Struct., vol. 44, no. 8, pp. 2135–2152, 2021.
[5] C. Xie, M. Cao, M. Khan, H. Yin, and J. Guan, "Review on different testing methods and factors affecting fracture properties of fiber reinforced cementitious composites," Constr. Build. Mater., vol. 273, no. 121766, p. 121766, 2021.
[6] C. Xie, M. Cao, J. Guan, Z. Liu, and M. Khan, "Improvement of boundary effect model in multi-scale hybrid fibers reinforced cementitious composite and prediction of its structural failure behavior," Compos. B Eng., vol. 224, no. 109219, p. 109219, 2021.
[7] "World Fire statistics," World Fire Statistics | CTIF - International Association of Fire Services for Safer Citizens through Skilled Firefighters. [Online]. Available: https://www.ctif.org/world-fire-statistics
[8] World_fire_statistics_2017.pdf.
[9] Y. Alarie, "Toxicity of fire smoke," Crit. Rev. Toxicol., vol. 32, no. 4, pp. 259–289, 2002.
[10] "NFPA - Reporter's Guide: The consequences of fire," Nfpa.org. [Online]. Available: https://www.nfpa.org/about-nfpa/press-room/reporters-guide-to-fire/consequences-of-fire.
[11] D. Martin, M. Tomida, and B. Meacham, "Environmental impact of fire," Fire Sci. Rev., vol. 5, no. 1, 2016.
[12] E. Ryu, Y. Shin, and H. Kim, "Effect of loading and beam sizes on the structural behaviors of reinforced concrete beams under and after fire," Int. J. Concr. Struct. Mater., vol. 12, no. 1, 2018.
[13] V. K. R. Kodur and A. Agrawal, "An approach for evaluating residual capacity of reinforced concrete beams exposed to fire," Eng. Struct., vol. 110, pp. 293–306, 2016.
[14] A. Agrawal and V. K. R. Kodur, "A novel experimental approach for evaluating residual capacity of fire damaged concrete members," Fire Technol., vol. 56, no. 2, pp. 715–735, 2020.
[15] R. Felicetti, "Assessment of fire damage in concrete structures: new inspection tools and combined interpretation of results in 8th International Conference on Structures in Fire Shanghai, China," 2014, pp. 1111–1120.
[16] Z. Huang, "The behaviour of reinforced concrete slabs in fire," Fire Saf. J., vol. 45, no. 5, pp. 271–282, 2010.
[17] H.-C. Cho, D. Lee, H. Ju, H.-C. Park, H.-Y. Kim, and K. Kim, "Fire damage assessment of reinforced concrete structures using fuzzy theory," Appl. Sci. (Basel), vol. 7, no. 5, p. 518, 2017.
[18] Osman, M. H., Sarbini, N. N., Ibrahim, I. S., Ma, C. K., Ismail, M., & Mohd, M. F. (2017, November). A case study on the structural assessment of fire damaged building. In IOP Conference Series: Materials Science and Engineering (Vol. 271, No. 1, p. 012100). IOP Publishing.
[19] Chin, S. C., Moh, J. N. S., Doh, S. I., Yahaya, F. M., & Gimbun, J. (2019). Strengthening of reinforced concrete beams using bamboo fiber/epoxy composite plates in flexure. Key Engineering Materials, 821, 465-471.
[20] Awoyera, P. O., Nworgu, T. A., Shanmugam, B., Prakash Arunachalam, K., Mansouri, I., Romero, L. M. B., & Hu, J. W. (2021). Structural retrofitting of corroded reinforced concrete beams using bamboo fiber laminate. Materials, 14(21), 6711.
[21] P. Knyziak, R. Kowalski, and J. R. Krentowski, "Fire damage of RC slab structure of a shopping center," Eng. Fail. Anal., vol. 97, pp. 53–60, 2019.
[22] P. O. Awoyera, A. Akin-Adeniyi, A. Bahrami, and L. M. Bendezu Romero, "Structural performance of fire-damaged concrete beams retrofitted using bamboo fiber laminates," Results Eng., vol. 21, no. 101821, p. 101821, 2024.
[23] P. M. Cuce et al., "Unlocking energy efficiency: Experimental investigation of bamboo fibre reinforced briquettes as sustainable solution with enhanced thermal resistance," Case Stud. Therm. Eng., vol. 60, no. 104680, p. 104680, 2024.
[24] A. Bala and S. Gupta, "Engineered bamboo and bamboo-reinforced concrete elements as sustainable building materials: A review," Constr. Build. Mater., vol. 394, no. 132116, p. 132116, 2023
[25] P. O. Awoyera, A. Akin-Adeniyi, F. Althoey, M. A. Abuhussain, K. Jolayemi, and L. M. B. Romero, "Green structural retrofitting materials for fire-damaged reinforced concrete buildings: Advances in sustainable repair of distressed buildings," Fire Technol., vol. 60, no. 3, pp. 1955–1991, 2024.
[26] "Effects of fire on concrete," Edtengineers.com. Available: https://www.edtengineers.com/blog-post/fire-effects-concrete.
[27] S. K. Personnel, "Fire damaged concrete," Sandberg, 30-Nov-2019. Available: https://www.sandberg.co.uk/site/inspection/fire-damaged-concrete/.

A SIMPLIFIED NUMERICAL MODEL FOR REINFORCED CONCRETE BEAM-COLUMN JOINTS

[a] Muhammad Azeem*, [b] Muhammad Fahim

a: Civil Engineering Department, University of Engineering and Technology, Peshawar, Pakistan. 16jzciv0102@uetpeshawar.edu.pk
b: Civil Engineering Department, University of Engineering and Technology, Peshawar, Pakistan. drmfahim@uetpeshawar.edu.pk
* Corresponding author.

Abstract- Reinforced Concrete Beam Column joints are most critical regions of any reinforced concrete structures. The performance of RC joints determines the performance of whole building during seismic loading. Many researchers have focused on the experimental study of RC joints to determine the seismic performance of RC structures. However, experimental tests are expensive and time consuming. Therefore, the alternative approach of numerical modeling is preferred to study a wide range of parameters affecting the behavior of beam-column joints. This study presents the result of macro modeling of RC beam-column joints using finite element based software SeismoStruct. The results of the numerical model are compared with the experimental results and found to be in excellent agreement. The peak strength of the numerical model was found to be 75.2 kN, which is 8% higher than that of experimental model and drift ratio at which peak strength of the numerical model was obtained is 4.33%, which is higher than that of experimental model by 2%. This shows good agreement of numerical results with the experimental results. It is also observed that the initial stiffness of numerical model is higher than that of the experimental model. The numerical model may be used for more comprehensive parametric study of the beam-column joints.

Keywords- Calibrated, Modeling, Macro Model, Stiffness.

1 Introduction

In the past beam-column joint region was assumed to be rigid during analysis, but this lead to overestimated results. Beam-column joints mostly have brittle failure, which may not contribute significantly to the ductility performance of the structures [1]. In the past earthquakes, most of buildings collapsed due to the failure of RC joints as shown in Figure 1 [2]. In RC frames the beam-column joint are important region to resist the seismic forces and determine response of the building during earthquakes [3]. Therefore, RC beam-column joint need to be studied comprehensively in order to ensure a safe design of RC structures.

Figure 1: Building collapses due to beam-column joint failure [4]

Extensive experimental studies have been conducted in order to study the response of the beam-column joints, based on which several codes have been improved [5]. Present joint design and detailing using ACI provides the adequate provision in joint against the gravity and seismic forces [6].

Sufficient development length and confinement is provided in the joint to resist the reversed cyclic loading. However, to satisfy these requirements, the joint region become very congested and the execution become a challenge on site. Therefore, this study aims to develop a numerical model to study various parameters contributing to the strength of the joint and which determines the governing failure type (shear failure of joint core, bar slippage etc.).
Failure mechanisms including Bar Slip Failure and Shear Panel Failure which are the two primary mechanisms determining the inelastic behavior of RC beam column joint can be studied using this model, to investigate whether the failure will occurs due to Bar Slip Failure or due to Shear Panel Failure of particular RC beam column joint.

2 Research Methodology

2.1 Numerical Modelling

Reinforced concrete structures can be modelled using both micro and macro approaches, both having pros and cons. This paper presents the results obtained using macro modelling of RC beam-column joints. The numerical model is first verified and calibrated with the experimental results and then a comprehensive parametric study is conducted to determine the contributing parameters in various failure scenarios.
Manders [7] model will be used for the modelling concrete (20.68 MPa) and Manegotto Pinto [6] model for modelling steel (413.5 MPa). A finite element based software package SeismoStruct is utilized for the numerical modelling of RC joints.

2.2 Simplified Joint Model

One of the simplified beam-column joint model was presented by Lowes et al [8]. This model is able to capture the mechanisms responsible for the nonlinear behavior of RC beam-column joints [8]. It is used in the two dimensional analysis of the RC frame and has the following characteristics: (1) it has 12 degree of freedom at the four exterior nodes (2) 4 interior degrees of freedom (3) It has eight anchorage failure components which are used to model the bar slip mechanism. The model also consists of joint core component which are used to capture the shear failure of joint core, and interface shear component to capture the shear at the interface as shown in Figure 2. Every component of this model needs an independent action-deformation response curve [9].

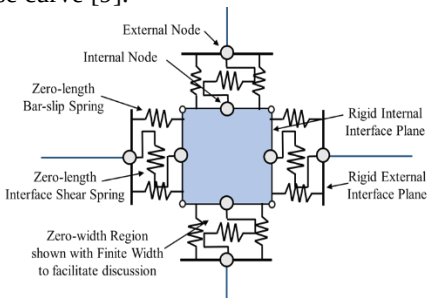

Figure 2: Beam Column Joint Spring Model by Lowes et al [8]

In the SeismoStruct, all these components are modeled using the "Joint Element" available in SeismoStruct [10]. The joint element is a three dimensional element with six degrees of freedom. As mentioned above, action deformation curve needs to be provided for every degree of freedom. There are 12 response curves available in SeismoStruct, and modified Tekeda curve will be used to model the response of the model. The parameters required to define the Tekeda curve are given in theTable 1.

Table 1: Tekeda Curve Parameters

Parameters		Bar Slip Component (Beam)	Bar Slip Component (Column)	Shear Panel Rotation
Yielding strength	Fy	9.64E+07	8.43E+07	1.73E+08
Initial stiffness	Ky	1.66E+11	1.29E+11	1.42E+12
Post-yielding to initial stiffness ratio	α	0.1	0.1	0.1
Outer loop stiffness degradation factor	β0	0.4	0.4	0.4
Inner loop stiffness degradation factor	β1	0.9	0.9	0.9

2.3 Description of Test Specimen

The numerical model was developed for a typical RC beam-column joint which was tested at Civil Engineering Department, University of Engineering and Technology, Peshawar. The numerical model and experimental test specimen are given in Figure 3. The specimen employed concrete with compressive strength of 20.68 MPa and steel had a yield strength of 413.5 MPa.

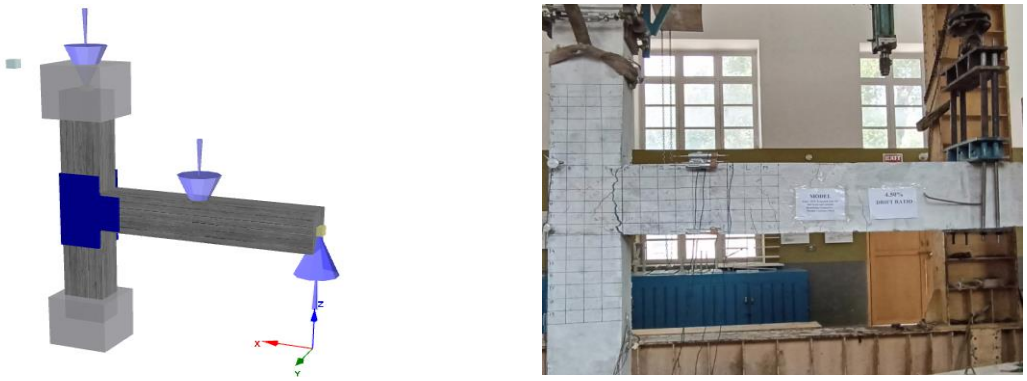

Figure 3: SeismoStruct Model (Left Figure) and Experimental Test Specimen (Right Figure)

3 Results

Figure 4 compare the numerical and experimental action deformation response. The strength and hysteristic reponse of numerical study agrees well with the expeimental results. For the Normal Concrete Model, the maximum load capacities of the test specimen were 75.2 kN. This capacity was higher than the experimental test by about 8.0% as shown in Table 22. Numerical results show high value for initail stiffness due to assumptions made during modeling.

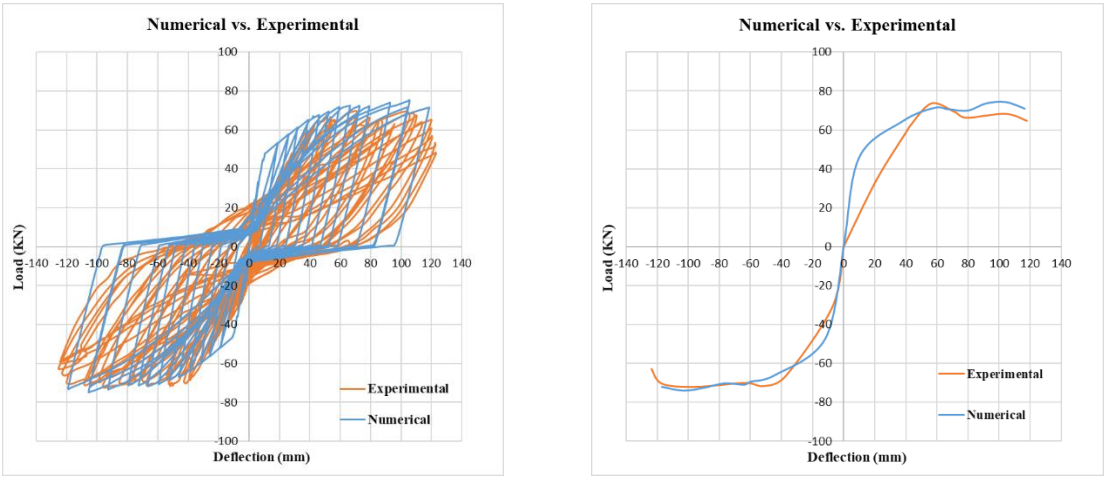

Figure 4: Numerical vs. Experimental Hysteretic Curves (Left Figure) and Envelope Curves (Right Figure)

Table 2: Comparison of Numerical and Experimental Results

Model	Loading Direction	Load max (KN)		Rmax
		Analytical Pmax (kN)	Experimental Pmax (kN)	
RC Model	Positive	75.2	69.6	1.08

4 Practical Implementation

Failure mechanisms including Bar Slip Failure and Shear Panel Failure which are the two primary mechanisms determining the inelastic behavior of RC beam column joint can be studied using this model, to investigate whether the failure will occurs due to Bar Slip Failure or due to Shear Panel Failure of particular RC beam column joint

5 Conclusion

Based on the above numerical results it can be concluded that :

1) The peak strength of the numerical model was found to be 75.2 kN, which is 8% higher than that of experimental model and drift ratio at which peak strength of the numerical model was obtained is 4.33%, which is higher than that of experimental model by 2%. This shows good agreement of numerical results with the experimental results.
2) The non linear response of the beam-column joint can be accuratetely modelled and simulated using the above mentioned simplified modeling technique using Seismostruct software.
3) The mechanisms like anchorage failure and joint core shear failure mechanisms responsible for the non linear response of the beam-column joint can be modeled and incorporated in the numerical analysis.
4) It is also observed that the initial stiffness of numerical model is higher than that of the experimental model because of the simplified approaches used in the numerical model.

Acknowledgment

The authors thanks every colleague who has helped in this research work.

References

[1] G. M. Kotsovou, D. M. Cotsovos, and N. D. Lagaros, "Assessment of RC exterior beam-column Joints based on artificial neural networks and other methods," *Engineering Structures*, vol. 144, pp. 1–18, 2017.
[2] I. Choi, J.-H. Lee, J.-H. Sohn, and J. Kim, "Investigation on Seismic Design Component and Load for Nonstructural Element," *Journal of the Architectural Institute of Korea Structure & Construction*, vol. 35, no. 5, pp. 117–124, 2019.
[3] M. J. Favvata, B. A. Izzuddin, and C. G. Karayannis, "Modelling exterior beam–column joints for seismic analysis of RC frame structures," *Earthquake engineering & structural dynamics*, vol. 37, no. 13, pp. 1527–1548, 2008.
[4] S. Park and K. M. Mosalam, "Experimental investigation of nonductile RC corner beam-column joints with floor slabs," *Journal of Structural Engineering*, vol. 139, no. 1, pp. 1–14, 2013.
[5] G. A. Diro and W. F. Kabeta, "Finite element analysis of key influence parameters in reinforced concrete exterior beam column connection subjected to lateral loading," *European Journal of Engineering and Technology Research*, vol. 5, no. 6, pp. 689–697, 2020.
[6] A.-D. G. Tsonos, "Performance enhancement of R/C building columns and beam–column joints through shotcrete jacketing," *Engineering Structures*, vol. 32, no. 3, pp. 726–740, 2010.
[7] J. B. Mander, M. J. Priestley, and R. Park, "Theoretical stress-strain model for confined concrete," *Journal of structural engineering*, vol. 114, no. 8, pp. 1804–1826, 1988.
[8] N. Mitra and L. N. Lowes, "Evaluation, calibration, and verification of a reinforced concrete beam–column joint model," *Journal of Structural Engineering*, vol. 133, no. 1, pp. 105–120, 2007.
[9] L. N. Lowes and A. Altoontash, "Modeling reinforced-concrete beam-column joints subjected to cyclic loading," *Journal of Structural Engineering*, vol. 129, no. 12, pp. 1686–1697, 2003.
[10] T. M. Elshafiey, A. M. Atta, H. M. Afefy, and M. E. Ellithy, "Structural performance of reinforced concrete exterior beam–column joint subjected to combined shear and torsion," *Advances in Structural Engineering*, vol. 19, no. 2, pp. 327–340, 2016.

PLASTIC STRENGTH OF EXTERNALLY WELDED CHS-TRANSVERSE PLATE T-JOINTS

[a]Ali Ajwad*, [b]Massimo Latour

a: DICIV, University of Salerno, Fisciano, Salerno, Italy. aajwad@unisa.it
b: DICIV, University of Salerno, Fisciano, Salerno, Italy. mlatour@unisa.it
* Corresponding author.

Abstract- Utilizing tube-like hollow sections (HSS) as columns in Moment Resisting Frames (MRFs) offers beneficial resolutions for overall structural performance. Nonetheless, the adoption of HSS columns is limited by the intricacy in engineering connections between columns and Double Tee Beams. One of most common approach for such types of joints is welding the beam externally to the chord using either fillet or full penetration butt welds. As per the EC3:1.8 guidelines, a so-called component method approach can be used for such types of joints to predict their plastic strength. The component method approach simplifies the joint design by breaking down the joint into its fundamental components, allowing for a detailed examination of each component's behaviour and interaction, thus ensuring precise evaluation of joint performance and reliability. In this study, the emphasis lies on delineating the strength attributes of welded joints in a T-shape, connecting Circular HSS chords and externally welded transverse plates. The component's mechanical response seeks to mimic connection dynamics between beam flange and chord in connections connecting CHS chords and welded IPE profiles. More precisely, this critical element has been isolated and thoroughly examined using results from theoretical approaches and numerical simulations, culminating in identification for the most suitable analytical design equation.

Keywords- Component Method, Parametric Analysis, Finite Element Modelling, Circular Hollow Sections, Externally Welded Double-Tee Beams, Resistance.

1 Introduction

Usage of Circular Hollow Sections (CHS) in modern structures, particularly for Moment Resisting Frames (MRFs), has seen a significant increase in recent years. The inherent geometric properties of CHS, such as their uniform strength characteristics and aesthetic appeal, make them highly suitable for use in high-load bearing applications [1]. This growing trend is supported by advancements in manufacturing and material science, which have improved the quality and availability of CHS for structural applications. The adoption of CHS in MRFs is further driven by their ability to dissipate energy efficiently during seismic events, making them a preferred choice in earthquake-prone areas [2-4]. Despite their increasing use in MRFs, CHS are predominantly utilized in portal frames rather than perimeter frames. Portal frames benefit significantly from the structural efficiency and simplicity of CHS, especially in industrial buildings and warehouses where large, clear spans are required. The preference for CHS in portal frames over perimeter frames can be attributed to the specific load distribution and architectural requirements that differ significantly between these two types of structures. Understanding the behaviour of joints in perimeter frames becomes crucial as the application of CHS expands beyond traditional portal frames. The joints in perimeter frames often undergo more complex stress distributions due to the variability in loading conditions and the architectural constraints associated with these structures. Currently in Eurocode 3 part 1.8 [5], there are well established guidelines available to design soldered and fastened joints with double Tee sections, however, in the case of CHS as column, it still uses a basic method from studies done in 1982 by Wardenier [6]. The procedure operates under assumption that the primary influence on flexural response stems from the chord face failure mode which can be considered the weakest component of the joint. This localized failure mode is conceptualized by modeling resistance of corresponding T-joints with branch plates multiplied with the beam depth (h_1) as depicted in Fig. 1. Building upon this, Wardenier, De Winkel, and Van Der Vegte [7-14] conducted numerous experimental campaigns and numerical studies and influenced CIDECT (International Committee for the Development and Study of Tubular Structures) to incorporate their findings into the organization's design guidelines [15].

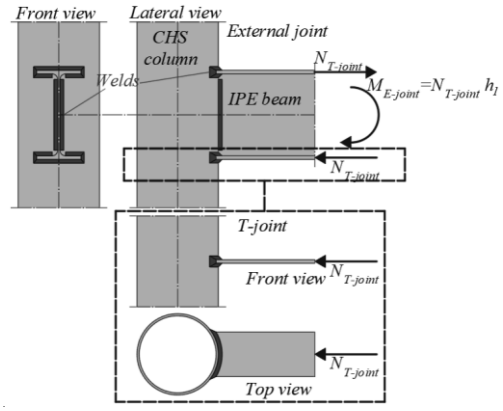

Figure 1: Approach of EC3 part 1.8 [5] approach for CHS-IPE Joints

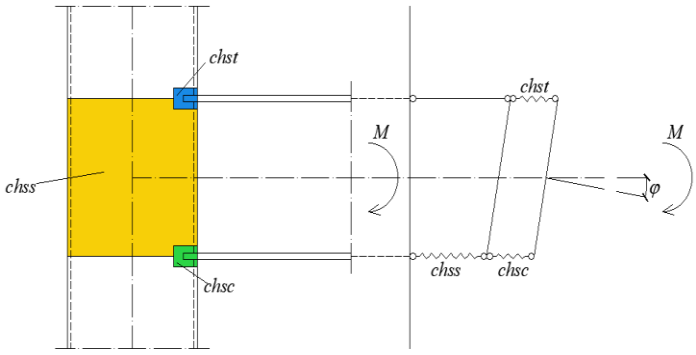

Figure 2: Components Identification

However, recent research conducted by Voth and Packer [16, 17] has shown that the equations suggested by CIDECT and EC3: 1-8 for predicting plastic resistance for T-joints are too conservative. This makes us question if these equations are suitable for beam-to-column connections. Precisely, the findings point out that both standards overlook the impact of plate thickness and fail to distinguish between tension and compression resistance, leading to overly conservative estimates. In this context, a study was conducted at the University of Salerno which involved experimentation, validation of numerical models against the same, conducting a parametric analysis using the validated models and comparing the results of the same with the current available analytical formulations which include EC3 [5], CIDECT [15] and Voth [17]. The present manuscript offers the analytical portion of this research which covers the validity of the available formulation to predict the CHS-Plate component of the joint. In actual, as per the EC3: Part 1.8 component method approach [5], three components can be identified when it comes to CHS-externally welded IPE joint (Fig. 2) which are explained in table 1.

Table 1: Components

Component	**Type**	**Equivalency**
chsc	Local Deformability	Plate-CHS T-Joint in compression
chst	Local Deformability	Plate-CHS T-Joint in Tension
chss	Shear Strength of Tube	Panel in Shear under beam action

This research will focus specifically on the resistance of chst/chsc components to evaluate the predictive accuracy of available formulations. The third component 'chss' will be used in the next part of this research where the whole joint will be studied in entirety.

2 Analytical Formulations

The T-joints involving Welded branch plates and CHS chords resist chord failure using Togo's ring model theory [18]. The ring model provides a framework for analyzing a CHS exposed to actions transmitted axially by a plate that is externally welded at 90^0. This helps like a simplified representation for a more complex issue, where the development of yield lines in three dimensions would typically govern failure under load as shown in Figure 3.

The equations currently used in estimating the resistance for T-joints under compression or tension (similar to those in connections between circular hollow section columns and double-tee beams) are shown as Equations 1, 2 and 3, and come from references [5], [15], and [16].

$$F_{pl,EC3} = (4 + 20\beta^2) f_{y0} t_0^2 \quad (1)$$

$$F_{pl,CIDECT} = 2.2(1 + 6.8\beta^2)\gamma^{0.2} f_{y0} t_0^2 \quad (2)$$

$$F_{pl,Voth} = k_1(1 + k_2\beta^2)(1 + 0.6\eta)\gamma^{k_3} f_{y0} t_0^2 \quad (3)$$

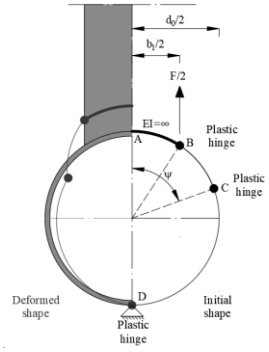

Figure 3: 'chst' Ring Model

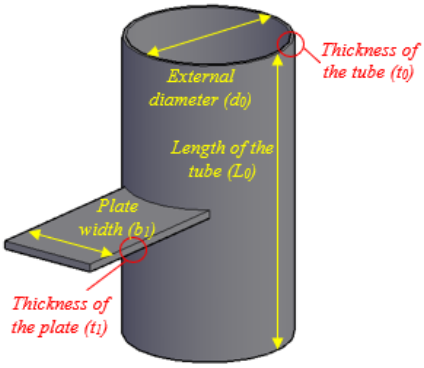

Figure 4: Strength influencing Geometric parameters

It's important to note that EC3 part 1.8 and CIDECT use the same equations for tension and compression. However, Voth adjusted the coefficients based on a large set of test results. In Eq. 3, for T-joints in tension, the coefficients k_1, k_2 and k_3 are 2.3, 2.5, and 0.55, respectively, whereas, $k_1 = 2.6$, $k_2 = 3$ and $k_3 = 0.35$ for compression behaviour. The other parameters involved in the equations are β, γ and η which are non-dimensional and depend on the geometry of the connections involved as depicted in figure 4 and shown below;

$$\beta = \frac{b_1}{d_o}, \gamma = \frac{d_o}{2t_o}, \tau = \frac{t_1}{t_o}$$

3 Parametric Analysis

For checking the accurateness level for equations 1-3, FE data from [19] was utilized. A simplified approach was adopted for the welds, employing zero-thickness Tie contacts to connect plates and chords. Mentioned generalization was intended at streamlining method of modelling, reducing computational period without losing in accuracy as already shown in [20]. The analysis involved a total of 40 cases with varying β, η, γ and τ (Table 2). Figures 5a and 5b compare the tension and compression strength from Forty Finite Element simulations for T-joints with predicted values by Eqs. 1-3.

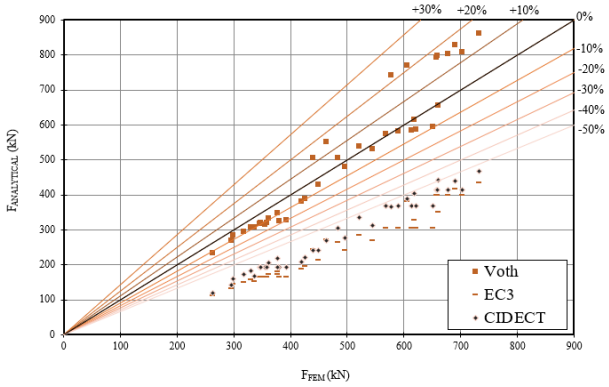

a) chst Component

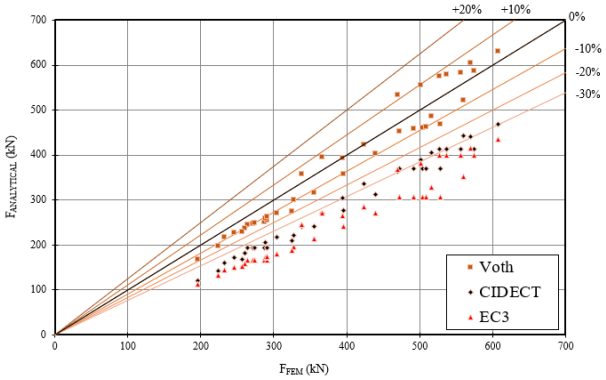

b) chsc Component

Figure 5: FE Models vs Analytical formulations

Table 2: Parametric analysis Cases [19]

Cases	*k* (kN/mm)	*β*	*γ*	*τ*	*η*
1-40	292-653	0.44-0.74	15.28-22.75	2-5.83	0.05-0.18

Assessment reveals that Voth's method correctly forecasts how strong the component is. In contrast, EC3-1.8 and CIDECT are cautious and forecast component's plastic resistance to be about 50% less in tension and 40% less in compression than it actually is. The difference stems from the assumption made by EC3 and CIDECT that the component's strength will be unvarying in both compression and tension, whereas in reality, that is not the case. The strength in tension component is relatively higher as compared to compression due to different buckling phenomenon. Furthermore, both overlook significant influence by the parameter 'η' on T-joint strength.

4 Conclusion

This paper focuses on investigating two components of CHS-externally welded double tee profiles which are effectively CHS-plate connection with either plate in tension and compression. There are equations present in design guidelines from EC3 and CIDECT to predict the plastic strength of these connections however, studies have shown that the equations tend to underpredict the actual strength exhibited by the same. Numerical data from [19] was taken to check the accuracy level of the equations from EC3 [5], CIDECT [15] and Voth [16] and the findings clearly show that Eurocode 3 Part 1.8 and CIDECT rules underestimate how strong the connections are. On the other hand, Voth's equations are very accurate. This highlights how important it is to consider plate thickness when making predictions.

Acknowledgement

The authors would like to express their gratitude to Prof. Dr. Gianvittorio Rizzano and Dr. Eng. Sabatino Di Benedetto for their invaluable guidance throughout the research.

References

[1]. Di Benedetto, S., Latour, M., Rizzano, G., Stiffness Prediction of Connections between CHS Tubes and Externally Welded I-Beams: FE Analyses and Analytical Study, *Materials*, 13, 3030; doi:10.3390/ma13133030, 2020.
[2]. Landolfo, R., Zandonini, R., Steel and Steel-Concrete composite structures in seismic area: advances in research and design, The research project RP3 of the ReLUIS-DPC 2014-18, 489 p, ISBN: 978-88-89972-74-8, 2018.
[3]. Das, R., Kanyilmaz, A. and Degee, H., Laser Cut passing-through Open-to-CHS Beam-to-Column Connections. *ce/papers*, 4: 964-972, 2021, https://doi.org/10.1002/cepa.1385.
[4]. Varughese, L.M., & Johny, E., Analytical Study on Effect of Dimensions of Tapered Cover Plates and vertical stiffeners on Replaceable I-Beam to CHS Column Joint. *International journal of engineering research and technology*, 2018.
[5]. CEN [2005]: EN 1993-1-8 *Eurocode 3: Design of Steel Structures. Part 1-8: Design of Joints*, CEN, European Committee for Standardization, 2005.
[6]. Wardenier, J., Hollow section joints, Delft University Press, Delft, The Netherlands, 1982.
[7]. Wardenier, J., Kurobane, Y., Packer, J.A., Dutta, D., Yeomans, N., Design guide for circular hollow section (CHS) joint under predominantly static loading, Ed. By Comité International pour le Développement et l'Etude de la Construction Tubulaire (CIDECT), Verlag TÜV Rheinland GmbH, Köln, Germany, 1991.
[8]. Kamba, T., Tabuchi, M., Database for tubular column to beam connections in moment resisting frames, IIW doc. XV-893-95, Dep. Of Architecture, Faculty of Engineering, Kobe University, Japan, 1995.
[9]. van der Vegte, G.J., The Static Strength of Uniplanar and Multiplanar Tubular T- and X-Joints, Ph. D. Thesis, Delft University Press, Delft, The Netherlands, 1995.
[10]. de Winkel, G. D., and Wardenier, J., Parametric Study on the Static Strength of Axially Loaded Multiplanar Plate to Circular Column Connections, Proceedings ISOPE Fifth International Offshore and Polar Engineering Conference, Vol. IV, The Hague, The Netherlands, 1995.
[11]. de Winkel, G. D., and Wardenier, J., The Static Strength and Behaviour of Multiplanar I-beam to Tubular Column Connections loaded with In-plane Bending Moments, Proceedings of the Third International Workshop Connections in Steel Structures III, Trento, Italy, 1995.
[12]. de Winkel, G. D., and Wardenier, J., Parametric Study on the Static behavior of Uniplanar I-beam-to-tubular Column Connections Loaded with In-plane Bending Moments Combined with Pre-stressed Columns, Proceedings of the Seventh Int. Symposium on Tubular Structures VII, Miskolc, Hungary, 1996.
[13]. de Winkel, G. D., The Static Strength of I-beam to Circular Hollow Section Column Connections, Ph. D. Thesis, Delft University Press, Delft, The Netherlands, 1998.
[14]. Wardenier, J., A uniform effective width approach for the design of CHS overlap joints, Proceedings of the 5th International Conference on Advances in Steel Structures (ICASS), Singapore, Research Publishing Services, Vol. II, pp. 155-165, 2007.
[15]. Wardenier, J., Kurobane, Y., Packer, J.A., van der Vegte, G.J., Zhao, X.L., Design guide for circular hollow section (CHS) joints under predominantly static loading, 2nd Ed., CIDECT, Geneva, Switzerland, 2008.
[16]. Voth, A., Branch Plate-to-Circular Hollow Structural Section Connections, Ph. D. Thesis, Toronto, 2010.
[17]. Voth, A.; Packer, J.A., Branch Plate-to-Circular Hollow Structural Section Connections. I: Experimental Investigation and Finite-Element Modeling, J. Struct. Eng. 2012, 138, 995–1006.
[18]. Togo, T., Experimental study on mechanical behavior of tubular joints, D. Eng. Thesis, Osaka University, Osaka, Japan, 1967.
[19]. Ajwad, A., Di Benedetto, S., Latour, M., Rizzano, G., A component method approach for single-sided beam-to-column joints with CHS columns and welded double-tee beam, Thin-Walled Structures, 112055, ISSN 0263-8231, https://doi.org/10.1016/j.tws.2024.112055, 2024.
[20]. Sato, A., Elettore, G., Ajwad, A., Di Benedetto, S., Latour, M., Francavilla, A.B., and Rizzano, G., Stiffness of Welded T-joints Between SHS Profiles and Through Plates, STESSA 2024, pp. 350,361, Lecture Notes in Civil Engineering, vol 519. Springer, Cham. https://doi.org/10.1007/978-3-031-62884-9_31.

PREDICTING THE INITIAL STIFFNESS OF EXTERNALLY WELDED CHS-TRANSVERSE PLATE JOINTS AT VERTICAL AND HORIZONTAL CONNECTIONS

[a]Ali Ajwad*, [b]Massimo Latour

a: DICIV, University of Salerno, Fisciano, Salerno, Italy. aajwad@unisa.it
b: DICIV, University of Salerno, Fisciano, Salerno, Italy. mlatour@unisa.it
* Corresponding author.

Abstract- This study performs an analytical examination of how transverse T-type plate-to-circular hollow section (CHS) connections behave when subjected to tension or compression forces from the branch plate. At present, EC 3: 1.8 focuses only on resistance prediction of tubular joints and does not address stiffness prediction. Consequently, in practical applications, tubular joints are frequently modelled using simplistic assumptions of either pinned or fully restrained conditions, resulting in inaccurate predictions due to the omission of stiffness considerations. This paper addresses the identified gap in Eurocode 3 Part 1.8 by proposing two equations, using Clapeyron theorem, for initial stiffness prediction of transverse plate-to-CHS joints using the Clapeyron theorem. The proposed equations aim to provide guidelines for stiffness prediction, which is currently absent in the code. Numerical comparisons were conducted with results from another study, analyzing 40 cases. The findings demonstrated that both equations accurately predicted stiffness, with mean values close to 1 and 1.03 and coefficients of variation (CoV) of 12% and 15%, respectively.

Keywords- Component Method, Finite Element Modelling, Parametric Analysis, Circular Hollow Sections, Externally Welded Double-Tee Beams, Stiffness.

1 Introduction

Circular Hollow Section (CHS) members are increasingly preferred as a substitute for steel open section members due to their visually appealing exposed steelwork. The enhanced compression resistance of CHS steel members often results in lighter and more cost-effective elements compared to open section members, despite the higher cost [1]. Moreover, CHS members generally have reduced painting costs due to their smaller surface area, lower transportation costs due to their lighter weight, and simpler installation procedures due to their reduced weight compared to open sections [2]. In the context of a CHS-plate joint, the joint exhibits high deformability as compared to traditional connections with open sections. This flexibility can result in excessive distortion or plastic deformation of the CHS connecting face, particularly at the interface with the transversally attached branch plate. As per the guidelines outlined by IIW (1989) [3], a face deformation limit of 1% of the main member (Circular Hollow Section) diameter is traditionally used as a serviceability deformation threshold. Therefore, accurately determining the initial stiffness provided by this type of connection is crucial for ensuring that the deformation remains within acceptable limits during serviceability. Despite the fact, Current design guidelines concerning circular hollow sections which are Eurocode 3 part 1.8 [4], AISC 316-16 [5] and CIDECT [6] have a notable limitation. They primarily address the assessment of resistance for externally welded plates but do not include provisions for predicting stiffness in these configurations. Building upon this limitation, the present study aims to bridge identified knowledge gaps by introducing analytical formulations using the Clapeyron theorem for stiffness determination. These formulations will be validated through comparison with numerical results obtained in a previous study [7]. The focus is on enhancing the understanding and prediction of stiffness in circular hollow section (CHS) connections, complementing the existing guidelines in Eurocode 3 Part 1.8 [4].

2 Parametric Study

In order to check the accuracy of the derived equation, numerical data of 40 selected cases (Table 1) obtained from [7] was utilized in this study which were validated using experimental data available in literature. The selected cases depended upon non-dimensional parameters τ, β, γ and (Figure 1), where;

$$\beta = \frac{b_1}{d_o}, \gamma = \frac{d_o}{2t_o}, \tau = \frac{t_1}{t_o}$$

A simplified approach was adopted for the welds, employing zero-thickness Tie contacts to connect plates and chords. Mentioned generalization was intended at streamlining method of modelling, reducing computational period without losing in accuracy as already shown in [8].

Table 1: Parametric analysis Cases [5]

Case	*k*(kN/mm)	β	γ	τ	Case	*k*(kN/mm)	β	γ	τ
1	292	0.62	16.14	3.33	**21**	487	0.61	15.28	3.13
2	299	0.62	16.14	3.75	**22**	553	0.65	15.28	3.13
3	308	0.62	16.14	4.17	**23**	630	0.70	15.28	3.13
4	323	0.62	16.14	5.00	**24**	714	0.74	15.28	3.13
5	335	0.62	16.14	5.83	**25**	430	0.44	20.32	2.50
6	577	0.65	15.28	3.13	**26**	469	0.47	20.32	2.50
7	603	0.65	15.28	3.75	**27**	514	0.49	20.32	2.50
8	621	0.65	15.28	4.06	**28**	558	0.52	20.32	2.50
9	628	0.65	15.28	4.38	**29**	606	0.54	20.32	2.50
10	653	0.65	15.28	5.00	**30**	191	0.55	21.91	5.00
11	485	0.49	20.32	2.00	**31**	227	0.55	19.92	5.00
12	511	0.49	20.32	2.50	**32**	265	0.55	18.26	5.00
13	534	0.49	20.32	3.00	**33**	307	0.55	16.85	5.00
14	552	0.49	20.32	3.50	**34**	353	0.55	15.65	5.00
15	241	0.54	16.14	4.17	**35**	342	0.62	22.75	4.00
16	261	0.57	16.14	4.17	**36**	395	0.62	21.00	4.00
17	284	0.59	16.14	4.17	**37**	449	0.62	19.50	4.00
18	336	0.65	16.14	4.17	**38**	506	0.62	18.20	4.00
19	366	0.67	16.14	4.17	**39**	304	0.45	22.23	3.00
20	442	0.57	15.28	3.13	**40**	342	0.45	20.92	3.00

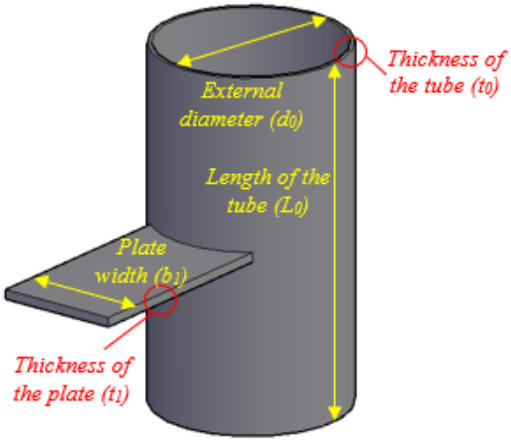

Figure 1: Geometric Factors Affecting Mechanical Performance of Specimen

3 Equation Derivation

The proposed method for stiffness prediction is built upon an analytical approach for the two-dimensional configuration depicted in Fig. 2. Finite element (FE) models indicate that, under low load levels, bottom semi of CHS chord experiences minimal deformation. Therefore, for simplification purposes, only a quarter of the tube is modeled, aligning with the reference configuration shown in Figure 1. Point A is fully restrained, and a guided support is placed at point B, where the plate connects to the tube. Because the system is hyperstatic, the principle of virtual work is used for calculating the reactions upon these supports.

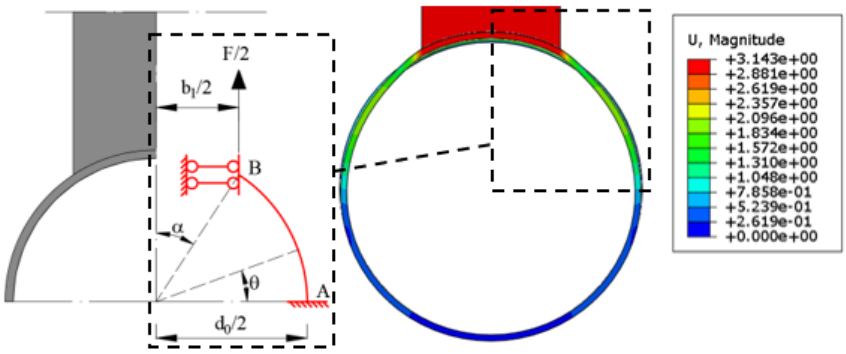

Figure 2: Simplified Procedure for Assessing Component Stiffness

After determining the reactions, the vertical displacement of node B (δ_B) in the tube is calculated using Clapeyron's theorem (Equation 1).

$$1 \cdot \delta_B = \int_0^{\frac{\pi}{2}-\alpha} M^s \chi^s \, dz + \int_0^{\frac{\pi}{2}-\alpha} T^s \gamma^s \, dz + \int_0^{\frac{\pi}{2}-\alpha} N^s \varepsilon^s \, dz \tag{1}$$

Comparisons and calculations showed that shear and axial deformability terms in Equation 1 only affect the displacement of node B (δ_B) by about 1%. To make things simpler, these terms are ignored. Using the integral from Equation 1, we can find the stiffness by dividing the force (F) by the displacement (δ_B), resulting in an easy-to-use equation.

$$k_{\mathrm{j}} = 226.5 \cdot \frac{E b_{eff} t_o^3}{d_o^3} \frac{0.03\beta^2 + 0.16\beta + 0.13}{(1 - 0.637\beta - 0.106\beta^3)^5 (0.26\beta^2 - 0.55\beta + 1.06)} \tag{2}$$

Here, b_{eff} stands for an effective width that considers how the material deforms in three dimensions and 'E' is the modulus of elasticity for the CHS chord member equal to 210 kN/mm^2. It is determined using three non-dimensional parameters: β, γ and τ. This approach follows the method previously used by the authors in [6]. Therefore, b_{eff} can be expressed as follows;

$$\frac{b_{eff}}{d_o} = c_1 \beta^{c_2} \gamma^{c_3} \tau^{c_4} \tag{3}$$

Using the numerical data from Table 1, a regression analysis was performed to find the coefficients in Equation 3. The resulting values are as follows: $c_1 = 1.33 \times 10^{-3}$, $c_2 = -2.7$, $c_3 = 1.57$, $c_4 = -0.21$, namely:

$$k_j = \frac{3}{80} E d_o \beta^{-2.7} \gamma^{-1.43} \tau^{-0.2} \frac{0.03\beta^2 + 0.16\beta + 0.13}{(1 - 0.637\beta - 0.106\beta^3)^5 (0.26\beta^2 - 0.55\beta + 1.06)} \tag{4}$$

Where;

$$\frac{0.03\beta^2 + 0.16\beta + 0.13}{(1 - 0.637\beta - 0.106\beta^3)^5 (0.26\beta^2 - 0.55\beta + 1.06)} \cong 37.3\beta^{4.4} \tag{5}$$

Because Equation 4 is too complicated for practical use, a simpler version has been developed. This simplified form achieves an average error below 3% for angles α between 25° and 50° (refer to Figure 2).

$$k_{j,sim.} = 1.4 E d_o \beta^{1.7} \gamma^{-1.4} \tau^{-0.2} \tag{6}$$

The accuracy of both equations was checked (Eqs. 4 and 6) by comparing their predictions with the numerical results in Table 1. Figure 3 shows that Eq. 4 predicts the numerical results very closely, averaging 1 and 12% variability. The simplified equation (Eq. 6) is to some extent less accurate in comparison to the derived equation, with an average of 1.03 and variability of 15%. However, for practical purposes, Eq. 6 strikes a good balance between simplicity and accuracy.

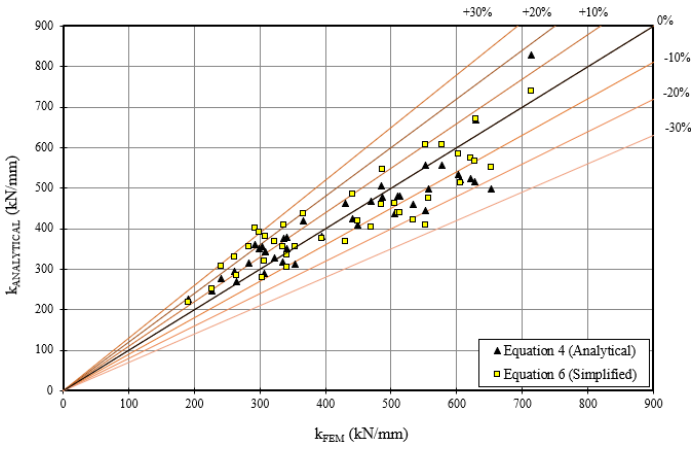

Figure 3: Stiffness formulations vs FE models

4 Conclusion

To address the absence of initial stiffness prediction formulations for CHS-to-transversally welded plate connections in Eurocode 3 Part 1.8 [4], a study was conducted to develop two equations for this purpose. Numerical data from 40 cases in a separate study [5] was used to validate these derived equations. The results demonstrated that both formulations achieved accuracy of good level when comparison is done to the numerical results. Specifically, analytical equation predicted initial stiffness with 1 as the mean value and 12% CoV, while the simplified equation yielded a mean value of 1.03 with 15% CoV. However, the equations are constrained by the defined limits of the parameters 'β', 'γ' and 'τ'. These limits are 0.44 to 0.74 for 'β', 15.28 to 22.75 for 'γ' and 2 to 5.83 for 'τ' respectively.

5 Recommendation for Future Research

This research can be further extended to the prediction of the initial stiffness of CHS-IPE joints in their entirety, where the CHS-Plate connection functions as an integral component.

Acknowledgement

The authors would like to express their gratitude to Prof. Dr. Gianvittorio Rizzano and Dr. Eng. Sabatino Di Benedetto for their invaluable guidance throughout the research.

References

[1]. Piscini, A., Passing-through Tubular Column Joints for Steel and Composite Constructions made by Laser Cutting Technology, PhD Thesis, University of Florence, 2019.
[2]. N. Kosteski and J.A. Packer, *Longitudinal Plate and Through Plate-to-Hollow Structural Section Welded Connections*, Journal of Structural Engineering, vol. 129(4), pp. 478-486, 2003, https://doi.org/10.1061/(ASCE)0733-9445(2003)129:4(478).
[3]. IIW, 1989: *Design recommendations for hollow section joints – Predominantly statically loaded*, 2nd Edition, International Institute of Welding, Sub-commission XV-E, Paris, France, IIW Doc. XV-701-89.
[4]. CEN [2005]: EN 1993-1-8 *Eurocode 3: Design of Steel Structures. Part 1-8: Design of Joints*, CEN, European Committee for Standardization, 2005.
[5]. American Institute of Steel Construction (AISC). (2016). Specification for Structural Steel Buildings (ANSI/AISC 316-16). Chicago, IL: AISC.
[6]. Wardenier, J., Kurobane, Y., Packer, J.A., van der Vegte, G.J., Zhao, X.L., Design guide for circular hollow section (CHS) joints under predominantly static loading, 2nd Ed., CIDECT, Geneva, Switzerland, 2008.
[7]. Ajwad, A., Di Benedetto, S., Latour, M., Rizzano, G., A component method approach for single-sided beam-to-column joints with CHS columns and welded double-tee beam, Thin-Walled Structures, 112055, ISSN 0263-8231, https://doi.org/10.1016/j.tws.2024.112055, 2024.
[8]. Sato, A., Elettore, G., Ajwad, A., Di Benedetto, S., Latour, M., Francavilla, A.B., and Rizzano, G., Stiffness of Welded T-joints Between SHS Profiles and Through Plates, STESSA 2024, pp. 350,361, Lecture Notes in Civil Engineering, vol 519. Springer, Cham. https://doi.org/10.1007/978-3-031-62884-9_31.

THE DEVELOPMENT OF FRAGILITY CURVES FOR MASONRY BUILDING- STATE OF ART REVIEW

[a] Saif Ur Rehman*, [b] Mohammad Ashraf

a: Department of Civil Engineering, University of Engineering and Technology, Peshawar, Pakistan. saifgandapur@uetpeshawar.edu.pk
b: Department of Civil Engineering, University of Engineering and Technology, Peshawar, Pakistan. mashraf@uetpeshawar.edu.pk
* Corresponding author.

Abstract- A significant portion of buildings worldwide are made of masonry, that is the reason that buildings are more vulnerable to earthquake damage. Fragility curves are crucial tools for evaluating seismic risk as they provide a quantitative measure of the probability of a building exceeding a particular damage condition in response to a given ground motion intensity. This review study provides a thorough analysis of the current knowledge in the development of fragility curves specifically for masonry buildings. The review starts by explaining the significance of fragility curves in earthquake mitigation techniques. The review article then investigates numerous methods for developing fragility curves for masonry buildings, such as the empirical method, analytical method, expert judgment, and hybrid approach. Following that, various findings of the researchers, the methodology they employed, and the crucial aspects they studied in order to construct the fragility curves are discussed.

Keywords- Fragility Curves, Fragility Analysis, Risk Assessment of Buildings, Non-linear Analysis.

1 Introduction

Seismic fragility curves illustrate the vulnerability of buildings to earthquakes. Figure 1 represent the general representation of fragility curves by showing the probability of structural failure as a function of an earthquake intensity measure [1].

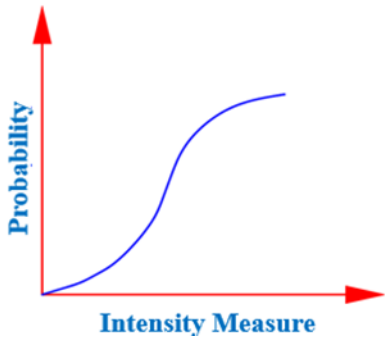

Figure 1: General representation of fragility curves [1]

Fragility curves tell us what's likely happen to our buildings when the ground starts shaking. Fragility curve are necessary to evaluate the vulnerability of structures to unforeseen events and for setting retrofit and/or repair priorities [2]. The fragility curve provides the possibility of exceedance of a specific damage level based on a chosen ground motion parameter [3]. According to D'Ayala [3] , there are various types of fragility curves,

1. Empirical method
2. Analytical method

3. Expert judgement
4. Hybrid method

Table 1: Pros and cons of each method [4]

Approaches	Advantages	Disadvantages
Empirical method	It shows the actual vulnerability It represents a realistic picture of the structure	Lack of data Inconsistency in damage observation
Analytical method	It is less biased It covers all types of uncertainties	It is quite costly Its computation takes a lot of time
Expert Judgement	This approach quite Simple It may include all the factors	It is very subjective It is totally dependent on the panel expertise It is not that much accurate
Hybrid method	It considers the post-earthquake data It can reduce the computational effort	It generally requires multiple data because of combination of experimental and analytical approaches

According to Table 1, each method has its strengths and weaknesses. An empirical approach is based on actual data, but can be hampered by data limitations. The analytical approach provides a rigorous and unbiased assessment, but with a large cost and time investment. Expert judgment offers simplicity and the ability to take different factors into account, although it is subjective and relies on expert knowledge. Finally, the hybrid approach aims to balance these factors by using post-event data and reducing computational requirements, although it requires extensive and diverse data sources. The choice of method depends on the specific context, the available resources and the required accuracy of the vulnerability assessment.

2 Methodology

In Pakistan, significant research work has been carried out in the past on masonry buildings including different building typologies such as unreinforced masonry building (URM), reinforced concrete frame structure, confined masonry building, and adobe buildings. Here we will shed light on some of the significant work on developing fragility for buildings carried out in the past.

[5] Provides an analytical procedure for developing the fragility curves for masonry buildings.

Figure 2 shows the fragility curves for masonry buildings having PGA on x axis and probability on the y axis which is developed by identifying all mechanical properties of masonry buildings that can vary (e.g. strength and stiffness), and using Monte Carlo simulations to generate random values for these properties. Then by performing nonlinear static and dynamic analysis of the building the fragility curves are obtained.

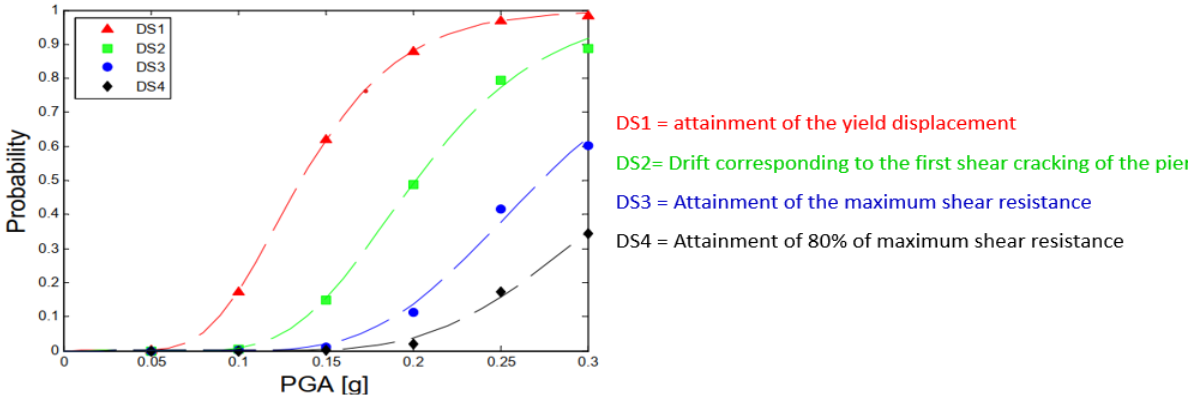

Figure 2: Masonry building fragility curves [5]

[6] developed empirical fragility curves for adobe buildings using methodology proposed by Giovinazzi (2005). Figure 3 shows the fragility curves for adobe buildings having intensity measures on x axis and probability of damage on y axis. They Compared damage potential of adobe buildings in Pakistan and Europe and found Pakistani buildings are more vulnerable to collapse.

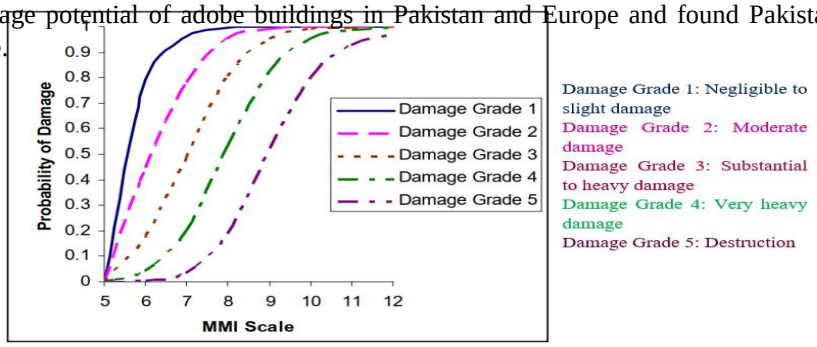

Figure 3: Adobe buildings fragility curves [6]

[7] developed the analytical fragility curves for masonry buildings based on Applied Element Method (AEM). Figure 4 depicts the fragility curves for masonry buildings having spectral acceleration on x axis and probability on y axis. AEM combines strengths of finite element method and discrete element methods for better simulation of complex structural behavior. Over 50 ground motion records were used to Studied the models. They concluded that AEM is a reliable tool for assessing earthquake risk in URM buildings.

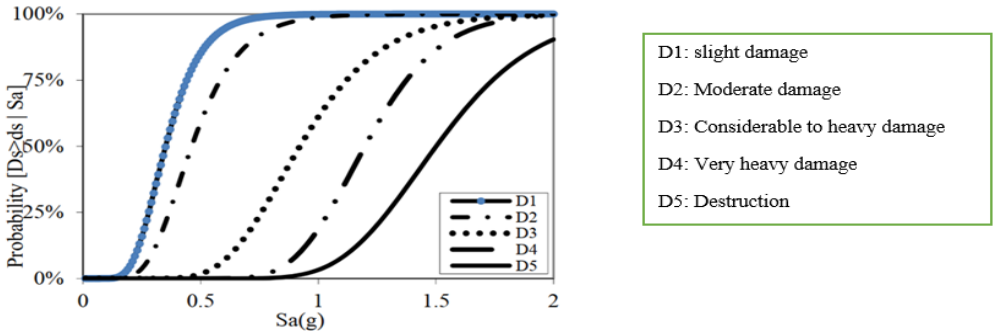

Figure 4: Brick Masonry Buildings fragility curves [7]

[8] developed the hybrid fragility curve for a confined masonry buildings in Lima, Peru. Figure 5 shows the fragility curves for confined masonry buildings having PGA on x axis and probability of exceedance on y axis They used a combination of field surveys, experimental tests, and computer simulations to create a database of information about these buildings. The results showed that confined masonry buildings in Lima are at moderate risk of damage from earthquakes. However, the risk of damage varies depending on the size and location of the building.

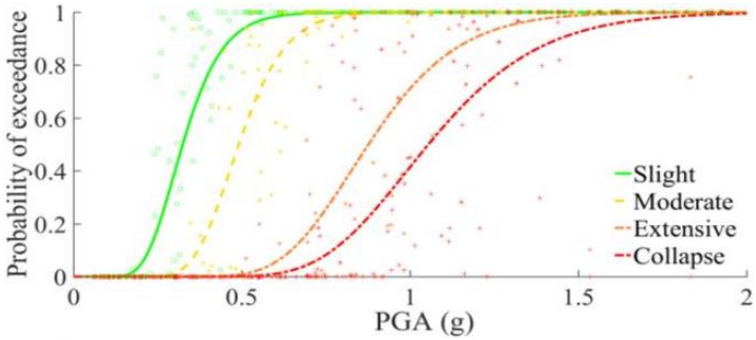

Figure 5: Confined Masonry Buildings fragility curves [8]

3 Practical Implementation

Engineers can use the seismic fragility curves to estimate the building's damage probability under different earthquakes. The information provided by the fragility curves can be directly used in prioritizing retrofitting efforts, establishing building codes, and implementing preventative measures, ultimately improving the seismic resilience of our masonry structures.

4 Conclusion

1. This review article thoroughly examines the fragility curves development for masonry buildings, which are an essential tool for assessing seismic risk.
2. The review showcased the effectiveness of these methodologies in evaluating the seismic vulnerability of various masonry structures through reviewing previous research.
3. Future research directions could focus on refining existing methodologies, incorporating regional construction practices, and developing fragility curves for a wider range of masonry building typologies.
4. By continuously improving fragility curve development, engineers can make informed decisions regarding earthquake risk mitigation strategies and ensure the safety and resilience of our built environment.

References

[1] C. Mai, K. Konakli, and B. Sudret, "Seismic fragility curves for structures using non-parametric representations," Front. Struct. Civ. Eng., vol. 11, no. 2, pp. 169–186, Jun. 2017, doi: 10.1007/s11709-017-0385-y.

[2] S. M. Lee, T. J. Kim, and S. L. Kang, "Development of fragility curves for bridges in Korea," KSCE Journal of Civil Engineering, vol. 11, pp. 165–174, 2007.

[3] D. D'Ayala et al., "Guidelines for analytical vulnerability assessment of low/mid-rise buildings," 2014.

[4] A. Muntasir Billah and M. Shahria Alam, "Seismic fragility assessment of highway bridges: a state-of-the-art review," Structure and infrastructure engineering, vol. 11, no. 6, pp. 804–832, 2015.

[5] M. Rota, A. Penna, and G. Magenes, "A methodology for deriving analytical fragility curves for masonry buildings based on stochastic nonlinear analyses," Engineering Structures, vol. 32, no. 5, pp. 1312–1323, May 2010, doi: 10.1016/j.engstruct.2010.01.009.

[6] M. M. Rafi, S. H. Lodi, H. Varum, and N. Alam, "Estimation of Losses for Adobe Buildings in Pakistan".

[7] A. Karbassi and P. Lestuzzi, "Fragility Analysis of Existing Unreinforced Masonry Buildings through a Numerical-based Methodology," TOCIEJ, vol. 6, no. 1, pp. 121–130, Nov. 2012, doi: 10.2174/1874149501206010121.

[8] H. Lovon, N. Tarque, V. Silva, and C. Yepes-Estrada, "Development of Fragility Curves for Confined Masonry Buildings in Lima, Peru," Earthquake Spectra, vol. 34, no. 3, pp. 1339–1361, Aug. 2018, doi: 10.1193/090517EQS174M.

[9] M. W. Khan, M. Usman, S. H. Farooq, M. Zain, and S. Saleem, "Effect of masonry infill on analytical fragility response of RC frame school buildings in high seismic zone," Journal of Structural Integrity and Maintenance, vol. 6, no. 2, pp. 110–122, Apr. 2021, doi: 10.1080/24705314.2020.1865624.

STRENGTHENING OF UNREINFORCED MASONRY STRUCTURE WITH FIBER-REINFORCED POLYMER

[a] Ahmad Suboor*, [b] Samiullah Qazi

a: Department of Civil Engineering, University of Engineering and Technology, Peshawar, Pakistan. ahamadsuboor.civ@uetpeshawar.edu.pk
b: Department of Civil Engineering, University of Engineering and Technology, Peshawar, Pakistan. samiullah.qazi@uetpeshawar.edu.pk
* Corresponding author.

Abstract- This study investigates the effect of carbon fibre-reinforced polymer (CFRP) in improving the seismic capacity of rural masonry structures prevalent in central Asia, where an overwhelming majority of masonry buildings lack reinforcement, rendering them susceptible to seismic events. Considering the situation, it is essential to reinforce these buildings using an efficient, cost-effective, and practical approach. CFRP partial bonding has been more economical compared to full jacketing; though, it comes with potential challenges such as interface delamination. As a result, this study utilizes the partial bonding method coupled with a CFRP anchorage system applied on the exterior of the structure. Two one-third scale unreinforced masonry structures (URM), designed to replicate typical village rooms, were constructed and subjected to displacement-controlled lateral loading and a constant normal load. The specimen reinforced with CFRP exhibited satisfactory performance in terms of observed failure modes and load response curves compared to the URM structure. In addition, the strengthening technique resulted in keeping the masonry structure intact over large drift ratios.

Keywords- Carbon Fiber Reinforced Polymer, CFRP Anchorage, Masonry Structures, Seismic Performance.

1 Introduction

Brick masonry is widely utilized in the construction industry around the world thanks to its practical application, local availability, heat insulation property, and affordable price. These structures are constructed either following engineering guidelines, referred to as confined masonry (CM), or without the use of confining elements, known as unreinforced masonry (URM). In Pakistan, however, a substantial 62% of the overall building stock is composed of brick masonry structures [1]. While unreinforced masonry (URM) structures exhibit satisfactory performance under gravity loads, their seismic resilience is limited, with the potential to withstand only minor earthquakes, rendering them susceptible to damage even in the case of moderate seismic events. The assessment conducted after the 2005 Kashmir earthquake revealed that the majority of the damaged or collapsed buildings were URM structures [2]. Moreover, URM structures suffered substantial damage in the 2015 Nepal earthquake and the 2016 Italy earthquake [3], [4]. Based on the occurrence of recent catastrophic seismic events and post-earthquake assessments, there is a crucial need for further research to enhance the seismic capacity of URM structures. Conventional seismic strengthening techniques, such as post-tensioning, member confinement, the centre core method, surface treatment, etc., have been explored to enhance the capacity of URM structures. Nevertheless, these techniques are accompanied by certain drawbacks such as mass increase, labour-intensive processes, and time consumption. On the contrary, Fibre-reinforced polymer (FRP) has captured the interest of researchers due to its inherent properties, such as its lightweight nature, high tensile strength, ease of application, corrosion resistance, and minimal alteration to the geometry of structural elements [5]. Many researchers have focused on strengthening of URM structural components such as walls, piers, or spandrels using FRP composites. Mustafaraj and Yardim [6] explored the effect of the diagonal compression test on brick masonry panels and reported a 27% increase in shear strength, a 645% increase in shear modulus, and an 1100% increase in ductility compared to that of the control specimen. Hernoune et al. [7] reinforced masonry panels constructed from hollow bricks using various carbon fibre-reinforced polymer (CFRP) configurations. The specimens strengthened with FRP showed a 3 to 4 times increase in shear strength and up to an 88%

increase in ductility. Although numerous studies have concentrated on strengthening individual components (pier, spandrel, or wall) of the URM structure, limited literature is available regarding the global response of FRP-strengthened masonry structures under seismic loading. Moon et al. [8] conducted tests on a two-storey unreinforced masonry (URM) structure both before and after retrofitting with fibre-reinforced polymer (FRP). The primary objective of the composite repair was not to strengthen the structure but rather to maintain the damaged structure intact over significant displacement. Notably, the FRP was not anchored to the masonry. However, no research has so far been conducted on the seismic performance of the typical village room structure that is typically constructed in rural areas of developing countries. In this type of structure mainly the outer wall is also used as a boundary wall whereas door and window openings are made in the parallel wall—open to in-house courtyards. Therefore, this research work presents the seismic performance of the URM structure that is prevalent in rural areas of developing countries and explores the effect of FRP reinforcement on the strengthening of such structures. Apart from that to improve the bonded CFRP strips two types of CFRP anchors are used.

2 Research Methodology

2.1 Specimens Preparation

The construction of the models is carried out in two stages. In the first stage, two one-third-scale unreinforced brick masonry room models are constructed. The decision to scale down the specimens is made based on the limitations in instrumentation and project funds. The geometric configuration of the model is such that it has one perforated wall and three solid walls. The model dimensions are 122 cm x 102 cm x 130 cm (length x width x height) with 7.5 cm thick walls laid in English bond. Each room model is constructed over a 15 cm reinforced concrete (RC) raft to ensure they do not incur any damage during transportation to and placement inside the steel reaction frame. After construction and a curing period, one of the specimens is whitewashed and positioned within the straining frame. Its base is securely fastened to the underlying steel girders through a nut and bolt connection. The model is then subjected to the displacement-controlled cyclic load and a constant vertical load.

In the second stage, the uncracked model is confined with unidirectional CFRP strips. In solid walls, all vertical strips running throughout the specimen are 7.5 cm in width, while the vertical strips, on the sides of the openings (door and window) in the perforated wall, are 5 cm in width. The horizontal strips and the vertical strips running up to the sill level are both 5 cm in width. The CFRP pattern and strip width are determined based on both local and global failures observed in the control specimen, as well as previous studies on CFRP-strengthened masonry walls. To minimize the occurrence of premature failure, 90-degree and 180-degree FRP anchor spikes are employed to anchor the CFRP strips to the masonry walls, RC slab, and raft foundation. The FRP strips were bonded to the masonry substrate using Chemdur 300 epoxy resin and were allowed to cure for 7 days before undergoing testing. The materials used in the preparation of the test specimens and the mixed proportions of mortar and concrete are kept similar to those of the study area. The specifications of CFRP reinforcement, as provided by the manufacturer, are illustrated in Table 1.

Table 1: Specifications of CFRP fabric

Fibre Type	**Areal Weight**	**Tensile Strength of Fibres**	**Tensile E-modulus of Fibres**	**Strain at Break of Fibres**
High-strength carbon fibres	220 g/m^2 ± 10 g/m^2	4100 N/mm^2	231000 N/mm^2	1.7%

2.2 Test Setup and Procedure

The instrumentation and isometric view of the test specimen are illustrated in Figure 1(a) and Figure 1(b) respectively. The displacement cycles are applied using a 500 kN capacity hydraulic jack fixed to the steel reaction frame and connected to the specimen at the roof slab. For brevity, the four walls of the structure are referred to as Wall A, Wall B, Wall 1, and Wall 2. Wall A and Wall B represent the perforated and solid in-plane walls, respectively. Wall 1 designates the out-of-plane wall where the load cell is attached, while Wall 2 signifies its parallel out-of-plane wall. To measure the displacement at various points of the structure, twelve Linear Variable Displacement Transducers (LVDT) are installed on steel reference frames and connected to the structure at various locations of interest through flexible steel wires. Each displacement cycle encompasses two amplitudes, one negative and one positive, with identical loading conditions applied in both directions.

Starting from 0.25mm, all displacement cycles are repeated three times. The test is continued till the structure fails or is excessively damaged.

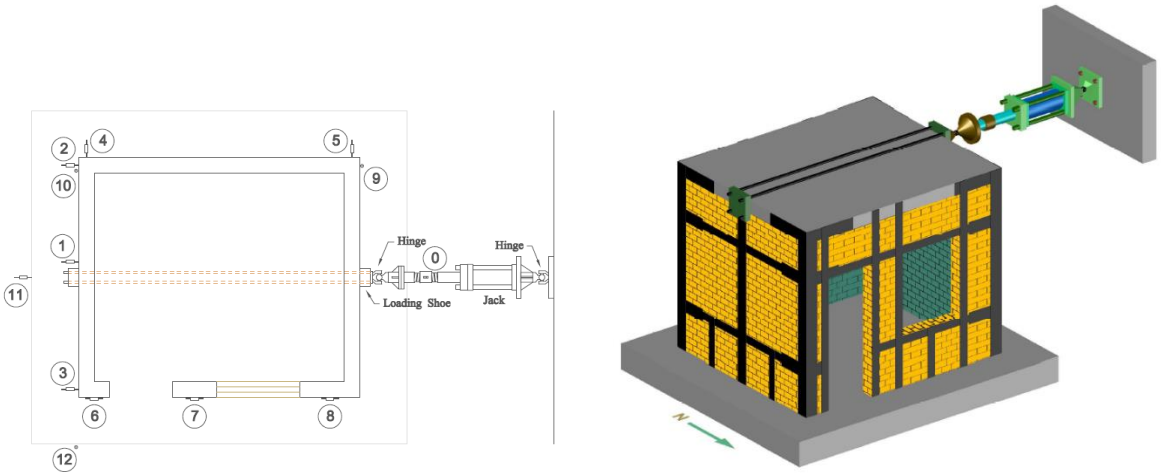

a) b)

Figure 1: Test specimen, a. instrumentation setup, and b. N-E isometric view

3 Results

3.1 Hysteresis Loops

In the URM specimen, a tight loop was formed at the initial displacement cycle corresponding to 0.02% drift. Beyond this drift, wide loops were observed. Tight loops show small energy dissipation while wide loops are an indication of higher energy dissipation. Rapid stiffness degradation occurred at 0.02% drift and reached almost zero at 0.15% story drift. This rapid stiffness degradation could be attributed to the brittle behaviour of unreinforced masonry. During the initial displacement cycles, wall B (solid in-plane wall) was undergoing sliding failure while wall A underwent diagonal shear failure. However, during the final displacement cycles, the failure mode of wall B altered to rocking while the existent diagonal cracks in wall A continued to widen.

In the case of the CFRP-confined specimen, Rapid stiffness degradation was observed till 0.1% story drift and thereafter continued to gradually decrease till the ultimate displacement cycle. FRP rupture initiated at 0.77% story drift followed by gradual failure of the composite at various locations. During the initial displacement cycles, fewer cracks were observed in the CFRP-strengthened specimen as compared to the URM specimen because the introduction of CFRP enhanced the stiffness of the structure. However, during the final displacement cycles, more cracks were propagated in the strengthened specimen as opposed to the URM specimen. Figure 2 illustrates the hysteresis loops and envelope curves of URM and CFRP-strengthened specimens.

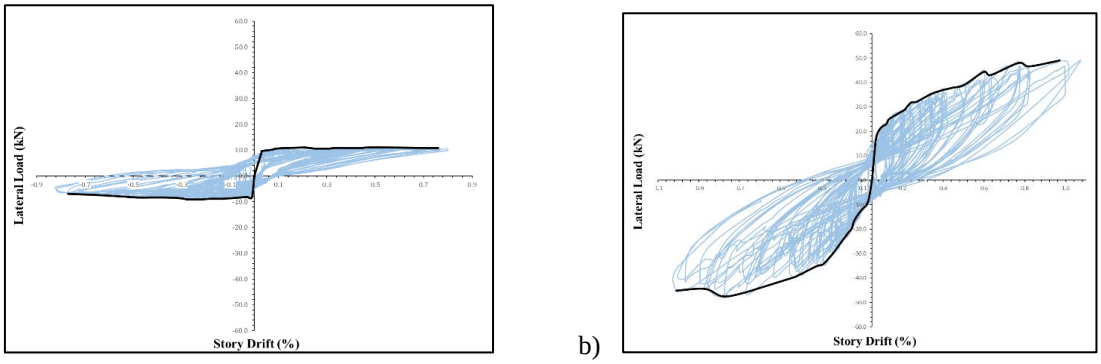

a) b)

Figure 2: Hysteresis loops, a. URM specimen, and b. CFRP-Strengthened specimen

3.2 Backbone envelope

The peak load and its corresponding displacement in each displacement cycle, for both positive and negative amplitudes, were joined to obtain the backbone curve for URM and CFRP-strengthened specimens. Initially, both control and strengthened models exhibited stiff behaviour. However, the stiffness of the URM specimen decreased substantially during the initial displacement cycles while the CFRP-strengthened specimen showed a gradual decrease in stiffness till the ultimate displacement cycle. URM specimen reached its maximum capacity of 9.98 kN at 0.19% story drift whereas the CFRP-strengthened specimen reached its ultimate capacity of 47.09 kN at a drift ratio of 0.7. The CFRP confinement dramatically enhanced the lateral resistance of the URM structure by a factor of 4.72. This was achieved as a result of the proper anchorage of CFRP strips to the masonry walls, RC slab, and raft foundation. A parametric comparison of URM and CFRP-strengthened Masonry is presented in Table 2.

Table 2: URM and CFRP-Strengthened Masonry Specimens Parametric Comparison

Parameters	Control Specimen	CFRP-Confined Specimen	Percent Increase due to CFRP Application
Peak Resistance (kN)	9.98	47.09	372%
Drift at Peak resistance (%)	0.19	0.7	268%
Ultimate Displacement (mm)	10	12	20%

4 Practical Implementation

Based on the experimental findings, the adopted strengthening technique can be used to enhance the seismic performance of non-engineered rural area masonry structures that do not satisfy the local building code's seismic requirements without displacing their occupants and in a shorter period as compared to conventional strengthening techniques.

5 Conclusions

- The adopted CFRP strengthening configuration improved the URM structure's seismic performance significantly.
- The CFRP bonding technique improved the strength of the URM structure by 372%.
- The adopted technique also improved the ultimate displacement of the structure by 20%.
- The adopted anchorage technique proved to be effective in preventing the delamination of CFRP strips from masonry, RC slab, and foundation.

References

[1] M. Ahmed, S. Lodi, M. Rafi, and N. Alam, "Transforming Census Data in Pakistan into Spatial Database for Earthquake Loss Estimation Models," *Lisb. Sn*, 2012.
[2] M. Javed, "Seismic risk assessment of unreinforced brick masonry buildings system of Northern Pakistan," *Civ. Eng. Dep.*, 2009.
[3] D. Dizhur, R. P. Dhakal, J. Bothara, and J. M. Ingham, "Building typologies and failure modes observed in the 2015 Gorkha (Nepal) earthquake," *Bull. N. Z. Soc. Earthq. Eng.*, vol. 49, no. 2, pp. 211–232, 2016.
[4] M. Çelebi *et al.*, "Recorded motions of the 6 April 2009 Mw 6.3 L'Aquila, Italy, earthquake and implications for building structural damage: overview," *Earthq. Spectra*, vol. 26, no. 3, pp. 651–684, 2010.
[5] A. Ahmed and V. Kodur, "The experimental behavior of FRP-strengthened RC beams subjected to design fire exposure," *Eng. Struct.*, vol. 33, no. 7, pp. 2201–2211, 2011.
[6] E. Mustafaraj and Y. Yardim, "In-plane shear strengthening of unreinforced masonry walls using GFRP jacketing," *Period. Polytech. Civ. Eng.*, vol. 62, no. 2, pp. 330–336, 2018.
[7] H. Hernoune, B. Benabed, M. Alshugaa, R. Abousnina, and A. Guettala, "Strengthening of masonry walls with CFRP composite: experiments and numerical modeling," *Ép. Online*, no. 1, pp. 2–11, 2020.
[8] F. L. Moon, T. Yi, R. T. Leon, and L. F. Kahn, "Testing of a full-scale unreinforced masonry building following seismic strengthening," *J. Struct. Eng.*, vol. 133, no. 9, pp. 1215–1226, 2007.

EXPERIMENTAL INVESTIGATION OF BRIDGE PIER SCOURING WITH RIP RAP ENCLOSED IN MESH

[a]Fardeen Javaid, [b] Muhammad Bilal*

a: Civil Engineering Department, Army Public College of Management and Sciences, Rawalpindi. fardeenkiyani999@gmail.com
b: Civil Engineering Department, Army Public College of Management and Sciences, Rawalpindi. malikbilal121912@gmail.com
* Corresponding author.

Abstract- Bridge pier scouring poses a significant risk to the stability and safety of transportation infrastructure, necessitating effective countermeasures to mitigate its impact. This study presents an experimental investigation aimed at evaluating the effectiveness of rip rap enclosed in mesh for reducing scour depth around bridge piers. Scaled models representing bridge piers were constructed in a laboratory flume, and rip rap enclosed in mesh was installed around the piers. Controlled experiments were conducted to simulate varying flow conditions and sediment transport processes. Data on water flow velocity, sediment transport rates, scour depth, and rip rap stability were collected and analyzed. The results demonstrate that the use of rip rap enclosed in mesh significantly reduces scour depth compared to unprotected scenarios. Taking Oblong pier as reference before installing riprap value of scouring was 0.83 which later was reduced to 0.62. Furthermore, the overall scouring that was reduced is 74.5%. Insights gained from this study contribute to the understanding of scour processes and the effectiveness of rip rap with mesh in mitigating bridge pier scouring. Practical recommendations are provided for the design and implementation of rip rap protection systems to enhance the resilience of bridge infrastructure against hydraulic scour.

Keywords- Bridge, Mesh, Rip Rap, Scouring.

1 Introduction

The erosive action of running water causes bridge pier scouring, which is a serious risk to the structural integrity and stability of bridges worldwide. As shown in figure 2. [1]. Scouring can undermine the foundations of bridge piers, leading to structural instability and potential collapse, with potentially catastrophic consequences. [2] Consequently, there is a pressing need for effective scour mitigation measures to safeguard bridge infrastructure and ensure public safety.[3] Among the various scour countermeasures, rip rap – loose stone or concrete rubble – has long been utilized to protect bridge piers from scour erosion. Rip rap functions by dissipating flow energy and resisting erosive forces, thereby reducing scour depth around bridge foundations. However, traditional riprap placement techniques may not always provide optimal protection, as sediment migration and instability can compromise its effectiveness.

To address these limitations, researchers and engineers have explored innovative approaches to enhance rip rap performance. One such approach involves enclosing rip rap within a mesh framework, which serves to contain the stones and prevent sediment displacement. By changing flow patterns and improving the riprap's structural stability, the mesh promotes sediment deposition and lessens scour. The purpose of this project is to conduct an experimental investigation into the efficacy of riprap contained in mesh as a bridge pier scour counter measure.[4] By subjecting scaled models of bridge piers to controlled flow conditions in a laboratory setting, this research aims to assess the effectiveness of rip rap with mesh in reducing scour depth and enhancing stability. The findings of this experimental study are expected to contribute valuable insights into the performance of rip rap enclosed in mesh as a scour mitigation measure. [5] These insights will inform the design and implementation of effective scour protection strategies for bridge infrastructure, ultimately enhancing resilience and safety in transportation systems. Scouring around bridge piers significantly threatens bridge stability and can cause tragic failures if not addressed effectively [8].

2 Research Methodology

A comprehensive experiment was conducted at the Water Resources & Hydraulics Engineering Laboratory of the University of Engineering and Technology, Taxila, focusing on mitigating bridge pier scour. The experiment utilized a 20-meter-long glass-sided flume equipped with adjustable features to control water flow characteristics precisely as shown in figure 1. A model pier resembling real-world designs was placed within distinct test sections of the flume, each evaluating different pier protection strategies [6]. These tactics comprised conventional riprap, bare piers, and several mesh-enclosed riprap designs with different mesh qualities. Instruments such as point gauges and depth sensors were strategically placed to quantify scour depth around the pier in each section [7]. The main experiment comprised operating water flow for a predefined amount of time, mimicking flood occurrences or observation periods, and monitoring the scour depth surrounding the pier during that time [9]. After the experiment, thorough analysis compared scour depth and patterns across sections, focusing particularly on the effectiveness of mesh-enclosed rip rap in reducing scour compared to traditional methods. This research aims to provide valuable insights into enhancing bridge safety and longevity through improved pier protection techniques [10].

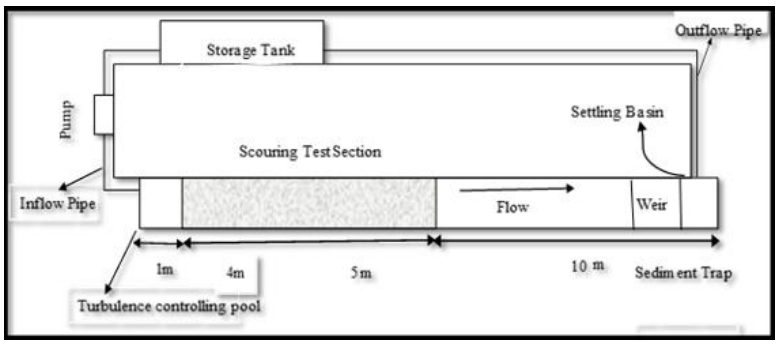

Figure 1: Schematic Diagram

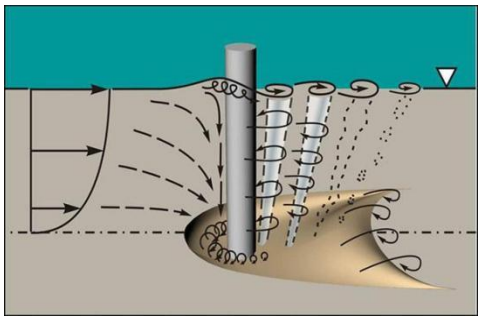

Figure 2: Local Scouring

3 Results

All the experiment was performed in clear water flow conditions, which means that the velocity of the flow was less or equal to the threshold velocity or critical velocity [V_C], in clear-water scouring conditions maximum scouring occurs at the threshold peak, where '*h*' is the flow depth, '*T*' is the time in hours, '*Q*' is the discharge, S is the separation distance, from the upstream submerged rip rap, *ysf* is the maximum scour at the upstream face of pier. Table: 1 shows the hydraulic parameters of the present experimentalstudy. As the figure 3 and 4 shows the relation between V/Vc and ds/D with mesh where 5 and 6 figure shows without mesh relation. As, V represent velocity and Vc is the critical velocity and ds represent the scouring depth and D is the dia of the pier in table 1. Rather of depending on weirs and other expensive techniques, we might choose a more economical course of action with easily accessible resources. Because it substantially lowers scouring at just a percentage of the expense, this alternate approach is preferred.

Table 1: Experimental Values

					Without Mesh			With Mesh		
Shape	**Discharge 'cm³/s'**	**Bed Depth 'cm'**	**V/Vc**	**Fr**	**Dia 'cm'**	**ds**	**ds/D**	**Dia 'cm'**	**ds**	**ds/D**
Oblong	22	15	0.47	0.019	6	5	0.833333333	6	5	0.625
	27	15	0.59	0.024	6	5.4	0.9	6	5.4	0.675
	32	15	0.71	0.029	6	5.9	0.983333333	6	5.9	0.7375
	38	15	0.84	0.034	6	6.4	1.066666667	6	6.4	0.8

	42	15	0.95	0.038	6	6.7	1.116666667	6	6.7	0.8375
Circle	22	15	0.47	0.019	6	5.3	0.883333333	6	5.3	0.6625
	27	15	0.59	0.024	6	5.7	0.95	6	5.7	0.7125
	32	15	0.71	0.029	6	6.2	1.033333333	6	6.2	0.775
	38	15	0.84	0.034	6	6.7	1.116666667	6	6.7	0.8375
	42	15	0.95	0.038	6	7	1.166666667	6	7	0.875
Square	22	15	0.47	0.019	6	5.5	0.916666667	6	5.5	0.6875
	27	15	0.59	0.024	6	5.9	0.983333333	6	5.9	0.7375
	32	15	0.71	0.029	6	6.4	1.066666667	6	6.4	0.8
	38	15	0.84	0.034	6	6.9	1.15	6	6.9	0.8625
	42	15	0.95	0.038	6	7.2	1.2	6	7.2	0.9

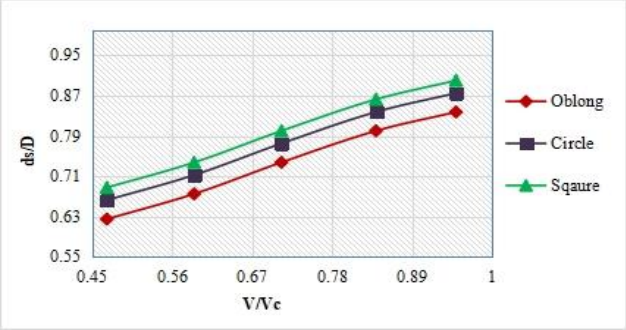

Figure 3. Graph with Mesh

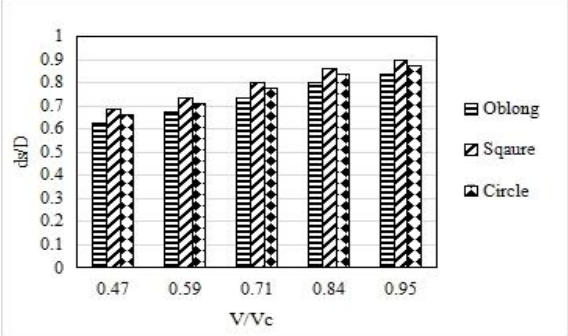

Figure 4. Graph with Mesh

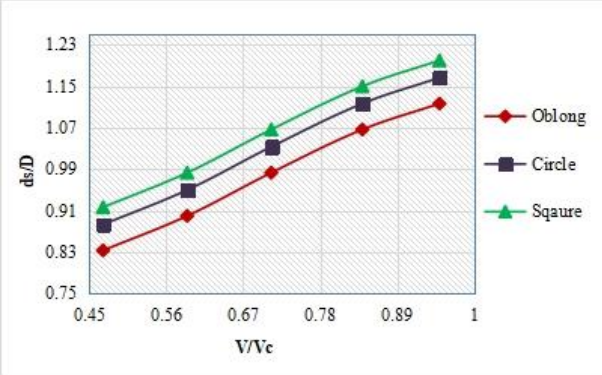

Figure 5. Graph without mesh

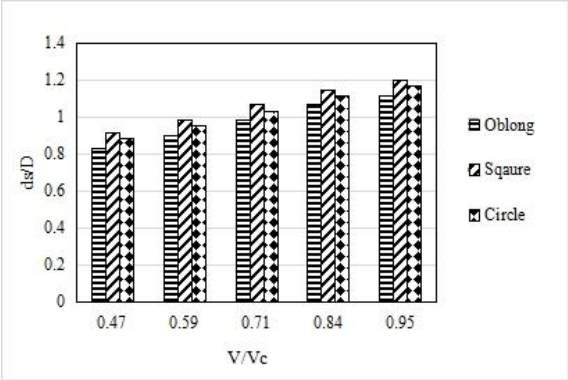

Figure 6. Graph without mesh

4 Conclusion

Using riprap that is covered with mesh greatly decreased scouring. After three distinct forms were tested (oblong, round, and square), the oblong design produced the best results. Both pre-and post-installation investigations show that the oblong pier greatly reduces scouring to the maximum degree. Using figure 3, 4, 5 and 6 we can see that before rip rap installation, scouring in the oblong pier measured was 0.83, but it dropped to 0.62 after installation, the lowest figure achieved across all shapes. When the findings before and after rip rap installation are compared, a 21% reduction in scouring is seen. Furthermore, using rip rap encased in mesh reduces scouring by 74.5%. This highlights the tremendous usefulness of rip rap, especially when paired with mesh reinforcement, in reducing scouring.

References

[1] Abudallah Habib, I., Wan Mohtar, W. H. M., Muftah Shahot, K., El-shafie, A., & Abd Manan, T. S. [2021]. Bridge failure prevention: An overview of self-protected pier as flow altering countermeasures for scour protection. Civil Engineering Infrastructures Journal, 54[1], 1-22.

[2] Bento, A. M., Gomes, A., Viseu, T., Couto, L., & Pêgo, J. P. [2020]. Risk-based methodology for scour analysis at bridge foundations. Engineering structures, 223, 111115.

[3] Ettema, R., Nakato, T., & Muste, M. V. I. [2006]. An illustrated guide for monitoring and protecting bridge waterways against scour [No. Project TR-515]. IIHR-Hydroscience & Engineering, University of Iowa.

[4] Valela, C. [2021]. Reduction of bridge pier scour through the use of a novel collar design [Doctoral dissertation, Université d'Ottawa/University of Ottawa].

[5] MARTIN MOYA, M. F. (2020). The use of geosynthetics as a countermeasure for scour at piers in rivers: experimental small case investigation.

[6] Panici, D., & de Almeida, G. A. (2018). Formation, growth, and failure of debris jams at bridge piers. *Water Resources Research*, *54*(9), 6226-6241.

[7] Zarafshan, A., Iranmanesh, A., & Ansari, F. (2012). Vibration-based method and sensor for monitoring of bridge scour. *Journal of bridge engineering*, *17*(6), 829-838.

[8] Baranwal, A., & Das, B. S. (2024). Scouring around bridge pier: A comprehensive review of countermeasure techniques. *Engineering Research Express*.

[9] Wang, C., Yu, X., & Liang, F. (2017). A review of bridge scour: mechanism, estimation, monitoring and countermeasures. *Natural Hazards*, *87*, 1881-1906.

[10] Frangopol, D. M., Kusko, C. S., & Sause, R. (Eds.). (2010). *Bridge Maintenance, Safety, and Management and Life-cycle Optimization*. Boca Raton, FL: CRC Press.

ASSESSING STRUCTURAL BEHAVIOUR OF FRP-CONFINED CFST COLUMNS THROUGH FINITE ELEMENT METHODS

[a] Muhammad Azan Iqbal*, [b] Ali Raza

a: Department of Civil Engineering, University of Engineering and Technology, Taxila, Pakistan.hafizazan196@gmail.com
b: Department of Civil Engineering, University of Engineering and Technology, Taxila, Pakistan. ali.raza@uettaxila.edu.pk
* Corresponding author.

Abstract- While several studies have examined the use of sparse and limited data to predict the load-carrying capacity (LC) of fiber-reinforced polymer (FRP)-confined concrete-filled steel tube (CFST) compression members (FCC). But none have examined the predictive accuracy of different modeling approaches with a large and comprehensive dataset. Creating a finite element model (FEM) to forecast the axial compressive performance of FCC compression components is the main goal of this research. The steel tube and FRP wraps are represented by bilinear and linear elastic models, respectively. The concrete is represented by a concrete damage plasticity model. The proposed FEA model showed minor variations of only 6.70% and 3.10% for the maximum LC and related axial shortening of FCC columns, respectively.

Keywords- Database, Finite Element Analysis, CFST, Damaged Plastic Model, Axial Strength.

1 Introduction

When restricted with steel tubes (ST) and fiber reinforced polymer (FRP), concrete compression members demonstrate remarkable mechanical performance and adaptability. In civil engineering projects like long-span bridges and multistory buildings, these members are heavily utilized [1]. A precise simulation of axial compression strength is achieved using a nonlinear finite element analysis (FEA) of concrete filled stainless steel tube (CFST) compression members, which use an updated concrete damaged plastic model [2]. There is a good consistency between numerical estimations and experimental results in another FEA investigation of CFST compression members that uses an upgraded damaged plastic model to evaluate axial load-deflection and load-bearing capacity with ABAQUS [3]. Raza et al. [4] investigated reinforced concrete compression members wrapped with FRP sheets using FEA, utilizing both the linear elastic model and an updated version of the damaged plastic model. To accurately replicate the structural behavior of compression elements, another study looked at the effects of a number of characteristics, such as lateral FRP confinements and the interaction mechanism between lateral steel-tubes, FRP wraps, and concrete [5]. Similarly, a general fiber element model was developed to incorporate ultimate strength and axial compression behavior to predict the load-bearing strength of CFST circular components [6]. Previous empirical models did not consider factors unique to FRP confinement, such as interaction between FRP wraps, steel tubes, and concrete. Instead estimated the load carrying capacity (LC) of FRP-confined CFST compression members (FCC) using sparse experimental data. Therefore, more study will be needed to create a more thorough sample that can estimate the load carrying capacity of FCC compression members. The authors of this study used an experimental database and ABAQUS-based FEA modeling to assess the effectiveness of FCC compression members.

2 Finite Element Analysis

2.1 General Methodology

Currently, ABAQUS 6.14 tool is being used to do the finite element analysis of FCC compression members [7]. To replicate the behavior of axial shortening, eight FCC compression members were selected [8]. The primary

characteristics of the modeled FCC members are shown in Table 1. To represent the restricted concrete, 4 node curved shell components and 8 node brick elements in 3D were used (see Figure 1), together with steel tubes (ST) and carbon fiber reinforced polymer (CFRP) wraps. These element kinds were chosen because they could faithfully depict the behavior of compression elements [4]. The concrete was poured into the steel tubes (ST) and stirred, in accordance with the guidelines of a prior study. A homogenous and flowable concrete mix was made in order to guarantee consistency of the mix inside the ST. The top of the ST was then welded with a steel plate to apply load. 150 mm x 150 mm x 150 mm cube samples were created to evaluate the concrete's compressive strength.

Table 1: Characteristics of modelled FCC samples

Sample name	H (mm)	D (mm)	D/t_s	t_s (mm)	t_{cf} (mm)	n_o	f'_{co} (MPa)	K_ε
D200-C40-L2	600	200	100	2	0.334	2	40	0.575
D200-C40-L4-S1	600	200	100	2	0.668	4	40	0.677
D200-C60-L2	600	200	100	2	0.334	2	60	-
D200-C60-L4-S1	600	200	100	2	0.668	4	60	0.567
D260-C40-L2	780	260	130	2	0.334	2	40	0.701
D260-C40-L4-S1	780	260	130	2	0.668	4	40	0.420
D260-C60-L2	780	260	130	2	0.334	2	60	-
D260-C60-L4-S1	780	260	130	2	0.668	4	60	0.449

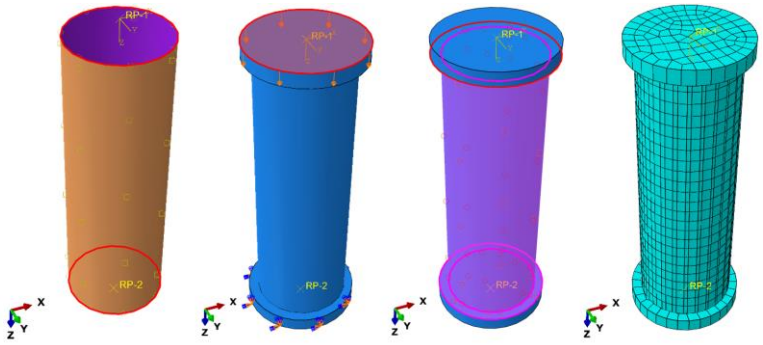

Figure 1: FEA simulations (a) steel tube, (b) application of loads, (c) interactions, and (d) meshed elements

The damaged plasticity model from the ABAQUS library was used to simulate restricted concrete, and it demonstrated a high degree of accuracy in representing the inelastic response of concrete under compression [6]. To precisely replicate the high-strength properties and damage behavior of CFRP wraps, the Hashin damage model [4] was used. Equations (6) through (9) of this model demonstrate its well-known capacity to characterize the beginning of damage in the medium and fibers under tensile and compressive loads [4].

Mode 1: fiber tension

$$f_1 = \left(\frac{\hat{\sigma}_{11}}{X^T}\right)^2 + \alpha\left(\frac{\hat{\sigma}_{12}}{S^L}\right)^2, \text{where } 0 \le \alpha \le 1 \quad (6)$$

Mode 2: fiber compression

$$f_2 = \left(\frac{\hat{\sigma}_{11}}{X^c}\right)^2 \quad (7)$$

Mode 3: matrix tension

$$f_3 = \left(\frac{\hat{\sigma}_{22}}{Y^T}\right)^2 + \left(\frac{\hat{\sigma}_{12}}{S^L}\right)^2 \quad (8)$$

Mode 4: matrix compression

$$f_4 = \left(\frac{\hat{\sigma}_{22}}{2S^T}\right)^2 + \left[\left(\frac{Y^c}{2S^T}\right)^2 - 1\right]\frac{\hat{\sigma}_{22}}{Y^c} + \left(\frac{\hat{\sigma}_{12}}{S^L}\right)^2 \quad (9)$$

Where, X^C denotes the compression strength of fibers, X^T shows the fibers' tensile strength measured in the normal direction whereas Y^C designates the compression strength. Similarly, Y^T depicts the tension strength reported in the transverse direction of wraps.

2.2 Discussion of FEM Results

The behavior and comparison of the whole load-deflection plot for each of the FCC samples that were included in the FEA model are shown in Figure 2. In the elastic and plastic zones of the load deflection plots, the sample performed admirably. The standard FEA model showed minor variations of only 6.70% and 3.10% for the maximum LC and related axial shortening, respectively. In contrast to all other models, sample D260-C40-L4-S1 showed the biggest divergence, with a value of 8.90% for the highest LC. Although the FEA model demonstrated a stronger correlation with experimental results in the plastic stage, it underestimated loadings in the elastic zone.

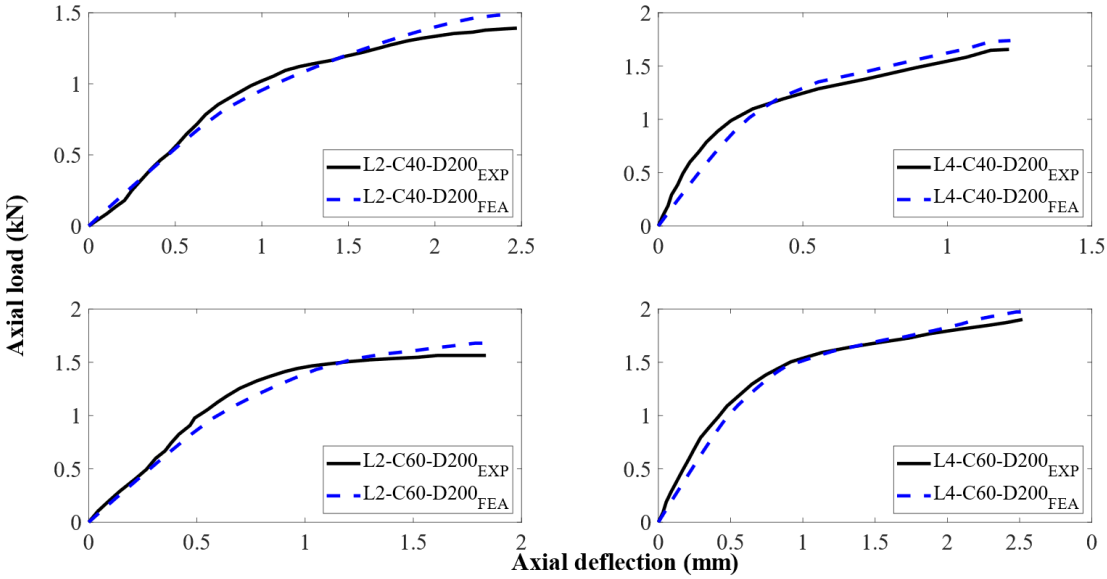

Figure 2: Running of FEA sample for the load deflection performance of FCC compression members

The study investigated the impact of increasing CFRP layers from two to four on Fiber-reinforced concrete (FCC) compression elements. Results showed a 19% and 21.50% increase in LC for D200-40 and D200-60 elements, respectively, with corresponding enhancements in axial shortening (see figure 3 and Figure 4). Similar improvements were observed for D260-40 and D260-60 elements. FEA calculations for D260-40 showed a 33.20% difference in ductility behavior and LC compared to experimental results, possibly due to disregarding residual stresses, variations in material properties, and assumptions in modeling.

2.2.1 Failure Patterns

Experimental testing of FCC members showed a linear elastic relationship between axial shortening and LC until ST yielding. Lateral confinement from CFRP wraps and ST led to a second linear segment in load-deflection, but LC dropped after CFRP fracture and ST buckling, indicating shear, and crushing failure. FE simulations matched lab results being visualized through positive principal plastic stains [9-10], showing shear failure in FCC members with fewer CFRP layers and higher core strength, and crushing failure in those with lower core strength (Figure 4).

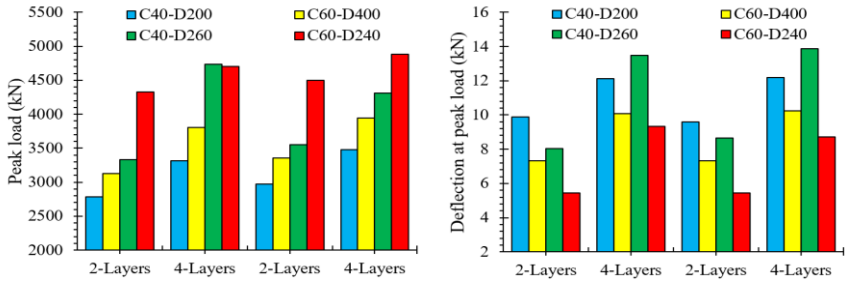

Figure 3: Influence of number of CFRP sheets (a) LC and (b) axial shortening of FCC compression members

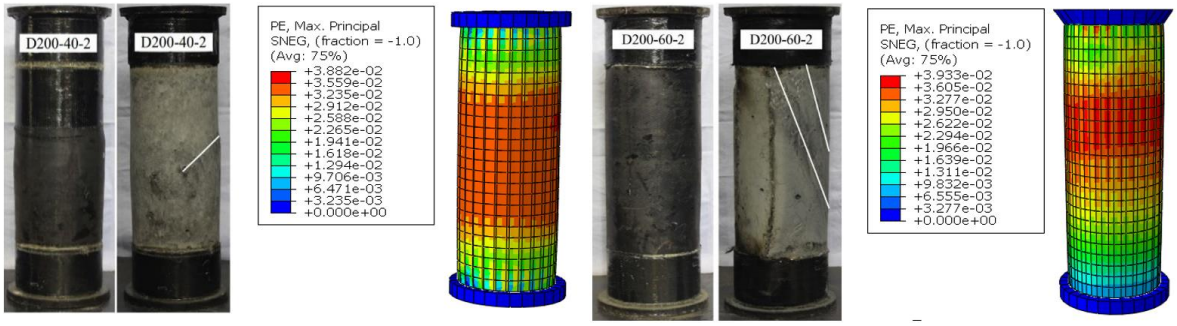

Figure 4: Failure modes of samples

3 Conclusion

This study's nonlinear finite element model, which accounts for the confinement offered by CFRP and ST confinement, successfully replicated the behavior of these parts. With differences of 5.72% and 2.83%, respectively, the FEA-based model's predictions for the members' axial shortening and LC exhibited only minor variations. The model used the Hashin damage model for CFRP covers, an updated concrete damage plasticity sample for the core concrete, and bilinear modeling for ST.

Reference

[1] Han, L.-H., W. Li, and R. Bjorhovde, Developments and advanced applications of concrete-filled steel tubular (CFST) structures: Members. Journal of constructional steel research, 2014. 100: p. 211-228
[2] Raza, A., et al. Axial performance of GFRP composite bars and spirals in circular hollow concrete columns. in Structures. 2021. Elsevier
[3] Raza, A., et al., Structural performance of FRP-RC compression members wrapped with FRP composites. Structures, 2020. 27: p. 1693-1709
[4] Raza, A., et al. Performance evaluation of hybrid fiber reinforced low strength concrete cylinders confined with CFRP wraps. in Structures. 2021. Elsevier
[5] Raza, A., et al. Prediction of axial load-carrying capacity of GFRP-reinforced concrete columns through artificial neural networks. in Structures. 2020. Elsevier
[6] Raza, A., et al., Finite element modelling and theoretical predictions of FRP-reinforced concrete columns confined with various FRP-tubes. Structures, 2020. 26: p. 626-638
[7] Fam, A., F.S. Qie, and S. Rizkalla, Concrete-filled steel tubes subjected to axial compression and lateral cyclic loads. Journal of Structural Engineering, 2004. 130(4): p. 631-640
[8] O'Shea, M.D. and R.Q. Bridge, Design of circular thin-walled concrete filled steel tubes. Journal of Structural Engineering, 2000. 126(11): p. 1295-1303
[9] Raza, A., El Ouni, M. H., & Hamza, M. (2024). Finite Element Modelling of Structural Behavior of Doubly Restrained Concrete Compressive Members. Technical Journal, 3(ICACEE), 20-29.
[10] Ghani, M. U., Ahmad, N., Abraha, K. G., Manj, R. Z. A., Sharif, M. H., & Wei, L. (2024). Review and Assessment of Material, Method, and Predictive Modeling for Fiber-Reinforced Polymer (FRP) Partially Confined Concrete Columns. Polymers, 16(10), 1367.

ENHANCING STRUCTURAL INTEGRITY AND RESILIENCE: A SYSTEMATIC APPROACH FOR RETROFITTING DESIGN OF A TWO-STORY HOSPITAL BUILDING IN KARACHI

[a] Hassan Tahir*, [b] Muhammad Numan

a: Structure Engineering Department, Designmen Consulting Engineers, Islamabad, Pakistan. hassantahir275@gmail.com
b: Infrastructure Engineering Department, Designmen Consulting Engineers, Islamabad, Pakistan. engr.numans@gmail.com
* Corresponding author.

Abstract- This paper presents a case study on the structural assessment and retrofitting design of a two-story hospital building in Karachi, Pakistan, constructed in 1992. To overcome this, a systematic approach was adopted, involving site visits, data gathering, the creation of as-built drawings, and detailed analysis and design using ETABS software. The assessment revealed vulnerabilities in the existing structure, particularly in the columns, which necessitated retrofitting measures. The retrofitting design included the incorporation of shear walls and the increase in column and beam sizes to enhance the building's seismic resilience. The successful completion of this project underscores the importance of a systematic approach in ensuring the structural integrity and resilience of existing buildings, especially in earthquake-prone regions. By prioritizing the preservation of human life and the enhancement of building safety, this study contributes to a more resilient built environment.

Keywords- Seismic Resilience, Structural Assessment, Retrofitting Design, Non-Destructive Testing.

1 Introduction

The devastating earthquake that struck the Northern region of Pakistan in 2005, commonly known as the Kashmir Earthquake [1], brought about significant destruction and loss of life. This natural disaster not only impacted the effective areas but also highlighted the need for a structured assessment and retrofitting of existing buildings to ensure their resilience against future earthquake events [2].

The impact of the earthquake on the existing buildings was catastrophic. Many structures including hospitals suffered expensive damage or collapsed entirely the lack of proper seismic design and retrofitting measures in these buildings exacerbated the destruction and resulted in the loss of critical healthcare facilities when they were needed the most.

In light of this, the present paper focuses on a case study involving a two-story hospital building in Karachi, constructed in 1992. The hospital has a ground floor and two upper floors, with existing column sizes measuring 6 in x 18 in and beam sizes measuring 6 in x 27 in. The scope of the project includes creating as-built drawings, making architectural notifications as requested by the client, conducting a retrofitting design of the structure, and outlining the methodology for implementing the retrofitting measures.

2 Research Methodology

The structural assessment and retrofitting design of the two-story hospital building involved a systematic approach to ensure successful project execution. A site visit was conducted to gather the necessary site data and details for creating accurate as-built drawings. This involved documenting the existing conditions of the building, including its architecture and structural elements. The Ferro Scanning test was conducted to identify the existing steel in the existing structural elements. Using the gathered data, as-built architecture and structure drawings were created in Revit [3]. These drawings served as a baseline for the retrofitting design process.

The model was analyzed and designed in the Etabs software using the ELF procedure. This analysis considered seismic forces and other relevant loadings to ensure the retrofitting design could withstand potential earthquakes. Based on the analysis and design outputs, final structure drawings and details were prepared. A comprehensive methodology report was prepared to outline the execution of the project.

3 Case Study

This case study revolves around the hospital in Karachi, established in 1992, according to the building code of Pakistan (BCP-2007), the Karachi region lies under the seismic zone 2B [4]. The structural system of the building is comprised of a Reinforced Concrete frame system (RCC column beam framing). Hollow block masonry has been used for infill wall panels along with seismic stiffeners.

3.1 Site Visit and Data Gathering

To assess the building's integrity, a team of senior structural engineers and architects carried out a visual inspection of the existing building. A conditional survey by visual inspection was based on ACI 201.1R-08 which serves as a Guide for Conducting a Visual Inspection of Concrete in Service and ACI 364.IR-07 which is used for the guide of evaluation of concrete structures before rehabilitation [5, 6]. In Figure 1, on-site investigations and measurements of visible cracks have been found at the slab (Figure 1a) and existing beam (Figure 1b), the cracks observed are due to a combination of factors, including the seismic activity and the overloading. [9].

a)

b)

Figure 1: Observed structural cracks, a. Existing roof slab, b. Existing concrete beam.

3.2 Creation of As-Built Drawings

One of the main challenges encountered was the absence of original construction drawings. To address this, a team of architects was engaged to create as-built architectural drawings of the building. For the preparation of structural drawings with exact steel reinforcement in the existing concrete elements, a ferro scanning test was conducted by professionals. The objective of the test is to determine the diameter of the steel bars, concrete cover, and spacing between the bars in beams, columns, and slabs. The equipment used consists of a rebar detection system named Profometer made by Proceq SA, Switzerland. For rebar detection, the profilometer was slid over the surface of the existing structural elements. The provided beams are of size 6 in x 30 in and flexural cracks were observed in the beams. Columns size consists of 8 in x 18 in with minor torsional cracks were observed.

3.3 Structural Analysis and Design

An analytical model of the existing building was developed within ETABS software, incorporating the two additional stories and precise steel reinforcement details obtained from the ferro-scanning report. This model was subjected to the existing loads and boundary conditions to assess its structural integrity. While the model demonstrated adequate performance under existing loads, the introduction of proposed additional stories and their corresponding loads revealed signs of failure in specific structural elements. Notably, the columns exhibited a demand-to-capacity ratio exceeding acceptable limits, necessitating immediate attention in the retrofitting design process. To address this, an iterative design

process was employed to incrementally increase the column and beam sizes until the building successfully passed all post-analysis checks including drift and torsional building checks.

Table 1: Drift limits before retrofitting

Storey Level	Storey Elevation (ft)	R	Δ_sEx (in)	Δ_sEy (in)	Δ_mEx (in)	Δ_mEy (in)	Storey Drift % Ex	Storey Drift % Ey
4	36	5.5	1.99211	1.481328	7.6696	5.7031	1.46	1.23
3	25	5.5	1.490297	1.061036	5.7376	4.0850	2.16	1.60
2	14	5.5	0.750679	0.513921	2.8901	1.9786	2.06	1.41
1	3	5.5	0.044387	0.030012	0.1709	0.1155	0.47	0.32

The initial structural analysis revealed that the maximum average drift in the x and y directions exceeded the allowable limit of 2%, reaching 2.16% and 1.60%, respectively as shown in Table 1, with a fundamental time period of 1.001 seconds.

Table 2: Drift limits after retrofitting

Storey Level	Storey Elevation (ft)	R	Δ_sEx (in)	Δ_sEy (in)	Δ_mEx (in)	Δ_mEy (in)	Storey Drift % Ex	Storey Drift % Ey
4	36	5.5	0.604753	0.385042	2.3283	1.4824	0.59	0.40
3	25	5.5	0.40392	0.249321	1.5551	0.9599	0.64	0.41
2	14	5.5	0.18294	0.108501	0.7043	0.4177	0.50	0.29
1	3	5.5	0.01044	0.00789	0.0402	0.0304	0.11	0.08

The implementation of retrofitting measures, including the addition of shear walls, effectively reduced the building's drift limits to 0.64% and 0.41% in the x and y directions, respectively as shown in Table 2. This reduction, coupled with a decreased time period of 0.441 seconds, indicates a substantial improvement in the building's seismic performance. The analysis and design process adhered to the guidelines outlined in the Building Code of Pakistan (BCP-2007), with an importance factor of 1.25 assigned to the hospital building.

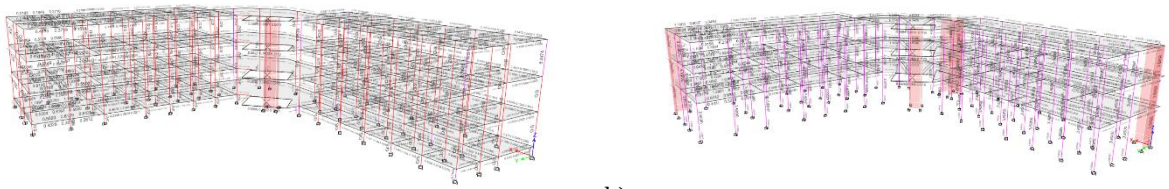

a) b)

Figure 2: Structural analysis and design in etabs, a. O/S sections before retrofitting, b. Pass sections after retrofitting

After the final analysis and design (Figure 2a), we determined the new column and beam sizes 15 in x 18 in and 12 in x 33 in as shown in Table 3. To control the drift, we considered the inclusion of 9 in-thick shear walls.

Table 3: Member sizes

Sr. No	Members	Existing Sizes before Retrofitting (in)	New Sizes after Retrofitting (in)
1	Slab	6	6
2	Beam	6 x 30	12 x 33
3	Column	8 x 18	15 x 18
4	Shear walls	Not provided	9

M/s strips were employed as a substitute for conventional stirrups. M/s strips, also known as steel straps or flat bars, are thin, flat steel elements used to confine concrete and enhance its ductility and shear strength [9]. In this context, they were strategically placed within the column and beam reinforcement to improve the stability of the columns to withstand lateral loads and seismic forces as shown in Figure 3. This choice was likely made due to the ease of installation and the potential for M/s strips to provide a more uniform distribution of confinement compared to traditional stirrups.

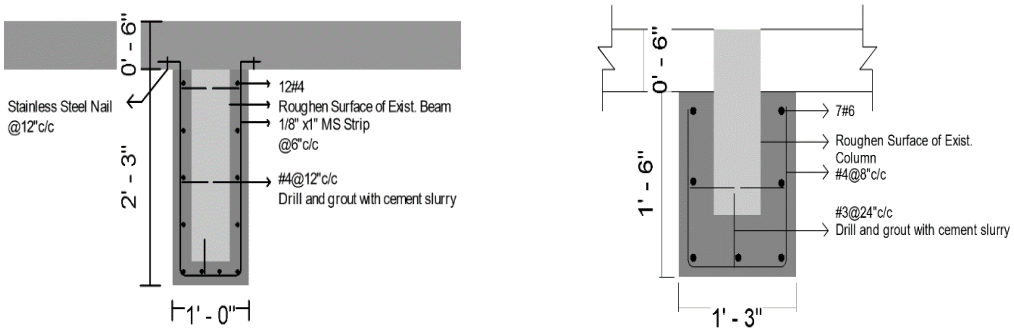

a) b)

Figure 3: Retrofitting details, a. Retrofitting detail of beam, b. Retrofitting detail of column

4 Conclusion

This case study underscores the importance of a systematic approach to structural assessment and retrofitting, particularly in the absence of original construction drawings. By utilizing a combination of site visits, data collection, the creation of as-built drawings, and advanced analysis and design tools, the structural integrity and resilience of existing buildings can be significantly enhanced. This approach not only ensures the safety of occupants but also contributes to a more resilient built environment in regions prone to seismic activity.

References

[1] T. Rossetto and N. Peiris, "Observations of damage due to the Kashmir earthquake of October 8, 2005 and study of current seismic provisions for buildings in Pakistan," Bulletin of Earthquake Engineering, vol. 7, no. 3, pp. 681–699, May 2009, doi: 10.1007/s10518-009-9118-5

[2] "Pakistan 2005 earthquake: Preliminary damage and needs assessment - Pakistan," ReliefWeb, Nov. 12, 2005.

[3] ASCE, "As-Built Documentation of Structural Components for Reinforced Concrete Construction Quality Control with 3D Laser Scanning," Computing in Civil Engineering (2012), doi: 10.1061/9780784412343.003.

[4] PEC"Buidling Code of Pakistan - Secismic Provisions" Pakistan Engineering Council - PEC, "Building Code of Pakistan,2007.

[5] "ACI 201.1R-08 Guide for conducting a Visual Inspection of concrete in service,".

[6] "ACI 364. 1R-07 Guide for Assessment of Concrete Structures before Rehabilitation".

[7] J. M. Bracci, S. K. Kunnath, and A. M. Reinhorn, "Seismic performance and retrofit evaluation of reinforced concrete structures," Journal of Structural Engineering, vol. 123, no. 1, pp. 3–10, Jan. 1997, doi: 10.1061/(asce)0733-9445(1997)123:1(3.

[8] "Vijayakumar, D.L. (2012) Pushover Analysis of existing reinforced concrete framed structures. European Journal of Scientific Research, 71, 195-202. - References - Scientific Research Publishing." https://www.scirp.org/reference/referencespapers?referenceid=1477367

[9] N. H. F. A. Halim, S. C. Alih, and M. Vafaei, "Efficiency of CFRP strips as a substitute for carbon steel stirrups in RC columns," Materials and Structures, vol. 53, no. 5, Oct. 2020, doi: 10.1617/s11527-020-01566-w.

A REVIEW ON FIRE DAMAGE ASSESSMENT OF REINFORCED CONCRETE STRUCTURES OF A BUILDING

[a] Ghazanfar Ali Anwar*, [b] Yousef Khan

a: Centre for Advances in Reliability and Safety, Hong Kong Science Park, Hong Kong. ghazanfar.an@gmail.com
b: Muhammad Saleem and Engineering Company, Islamabad, Pakistan. yousakhanenge2139@gmail.com
* Corresponding author.

Abstract- Performance-based engineering methods have been recently developed for fire hazards providing enhanced prediction of the structural response and subsequent damage and loss assessments. In this context, this paper presents an overview of the fire damage and loss assessment of reinforced concrete structures under fire hazards by utilizing performance-based assessment methodologies. Hence, fire hazard models and the stages of fire initiation, propagation, and decay are discussed. Then, a six-step methodology is formulated comprising hazard modeling, structural modeling, performance modeling, collapse fragility assessment, building response assessment, and loss assessment. Finally, the methodology is illustrated by utilizing a four-story building model built in the OpenSEES framework.

Keywords- Buildings, Damage, Fire-Hazard, Performance-Based, Reinforced-Concrete.

1 Introduction

Fire hazard-related accidents can significantly damage the structure and could result in catastrophic failure due to extreme heat that could result in structural and material degradation [1]. The building structures could experience a fire hazard during the service life of a structure and hence it is crucial to understand the fire behaviors during an event of a fire hazard. The fire hazard may significantly enhance the degradation process of the structures and could result in socioeconomic and environmental consequences increasing the risk of the built environment [2].

Performance-based methods could be utilized to assess the structural response to the fire hazard and subsequently assess the damage to the buildings. The damage assessment requires fire hazard modeling and structural modeling to determine the engineering demand parameters including drifts, and deformations, among others resulting from the additional loads due to fire hazards. Furthermore, fire hazard scenarios also reduce the structural strength of the building that also needs to be addressed. The structural analysis of the structure given fire hazard scenarios can then be correlated with the damage to the building by utilizing fragility functions that are lognormal cumulative distribution functions providing the probability of damage to the building structure given fire hazard scenario [3]. The fragility functions are represented for different damage states including slight, moderate, extensive, and complete damage states. Also, fragility functions can be developed for collapse state or irreparable states to assess the repair, maintenance, or demolition conditions in the post-hazard conditions [4].

Concrete is a relatively durable material that can comparatively perform well under fire scenarios due to several reasons including its low thermal conductivity and relative incombustibility as compared to other structural materials such as timber, wood, and steel, among others. Furthermore, reinforced concrete structures that are designed according to the recent building design codes and according to the required construction quality with adequate reinforcement steel can reasonably perform well in the event of a fire by redistributing the loads from the damaged part of the structure to the relatively undamaged part of the structure due to reinforcement yielding and stiffness degradation of the structural members [5].

Subsequently, the probability of complete collapse of the reinforced concrete structures is relatively minimized. Nonetheless, reinforced concrete structures still could witness severe damage that may significantly affect the functionality of the structure and often require subsequent rehabilitation or repair. Post-hazard repair may be economically viable as compared to demolition of structures and building new construction. Furthermore, socioeconomic and environmental consequences resulting from new construction are significantly higher as compared to repair of the structure. Also, considering the economic constraints of developing countries, repair and rehabilitation of reinforced concrete structures in the post-hazard condition is often seen as a viable approach. Nonetheless, before making these decisions, a comprehensive assessment of the structures under fire hazard scenarios needs to be considered [6].

In this context, this paper presents the overview of the performance-based assessment approach to assess the structural response of reinforced concrete buildings under fire hazards and subsequent repair and rehabilitation strategies that could be utilized depending upon the level of damage to the building. The framework is provided by utilizing a four-story building under a fire hazard scenario. The subsequent section discusses the performance-based assessment methodology for fire hazard scenarios to assess the damage to reinforced concrete buildings.

2 Performance-Based Methodology For Fire Hazard

The performance-based methodology originally proposed for the seismic hazard scenarios to assess the structural response, damage to the buildings, and subsequent socioeconomic and environmental consequences can be utilized to assess the fire hazard scenarios with modifications. Conventionally, performance-based methodology requires steps including hazard assessment, structural analysis, damage assessment, and consequence assessment. Herein, we propose a performance-based assessment framework for fire hazard assessment that consists of six steps as shown in Figure 1. The first step includes fire hazard modeling which is the crucial step in the performance-based methodology. Then, a structural model is built to assess the structural response given the fire hazard scenario. Also, building performance models are developed for considered structural and non-structural components of a building to assess the damage states for all the components given the fire hazard. The collapse fragility is utilized to determine and probability of collapse of a structure and structural response is utilized to determine engineering demand parameters given fire hazard and structural model. Finally, component damage, repair costs, and total costs of damage can be determined in the loss assessment step. A detailed discussion of the individual steps can be seen in the study conducted in.

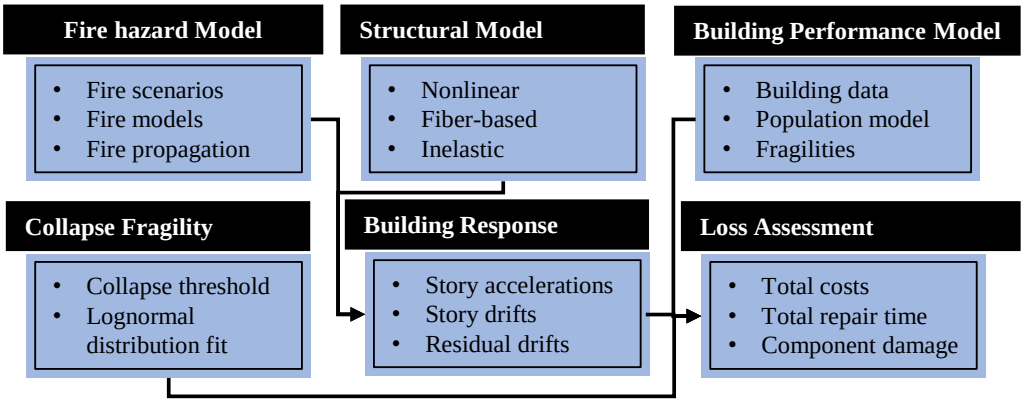

Figure 1: Performance-based assessment methodology for damage and loss assessment given fire hazard scenarios

3 Fire Hazard Modelling

The fire models vary from considering just a fully developed fire assuming that structural fire resistance of structures under fire only depends on the post-flashover fire. Nonetheless, recent models have been developed that considered localized and traveling fire scenarios that are in the initial stages, spreading stages, or the pre-flashover phase. However, most of the data gathered related to the stages is based on empirical and experimental evidence. Subsequent analytical formulations developed are also based on the empirical evidence gathered from the real-life fire hazard scenarios observed during and after a fire hazard event. There has been a recent trend to realistically model the fire hazard scenarios to accurately predict the structural analysis and damage under fire events. Realistically representing fire hazard load requires some key issues

to be resolved including defining the boundary conditions for the heat transfer of fire load, and accurately modeling the temperature differences around the structural components, fire durations, and geometry of burning conditions, among others [7]. The most important parameter to determine the structural damage of the buildings under fire hazard is the fuel load. The fuel load can be regarded as the structural load that can be utilized to determine the structural response by utilizing performance-based assessment methodologies. The fire hazard can be divided into several stages including pre-flashover and post-flashover as shown in Table 1.

Table 1: Fire stages for the fire hazard in a compartment

Investigated time	Pre-Flashover	Post-Flashover
First part	Initiation	Fully developed
Second part	Growth	Decay

The pre-flashover fire stages include the initiation stage and the growth stage as shown in Figure 2. After the growth phase, a flashover threshold is reached when the fire gets fully developed and enters a post-flashover stage where it remains fully developed for a given time and then starts to decay. Various fire hazard models exist that could be utilized in performance-based engineering for structural fires including zone models, traveling fire models e.g., Clifton's model and Rein's model, ETFM model, among others [8]. For instance, traveling fire models representing near and far field developed by the Reins model is shown in Figure 3.

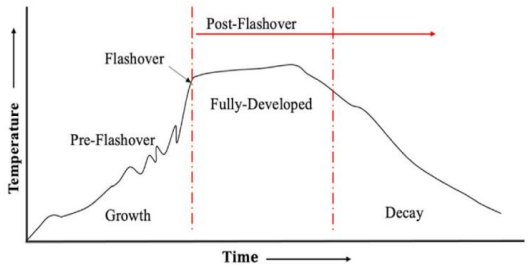

Figure 2: Fire stages for the fire hazard in a compartment

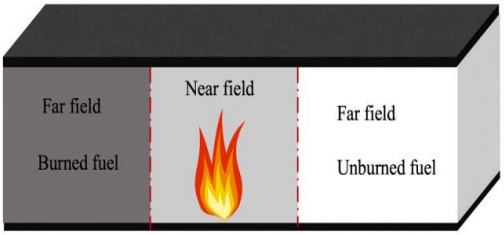

Figure 3: Travelling fire representing the near and far field [7]

4 Loss Assessment

The finite element structural models are required to assess the structural response of reinforced concrete structures under fire hazards. For that purpose, nonlinear structural models could be built that are capable of modeling the post-yield behavior of structures. In this context, an OpenSEES model is built that is capable of assessing the nonlinear structural response of the considered structure. The model is utilized to determine engineering demand parameters that can then be correlated to assess the structural damage. For instance, structural response a four-story building model under increasing fire hazard can be seen illustratively in Figure 4.

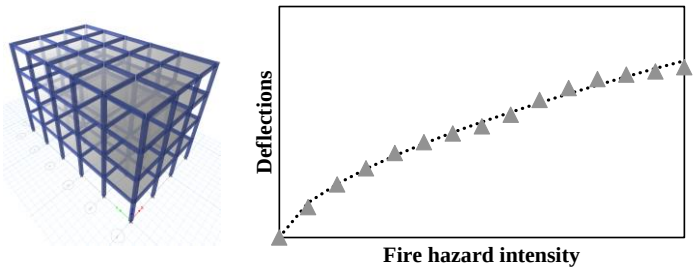

Figure 4: Structural response in terms of story deflections under increasing fire hazard

The structural fire response of a building by utilizing the finite element models can then be utilized to assess the structural damage of the building by utilizing fragility functions that can provide the probability of a damage state given the fire load intensity [9]. This information can be utilized to assess the losses resulting from the considered fire hazard scenario and for the subsequent repair and rehabilitation works. An illustrative representation of the fragility function and loss assessment given the fire hazard is shown in Figure 5.

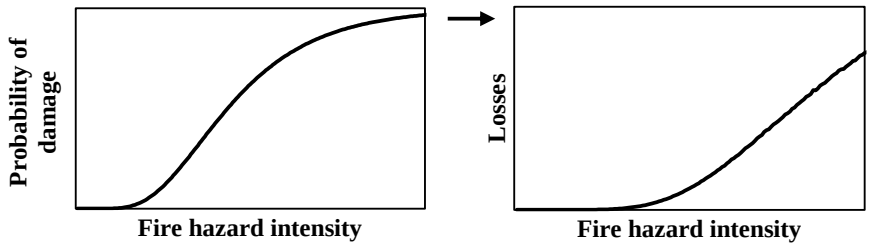

Figure 5: Structural response in terms of story deflections under increasing fire hazard

5 Conclusion

This paper provides an overview of fire damage assessment of reinforced concrete buildings under fire hazard by considering performance-based methods. In this context, a performance-based approach is formulated that consists of six steps including fire hazard modeling, structural modeling, building performance model, collapse assessment, building response assessment, and loss assessment. Subsequently, fire hazard modeling of the performance-based assessment methodology and discusses various stages of the fire and different fire hazard models utilized in the performance-based assessment methodology. Finally, the loss assessment part is discussed by utilizing a four-story reinforced concrete building as an illustrative example.

Acknowledgment

The work presented in this article is supported by Centre for Advances in Reliability and Safety (CAiRS) admitted under AiR@InnoHK Research Cluster.

References

[1] M. A. Khan, A. A. Khan, R. Domada, and A. Usmani, "Fire hazard assessment, performance evaluation, and fire resistance enhancement of bridges," in *Structures*, 2021, vol. 34, pp. 4704-4714: Elsevier.

[2] G. A. Anwar, "Life-cycle performance enhancement of deteriorating buildings under recurrent seismic hazards," *Soil Dynamics and Earthquake Engineering*, vol. 180, p. 108600, 2024.

[3] Z. Zhou, G. A. Anwar, and Y. Dong, "Performance-Based Bi-Objective Retrofit Optimization of Building Portfolios Considering Uncertainties and Environmental Impacts," *Buildings*, vol. 12, no. 1, p. 85, 2022.

[4] Y. Zheng, Y. Dong, B. Che, and G. A. Anwar, "Seismic damage mitigation of bridges with self-adaptive SMA-cable-based bearings," *Smart Structures and Systems, An International Journal*, vol. 24, no. 1, pp. 127-139, 2019.

[5] A. Franchini, C. Galasso, and J. L. Torero, "Consequence-oriented fire intensity optimization for structural design under uncertainty," *Journal of Structural Engineering*, vol. 150, no. 4, p. 04024020, 2024.

[6] M. Roohi, S. Farahani, A. Shojaeian, and B. Behnam, "Seismic Multi-Hazard Risk and Resilience Modeling of Networked Infrastructure Systems," in *Automation in Construction toward Resilience*: CRC Press, 2024, pp. 389-406.

[7] A. A. Khan, A. Usmani, and J. L. Torero, "Evolution of fire models for estimating structural fire-resistance," *Fire safety journal*, vol. 124, p. 103367, 2021.

[8] D. Chen, L. Chen, Y. Zhang, S. Lin, M. Ye, and S. Sølvsten, "Automated fire risk assessment and mitigation in building blueprints using computer vision and deep generative models," *Advanced Engineering Informatics*, vol. 62, p. 102614, 2024.

[9] G. A. Anwar, Y. Dong, and Y. Li, "Performance-based decision-making of buildings under seismic hazard considering long-term loss, sustainability, and resilience," *Structure and Infrastructure Engineering*, vol. 17, no. 4, pp. 454-470, 2020.

BRIDGE BEARINGS REPLACEMENT CHALLENGES – A REVIEW

[a] Mustafa Zwain, [b]Furqan Qamar*

a: Graduate Engineer, WSP UK, mustafa.moussa@wsp.com
b: Associate Director, WSP UK, furqan.qamar@wsp.com
* Corresponding author.

Abstract **-** Bearings are a critical element of bridge structures and play a key role in the distribution of loads from superstructure to substructure. Bearings are of various types and installed in bridge structures based on articulation requirements. Depending on the type of bearing, there is a variation in service life. Bearings also require different types of maintenance work ranging from routine cleaning and greasing to full replacement. This paper focus is based on major maintenance works i.e. full replacement of bearings during their design life. The replacement of bearings poses various design and construction challenges which are highlighted in this paper. Various solutions, which have been implemented in numerous past schemes, are proposed to overcome these design and construction challenges. These solutions provide insight to the reader to overcome these challenges in their schemes at preliminary design stages and can help in the preparation of efficient and economical design.

Keywords **-** Bearings, Design Challenges, Construction Challenges, Jacking, Replacement.

1. Introduction

Bearings are critical components of a bridge. They transfer loads between the superstructure and substructure while maintaining the articulation of the bridge. Different types of loading act on bridges which include self-weight (dead load), superimposed, traffic, wind and temperature. These loads create translation and rotational movements which bridge bearings need to accommodate during service life. Bearings are of many types depending on material and fixity [1, 2]. These can be elastomeric (*Figure 1a*), roller (*Figure 1b*), pot (*Figure 1c*), knuckle (*Figure 1d*), leaf (*Figure 1e*), guided and plane sliding (*Figure 1f*). An elastomeric bearing comprises a block of elastomer that may be reinforced internally with steel plates or may be unreinforced [3]. A roller bearing consists essentially of one or more steel rollers between parallel upper and lower steel plates. Pot bearings consist of a metal piston supported by a disc of unreinforced elastomer that is confined within a metal cylinder. Knuckle bearings comprise of two or more members with curved surfaces and allow rotation by sliding one part on another. Leaf bearings have a pin passing through plates fixed alternately to the upper and lower bearing plates. Guided bearings provide restraint in only one horizontal direction and plane sliding bearings only provide translation.

According to British Standards BS 5400 Part 1 [4] and Part 9 [5], bearings are required to be designed for 120 years. During this period bearings should be maintained and serviced as per manufacturer requirements. Bearings can be maintained through routine or minor maintenance prior to full refurbishment and replacement. Routine or minor maintenance includes cleaning or re-greasing of bearings and patch re-painting. Niemierko produced a paper on "Modern bridge bearings and expansion joints for road bridges" [6] however the focus was on the bearing components themselves rather than on the design and construction challenges of bearings. Three bridges were studied by Van Lund [7] with various construction challenges discussed, however, design challenges were not considered. Furthermore, the paper was published in 1995 with some of the bridges studied being nearly 100 years old. The purpose of this paper is to discuss present design and on-site challenges related to the replacement of bearings and conclude solutions to overcome these challenges. These solutions will provide insight to the reader to deal with challenges for their future schemes.

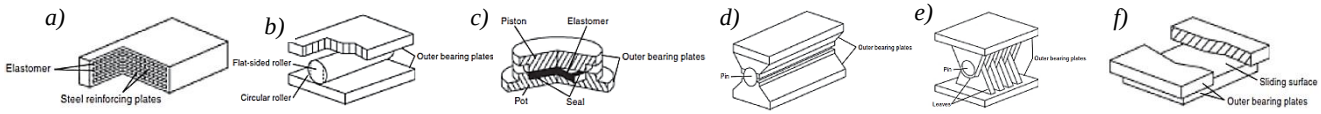

Figure 1: a) elastomeric bearing, b) roller bearing, c) pot bearing, d) knuckle bearing, e) leaf bearing, f) plane sliding bearing

2. Procedural Steps for Bridge Bearing Replacement

The design process for bridge bearings replacement has the following main activities: determination of the articulation and condition of the existing bearings, modelling of the bridge deck to confirm the loading on the bearings, development of a bearing schedule, modelling of jacking arrangements, production of a jacking schedule and temporary works design to undertake the bearing replacement work.

The process begins with a comprehensive preliminary assessment. This involves gathering information about the existing bearings from as-built design drawings as well as from inspection and maintenance reports. On-site surveying of the existing bearings should be undertaken to identify signs of deterioration or damage. Furthermore, surveying is necessary to understand precisely which bearings are in need of a replacement. It is possible that only a particular group of bearings need replacement i.e. the free bearings or mechanical bearing with PTFE. After determining which bearings need to be replaced, finite element analysis (FEA) modelling is undertaken to find the loading applied on bearings from the bridge deck. The model encompasses all the structural constituents of the deck (e.g. main beams, deck slab, parapet beams…) including the geometry and material properties. Furthermore, the modelling includes the various types of loading subject to the bearings such as deck dead, superimposed and live loads. These are calculated using relevant design standards. Finally, the model loading outputs are to be combined in accordance with design standards.

A bearing schedule, which is a detailed document that outlines the specifications and requirements for bridge bearings, is produced. Standard bearing schedule layout can be found in BS 5400 Part 9 [5] but this standard has been withdrawn in 2010 and since replaced with BS EN 1337 Part 1 [8]. The bearing schedule includes information such as the type of bearings required, their dimensions, the load capacities of the bearings from modelling analysis, material compositions of the bearing seating faces as well as specific installation requirements e.g. type of fixing. The overarching purpose of the bearing schedule is to provide information for the design of new bearings. In order for the bearings to replaced, the bridge deck must be jacked. A jacking arrangement is tested using FEA modelling software such as LUSAS [9] or MIDAS Civil [10] to simulate the loading experienced by the hydraulic jacks to ensure they can withstand the forces and stresses encountered during the jacking process. Furthermore, by modelling the jacking arrangement the stresses experienced by various bridge components (e.g. diaphragm or main beams) can be studied to ensure that they are within acceptable limits.

3. Discussions

3.1 Design Challenges

There are various design challenges with the replacement of bridge bearings. Unknown concrete strength is a significant challenge. Replacing bearings involves jacking entire bridge sections. It is particularly important to know the strength of the section being lifted by the jack e.g. the diaphragm. Design calculations are undertaken to ensure that the concrete section being lifted by a jack can handle the stress from lifting. Suitably sized jacking plates are selected to avoid concrete crushing from excessive stress. If the concrete strength is unknown, it may be necessary to sanction concrete testing of the affected sections. Otherwise, the designer would need to plan for the worst-case scenario (very low strength). This would present additional challenges with finding a jacking and temporary works design that would pass all the design checks.

Figure 2: Hydraulic jack placed on column with limited space

The age of bridge structure is a design challenge. Older bridges were designed using design codes that have since been withdrawn and replaced with newer standards. It is normally the case that new design standards have more strict requirements. In the case where there is a contractual obligation to satisfy the current design standards, there can be various challenges in finding an acceptable solution for bearing replacement. An example is where new design standards define that the deck main beams have a lower loading capacity than what was calculated in the original design. This could cause difficulty in selecting a temporary works design that does not cause the main beams to exceed their new, lower loading capacity.

Another challenge is the limitation of space for the placement of hydraulic jacks. To undertake a bearing replacement scheme, jacks of specific type and size must be placed in positions according to the temporary works design. However, due to poor bridge design, it can be very challenging to find a suitable position for the jacks. For example, the height between the bearing plinth and the bridge deck beam may be too small to fit a suitable jack. It is observable in ***Figure 2*** that there is a limit in available height so only a small jack could be safely placed on the column. Furthermore, it can be seen that there is no space for placing a second jack on this column. There are solutions for these types of limitations such as constructing a temporary shoring tower on which to place jacks, however, the solutions are far more expensive than the conventional method of placing jacks on the existing bridge substructure.

3.2 Construction Challenges

There are various construction challenges that can be faced as shown in *Table 1*. A major construction challenge is when it is discovered on site that the bridge is not as per as built drawings. For example, it is discovered that the spacing between bearings is less than previously known. This may require a change to the jacking arrangement and therefore a new design for temporary works. There may be a delay of weeks for the designer to check and approve an alternative jacking arrangement. Not only would there be a time delay, but there would also be a significant cost to cancel and reschedule equipment, personnel and road closures that were reserved for a particular time to undertake the bridge bearing replacement.

Table 1: Key construction challenges and solution

Construction Challenges	**Potential Solution 1**	**Potential Solution 2**
Services/STATs within the work area	Undertake calculations to check if services can allow displacement from jacking	Liaise with the service provider to find a solution e.g. temporarily shutting down the service
Inaccurate information from as-built drawings	Undertake on-site survey	Check if there is enough design tolerance to proceed
Difficulty with removing fixed bearing	Hydro-demolition around the old fixed bearing followed by restoration of the structural member	Implementation of other demolition methods such as drilling and cutting
Traffic Management	Ensure that there are satisfactory lane closures	Ensure that the traffic diversion route is satisfactory
Inadequate Space for equipment to allow breakout of concrete	Acquiring and using more compact equipment	Consider alternative demolition methods

Before undertaking bridge bearing replacement, it is vital to identify and coordinate with the owners of services that may be located near or within the bridge structure. This coordination ensures that services are properly protected. If necessary, services may need to be relocated or temporarily shut down during construction work. If there is a service line that was not accurately identified, there is a risk of damage to that service. Not only can this cause disruption to the service, costly repairs, and financial penalties, it may present a major safety challenge. For example, if the unidentified service was a gas pipe and it was broken during the jacking of the bridge, it would leak gas and possibly cause an explosion. If the service was identified on site just as construction work was getting started, there may be a delay to the project to agree with the service owner whether the service would need to be temporarily shut down or relocated.

Bearings with fixity can present additional challenges that free bearings are not affected by. It is often the case that fixed bearings are bolted in the bridge abutment or beam. There may be a range of issues with removing fixed bearings. The bolts may have corroded or deteriorated over time making them difficult to remove. There may be restrictions related to

access, such as limited space, making it challenging for the contractor to use the required equipment for disassembly. It is often the case that the contractor must remove the concrete around the bearing bolts to remove the old bearing. This presents further challenges associated with maintaining the bridge's structural integrity during the bearing replacement work as well as with ensuring that the damaged bridge structural component is refurbished to an acceptable condition.

There are challenges associated with providing temporary fixity or additional restraint to a bridge during bearing replacement work. There is the potential for damage if fixity or restraint systems are improperly installed. This may cause issues, such as overstressing bridge components and causing damage to concrete. These issues can threaten the structural integrity of the bridge. The contractor must ensure that restraint systems are installed correctly and in the case of causing damage to the bridge, there must be liaison with the designer before continuation of works to ensure that necessary repairs are undertaken so that the bearing replacement work is carried out safely.

If a bridge is to have bearings replaced at various abutment or pier locations, then it is necessary to follow a precise plan for the various stages of bearing replacement. It is a construction challenge to successfully coordinate the activities across multiple stages of bearing replacement work while minimising disruption and ensuring there are no delays. This requires effective communication with the various project stakeholders including the designer, principal contractor, sub-contractors and transportation authorities. Furthermore, bearing replacement projects often require lane closures to ensure the safety of workers and bridge users. Managing traffic flow during these closures is challenging and requires effective planning, particularly in heavily travelled routes or where alternative routes are limited.

4. Conclusions

The design and replacement of bridge bearings involves careful consideration of multiple factors to ensure successful implementation. ***Section 2*** of this paper provides a structured approach to the design process behind the replacement of bridge bearings. Various challenges faced in bearing replacement projects were discussed, such as unknown concrete strength, bridges designed under old design codes and access limitations for placing hydraulic jacks. These challenges require innovative solutions and often necessitate additional testing and conservative design assumptions. Furthermore, construction challenges, including discrepancies between site conditions and as-built drawings, the presence of utility services, and the necessity of maintaining bridge structural integrity during bearing removal and replacement, demand thorough planning and effective communication among various stakeholders. Overcoming these challenges is crucial for the successful and safe replacement of bridge bearings, ensuring an extended lifespan and satisfactory performance of bridge structures. Awareness of these challenges can lead to efficient and economical design.

Reference

[1] Kennedy Reid I. L., Milne D. M. and Craig R. E. Steel Bridge Strengthening. On behalf of Highways Agency and WS Atkins. Thomas Telford, London, 2001.
[2] Lee D. J. Bridge Bearings and Expansion Joints, 2nd edn. E& FN Spon, London, 1994.
[3] Ramberger G. Structural Bearings and Expansion Joints for Bridges. Structural Engineering Documents 6. International Association for Bridge and Structural Engineering (IABSE- AIPC-IVBH ETH Ho¨nggerberg), 2002.
[4] BS 5400-1:1988 Steel, concrete and composite bridges — Part 1: General statement
[5] BS 5400-9:1983 - Steel, concrete and composite bridges - Code of practice for the design of prestressed concrete bridge
[6] A. Niemierko "Modern bridge bearings and expansion joints for road bridges", *Transportation research procedia*, vol. 14, pp. 4040-4049, 2016
[7] Van Lund JA "Bridge bearing replacement", *InProc., 4th Int. Bridge Engineering Conf. Washington, DC: National Academy Press*, 1995
[8] BS EN 1337-1:2018 - Structural bearings - Part 1: General requirements.
[9] LUSAS Engineering analysis + design software [Online], Available: https://www.lusas.com/. [Accessed May 31, 2024]
[10] MIDAS Civil [Online], Available: https://www.midasoft.com/bridge-library/civil/products/midascivil. [Accessed May 31, 2024]

DESIGN AND ANALYSIS OF GREEN HIGH-RISE BUILDING USING RECYCLED MATERIALS

[a] Muhammad Bilal Subhani*, [b] Minahal Azad

a: Department of Civil Engineering, Mirpur University of Science and Technology, Mirpur, Pakistan. mbilalsubhani@gmail.com
b: Department of Civil Engineering, Mirpur University of Science and Technology, Mirpur, Pakistan. minahalazad121@gmail.com
* Corresponding author.

Abstract- This project deals with the design and analysis of high-rise building by using eco-friendly building materials. The locally developed building materials from recycled waste were used as concrete and bricks. A ten-story high-rise building was designed using the software ETABS. The concrete comprised of 10% partial replacement of cement by red brick powder (RBP) and the bricks contained 25% mass of clay replaced by the RBP. These materials were cast and their properties were determined as per ASTM standards. The characteristics were incorporated in the software and the building was designed and analyzed. The designed building was compared with that containing conventional concrete and bricks. It was found that the design having waste materials resulted in the saving of 160 tons of cement, and 440 cubic meters of fertile clay. This will avoid a Carbon emission of 144 tons to the atmosphere and a significant saving in energy required to manufacture cement. The building containing waste materials is also PKR. 5.67 million less in cost than that containing conventional materials.

Keywords- Green Design, High-rise Buildings, Recycling, Waste, Environmental Impact, Cost.

1 Introduction

In daily construction activities, it is observed that the concrete is made up of three main constituents i.e. cement, sand and aggregates. Cement being the main constituent, significantly affects the environment as well as sustainability. Cement while its production causes severe environmental impacts such as CO_2 emission which causes the global warming, production of cement requires a high temperature around 1400°C which is primarily done by igniting fossil fuels which are also decreasing day by day and its production is causing resource depletion and air pollution (emission of Nitrogen oxides & Sulphur oxides). It is required to reduce these effects to make the construction practices sustainable and reduce the environmental impact of concrete

Red brick powder is a local material and has been used in a variety of ways in the archeological sites of the sub-continent. Locally, it is known as "surkhi" [1], [2]. Arif et al. studied the effect of red brick powder (RBP) as a partial substitute of cement in concrete [3]. The results showed that for the replacement of 10% of cement provided improved mechanical properties and work ability due to its particle shape and size, and improves compressive, flexural, and tensile strengths due to its pozzolanic properties. It also improves the compressive strength and durability of concrete. On the other hand, it causes reduction of carbon and energy consumption in cement production and recycling of construction waste [3]. Riaz et examined the effect of red brick powder on the properties of clayey bricks. The study found that incorporating RBP increased brick porosity, making them suitable for moderate weather resistance and insulation, but decreased unit weight, leading to lighter and more economical structures. Moreover, compressive strength reduced with RBP addition but remained adequate for second-class bricks up to 15% RBP. Flexural strength also remained satisfactory even with 25% RBP. RBP incorporated in the production of clayey bricks saved 25% of fertile clay, leading to environmentally friendly construction [4]. Shah et studied the harnessing of red brick powder as a sustainable cement alternative. The findings revealed that RBP was a viable alternative to cement, enhancing the compressive strength of the concrete, particularly at an optimal dosage of 15%, which resulted in a 9% increase in strength at 28 days compared to the control mix. Moreover,

split tensile strength also saw a 15% improvement with 15% RBP substitution. Overall, incorporating RBP into concrete not only improved its structural integrity but also promoted sustainable waste management and cost efficiency [5].

This work deals with the design and analysis of an RCC high-rise building. In the design, concrete containing 10% RBP as a partial replacement of cement was used. Additionally, the partition walls were made of red bricks, in which 25% fertile clay was replaced by the RBP. The aim was to design a sustainable building based on the materials previously developed in our research group. The benefits of using locally developed materials were assessed by designing an actual RCC structure and comparing it with the conventional building in terms of environmental and cost. This work aims to provide the benefits of a green building in terms of waste reduction and utilization in accordance with the sustainable development goals of UNO [6]. A 10-story building was chosen as a test case. The design and analysis were carried out using ETABS. The benefits of green building are presented in the form of reduction in greenhouse gas emission, the use of natural resources, energy and cost.

2 Research Methodology

2.1 Dimensions of the Proposed Building

The proposed plan for the high-raised building is shown in Figure 1. It has dimensions of 37m x 36.57m with a height of 32m including ground floor. In this design, four shear walls were provided as per recommendations of ASCE 7-17 [7]. One shear wall each was provided along the longer side and two central shear walls were provided in the middle along the shorter side. The building was subjected to dead, live, wind and earthquake as per Universal Building Codes 97 [8].

a) 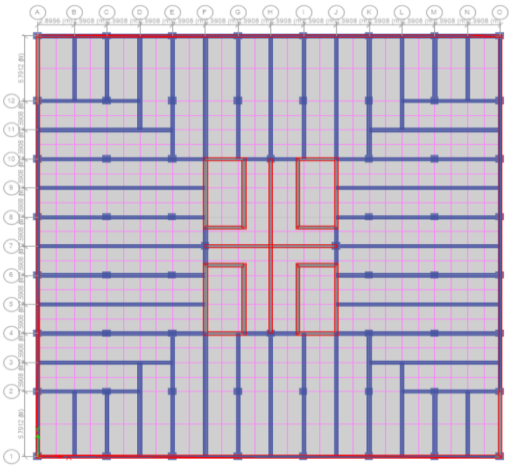 a) 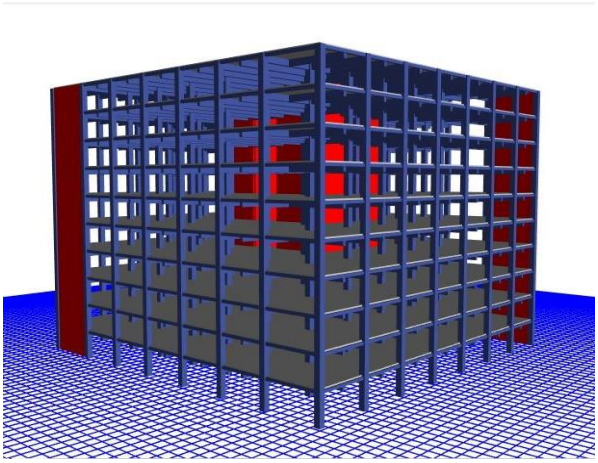

Figure 1: Two- & Three-Dimensional Plan of proposed model

2.2 Analysis and Design

The proposed building was modeled using ETABS, and properties of the materials resulting from past researches were assigned to the components of the building, i.e., slabs, columns, beams, walls, etc. The material properties used in the design are shown in Table 1.

Table 1: Properties of green materials used

Materials	Compressive Strength (MPa)	Density (kg/m^3)	Poisson's Ratio	Modulus of Elasticity (GPa)
Conventional concrete	27.5	2402.8	0.2	24.55
10% RBP in Concrete	30.3	2324.76	0.2	25.871
Conventional brick	9.13	2162	0.2	12.4
25% RBP in Bricks	5.95	1274.65	0.2	11.5

3 Results

After designing the model in ETABS, the dimensions of different components of green building (i.e. slabs, beams, columns and walls) for all stories were obtained and are described in Table 2:

Table 2: Dimensions obtained from design

Components	Width (mm)	Depth (mm)
Slabs	-	175
Beams	300	750
	300	300
Columns	560	560
Shear Walls	300	-
Perimeter Walls	228	-

After analyzing the model, the parameters were checked by the given ACI code (i.e. ACI-318-14) [9] using ETABS. The International Building Code (IBC) (for earthquake as load) specify a maximum story drift of 0.015-0.02 whereas it is 0.00016 & 0.000031 in x and y direction respectively, and a story displacement of 45-60 mm for a story height of 3 m [10] whereas it results in 4.06mm and 4.01mm, respectively. Moreover, the overturning moments was obtained as -540 KN-m, which normally depends on foundation soil conditions. This implies that the given structure is within the safe limits. The comparison of different parameters that are linked with sustainability are given in Table 3:

Table 3: Sustainability Parameters

Parameters	Conventional Building	Green Building	Savings	Cost Effectiveness
Cement (tons)	1088.222	927.924	160.398	4.65154 Million Rupees
Carbon Dioxide (tons) [11]	979.399	835.04	144.358	-
Electricity (kWh)[12]	119704.403	102060.6	17643.803	0.70575 Million Rupees
Clay (m^3)	1761.822	1321.36	440.46	0.308319 Million Rupees
Structure weight (MN)	169.22	142.36	26.86	-
			Total saving in Rs. Million	5.67

The Table 3 indicates that use of eco-friendly materials is a cost-effective sustainable solution: it provides savings in the use of cement, the emission of greenhouse gases, and the energy requirements. Additionally, the use of 25% RBP provides an economy of 440 m^3 of fertile clay. Nevertheless, the structure is also lighter than that consisting of the conventional materials.

4 Conclusions

This work deals with the design of a 10-story RCC building using green materials, developed in the lab. Based upon the simulations, the following conclusions are withdrawn:

1. The designed building provides a saving of 160.39 tons of cement, and 440 m^3 of fertile clay.
2. The saving in cement corresponds to a reduction of 144 tons of CO_2 to the atmosphere, and an energy conservation of 17.64 MWh.
3. The proposed green design assures a cost reduction of 5.67 million PKRs.

4. The building incorporating waste materials is 16% lighter than that containing conventional materials.

References

[1] A. Khitab, R. A. Khan, M. S. Riaz, K. Bashir, S. Tayyab, and R. B. N. Khan, "Utilization of Waste Brick Powder for Manufacturing Green Bricks and Cementitious Materials," in *Ecological and Health Effects of Building Materials*, Cham: Springer International Publishing, 2022, pp. 361–370.

[2] H. Talib, R. B. N. Khan, A. Khitab, O. Benjeddou, and R. A. Khan, "Scanning through multidisciplinary techniques and recreation of historic mortar: Case study of Rohtas Fort," *Case Stud. Constr. Mater.*, vol. 18, p. e02052, Jul. 2023.

[3] R. Arif *et al.*, "Experimental analysis on partial replacement of cement with brick powder in concrete," *Case Stud. Constr. Mater.*, vol. 15, p. e00749, Dec. 2021.

[4] M. H. Riaz, A. Khitab, and S. Ahmed, "Evaluation of sustainable clay bricks incorporating Brick Kiln Dust," *J. Build. Eng.*, vol. 24, p. 100725, Jul. 2019.

[5] S. A. Shah, "Revolutionizing Construction - Harnessing the Power of Brick Kiln Dust as a Sustainable Cement Alternative," *Int. J. Res. Appl. Sci. Eng. Technol.*, vol. 12, no. 1, pp. 1164–1171, Jan. 2024.

[6] United Nations, "The Sustainable Development Goals Report 2020," 300 East 42nd Street, New York, NY, 10017, United States of America., 2020.

[7] ASCE/SEI 7-17, *Minimum Design Loads and Associated Criteria for Buildings and Other Structures*. Reston, VA: American Society of Civil Engineers, 2017.

[8] International Code Council, *1997 Uniform Building Code*, First. United States of America: International Conference of Building Officials, 1997.

[9] ACI CODE-318-14, *Building Code Requirements for Structural Concrete and Commentary*. United States of America: American Concrete Institute, 2014.

[10] M. Paz and W. Leigh, "International Building Code IBC-2000," in *Structural Dynamics*, Boston, MA: Springer US, 2004, pp. 757–781.

[11] O. E. Ige, D. V. Von Kallon, and D. Desai, "Carbon emissions mitigation methods for cement industry using a systems dynamics model," *Clean Technol. Environ. Policy*, vol. 26, no. 3, pp. 579–597, Mar. 2024.

[12] M. R. Karim, M. F. M. Zain, M. Jamil, F. C. Lai, and M. N. Islam, "Use of Wastes in Construction Industries as an Energy Saving Approach," *Energy Procedia*, vol. 12, pp. 915–919, 2011.

ENHANCING STRUCTURAL DESIGN EFFICIENCY IN PAKISTAN: A CASE STUDY ON THE IMPACT OF BIM INTEGRATION

[a]Hassan Tahir*, [b]Muhammad Umair

a: Structure Engineering Department, Designmen Consulting Engineers, Islamabad, Pakistan. hassantahir275@gmail.com
b: Department of Construction Engineering and Management, NUST, Islamabad, Pakistan. mumair.ms22nice@student.nust.edu.pk
* Corresponding author.

Abstract- This study explores the implementation of Building Information Modeling (BIM) workflow in traditional structural design processes, with a focus on interoperability challenges and comparative analysis. A live project served as the basis for examining both conventional and BIM-based approaches to structure design. The study reveals significant differences in time consumption, coordination, error reduction, and rework between the two methods, with the BIM-based approach demonstrating notable advantages. Through the integration of 3D modeling and project browser features in Revit, stakeholders benefit from enhanced visualization, collaboration, and flexibility in design adjustments. Overall, BIM-based design in Revit proves to be a highly efficient and error-minimizing solution for structural design processes.

Keywords- Automation, BIM, Design Workflow, Structure Design.

1 Introduction

The design workflows in construction industry are continuously looking for more efficient methods. The only way is to automate manual processes and utilize better software for reduced cost and time. Introduction of modern technologies in the design workflows is important in achieving these desired efficiencies in the industry. The construction industry is in continuous implementation of new technologies due to ever evolving nature of this field [1], [2]. However, these technologies should facilitate digital building information in construction industry to transform it into dynamic environment [3]. New development in technologies have led to advanced building design tools [4]. BIM methodology is one example of such tools, which has been widely acknowledged and implemented within the construction sector. BIM can help to facilitate communication among design teams to prevent discrepancies in work output by individual team members that can otherwise affect the productivity rates. BIM is based on the idea of having a centralized database which contain digital three-dimensional model of each design parameter. Consequently, data exchange among different participants is easier. Multiple methodologies are being implemented for the use of BIM software in designing structures. These methodologies can help with quick design generation, increase efficiency, and alternatives to cut down discrepancies within design drawings [5]. For this reason, it is suggested that BIM has a significant role in assisting structural designer in their field of activity, and therefore should be adopted by the industry professionals [6]

Structural design is an activity that necessitates proficient management of available software, both in terms of the modelling process and analysis practice [7]. The process of structural design, backed by BIM software, has been extensively researched. A common finding across these studies is the identification of the interoperability capacity of the systems as a primary constraint on BIM implementation in this segment of construction [8], [9]. The percentage of structural projects where BIM software is utilized, revealed an average of 50% in tasks related to inter-discipline coordination, predication of documentation (drawings), and analyses and design [10], [11]. So, interoperability is an essential step that requires careful consideration in project design offices. This study examines and presents the implementation of BIM integration in structural design within a real-world project in Pakistan. The novelty of this study lies in its empirical comparison of BIM and traditional methods, highlighting the practical benefits and efficiency gains of BIM integration. This unique focus provides valuable insights into the implementation of BIM within the local context. Therefore, this study focusses on two main objectives:

1 Implementation of BIM workflow in the traditional structure design process.
2 Comparison of Traditional and BIM based structure design process.

2 Research Methodology

This study follows the methodology as elaborated in Fig. 1. A live project is chosen for study purposes. The structure design of the project has been conducted using the traditional approach practiced in design consultancy. Subsequently, the structure design process is repeated using BIM based approach, resulting into exploration of interoperability compatible BIM methodology for structure design processes and comparison of traditional and BIM based structure design approaches.

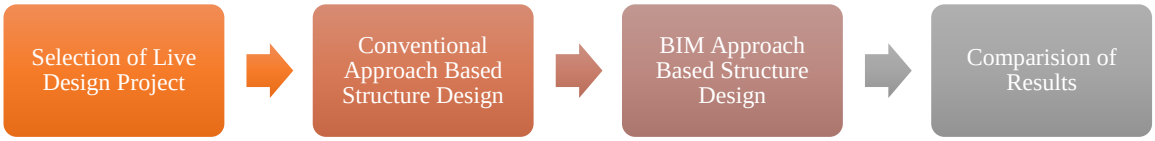

Figure 1: Research Methodology

3 Case Study

The live project involved the construction of a mosque in the Islamabad region, comprising two floors. The design process commenced with a soil investigation, followed by a site visit to assess soil profile, topography, and other site characteristics. Multiple plans were drafted by the architect according to client's specifications. Upon client's approval, one architectural draft plan was finalized, with column locations marked on for structural design. These architectural plans were then passed to the structural design engineer for framing, analysis, and design of the structure of mosque.

1.1 Conventional Design Approach

The conventional design approach involves the designing of the frame structures on the plans received from the architect. This task is accomplished using specialized software tools such as Etabs, which facilitate detailed and accurate structural analysis and design. The dimensions of the structural members and required steel reinforcements are then provided to the structural draftsmen. Equipped with this information, the draftsmen proceed to create detailed plans in accordance with the provided framing. Despite being time-tested, this methodology necessitates careful coordination and clear communication between all parties involved to ensure the successful completion of the project.

1.2 BIM based Design Approach

In a BIM-based approach, the architect provided CAD files of the architectural plan to the structural engineer for initial column sizing. Simultaneously, the architect began developing an architectural model in Revit for future collaboration and clash detection. The structural engineer linked the CAD file to Revit and created a 3D Structural Framing Model using a Revit structure template. A BIM studio plugin was utilized for automatic column placement based on the linked CAD file, reducing modeling time. Once the framing was verified, the engineer imported the model to CSI ETABS for analysis and design. Following analysis and design, the model was transferred back to Revit for validation. In order to ensure a smooth transferring of model between two software, CSiXRevit plugin was used. Rebar modeling using the CAD Rebar Extension ensued, resulting in the preparation of detailed construction drawings with 3D views and quantity estimation using BIM. Fig 2. shows the workflow begins with an initial framing geometrical model in Revit as shown in fig 2a. this basic 3D model lacks detailed load and boundary condition information. Fig 2b. shows an analytical model which was prepared in Revit incorporating loads and boundary conditions. Fig 2c. demonstrates the results of shear stress distribution after analyzing the analytical model in Etabs, and Fig 2d. represents the final reinforcement model in Revit that was based on the output reinforcement results from Etabs.

4 Results

The study showed a big difference in time consumption, coordination issues, errors, and rework between the BIM-based approach and the conventional design-based approach. The results are shown in Table 1 and Table 2. The conventional approach took 8.5 days, while the BIM-based approach only took 3 days.

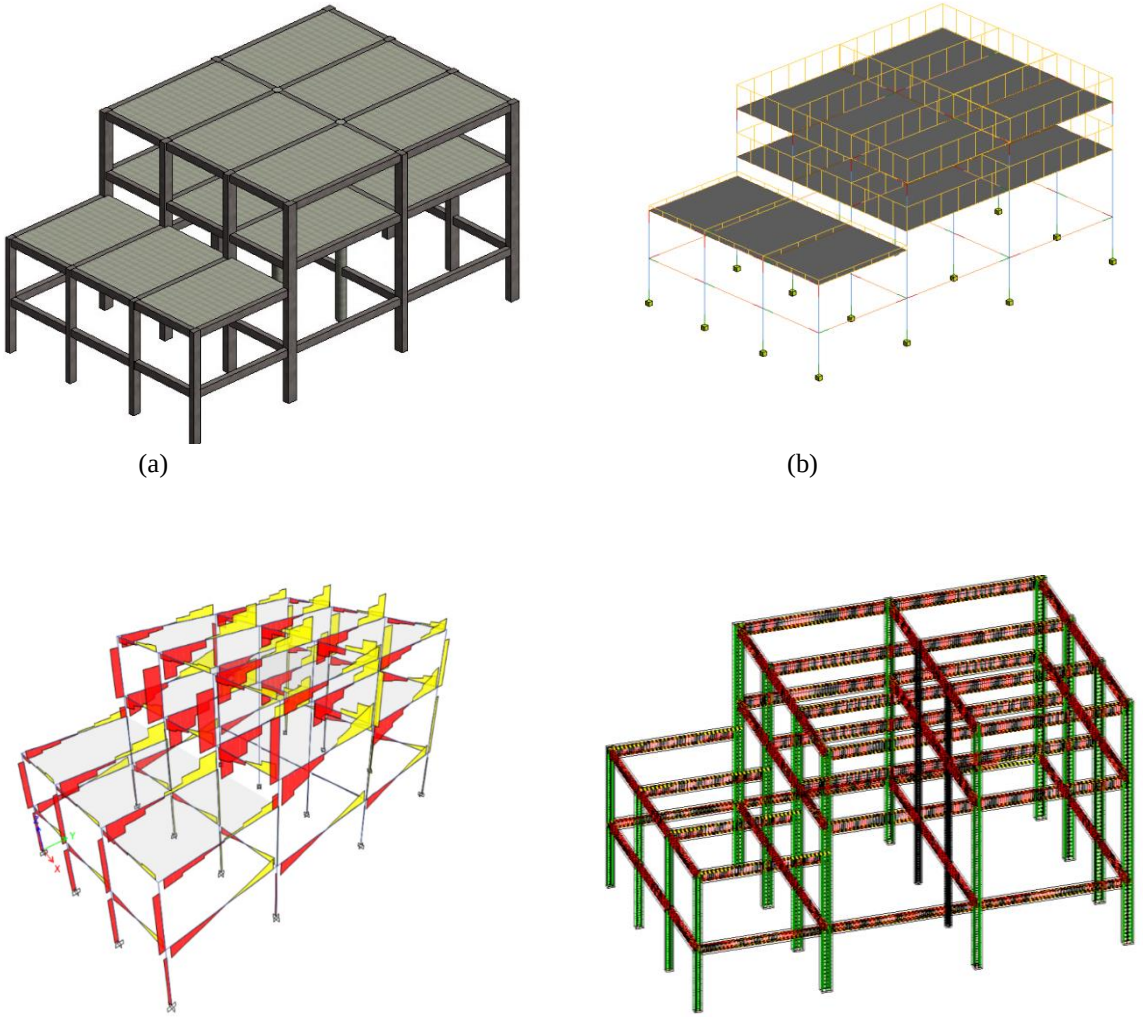

Figure 2: BIM design approach, a. Initial geometrical model, b. Revit analytical model, c. Etabs analysis model and d. Finalized reinforced model of Revit.

In the conventional design approach, the architect took 1 day to create the initial concept and CAD plan. Next, the structural draftsman took 1.5 days to prepare the initial structural drawings. Then, the structural engineer needed 2 days for detailed structural analysis and design. After that, the structural engineer spent another 2 days to create detailed structural drawings. Finally, the revision process took 2 more days to finalize the design and drawings. Overall, it took 8.5 days to complete the design and drafting process.

In contrast, with the BIM-based approach, the architect also took 1 day to create the initial CAD plan. After that, the structural engineer completed the design and detailing process using BIM tools in just 2 days. So, the entire process took only 3 days. This shows that the BIM-based process is 2.83 times faster than the conventional process. This significant timesaving highlights the efficiency of using BIM tools in design and drafting.

All in all, the conventional approach is already well established, and users are familiar with its workflow, which results in more predictability in the earlier stages of the project. However, it is time-consuming, as indicated by the results showing that it took 8.5 days for the entire process, and comparatively there is still a high probability of errors and rework. On the other hand, the BIM-based approach is more time-efficient, well-coordinated, and has a comparatively lower probability of errors and rework. However, the initial efforts in terms of setting up a BIM-based design environment, including the hard resources such as systems and soft resources such as software purchasing and recruiting people with the required skills, are comparatively high.

Table 1: Conventional Design Approach

Sr. No	Activity	Performed By	Time
1.	Initial CAD plan	Architect	1 day
2.	Structural CAD plan	Structure draftsman	1.5 days
3.	Structure analysis and design	Structure engineer	2 days
4.	Preparation of structure detailing	Structure draftsman	2 days
5.	Revisions	Architect and structure engineer	2 days

Table 2: BIM Base Design Approach

Sr. No	Activity	Performed By	Time
1.	Initial CAD Plan	Architect	1 day
2.	CAD to Revit	Structure engineer	1 day
3.	Integration of Revit model to Etabs for analysis and design	Structure engineer	
4.	Placement of reinforcement in Revit	Structure engineer	1 day
5.	Detailing in Revit	Structure engineer	

5 Conclusion

The study implemented the BIM based structure design process on a live project and drawn comparison with conventional approach. From this study, it is concluded that:

1. BIM-based design in Revit ensures minimal errors and high efficiency due to precise coordinate input and seamless propagation of modifications across all views, saving significant time in the design process.
2. The integration of 3D modeling and project browser in Revit enhances visualization, fosters collaboration, and minimizes inconsistencies across disciplines, further reducing design time.

References

[1] A. Naamane and A. Boukara, "A Brief Introduction to Building Information Modeling (BIM) and its interoperability with TRNSYS," Renewable Energy and Sustainable Development, vol. 1, no. 1, pp. 126–130, Aug. 2015, doi: 10.21622/RESD.2015.01.1.126.

[2] J. Brozovsky, N. Labonnote, and O. Vigren, "Digital technologies in architecture, engineering, and construction," Autom Constr, vol. 158, p. 105212, Feb. 2024, doi: 10.1016/J.AUTCON.2023.105212.

[3] A. Khudhair, H. Li, G. Ren, and S. Liu, "Towards Future BIM Technology Innovations: A Bibliometric Analysis of the Literature," Applied Sciences 2021, Vol. 11, Page 1232, vol. 11, no. 3, p. 1232, Jan. 2021, doi: 10.3390/APP11031232.

[4] R. Sacks, C. M. Eastman, and G. Lee, "Parametric 3D modeling in building construction with examples from precast concrete," Autom Constr, vol. 13, no. 3, pp. 291–312, May 2004, doi: 10.1016/S0926-5805(03)00043-8.

[5] D. Migilinskas and L. Ustinovichius, "Computer-Aided Modelling, Evaluation and Management of Construction Projects According to PLM Concept," Lecture Notes in Computer Science (including subseries Lecture Notes in Artificial Intelligence and Lecture Notes in Bioinformatics), vol. 4101 LNCS, pp. 242–250, 2006, doi: 10.1007/11863649_30.

[6] I. F. Varouqa and M. A. Alnsour, "A method of building information modelling implementation for structural engineering firms," MethodsX, vol. 12, p. 102685, Jun. 2024, doi: 10.1016/J.MEX.2024.102685.

[7] T. Hamidavi, S. Abrishami, and M. R. Hosseini, "Towards intelligent structural design of buildings: A BIM-based solution," Journal of Building Engineering, vol. 32, p. 101685, Nov. 2020, doi: 10.1016/J.JOBE.2020.101685.

[8] "Sequeira, P. (2022) Analysis of BIM Technology Capabilities in the Generation of 4D Models. Master's Thesis, University of Lisbon, Lisbon. - References - Scientific Research Publishing." Accessed: Jul. 16, 2024. [Online]. Available: https://www.scirp.org/reference/referencespapers?referenceid=3548887

[9] A. Z. Sampaio and A. M. Gomes, "BIM Interoperability Analyses in Structure Design," CivilEng 2021, Vol. 2, Pages 174-192, vol. 2, no. 1, pp. 174–192, Feb. 2021, doi: 10.3390/CIVILENG2010010.

[10] "STRUCTURE magazine | BIM and the Structural Engineering Community." Accessed: Jul. 16, 2024. [Online]. Available: https://www.structuremag.org/?p=5359

[11] R. Ren, J. Zhang, and H. N. Dib, "BIM Interoperability for Structure Analysis," Construction Research Congress 2018: Construction Information Technology - Selected Papers from the Construction Research Congress 2018, vol. 2018-April, pp. 470–479, 2018, doi: 10.1061/9780784481264.046.

SUSTAINABLE DESIGN OF A MULTI-STORY BUILDING USING WASTE MARBLE AND CERAMIC

[a] Muhammad Haroon Kabir*, [b]Anwar Khitab

a: Department of Civil Engineering, Mirpur University of Science and Technology, Mirpur, Pakistan.muhammadharoonkabir42@gmail.com
b: Department of Civil Engineering, Mirpur University of Science and Technology, Mirpur, Pakistan. anwar.ce@must.edu.pk
* Corresponding author.

Abstract- This project deals with the design of a High-rise building by using waste materials. The locally developed building materials from recycled wastes were used in manufacturing concrete and bricks. A ten-story high-rise building was designed using the software ETABS. The concrete comprised of 10% partial replacement of cement by waste marble powder (WMP) and the bricks contained 12% waste ceramic powder and 15% waste brick powder as replacement of clay. These materials were developed in the lab, and their properties were determined as per ASTM standards. The characteristics were incorporated in the software and the building was designed and analyzed. The designed building was compared with that containing conventional concrete and bricks. It was found that the design having waste materials resulted in the saving of 164 tons of cement, and 475 m3of fertile clay, while meeting the stability standards as documented in the building codes. The design prevents the emission of 148 tons of carbon into the atmosphere and significantly saves energy required for cement manufacturing. Additionally, the building incorporating waste materials costs Rs. 5.8 million less than one made with conventional materials.

Keywords- High-Rise Buildings, Recycling, Waste Marble, Waste Ceramic, Environmental Impact, Cost Effectiveness.

1 Introduction

In today's modern world, concrete is widely used in the construction of civil engineering structures. Concrete comprises of three main constituents: cement, sand, and coarse aggregate. The production of cement produces a huge amount of carbon dioxide and contributes significantly to global warming. Its manufacturing requires a temperature of 1400 ºC, which is achieved by burning fossil fuels [1]. Thus, it also causes the depletion of fossil fuels. It is necessary to reduce the use of cement to make the construction sustainable and eco-friendly.

Marble is one of the most important and widely used stones. It is calcareous in nature and is the metamorphic form of limestone. Majeed et al. studied the effect of waste marble powder (WMP) on the properties of concrete. The results showed that up to 10% replacement of WMP, the compressive and tensile strengths of concrete are improved. The increase in mechanical strength was attributed to the pozzolanic and cementing characteristics of the Marble [2]. Memon et al. studied the effect of partial replacement of marble dust with cement on the fresh and hardened properties of concrete. The results showed greater compressive strength in concrete and a decline in workability [3]. Özkılıç et al. examined the effect of marble powder on the performance of concrete. The authors partially replaced cement with 10-40 % of waste marble powder. The authors recommended a dosage of 10% waste marble powder as a partial replacement cement, based on the mechanical and sustainability aspects [4]. Khitab et al. examined the effect of waste brick powder (WBP) and waste ceramic powder (WCP) as replacements for clay in bricks. The study found that incorporating 15% WBP and 12% WCP resulted in the same density as with 100% clay [5]. An increased brick porosity was also obtained as compared to clay bricks, making them suitable for moderate weather resistance and insulation. Moreover, compressive strength reduced with 15% WBP and 12% WCP addition but remained adequate for second-class bricks. There was a 27% decrease in the initial water absorption rate in bricks with the replacement. Additionally, there was no efflorescence in the bricks. The

incorporation of WBP in the production of clayey bricks saved 27% of fertile clay, leading to environmentally friendly construction [5].

This work deals with the design and analysis of an RCC high-rise building. In the design, concrete containing 10% WMP as a partial replacement of cement was used. Additionally, partition walls of red bricks were provided, in which 27% fertile clay was replaced by a mixture of 10% WCP and 12% WBP. The aim was to design a sustainable building based on the materials previously developed in our research group. The benefits of using locally developed materials were assessed by designing an actual RCC structure and comparing it with the conventional building in terms of environmental impact and cost. This work aims to provide the benefits of a green building in terms of waste reduction and utilization in accordance with the sustainable development goals of UNO [6]. A 10-story building was chosen as a test case. The design and analysis were carried out using ETABS. The benefits of green building are presented in the form of reduction in greenhouse gas emission, the use of natural resources, energy and cost.

2 Research Methodology

2.1 Dimensions of the Proposed Building

The proposed plan for the high-raise building is shown in Figure 1. It has dimensions of 37m x 36.57m with a height of 32m including ground floor. In this design, 4 shear walls were provided as per recommendations of ASCE 7-17 [7].

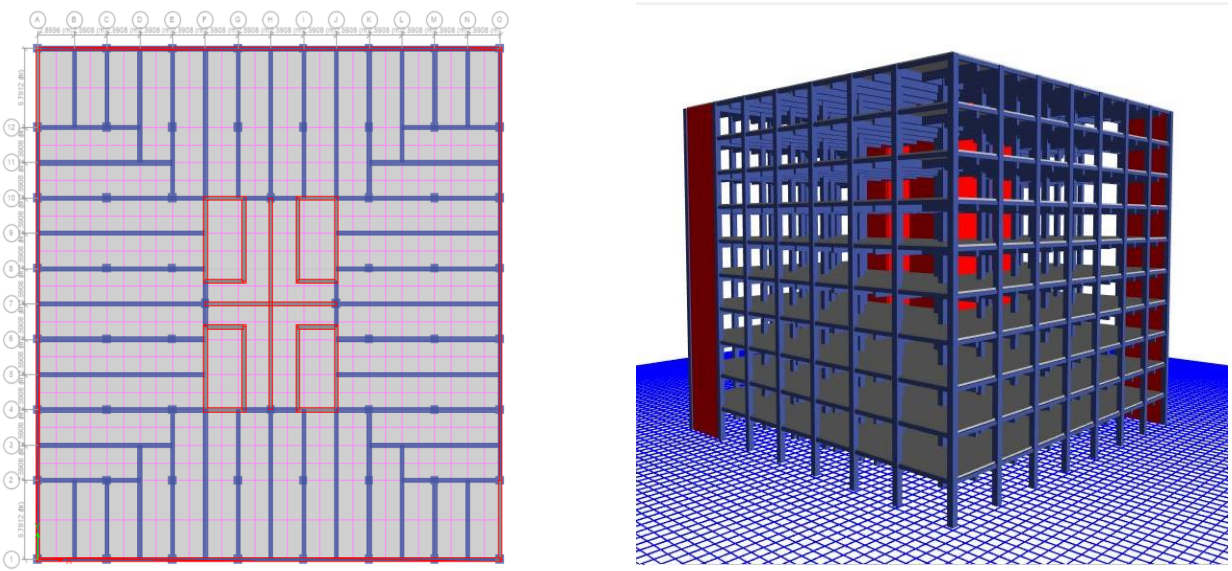

a) b)

Figure 1: Two- & Three-Dimensional Plan of proposed model

The shear walls are highlighted with red ink in Figure 1. One shear wall each was provided along the longer side and two central shear walls were provided in the middle along the shorter side. The building was subjected to dead, live, wind and earthquake as per Universal Building Codes 97 [8].

2.2 Design & Analysis

The proposed building was modeled using ETABS, and properties of the materials resulting from past research were assigned to the components of the building, i.e., slabs, columns, beams, walls, etc. The material properties used in the design are shown in Table 1. These properties were acquired from our previous researches [5], [9].

Table 1 Properties of materials used [5], [9]

Materials	Compressive Strength (MPa)	Density (kg/m^3)	Poisson's Ratio	Modulus of Elasticity (GPa)
Conventional concrete	25	2385	0.2	23.5
10% WMP in Concrete	32	2410	0.2	26.6
Conventional brick	9.31	2162	0.2	12.4
15% WBP + 12% WCP in Bricks	9	1400	0.2	14.1

3 Results

After designing the model in ETABS, dimensions of the components of green building (i.e. slabs, beams, columns and walls) for all stories are shown in table 2.

Table 2: Dimensions obtained from design

Components	Width (mm)	Depth (mm)
Slabs	-	175
Beams	300	750
	300	300
Columns	560	560
Shear Walls	300	-
Perimeter Walls	228	-

After analyzing the model, the parameters were checked by the given ACI code (i.e. ACI-318-14) [10] using ETABS, which indicated that the building was stable. Some significant limit state parameters are provided in Table 3.

Table 3: Analysis Parameters

Display Type	Load	Max. (X-direction)	Max. (Y-direction)	Max. Limit
Story Drift (Unit less)	Earthquake	0.000141	0.0000136	0.0015
Max. story Displacement (mm)	Earthquake	3.63	3.66	30
Overturning Moments (KN-m)	Earthquake	558434	-480000	Depends on foundation soil

Story drift is a parameter, which shows the relative displacement of a floor with respect to the next floor. According to Indian Standards IS 1893 (Part 1) [11], the maximum story drift should be less than 0.004, whereas the Appendix C of ASCE 7 put a limit ranging from 0.005 to 0.0015 [7]. The story displacements are well within the limits[12]. The comparison of different parameters that are linked with sustainability are given in Table 4:

Table 4: Sustainability Parameters

Parameters	Conventional Building	Green Building	Savings	Cost Effectiveness (Millions of Rs.)
Cement (tons)	1088	924	164	4.75
Carbon Dioxide (tons) [13]	979	813	148	-
Electricity (kWh)[14]	119704	101597	18167	0.73
Clay (m^3)	1762	1287	475	0.332
Structure weight (MN)	169.22	141.8	27.4	-
			Total saving in Rs. Million	5.812

The use of green materials, which have been tested in the labs, is an eco-friendly approach: this not only provides saving in cement, but also in the associated greenhouse gas emissions. The energy requirements can be reduced owing to lesser manufacturing of cement. Additionally, the incorporation of 27% waste in bricks results in a significant reduction of fertile clay, which can be preserved for crops, vegetables and fruit.

4 Conclusions

This work deals with the design of a 10-story RCC building using green materials, developed in the lab. Based upon the simulations, the following conclusions are withdrawn:

1. The designed building provides a saving of 164 tons of cement, and 475 m^3 of fertile clay.
2. The saving in cement corresponds to a reduction of 513 tons of CO_2 to the atmosphere, and an energy conservation of 18.2 MWh.
3. The proposed green design assures a cost reduction of 5.8 million PKRs.
4. The building incorporating waste materials is 16% lighter than that containing conventional materials.

References

[1] A. Khitab and W. Anwar, "Classical Building Materials," 2016, pp. 1–27.
[2] M. Majeed, "Evaluation of Concrete with Partial Replacement of Cement by Waste Marble Powder," *Civ. Eng. J.*, vol. 7, p. 13, 2021.
[3] F. A. Memon, "Effect of Marble Dust as a Partial Replacement of Cement on Fresh and Hardened Properties of Concrete," in *International conference on sustainable development in civil engineering*, 2017, p. 6.
[4] Y. O. Özkılıç *et al.*, "Optimum usage of waste marble powder to reduce use of cement toward eco-friendly concrete," *J. Mater. Res. Technol.*, vol. 25, pp. 4799–4819, Jul. 2023.
[5] A. Khitab *et al.*, "Manufacturing of Clayey Bricks by Synergistic Use of Waste Brick and Ceramic Powders as Partial Replacement of Clay," *Sustainability*, vol. 13, no. 18, p. 10214, Sep. 2021.
[6] United Nations, "The Sustainable Development Goals Report 2020," 300 East 42nd Street, New York, NY, 10017, United States of America., 2020.
[7] ASCE/SEI 7-17, *Minimum Design Loads and Associated Criteria for Buildings and Other Structures*. Reston, VA: American Society of Civil Engineers, 2017.
[8] International Code Council, *1997 Uniform Building Code*, First. United States of America: International Conference of Building Officials, 1997.
[9] M. Majeed, A. Khitab, W. Anwar, R. B. N. Khan, A. Jalil, and Z. Tariq, "Evaluation of concrete with partial replacement of cement by waste marble powder," *Civ. Eng. J.*, vol. 7, no. 1, 2021.
[10] ACI CODE-318-14, *Building Code Requirements for Structural Concrete and Commentary*. United States of America: American Concrete Institute, 2014.
[11] S. Gawande *et al.*, "Seismic Analysis of Tall Structures," *IOP Conf. Ser. Earth Environ. Sci.*, vol. 822, no. 1, p. 012028, Jul. 2021.
[12] B. Burak and H. G. Comlekoglu, "Effect of Shear Wall Area to Floor Area Ratio on the Seismic Behavior of Reinforced Concrete Buildings," *J. Struct. Eng.*, vol. 139, no. 11, pp. 1928–1937, Nov. 2013.
[13] O. E. Ige, D. V. Von Kallon, and D. Desai, "Carbon emissions mitigation methods for cement industry using a systems dynamics model," *Clean Technol. Environ. Policy*, vol. 26, no. 3, pp. 579–597, Mar. 2024.
[14] M. R. Karim, M. F. M. Zain, M. Jamil, F. C. Lai, and M. N. Islam, "Use of Wastes in Construction Industries as an Energy Saving Approach," *Energy Procedia*, vol. 12, pp. 915–919, 2011.

AN OVERVIEW ON FIRE DAMAGE QUANTIFICATION AND RETROFITTING OF LOW-RISE REINFORCED CONCRETE STRUCTURES

[a]Javaria Mehwish*, [b]Waseem Akram

a: Civil & Environmental Engineering, Brunel University London, UK., javaria.mehwish@brunel.ac.uk
b: TEVTA (Punjab), Pakistan. , wwaseem45@gmail.com
* Corresponding author.

***Abstract*:** Reinforced concrete (RC) structures are exceedingly susceptible to fire damage, which may induce substantial degradation of the material. Concrete does not ignite at ambient temperature; however, it can significantly alter its mechanical, chemical, and structural characteristics when subjected to elevated temperatures. The extent of a fire damage is primarily determined by its severity and duration. Small fires for short duration, burning, results limited damage, larger fires that persisting over time leads to substantial damage or even structural collapse. This study examines the response of concrete to fire, the potential damage that reinforced concrete buildings may sustain, and the retrofitting solutions that are currently available. Additionally, it contains an incident report regarding a textile market fire that was precipitated by a short circuit. This case study examines ecological retrofitting solutions and concentrates on reinforced concrete buildings on lower stories. In this investigation, we investigate the potential of natural fiber laminates to retrofit buildings and the ability of cement slurry to repair damaged concrete.

***Keywords*-**Bamboo Fiber Laminates, Concrete Structures, Fire, Retrofitting Techniques.

1 Introduction

The danger of fire causes a substantial risk to the structural stability of reinforced concrete (RC) buildings. Although concrete is categorized as a non-combustible substance, it can undergo physical and chemical alterations when subjected to high temperatures. These alterations can cause significant deterioration in the mechanical characteristics of the object, which may result in potentially disastrous structural failures [1,2]. The magnitude of harm sustained by concrete buildings during a fire occurrence is impacted by several aspects, such as the strength and length of the fire, as well as the distinct characteristics of the concrete and steel reinforcing [3].Concrete degradation when exposed to high temperatures is primarily caused by water vapor pressure, the breakdown of hydrated cement compounds, and the incompatibility between the thermal reactions of aggregate and hydrated cement [4]. At temperatures over 400˚C, concrete undergoes a process where water is expelled from the gel, capillary, and interlayer pores. Calcium hydroxide decomposes at around 400˚C, while combined water and C–S–H break down at temperatures ranging from 500˚C to 800˚C [5]. In most of the fire events, the intensity and length of the fire impair the structural integrity and rigidity of concrete structures to the extent that repairing them becomes a more practical and cost-effective alternative than dismantling and rebuilding the damaged structures [6].

Various deterioration and damage processes can affect RC structures, each with its own set of pros and cons. "Concrete jacketing" applies a new layer of reinforced concrete to enhance the strength and ductility of existing columns or beams. Modifications to the base can be required due to the method's effect on the enlargement and weight of structural parts [7]. Spending a significant amount of money on this could potentially change the appearance of the building. Installing steel braces or frames enhances the structural stability and lateral resistance of damaged constructions. The execution of this technique will determine whether altering the building's aesthetic is necessary or not. Factors such as the design of the

building and the placement of the bracing determine the effectiveness of the retrofit. Furthermore, significant bracing may lead to financial concerns [8]. When choosing an appropriate retrofitting method for burnt concrete structures, one must carefully consider factors such as increased strength and stability, expenditures, structural alterations, and the type of damage.

This study investigates the behaviour of concrete when exposed to fire, the many forms of damage that can occur to reinforced concrete structures because of fire, and the retrofitting options that are now available. Visual inspections and non-destructive tests quantify reinforced concrete fire damage. The procedures measure material properties, internal flaws, and structural integrity. These approaches provide a comprehensive representation of the damage caused by fire in concrete buildings. The case study examines the harm inflicted on low-rise reinforced concrete structures due to a fire triggered by a short-circuit in a nearby fabric market. It also investigates retrofitting methods that are ecologically sustainable. Several natural fibers exhibit potential as laminate materials for concrete retrofitting; nevertheless, there is a lack of research on the recommendations for their use. The paper looks at the possibilities of natural fiber laminates in combination with cement slurry for the purpose of retrofitting, with the goal of restoring concrete stiffness and stability.

2 Concrete Behaviour Under Fire

Concrete, a commonly utilized material in the construction industry owing to its strength and long-lasting properties, experiences substantial degradation when subjected to elevated temperatures. Comprehending the behaviour of concrete during fire situations is essential for evaluating harm and devising efficient retrofitting techniques. Concrete undergoes physical and chemical changes when exposed to high temperatures. Above 100°C, moisture evaporates, creating internal steam pressure that causes micro-cracking and spalling on the concrete surface [9]. Chemical decomposition begins at approximately 300°C, causing hydrated cement paste to dehydrate. This leads to the breakdown of calcium hydroxide into calcium oxide and water vapor, significantly weakening the cement paste and reducing its compressive strength [2]. Aggregate deterioration occurs when siliceous aggregates break down about 600°C, but calcareous aggregates maintain greater stability at higher temperatures, leading to further structural vulnerability [4].

Fire exposure drastically alters concrete's mechanical properties. Temperatures exceeding 300°C can reduce its compressive strength by around 50%, primarily due to moisture loss, chemical degradation, and the breakdown of the aggregate-cement bond [9]. The bad impact on tensile strength is greater than that on compressive strength, principally because of the development of micro-cracks and spalling, which undermine the material's capacity to endure tensile stresses [2]. The elastic modulus of concrete decreases with higher temperatures, increasing deflections and deformations under load. This poses risks to the structural integrity and load-bearing capacity of fire-exposed concrete elements [4]. Some of the common changes to concrete at high temperature are found in a study carried out by Osman et al. [l0] are shown in table below.

Table 1: The behavior of concrete at varying temperatures [10]

Temperature Range ◦C	Exposed Color	Surface Texture	Deterioration/Condition
Ambient-300◦C	Unaffected	Unaffected	Unaffected
(300–600) ◦C	Pink to red	Cracking, crazing, and aggregate pop-outs on the surface	Safe but capacity might be affected
(600–950) ◦C	Whitish grey	Exposure steel reinforcement and Spalling	Weakened
Above 950 ◦C	Buff	Extensive spalling	Significantly damaged

3 Fire Damages to RC Structures

Fire damages present a substantial risk to reinforced concrete (RC) structures, resulting in the deterioration of materials and a decrease in structural integrity. Crazing manifests as uneven, slender lines on the surface, signifying the early thermal harm caused by differential thermal expansion [9]. Rising temperatures result in thermal expansion and contraction, which in turn leads to the development of more severe fractures, including deeper structural fissures that weaken the connection between concrete and steel [2]. Spalling is the process in which the internal pressure of steam inside concrete becomes

greater than the concrete's ability to withstand tension. This leads to the loss of surface material and exposes the underlying concrete and reinforcing to heat [4]. The loss of concrete cover results in the vulnerable exposure of reinforcing steel, causing a quick decline in strength and a considerable decrease in load-bearing capacity [11]. Fire exposure may significantly impair the load-bearing capacity of reinforced concrete (RC) structures, putting them at high danger of partial or full collapse. This is caused by the deterioration of concrete, loss of bond, and degradation of reinforcing steel [12].

A recent fabric market fire as an example of the devastating impact of fire on reinforced concrete structures located at lower levels. An electrical short-circuit started the fire, which moderately damaged the surface, with spalling and splitting as its main characteristics. When the structure experiences crack due to thermal expansion and contraction, the loss of concrete cover worsens its vulnerability. In severe weather, the cement that holds the aggregate together may dissolve or deteriorate, releasing the aggregate and weakening the building. The results of a moderate fire that occurred in a low-rise RC structure that was commercially oriented are depicted in Figure 1. The fire was initiated by an electrical short-circuit on the second floor. It raged for eight hours, resulting in the death of one individual, moderate structural damage, and a significant amount of property loss. The fire incident that was detailed resulted in Level III structural damage, which is defined as extensive concrete degradation and fracture. This underscores the importance of efficient retrofitting solutions.

Figure 1: Damages to RC structure: a) RC structure under fire, b) Crazing, c) Cracking and loss of cover, d) Exposure of aggregate

3 Retrofitting of Fire Damaged Structures

The retrofitting approaches for fire-damaged reinforced concrete (RC) structures include both conventional and innovative technologies. One traditional approach is epoxy injection, which can seal fractures but does not much improve the structural load capacity, also bonding steel plates can enhance both flexural and shear strength. However, it is crucial to ensure exact installation in order to achieve optimal performance [13]. Carbon Fiber-Reinforced Polymers (CFRP) are preferred due to their superior strength-to-weight ratio and resistance to corrosion. They provide significant improvements in structural performance, although they are more expensive and require specialised application techniques [13,14]. Current study is centred around using natural fibre laminates, including jute, hemp, and bamboo, as sustainable alternative. These materials possess desirable mechanical qualities and have a reduced environmental effect compared to conventional options [11]. The renewable and biodegradable nature of these natural fibres makes them a cost-effective alternative.

Incorporating cement slurry with natural fibre laminates can improve adhesion to the concrete surface, therefore repairing cracks and voids and restoring rigidity and structural strength [4, 11]. Table 2 shows several retrofitting options available. Some of them have drawbacks as well, such as rising element cross-sections, expense, and brittleness. Restoring the ductility of beams that have been burned provides important information on how these structures failed, and BFRP laminates are great at this. BFRP laminates, an environmentally friendly alternative to conventional synthetic FRP composites, significantly increase the capacity of RC beams damaged by fire and subsequently reduce deflection, making them a viable retrofitting choice.

Table 2. Retrofitting techniques suggested by the researchers in their studies

Sr #	Member	Damage	Retrofitting Techniques	Reference
1	Columns	Severe	Jackets, RC concrete	[12]
2	Beams		Jacketing, Ferro cement (FC)	[15]
3	Beams	Moderate	Laminates, Bamboo fiber reinforced polymer (BFRP)	[11]
4	Beams		Glass fiber-reinforced polymer(GFRP)	[15]
5	Beams	Mild	Jacketing, Slurry-infiltrated fibrous concrete (SIFCON)	[16]
6	Columns		Wrap jackets, Carbon fiber reinforced polymer (CFRP)	[17]

5. Discussion

A recent fire in a nearby cloth market caused mild surface damage to a low-rise reinforced concrete structure due to a short-circuit. Post-fire evaluation revealed significant spalling, cracking, and slight steel reinforcement deformation, compromising structural stability despite the short duration of the fire. Retrofitting is recommended, starting with visual inspections and structural analysis. Cleaning damaged area, repairing with cement slurry for crack restoration and bonding, and reinforcing with natural fiber laminates (bamboo or jute) to enhance load-bearing capacity and structural performance.

6 Conclusions

Studying the effects of fire damage on reinforced concrete (RC) structures emphasises the need of comprehending material behaviour in extreme circumstances, since deterioration processes can greatly endanger structural integrity. Current progress in sustainable retrofitting methods, namely employing natural fibre laminates, provide lightweight, durable alternatives that are in line with environmental objectives. Although natural fibres help to decrease carbon footprints, their inherent variability requires standardisation in order to ensure consistent and dependable use. The transition to environmentally sustainable materials is crucial for tackling climate change and advancing the preservation of resources.

Acknowledgment

The Authors would like to thank Professor Dr. Majid Ali and Dr. Mehran Khan for their kind guidance and support.

References

[1] Kodur, V. (2007). Fire performance of concrete structures. Canadian Journal of Civil Engineering, 34(1), 6-12. https://doi.org/10.1139/l06-058.
[2] Zhang, H.Y., Li, Q.Y., Kodur, V., & Lv, H.R. (2021). Effect of cracking and residual deformation on behavior of concrete beams with different scales under fire exposure. Engineering Structures, 245, 112886. https://doi.org/10.1016/j.engstruct.2021.112886.
[3] Khoury, G.A. (1992). Fire resistance of concrete structures. Cement and Concrete Research, 22(5), 800-815. https://doi.org/10.1016/0008-8846(92)90007-J.
[4] Usman, M., Yaqub, M., Auzair, M., Khaliq, W., Noman, M., & Afaq, A. (2021). Restorability of strength and stiffness of fire damaged concrete using various composite confinement techniques. Construction and Building Materials, 272, 121984. https://doi.org/10.1016/j.conbuildmat.2020.121984.
[5] Haddad, R.H., & Yaghmour, E.M. (2020). Retrofitting heat-damaged concrete beams using different profiles of side NSM CFRP strips. Structures, 28, 2232–2243. https://doi.org/10.1016/j.istruc.2020.10.027.
[6] Haddad, R.H., & Almomani, O.A. (2017). Recovering flexural performance of thermally damaged concrete beams using NSM CFRP strips. Construction and Building Materials, 154, 632–643. https://doi.org/10.1016/j.conbuildmat.2017.07.211.
[7] Zaiter, A., & Lau, T.L. (2021). Experimental study of jacket height and reinforcement effects on seismic retrofitting of concrete columns. Structures, 31, 1084–1095. https://doi.org/10.1016/j.istruc.2021.02.020.
[8] Rahimi, A., & Maheri, M.R. (2020). The effects of steel X-brace retrofitting of RC frames on the seismic performance of frames and their elements. Engineering Structures, 206, 110149. https://doi.org/10.1016/j.engstruct.2019.110149.
[9] Qin, D., Gao, P.K., Aslam, F., Sufian, M., & Alabduljabbar, H. (2022). A comprehensive review on fire damage assessment of reinforced concrete structures. Case Studies in Construction Materials, 16, e00843. https://doi.org/10.1016/j.cscm.2021.e00843.
[10] Osman, M.H., Sarbini, N.N., Ibrahim, I.S., Ma, C.K., Ismail, M., & Mohd, M.F. (2017). A case study on the structural assessment of fire damaged building. IOP Conference Series: Materials Science and Engineering, 271(1).
[11] Awoyera, P.O., Akin-Adeniyi, A., Bahrami, A., & Romero, L.M.B. (2024). Structural performance of fire-damaged concrete beams retrofitted using bamboo fiber laminates. Results in Engineering, 21, 101821. https://doi.org/10.1016/j.rineng.2024.101821.
[12] Belakhdar, A.R., Dimia, M.S., & Baghdadi, M. (2023). Post-fire behavior of RC columns repaired with square hollow section steel tube and RC concrete jackets. The Journal of Engineering and Exact Sciences, 9(6), 161456-01e.
[13] Pacheco-Torgal, F., Jalali, S., & Sato, H. (2012). Eco-efficient repair and retrofitting of concrete structures. Construction and Building Materials, 29, 34-40. https://doi.org/10.1016/j.conbuildmat.2011.11.055.
[14] Borghese, V., Contiguglia, C.P., Lavorato, D., Santini, S., Briseghella, B., & Nuti, C. (2024). Sustainable retrofits on reinforced concrete infrastructures. Structural Engineering. https://doi.org/10.4430/bgo00436.
[15] Anasco Bastin, D.R., Sharma, U.K., & Bhargava, P. (2017). A study on different techniques of restoration of fire damaged reinforced concrete flexural members. Journal of Structural Fire Engineering, 8(2), 131-148.
[16] Elsheikh, A., & Alzamili, H.H. (2024). Behavior of Fire-damaged RC Beams After Strengthening with Various Techniques. Civil Engineering Journal, 10(1), 189-209.
[17] Izzat, A.F. (2015). Retrofitting of Reinforced Concrete Damaged Short Column Exposed to High Temperature. Journal of Engineering, 21(3), 34-53.

OPERATION AND MAINTENANCE OF GREEN BUILDINGS: A CASE STUDY

[a] Muhammad Fahad*, [b] Hafiz Aiman jamshaid

a: Department of Civil Engineering, university of Central Punjab, Lahore, Pakistan. l1f20bsce0005@ucp.edu.pk
b: Department of Civil Engineering, university of Central Punjab, Lahore, Pakistan. aiman.jamshaid@ucp.edu.pk
* Corresponding Author.

Abstract- Conventional construction has played a massive role in contributing towards pollution and global warming which eventually leads to different diseases that have caused death but also created energy problems. To tackle this major issue, we need to convert our construction to green buildings and operate and maintain buildings according to Leed rating system. There are different systems for green buildings like Breeam, Green Globes etc. but we opted for Leed rating system as it covers more aspects of the building than any other system. A case study has been done on 3 Marla (816.752 square feet) house to show how we can operate and maintain a house according to Leed rating system. We use energy efficient sources, materials and items that can not only reduce pollution but also have a positive impact on the environment. We mainly focus on the sources, materials and items which are easily available in our country to make it more convenient and easy for the people. But the most important part of constructing or operating and maintaining a house according to LEED rating system is the return on investment (ROI) factor.

Keywords- Green Buildings, Leed, Rating Systems, Operation and Maintenance.

1 Introduction

The construction industry is one of the oldest industries that continues to contribute to the financial development of Malaysia [1,2]. The local construction industry needs to keep evolving by following in the footsteps of the Industrial Revolution 4.0 so that improvements can be made [3,4] Operation and maintenance of green buildings using the LEED rating system begins by exploring history of the green building movement. Many people contribute to the modern green building movement in the United States to the creation of the US Green Building Council in 1993 [5]. One of the most well-known green building rating systems in the United States is the LEED (Leadershipin Energy and Environmental Design) rating system. Created by the US Green Building Council,the LEED rating system provides a framework to create healthy, highly efficient, and cost-saving green buildings. This essay focuses on a relatively new area of sustainability as it applies to greenbuilding operation. During the past few decades, the use of green building operation has significantly increased. "Operation" refers to the decisions, systems, and methods used to ensure that a building performs and functions as intended. "Maintenance" signifies the continuous processof identifying, prioritizing, and carrying out recurring and non-recurring work [6].

2 Green Buildings

2.1 Overview of Green Buildings

As the process of urbanization more and more developed, the problems of environment and energy have further attracted people and society's concern [1]. The concept of green buildings has thus assumed the mantle of the overall theme in the contemporary construction process [9]. Green buildings' focus influences are to diminish the general impact of the

prescribed construction on inhabitants' wellbeing and the physical environment through efficient use of vitality, water and other resources, enhancing tenant health and boosting workers' productivity, reducing waste, pollution and ecological degradation.

2.2 LEED Rating System

LEED (Leadership in Energy and Environmental Design) is the world's most extensively used green structure standing system. LEED instrument provides a frame for healthy, largely effective, and cost- saving green structures, which offer environmental, social and governance benefits. To achieve LEED instrument, a design earns points by clinging to prerequisites and credits that address carbon, energy, water, waste, transportation, accoutrements, health and inner environmental quality. Green buildings are innovative structures of sustainable development in this age; since they create harmony of social, economic and environmental sustainability [7].

3 Methodology

The Figure 1 shows that a 3 Marla (816.752 square feet) house has been selected and we converted it into a green building by operating and maintaining it by using energy efficient items, sources and materials. We have replaced conventional items with energy efficient ones which obviously costed more but it will return our investment in a year or two as we don't need to pay electricity bills as we have installed a solar panel in this house. Similarly, there are other efficient items and materials also used as listed in the cost analysis Table 1. We have used items that are easily available in Pakistan. The cost that we need is around 25-26 lakhs PKR to make this house energy efficient and environment friendly which is obviously not high when we consider a return on investment (ROI) factor.

4 Result

The case study in this paper proves that green building is not only energy efficient and environment friendly but also decreases the monthly operating and maintaining cost of a house. We have operated this house for about four months and observed significant decrease in electricity bills and reduction in water consumption as low flow faucets were installed. Moreover, quality of indoor air has also improved in the house. The result shows that return on investment is 78.56% and also increase in property values ranges from 1.2% to 3.28%.

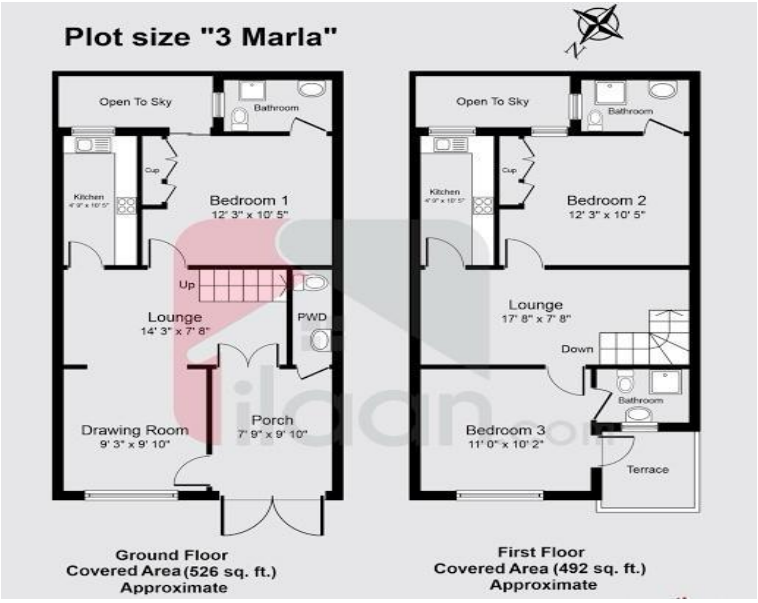

Figure 1: Drawing of 3 Marla (816.752 sq. ft.) House

All the lights are replaced with LED ones and after replacing all the electricity items such as normal refrigerators with low impact refrigerators and other items with efficient ones they are operated on solar panels which greatly reduces the electricity bills to almost nil. In this part of the world where we don't have much rain and its mostly sunny days we can't store water instead we can reduce water consumption by placing low flow faucets which makes the house water efficient. To prevent direct sun light coming into the house which eventually heat up the house double glazed windows are used instead of the conventional windows which are single glazed. Non- Toxic paints are also used which improves the indoor air quality and insulation sheets are also installed which prevents the house from heat in summers and cold in winters.

Table 1: Cost Analysis

Materials	**Quantity**	**Cost (RS)**
Solar Panel(complete system)	10	(5 kw) = 750000
LED lights.	8	Rs 5675/(8 pieces) = 5675 RS
Double glazed Bedroom#3 windows 6×8(ft.)	1	Rs 1900/sq. ft. Window = 91200 RS
Non-toxic paints	40 Gallons	Rs 4000/Gallon = 160000
Insulation sheets	500 sq. m	13000 RS
Bathroom windows 2×2(ft)	3	22800 RS
Kitchen windows 3×4(ft.)	2	45600 RS
Double glazed Bedroom#1&2 windows 2.5×3(ft.)	2	28500 RS
Drawing room windows 6×8(ft.)	1	91200 RS
Low flow faucets	10	8000/faucet= 80000 RS
Automated HVAC system	1	800,000 RS
Fiber doors (Inside the house)	12	8000/door = 96000 RS
Natural Repellents	4	926/ repellent = 3704 RS
Solar shades	5	230/sq. ft. = 16445 RS
Tank less water heaters	3	14000/tank = 42000 RS
Air purifiers	3	15,499/purifier = 46497 RS
Low Impact Refrigerators	2	112024/refrigerator = 224048 RS
Locally source building materials	Steel, fly ash bricks,	According to requirements -
Green Roof Materials	-	-
VOC-Free adhesives	-	1300-1500 RS/ bag
Green concrete	-	According to requirements
Sensor lights	8	4000/light = 32000

6 Practical Implementation

This experimentation helps in selecting the most effective materials and items to enhance the building's efficiency and make it environmental friendly.

7 Conclusion

In conclusion, the paper has articulated a set of comprehensive strategies for maintain and operate a home based on the LEED principles. As it is clearly mentioned above that by replacing the conventional items with energy efficient ones as they are mentioned in the Cost Analysis Table 1 the efficiency of the house improves. The objectives of the strategies have been energy and water efficiency as low flow faucets are installed, using of sustainable materials and incorporation of smart technology in operation. Home owners that can afford the investment stand a chance to reap long-term benefits as the utility costs will reduce. More so, the environmental footprint will be minimal compared to the beginning. This is even though will be costly at the start. Additionally, the paper has shown some of the financial reports and the environmental benefits of the adoptions and practices of the assessed strategies, and they are a wise and responsible decision of homeowners who want to have greener more comfortable home. More so, the LEED rating system is vital in operating and maintaining green buildings.

References

[1] Ali Hauashdh, Sasitharan Nagapan, Junaidah Jailani, Yaser Gamil, An integrated framework for sustainable and efficient building maintenance operations aligning with climate change, SDGs, and emerging technology, Results in Engineering,Volume 21,2024,

[2] Alaloul, W.; Musarat, M.; Rabbani, M.; Iqbal, Q.; Maqsoom, A.; Farooq, W. Construction Sector Contribution to Economic Stability: Malaysian GDP Distribution. Sustainability 2021, 13, 5012.

[3] Musarat, M.A.; Alaloul, W.S.; Hameed, N.; Qureshi, A.H.; Wahab, M.M.A. Efficient Construction Waste Management: A Solution through Industrial Revolution (IR) 4.0 Evaluated by AHP. Sustainability 2022, 15, 274.

[4] Gamil, Y.; Abdullah, M.A.; Rahman, I.A.; Asad, M.M. Internet of things in construction industry revolution 4.0: Recent trends and challenges in the Malaysian context. J. Eng. Des. Tech. 2020, 18, 1091–1102.

[5] J. Si et al. Assessment of building-integrated green technologies: a review and case study on applications of Multi-Criteria Decision Making (MCDM) method Sustain. Cities Soc. (2016)

[6] Y. Zhang et al. Comparison of evaluation standards for green building in China, Britain, United States Renew. Sustain. Energy Rev. (2017)

[7] A. Valentin et al. A guide to community sustainability indicators Environ. Impact Assess. Rev. (2000)

[8] S.W. Yoon and D. K. Lee, "The development of the evaluation model of climate changes and air pollution for sustainability of cities in Korea," Landscape and Urban Planning, vol. 63, no. 3, pp. 145–160, Apr. 2003, doi:

[9] "LEED v4: Building Operations + Maintenance Guide | U.S. Green Building Council," www.usgbc.org.

OPTIMIZING ENERGY PERFORMANCE OF BUILDINGS IN PAKISTAN USING BIM

[a] Said Haseebullah*, [b] Fahad Aslam

a: Civil Engineering Department, COMSATS University Islamabad, Abbottabad Campus, Pakistan. saidhaseebullah195@gmail.com
b: Civil Engineering Department, University of Engineering and Technology, Taxila, Pakistan. aslamfahad113@gmail.com
* Corresponding author.

Abstract- An unprecedented increase in global and national energy demand has arisen due to the rapid development of infrastructures and population growth. The residential sectors consume the major share of energy resources, up to 22% of the world's total energy consumption. In Pakistan, the residential sector consumes an average of 45% of the nation's energy resources. To address this issue and mitigate the escalating demand, the optimization of energy resources is required. The Phase Change Material (PCM) has been approved as a vital source for enhancing energy usage worldwide. In PCM, the material can store and release energy as it undergoes the transition stage. Utilizing the PCM in the building envelope, particularly in Peshawar, with distinct heating and cooling requirements, makes it possible to reduce energy consumption substantially. Extensive analysis reveals that PCM A25H exhibits the highest performance, achieving an impressive energy efficiency of 8.82%. To further investigate the impact of PCM thickness and its strategic placement within walls and roofs. The analysis outcomes demonstrate that applying a 40mm PCM coating on the interior side of building walls and roofs in Peshawar can significantly reduce energy consumption.

Keywords- Energy Performance, BIM, Phase Change Material, Energy Model.

1 Introduction

In recent years, it has been observed that the development of infrastructures has increased exponentially, which results in more energy consumption of valuable resources. Pakistan is an underdeveloped country with very limited energy resources, and the residential sector is the major source of energy consumption. In the last two decades, the usage and optimization of energy resources in Pakistan have not been done properly as the world is moving towards sustainable infrastructure development and maximum utilization of available natural resources to decrease energy resource usage [1]. Building Information Modeling (BIM) has emerged with the immense potential to revolutionize building design, construction, and operation using Phase Change Materials (PCM). Therefore, extensive studies are required to provide the roadmap for future residential constructions in Pakistan, understand the applications of PCM in Pakistan, and optimize energy performance [2].

Concerns about the dependability of the energy supply are growing due to the expansion of the population and industrialization. Based on UN estimates, assuming the growth rate remains constant at 1.07% starting from 2020, with a population of 7.8 billion, the global population is projected to reach 9.7 billion by the conclusion of 2050 [3]. Similarly, it is expected that there would be a 19% rise in the worldwide energy consumption by the conclusion of 2040. With the rapid growth of the world's population, there is a corresponding increase in people's reliance on equipment and appliances for their comfort and mobility. Consequently, this exacerbates the issue of global warming. These factors are contributing to the global increase in energy consumption [4]. Given the rising energy demand in Pakistan, there has been a noticeable increase in the disparity between energy supply and demand. Therefore, it is crucial to implement necessary measures to address the energy crisis. To ensure rigorous adherence to construction regulations for thermal efficiency in buildings, the most widely used method is to augment the insulation thickness. The lightweight façade option, sometimes known as

curtain walls, has experienced an increase in popularity due to limited space constraints. Lightweight construction has benefits such as accelerated construction timeframes, more design flexibility, and cost-effectiveness [5]. Given these conditions, there is a growing interest in thermal energy storage devices that can conserve energy in buildings. Phase change materials (PCMs) with latent heat storage capabilities have attracted considerable study. These phase change materials (PCMs) have a high thermal energy storage capacity and are efficient at retaining heat. [6] Through the process of absorbing heat throughout the daylight and subsequently releasing it during cooler periods. PCMs play a crucial role in managing temperature management within buildings, leading to substantial reductions in energy consumption. Several energy-saving rules have been created, including Pakistan's building codes established in 2013 [7]. However, these codes are not being enforced in the construction of residential buildings, which are still being built using old materials. To achieve energy efficiency, it is necessary to consider strategies for low-carbon buildings and techniques for net-zero energy buildings [8]. The PCM method has demonstrated superior outcomes due to its specific temperature needs. PCM can be controlled by the utilization of fans and natural air circulation during the summer, leading to a reduction in the need for supplementary cooling devices and resulting in lower temperatures in walls and rooms.

To successfully integrate Phase Change Materials (PCM) into buildings, several key elements must be considered. These include the specific type of PCM to be used, the prevailing local temperature conditions, the weight restrictions, and the most suitable sites for installation. Although PCMs have potential applications in both active and passive building energy systems, there is a lack of research on incorporating PCMs into building envelopes in Pakistan. Hence, it is imperative to conduct more extensive research that considers numerous design components and the varied climatic conditions prevalent in different cities of Pakistan. These investigations will offer useful insights into the possible advantages of PCM integration in the Pakistani environment.

2 Research Methodology

The study evaluates the impact of incorporating phase change material (PCM) into a building's structure to improve insulation. For improved insulation, PCM was added, double-pane windows were used, and the window-to-wall ratio was decreased. The study uses variable energy models to predict the behavior of PCM during charging and discharging, considering their volatile nature. Autodesk Revit (Student Version) software is used for modelling, while the Insight Building performance analysis program performs dynamic energy modelling and heat transfer calculations [10]. The models integrate internal loads, including occupants, machinery, and lighting, allowing comprehensive evaluations of power and energy use. The Figure 1 shows the 3D view of a proposed building. This tool is crucial for architects, engineers, and designers to optimize energy efficiency and minimize environmental impact in building design and operation.

Figure 1: 3D view of Proposed Building

2.1 Phase Change Materials (PCMs)

The research aim is to assess several Phase Change Materials (PCMs) and determine the best appropriate PCM for the climatic conditions in Peshawar. The choice of PCM is determined by the standard room temperatures (18–25°C) often observed in residential properties in Pakistan. Previous research has thoroughly examined these Phase Change Materials (PCMs) and demonstrated their potential to enhance the energy efficiency of buildings. Table 1 displays the essential attributes of the chosen PCM. To evaluate the efficiency of each Phase Change Material (PCM) in terms of the building's

yearly energy consumption, they are separately integrated into the building's structure. The study attempts to identify the most efficient phase change material (PCM) for minimizing energy usage in buildings by analyzing the energy performance of several PCMs.

Table 1: Property of Phase Change Material

Material Name	(Melting, freezing Temp (℃)	Freezing Temperature (℃)	Density (kg/m^3)	Thermal conductivity (W/m.K)	Specific Heat (KJ/KG.K)
RT21HC	21	20	825	0.2	2
RT22HC	22	20	730	0.2	2
RT25HC	25	22	825	0.2	2
SP25E2	25	24	1450	0.5	2
A25H	25	25	810	0.18	2.15
M182/Q21	24	21	235	0.11	1.97

2.2 Energy Model of Building

Building performance analysis often begins with designing a conceptual model in Revit, which can be transformed into an energy model that can be analyzed in Insight. Figure 2 shows the energy model of the building. This model can be adjusted to suit unique requirements and project constraints. The energy model's generation and forecasting precision depend on energy choices. Users can fine-tune the model's behavior to fit their specific requirements. Adding more specific data, such as material parameters and thermal space properties, improves the model's accuracy. This allows for a more comprehensive evaluation of the building's energy performance and better decisions regarding sustainability and energy efficiency solutions. Insight helps identify desired outcomes and identify areas for improvement. With sustainability goals like the 2030 Challenge and Net Zero, Insight is a vital tool for achieving sustainability goals.

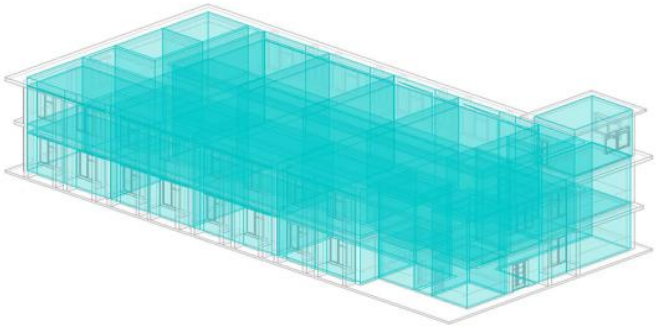

Figure 2: Energy Model of Building

2.3 Optimal Energy Reduction Option

The initial window-to-wall ratio in the study was 58%. The ratio was subsequently decreased to 30% and 20% to improve energy efficiency. Application of various phase change materials (PCMs) and evaluation of changes in energy usage resulted in analysis. The observed effects of these modifications and the integration of PCMs on energy performance are depicted in the accompanying. The studies showed that the PCM A25H is the most efficient for energy savings after extensive examination. This PCM choice produced a noteworthy 8.84% annual total energy reduction. The choice of PCM A25H as the best option highlights its potential for significant energy savings and underlines its suitability for boosting building energy efficiency. Table 2 shows the comparison between all three conditions

Table 2: Annual Consumption of Heating and Cooling with Different Condition

CM	Heating Condition			Cooling Condition		
	Existing Condition (kw-h)	PCM with 30% Win/wall (kw-h)	PCM with 20% Win/wall (kw-h)	Existing Condition (kw-h)	PCM with 30% Win/wall (kw-h)	PCM with 20% Win/wall (kw-h)
RT21HC	175582.7059	174912.4523	174437.3841	618868.2777	620665.0964	619655.4664
RT22HC	175595.308	175770.8576	174444.4178	618880.2934	625558.7976	619669.8269
RT25HC	175570.69	174899.8503	17663.4866	62008.86255	620648.6844	617895.2814
SP25E2	175796.3	175348.2491	174885.1967	619880.34	626159.5933	625319.0654
A25H	175436.4635	174752.4335	174266.8176	618051.4883	619840.3943	618810.2494
M180	175716.3464	175051.9542	174575.4206	619283.8523	621112.6159	620128.4832

3 Conclusion and Recommendations

The study suggests that Pakistan's growing population and urbanisation may lead to an energy crisis. To address this, a guide for designing energy-efficient residential buildings in Peshawar is presented, focusing on the use of Phase Change Materials (PCMs). Simulations using DOE-2 algorithms and Revit Insight were conducted on six PCMs, double-pane windows, and reduced window-to-wall ratios. The findings show that using A25H with a 20% window-to-wall ratio and double-pane windows can reduce heating and cooling energy consumption by up to 8.84%. Further research is needed to assess the effects of PCM features on heat transport and transition temperature. The feasibility and financial sustainability of incorporating PCM technology in construction projects need to be evaluated.

References

[1] Khan, M.,Ahmad, H., Tariq Shah, Taimur Mazhar Sheikh, & Shoaib Muhammad. (2024). https://uow.edu.pk/ORIC/MDSRIC/Publications/8th%20MDSRIC-154.pdf.MDSRIC,1–5

[2] H. M. A. Iqbal, I. G. Chaudhry, and S. M. Cheema, "Exploring the Role of BIM In Supporting Sustainable Design and Construction of Green Buildings", AHSS, vol. 5, no. 2, pp. 14–25, Apr. 2024

[3] "World Population Prospects 2019: Highlights," Statistical Papers - United Nations (Ser. A), Population and Vital Statistics Report, Jun. 2019, Published, doi: 10.18356/13bf5476-en.

[4] "World Energy Outlook 2020 - Annex B - Data Tables," World Energy Outlook 2020, Oct. 2020, Published, doi: 10.1787/3e2fe963-en.

[5] V.Cheng and E. Ng, "Comfort Temperatures for Naturally Ventilated Buildings in Hong Kong," Archit Sci Rev, vol. 49, no. 2, pp. 179–182, Jun. 2006, doi: 10.3763/asre.2006.4924.

[6] J. Kośny, PCM-Enhanced Building Components. Cham: Springer International Publishing, 2015. doi: 10.1007/97831914286-9.

[7] Z. Usman and K. Ibrahim, "A Comparative Analysis of Energy Provisions of Pakistan Building Code with Indian and USA Building Energy Codes," Journal of Art, Architecture and Built Environment, vol. 1, no. 1, pp. 52–68, May 2018, doi: 10.32350/jaabe/11/03

[8] M. M. Rafique and S. Rehman, "National energy scenario of Pakistan – Current status, future alternatives, and institutional infrastructure: An overview," Renewable and Sustainable Energy Reviews, vol. 69, pp. 156–167, Mar. 2017, doi: 10.1016/j.rser.2016.11.057..

[9] A. G. Anter, A. A. Sultan, A. A. Hegazi, and M. A. E. Bouz, "Thermal performance and energy saving using phase change materials (PCM) integrated in building walls," Journal of Energy Storage, vol. 67, p. 107568, Sep. 2023, doi: 10.1016/j.est.2023.107568

FACTORS EFFECTING STAKEHOLDER ENGAGEMENT IN DESIGN BID BUILT

[a] Mehar Ali*, [b] Abdul Qadeer

a: Department of Civil Engineering, University of Engineering and Technology, Taxila, Pakistan. meharaliali25@gmail.com
b: Department of Civil Engineering, University of Engineering and Technology, Taxila, Pakistan. abdul.qadeer@uettaxila.edu.pk
* Corresponding author.

Abstract-. This study examines stakeholder management in Design-Bid-Build (DBB) projects, a previously under-researched area. Using a mixed-method survey with expert input, we highlight the critical role of early stakeholder involvement, particularly during project selection. The research also identifies opportunities for improvement, such as ongoing needs assessment, culturally adaptable project structures, and fostering stakeholder awareness of social, economic, and environmental (SEEEEPLL) considerations. We propose a strategic approach focused on early engagement, continuous needs evaluation, and culturally sensitive structures. This approach, combined with enhanced SEEEEPLL understanding, can significantly improve stakeholder participation and project outcomes in DBB environments.

Keywords- DBB Projects, Stakeholder Management, Project Management, Stakeholder Engagement.

1 Introduction

According to the PMI a stakeholder is defined as "Stakeholders can be individuals, groups, or organizations that may affect, be affected by, or perceive themselves to be affected by a decision, activity, or outcome of a portfolio, program, or project. Stakeholders also directly or indirectly influence a project, its performance, or outcome in either a positive or negative way" [1]. The terminology stakeholder is broadly explained by various professional and well-known organizations such as Project Management Institute (PMI) in his book PMBOK 7th edition. According to this a stakeholder can affect a project in many ways in terms of scope, cost, scheduling, outcomes, success etc. and these are not limited. In most cases the stakeholder is engaged throughout the project life cycle. With the traditional Design-Bid-Build (DBB) project delivery system, the project owner contracts with different organizations for the design and construction stages. The design phase is completed first in DBB, and then contractors bid for the building work using the finalized blueprints. Insufficient management of stakeholders can lead to significant problems, such as delays or exceeding the budget. Therefore, it is important to consider the needs and concerns of all stakeholders at every stage of a project. This article will delve into the importance of stakeholder management in project management. To gain a more comprehensive understanding of the topic, we will analyze examples and theories from past studies.

2 Literature Review

Project delays, public conflicts, and legal disputes resulting from inadequate stakeholder management at the Zhuhai-Hong Kong-Macao Sea crossing bridge demonstrate the need to involve stakeholders in projects. Numerous research confirms the need of include stakeholders in building projects and show how it can improve important aspects like quality, cost, and schedule [2]. Still, a large amount of the literature now in publication focuses on collaborative delivery techniques like Integrated Project Delivery (IPD), which leaves a dearth of studies that particularly address stakeholder management inside the Design-Bid-Build (DBB) paradigm [3]. Dealing with competing interests in DBB contracts and engaging with stakeholder's present difficulties, as has been acknowledged [4] in-depth examination of other stakeholder management

strategies in Design-Bid-Build (DBB) projects is yet lacking [5]. Engaging stakeholders is essential to project success, sustainable development, and handling complex socioeconomic dynamics [6].
Either internal or external stakeholders have a big influence on how a project turns out. For one to control their impact and expectations, one must assess and communicate clearly [7]. Important phases in this process are identifying and classifying

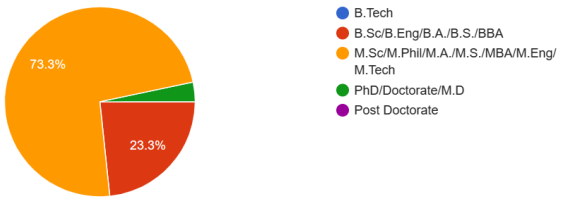

Figure 1: Highest academic qualification

stakeholders and depending on professional opinion [8]. By analyzing the duties, contributions, and commitments of stakeholders, one can better understand their interests and power relations, which makes coalitions and partnerships that support project success possible [9]. We will look at many points of view on these issues and offer original fixes that work inside the DBB framework. Various studies underscore the importance of stakeholder engagement in construction projects, emphasizing its positive influence on key success factors such as cost, schedule, and quality [1] [2].However, much of the existing literature primarily focuses on collaborative delivery methods like Integrated Project Delivery (IPD), leaving a gap in research specifically addressing stakeholder management within the Design-Bid-Build (DBB) framework [3]. Challenges related to stakeholder communication and conflicting interests in DBB contracts have been acknowledged [4]. While some studies suggest Building Information Modeling (BIM) to enhance stakeholder collaboration, comprehensive analysis of unconventional solutions for DBB stakeholder management remains limited [5]. A recent study highlights the importance of integrating advanced stakeholder management practices to address the dynamic challenges in modern construction projects (Doe, 2024). This paper aims to fill this void by providing a targeted examination of stakeholder management challenges in DBB projects and proposing innovative solutions tailored to this framework. Effective stakeholder engagement is crucial for project success, facilitating sustainable development and addressing complex socio-economic interactions [6]. Stakeholders, whether internal or external, play pivotal roles in project outcomes, necessitating careful analysis and communication to manage their influence and expectations [7]. We will explore unique perspectives on these challenges and propose innovative solutions that can be applied within the DBB framework. This study uniquely addresses stakeholder management within the Design-Bid-Build (DBB) framework, which has been under-researched. By focusing on early stakeholder involvement and continuous needs assessment, the research provides novel strategies to improve project outcomes in DBB projects. This work contributes significantly to the field of project management by offering practical solutions to enhance stakeholder engagement and project success. Existing literature focuses mainly on collaborative delivery methods like Integrated Project Delivery (IPD), leaving a gap in research on stakeholder management in the Design-Bid-Build (DBB) framework. This study addresses this gap by exploring DBB-specific challenges and proposing solutions, emphasizing early stakeholder involvement and ongoing needs assessment. Recent studies highlight the significance of stakeholder engagement in construction projects for enhancing value creation and overall project performance. For instance, Landorf (2024) emphasizes the role of early and continuous stakeholder involvement in achieving sustainable project outcomes. Similarly, Nguyen et al. (2024) discuss innovative strategies for managing external stakeholders to mitigate conflicts and improve project delivery.

3 Research Methodology

This study employs a robust mixed-methods approach to thoroughly examine stakeholder management in Design-Bid-Build (DBB) projects, ensuring both depth and relevance in its findings.
1. Expert Consultation: The Delphi Technique was utilized to harness the insights of seasoned experts with 15 to 20 years of experience in project management, engineering, and stakeholder engagement. This structured method involved multiple rounds of consultation to integrate expert opinions into the study design (see Figure 1).

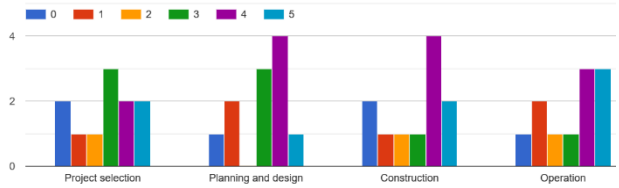

Figure 2: Understanding stakeholder interest and its dynamics.

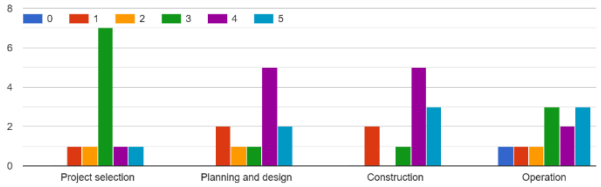

Figure 3: Exploring stakeholders' needs and its dynamics.

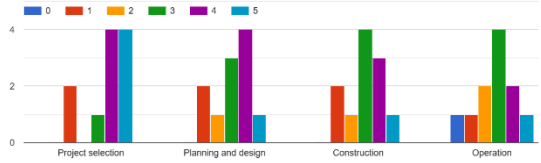

Figure 4: Flexible project organization and its cultural attributes.

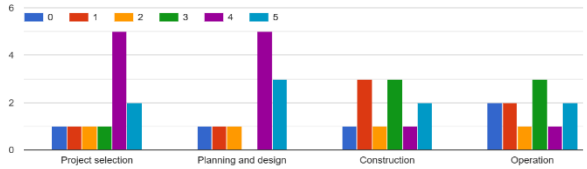

Figure5: Managing project responsibilities and its dynamics (social, economic, ethical, environmental, ecological, political legal and cultural).

2. Survey Design: Leveraging the expert insights, a comprehensive online questionnaire was developed using Google Forms. This survey covered critical aspects of stakeholder management, including identification, engagement, and the impact of cultural and organizational factors (see Table 1 for the detailed survey structure).
3. Data Collection: The survey was widely distributed among professionals engaged in DBB projects, collecting valuable data on stakeholder engagement activities and their effectiveness across various project phases.
4. Data Analysis: The collected responses were meticulously analyzed to identify prevalent practices and challenges in stakeholder management within the DBB framework. Advanced statistical methods were applied to evaluate the significance of different factors affecting stakeholder engagement (see Figure 2).
5. Validation: To ensure the accuracy and relevance of the findings, follow-up interviews were conducted with selected experts, providing a layer of validation to the study results.
This detailed and methodical approach ensures a comprehensive understanding of stakeholder dynamics in DBB projects, offering actionable insights to enhance stakeholder management practices effectively.

Table 1: Stakeholder Engagement Activities in Design-Bid-Build (DBB) Project

Project Phase	**Stakeholder Engagement Activities**
Selection	Early stakeholder involvement - Needs assessment workshops - Stakeholder forums for input
Planning	Regular stakeholder meetings - Incorporating feedback into designs
Construction	Ongoing communication - Site visits and tours - Addressing concerns and conflicts
Operation	Continuous engagement - Feedback mechanisms - Forums for long-term impacts

4 Results and Discussion

The survey results provide a comprehensive overview of stakeholder management in Design-Bid-Build (DBB) projects. The findings reveal that stakeholder interests are most significant during the project selection phase (see Figure 2). Early stakeholder engagement is critical, as it allows project managers to align project goals with stakeholder expectations, facilitating smoother project execution. As the project progresses, the impact of stakeholder interests tends to diminish. During the project selection phase, the importance of needs assessment workshops and stakeholder forums becomes evident. These early engagements help identify potential issues and align project objectives with diverse stakeholder interests, thereby reducing conflicts and delays later in the project. The planning and design phase also benefits significantly from regular stakeholder meetings and incorporating feedback into designs. This continuous engagement ensures that stakeholder needs are consistently addressed, contributing to a more refined and acceptable project design. During the construction phase, ongoing communication through regular meetings, site visits, and addressing concerns promptly were highlighted as effective strategies for maintaining stakeholder engagement (see Table 1). These activities are vital for managing expectations and ensuring the continuous incorporation of stakeholder feedback.

In the operation phase, continuous stakeholder engagement through feedback mechanisms and forums is essential to address long-term impacts and ensure sustained stakeholder satisfaction (see Figure 3). Interestingly, the survey indicated that social, economic, ethical, environmental, ecological, political, legal, and cultural (SEEEEPLL) responsibilities have a lesser impact on stakeholder engagement across the project lifecycle (see Figure 4). Survey findings show that SEEEEPLL duties are not seen to have much of an influence on the project lifetime (see Figure 5). These results provide important new information for raising stakeholder management in DBB initiatives. The little effect that SEEEEPLL duties are shown to have implies that stakeholders need to be made more aware of them. Project success may be much influenced by the efficient management of various (social, environmental, ethical, etc.) elements. This suggests a need for increased awareness and integration of SEEEEPLL considerations in stakeholder management practices. The mixed responses on project organization and cultural characteristics indicate a need for greater flexibility in project structures to accommodate diverse stakeholder needs. Promoting cultural awareness within project teams can improve stakeholder interactions and contribute to project success. Follow-up interviews with experts validated the survey findings, reinforcing the importance of early engagement, continuous communication, and flexible project structures. These practices are essential for effective stakeholder management and successful project outcomes in the DBB framework. By expanding on these key findings, the paper provides a comprehensive analysis of stakeholder management in DBB projects, offering practical insights and recommendations for improving stakeholder engagement practices. The data analysis in this study is primarily explained through detailed charts and figures rather than tables. While tables are useful, the use of charts and figures ensures complex information is communicated more effectively.

5 Practical Implementation

To address this diversity, we provide a strategic approach to managing stakeholders that emphasizes early involvement, incorporates ongoing evaluation of stakeholder demands throughout the duration of the project, and promotes flexible project structures that consider cultural settings. An enhanced and sustainable strategy for achieving project success may be achieved by increasing the understanding and commitment of all project participants towards their SEEEEPLL responsibilities. DBB project teams may use stakeholder participation to enhance the groundwork for a victorious project delivery and project results.

6 Conclusion

This research using multiple methods looked at stakeholder management procedures in DBB projects. The results confirm earlier studies on the value of early stakeholder involvement, especially in the process of choosing a project. Ongoing needs assessment, project organization flexibility, and knowledge of SEEEEPLL concerns are among the areas where the study also points up room for development.

References

[1] P. M. I. P. M. Institute, A Guide to the Project Management Body of Knowledge (PMBOK® Guide) – Seventh Edition and The Standard for Project Management (ARABIC) Section (3.3) page 31. Project Management Institute, 2021.
[2] R. E. Freeman, Strategic management: A stakeholder approach. Cambridge university press, 2010.
[3] G. Ballard. "Integrated Project Delivery (IPD): A new paradigm for project success." https://en.wikipedia.org/wiki/Integrated_project_delivery (accessed.
[4] C. M. Wong, Holt, G. D., & Li, H. (2012). "Managing conflicting interests in DBB construction contractsts: A stakeholder perspective. Construction Management and Economics," pp. 30(8-9), 723-744., 2012.
[5] A. Bahadorestani, N. Naderpajouh, and R. Sadiq, "Planning for sustainable stakeholder engagement based on the assessment of conflicting interests in projects," Journal of Cleaner Production, vol. 242, p. 118402, 2020/01/01/ 2020, doi: https://doi.org/10.1016/j.jclepro.2019.118402.
[6] P. M. I. P. M. Institute, A Guide to the Project Management Body of Knowledge (PMBOK® Guide) – Seventh Edition and The Standard for Project Management (ARABIC) Section (1.3) Project Management Institute, 2021.
[7] Y. Riahi, "Project stakeholders: Analysis and management processes," SSRG International Journal of Economics and Management Studies, vol. 4, no. 3, pp. 37-42, 2017.
[8] J. FERNANDO. "What Are Stakeholders: Definition, Types, and Examples." https://www.investopedia.com/terms/s/stakeholder.asp (accessed
[9] P. M. Institute, A Guide to the Project Management Body of Knowledge: PMBOK Guide Section 13.1 page (391-398). Project Management Institute, 2013.

AN INSIGHT INTO PROSPECTS AND CHALLENGES OF 3D PRINTING IN DEVELOPING COUNTRIES

[a] Sadia Sajid Khan*

a: Kinetics Contracting LLC, Ajman, United Arab Emirates. sadialohani@hotmail.com
* Corresponding author.

Abstract- The incorporation of 3D printing technique in construction demonstrates substantial promising opportunities for developing and under developing countries, that includes notable improvements in productivity, considerable cost minimizing, and eco-friendly construction provisions. This paper reviews the achieved milestones, prospects, and challenges linked with the integration of 3DP in the construction industry. Regardless of its benefits, such as reduced construction time and less material wastage, several challenges restrict its prevalent implementation. These challenges include high initial capital, lack of skilled labour, insufficient codes and regulatory frameworks, and technical risks related to material properties and printability. This review focuses the need of strategic resource allocation, organizing the training programs, and the establishment of regulatory guidelines. Emphasis is also placed on the importance of collaborative efforts between governments, academia, and industry stakeholders to encounters these challenges and utilize the full potential of 3DP technology in the construction sector.

Keywords- Additive Manufacturing, Material Optimization, Process Efficiency, Regulatory Challenges.

1 Introduction

The construction industry is a key element of economic prosperity and societal development, but it also reflects one of the most environmentally adverse sectors worldwide [1]. Conventional construction methods are often overwhelmed by shortcomings, high capital cost, and notable carbon footprints, adding to approximately 40% of global carbon emissions. To counter these challenges, the introduction of additive manufacturing, most familiar by the term of 3-Dimensional Printing technology, unveils the transformative step towards sustainable and optimized construction practices [2]. 3D printing in construction encompasses the layer-by-layer addition of materials under computer control to create three-dimensional structures. This technique has numerous benefits, that entails lessened material waste, less manpower, and the ability to build complex designs that are not do-able with conventional methods. Regardless of these benefits, the implementation of 3D printing in construction, particularly in developing countries is difficult.

One of the crucial challenges is the high initial cost of 3D printing construction and the specific machinery and instrumentation required. Developing countries often face difficulties with limited finances, that makes it impossible to allocate resources in such advanced technologies. Furthermore, there is a shortage of skilled labor to operate and handle 3D printing machinery, thus impeding its general adoption. Moreover, regulatory and standardization issues pose substantial barriers. Many developing countries lack comprehensive regulations and standards for 3D-printed structures, leading to concerns about the safety, durability, and quality of these buildings [3]. Without preset standards, it is difficult for construction firms to obtain the necessary approvals and certifications, slowing the incorporation of 3D printing technology into mainstream construction practices. Regardless of all challenges and risks, the prospects of 3D printing construction are promising. It has the potential to resolve the issue of housing and infrastructure deficits that many developing countries face. For instance, 3D printing can notably shorten the construction times, accelerating emergency shelters and necessary infrastructure. Moreover, the environmental and economic benefits of reduced waste and carbon dioxide emissions are the main milestones towards sustainable construction, placing 3D printing as a promising option towards green building initiatives [4].

2 3D Printing Technology in Construction Industry

Additive Manufacturing is well known by the term of 3D printing technology. It encompasses modeling of any multi-dimensional object by adding material in layers according to 3D digital file. The first 3D object was developed in 1987 by 3D printing system [5]. 3D printing allows for more geometric freedom and complexity. The structural reliability of 3D-printed constructions depends on both the factors kept under consideration and overall print quality. Bond strength, deformation resistance and other strength parameters depends on equipment selection i.e., shape and size of nozzle, thickness of layer and layering time, pump speed, its printing time and printing path.

The construction process of structure by 3D printing technology has three main steps [1]. The design step involves the preparation of 3D model using computer aided design (CAD) software. This design can be obtained by 3D scanning of the existing object. This CAD model is then converted into stereolithography file. The STL file is then imported into slicing software that splits the model into multiple thin layers and gives programming G-code file which has detailed instructions for parameters for every layer to be printed. The 3D printer deposits material layer by layer in accordance with the G-code instructions in a bottom – up sequence. Numerous materials like ceramic, metal, resin, and plastic can be used in this technology. Post - processing of the final object may need curing, painting or other finishing procedures. D – shape or powdered based printing machines are used in the concrete construction. In a powder - based system, four major parts controls the whole system. A thermal head is coupled with a robot and two hose pumps. The concrete material is supplied by the first pump, while the accelerator is supplied by the second and micro-controller controls all the three parts. In Gantry based system, a peristaltic pump is connected to the thermal head which is controlled by using a four-degree of freedom mechanism. The printer head is attached to the vertical arm, it has a nozzle attached to it, which is usually composed of steel. The nozzle size and shape depend on the selected technique. Predominant techniques used in 3D printing technology for concrete structures are counter crafting, Powder Jetting method [3], and 3D printed formwork methods [6].

3 Attainment in Developed Countries

Notable 3D printed buildings are constructed worldwide which reflects the potential of this technique. In Wellington, USA, Printed Farms marks a significant milestone, comprises a covered area of approx. 10,000 sq.ft. Apis Coir constructed a 38 m^2 house in Moscow in 24-hours which had a unique shape. That shape was chosen to manifest its adaptability to construct any building shape and 50-70% cost reduction was reported as compared to conventional block wall method. During the construction of mentioned buildings, severe winters followed by -35 degree Celsius was recorded and the 3D printable mixture was workable only till -5 degree Celsius, so additional insulations were done. Similarly, the same reputed company constructed Office of the Future in Dubai which was reported to reduce the construction cost by 50-70 percent, waste reduction by 60 percent and labor expense by 50-70 percent. Pedestrian bridge in China is one of the milestones of 3D construction which highlights its capability to adapt to structures other than housing. In this project, 33% cost reduction was reported mainly due to the elimination of moulds and reinforcing bars. Some other examples of such structures are given in Table 1 given below.

Table 1:Notable projects in 3D printing construction [5], [6], [7], [8]

S. No	Buildings	Countries
1	Printed Farms Equestrian Facility	Wellington, Florida, USA
2	Detroit's First 3D Printed Home	Detroit, Michigan, USA
3	Wildfire-Resistant Home	Redding, California, USA
4	3D-Printed 5 story building by Win sun Company	Jiangsu Province, China
5	Florida's First 3D Printed House	Tallahassee, Florida, USA
6	Office of the Future	Dubai, UAE
7	12-meter-long bridge	Amsterdam
8	Pedestrian Bridge	Shanghai, China
9	The Lewis Grand Hotel Suite	Philippines
10	Apis Cor House	Russia

4 Prospects and Challenges for 3D Printing in Developing Countries

AM Technique have promising prospect along with challenges as well. Viability of this technique can be seen in seven major categories that includes material, manpower, process efficiency, logistics, sustainable construction, structural strength and cost. It offers rapid prototyping, reduced waste, less time in one dimension, adaptability to any geometrical design and less manpower but also coupled with multiple risks and challenges. If cost of structure is considered it includes three major dimensions i.e., material, manpower and facilities. 3D printing will reduce the labor demand and remedial

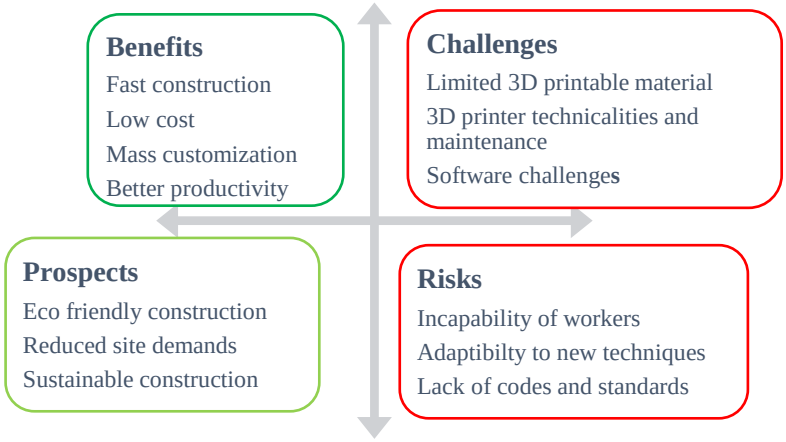

Figure 1: SWOT Analysis of 3D printing construction

works. Therefore, to evaluate this technique, it is desirable to calculate the financial performance in the whole process including all factors. Printability, buildability and open time are major concerns when material is considered while 3D printer itself comes with numerous challenges i.e., scalability and geometrical limitations [9]. Similarly, unskilled labor and inadequacy of knowledge also hinders the adaptation of the technique. Lack of codes and standards makes 3D printing questionable. It allows to complete large-scale project in less time but printing too quicky can also affects the strength [10]. Optimization of materials, expertise while maintaining speed is a delicate balance between benefits and challenges. Need of the hour is to create a standardized procedure and specify the design steps, standard codes and practices and construction guidelines which would give every organization a direction to stimulate research for the gaps so that implementation can be promoted. To effectively summarize the benefits, prospects and challenges, SWOT analysis of this technology is given in Fig.1.

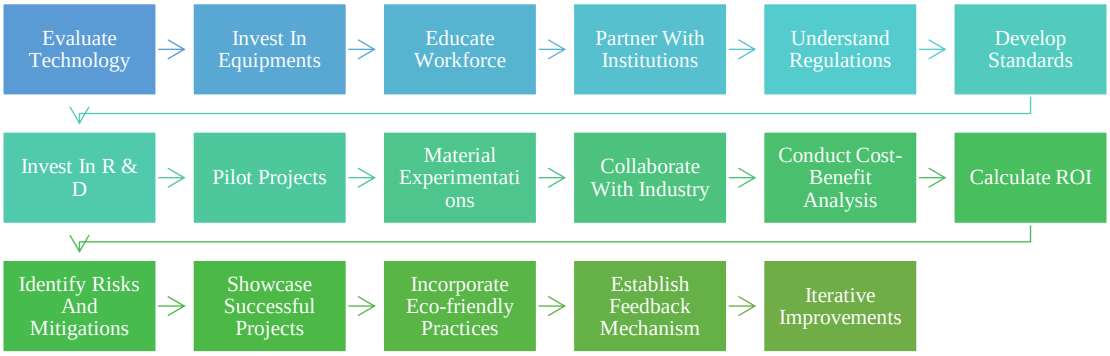

Figure 2 : Guidelines for adoption of 3D printing technology

5 Guidelines for Adoption of 3D Printing Technology in Construction Industries

Diversified models have been designed to better understand different attributes that may affect the implementation process of 3D printed construction. The technology-organization-environment (TOE) framework is the most consistent framework

that covers all the aspects that should be considered for the adaption of innovative technology at organizational level [11]. Technological dimensions include evaluation of technology, material experimentation and exploration, developing standards and codes while Organizational dimensions comprise of cost-benefit analysis, collaboration with industry, training programs, invests capital in equipment's related to 3D printing. Environmental aspects have life cycle assessment, identification of risks and mitigations, incorporation of eco-friendly practices [12]. Fig.2 explains the adoption guidelines under the light of TOE framework.

6 Conclusion

The application of 3D technology in construction has a high potential for bringing down construction time and ultimately reducing manpower, therefore indicating clear cost and resource savings. However, the applicability of this in multi-story buildings is not clearly assessed. With this, comprehensive analytical studies are needed to evaluate life cycle assessments using BIM, which would enable one to understand the environmental impacts and the actual project costs associated with an emerging technology. Steel has a significant impact on the cost of concrete structures. Accordingly, the study of methods of enhancing 3D buildings that are printed using steel or otherwise has to be conducted. Moreover, the design and construction criteria for this technology still remain to be developed. Proper codes and rules need to be drawn up if this technology is to be used practically.

Its implementation could affect the employment circumstances. But there are chances of new fields yet to be explored for developing 3D printing equipment and exploring materials to be used in this technology. Overall review concludes that legislative and economic perspectives still need to be explored.

Acknowledgment

The author would like to thank Dr Majid Ali and Engr Abrar Ahmed who helped throughout the research work.

References

[1] S. J. Schuldt, J. A. Jagoda, A. J. Hoisington, and J. D. Delorit, "A systematic review and analysis of the viability of 3D-printed construction in remote environments," Autom Constr, vol. 125, p. 103642, 2021.
[2] X. Ning, T. Liu, C. Wu, and C. Wang, "3D Printing in Construction: Current Status, Implementation Hindrances, and Development Agenda," Advances in Civil Engineering, vol. 2021, 2021, doi: 10.1155/2021/6665333.
[3] T. Wangler et al., "Digital concrete: opportunities and challenges," Rilem technical letters, vol. 1, no. 1, pp. 67–75, 2017.
[4] A. Alkhalidi and D. Hatuqay, "Energy efficient 3D printed buildings: Material and techniques selection worldwide study," Journal of Building Engineering, vol. 30, Jul. 2020, doi: 10.1016/j.jobe.2020.101286.
[5] E.-A. Alawneh and M. Alawneh, "THE WORLD'S FIRST 3D-PRINTED OFFICE BUILDING IN DUBAI."
[6] D. Lowke, E. Dini, A. Perrot, D. Weger, C. Gehlen, and B. Dillenburger, "Particle-bed 3D printing in concrete construction–possibilities and challenges," Cem Concr Res, vol. 112, pp. 50–65, 2018.
[7] N. Labonnote, A. Rønnquist, B. Manum, and P. Rüther, "Additive construction: State-of-the-art, challenges and opportunities," Autom Constr, vol. 72, pp. 347–366, 2016.
[8] "TECHNOLOGY READINESS AND ADOPTION OF 3D-PRINTING IN THE CONSTRUCTION INDUSTRY," 2018.
[9] S. El-Sayegh, L. Romdhane, and S. Manjikian, "A critical review of 3D printing in construction: benefits, challenges, and risks," Archives of Civil and Mechanical Engineering, vol. 20, no. 2. Springer, Jun. 01, 2020. doi: 10.1007/s43452-020-00038-w.
[10] S. A. Khan, M. Koç, and S. G. Al-Ghamdi, "Sustainability assessment, potentials and challenges of 3D printed concrete structures: A systematic review for built environmental applications," Journal of Cleaner Production, vol. 303. Elsevier Ltd, Jun. 20, 2021. doi: 10.1016/j.jclepro.2021.127027.
[11] C.-C. Yeh and Y.-F. Chen, "Critical success factors for adoption of 3D printing," Technol Forecast Soc Change, vol. 132, pp. 209–216, 2018.
[12] H. Tu, Z. Wei, A. Bahrami, N. Ben Kahla, A. Ahmad, and Y. O. Özkılıç, "Recent advancements and future trends in 3D concrete printing using waste materials," Developments in the Built Environment, vol. 16. Elsevier Ltd, Dec. 01, 2023. doi: 10.1016/j.dibe.2023.100187.

OPTIMIZING ENERGY EFFICIENCY IN GREEN BUILDINGS USING BIM-INTEGRATED ENERGY ANALYSIS TOOLS

[a] Muhammad Sohaib*

a: Civil Engineering, University of Engineering & Technology, Peshawar, Pakistan. 19pwciv5321@uetpeshawar.edu.pk
*Corresponding Author.

Abstract- The construction industry is one of the major contributors of GHG (Greenhouse Gas) Emissions, in which commercial and residential buildings play a major role. Most of these emissions are attributed to lack of energy conservation measures, outdated methods of design and construction. In this project, an analysis is made based on the comparison of energy consumption of a building constructed from conventional materials, having no sustainable design strategies. And another building that is designed with consideration to sustainable techniques such as energy efficient materials that have low thermal conductivity, lower U-value (thermal transmittance) glazing, and oriented at different angles to suit the best conditions of sun path for optimum heat transfer. A BIM-based approach is adopted. Both the models are designed in Autodesk Revit and then analyzed through the built-in Revit plug in: Autodesk Insight, which performs iterative energy analysis on cloud. The results for both the buildings are compared and conclusions are drawn based on energy and cost savings in the long run. The study concludes with the design and energy audit of a commercial plaza building, revealing the large energy and cost savings available via intelligent design decisions.

Keywords- Green Buildings, Energy Simulation, BIM, Sustainable Buildings, Energy Efficiency.

1 Introduction

Global warming is a major global issue rising rapidly and causing numerous problems for all species on Earth. One of its major contributors is Green House Gass emissions from combustion of fossil fuels for meeting energy demands. A large amount of this demand comes from operating residential and commercial buildings. Due to the rising population and intense urbanization, we have an all-time growing demand for energy. Our cities generate roughly 60% greenhouse gas emissions and account for 78% of the total energy consumption [1], where commercial buildings consume more energy than residential buildings [4]. Most of the buildings we have been constructing till recent years—especially in developing countries—did not include energy conservation strategies in their design and were unable to make energy savings. A huge amount of energy and money is wasted annually due to poor designs, inefficient materials, lack of knowledge and technical skills, and many other factors in the whole construction industry and in commercial buildings in particular.

The energy efficiency of buildings is paramount in reducing heating and cooling energy demands, with the building envelope playing a critical role by keeping the indoor temperatures at optimum[1]. Enhanced thermal resistance through improved insulation, strategic orientation, and design can significantly lower HVAC (Heating, Ventilation and Air-Conditioning) loads and overall energy consumption[2]. Extensive research has proved that green buildings outperform conventional buildings in terms of energy savings (up to 25%) and carbon emission reduction (up to 46.8%)[3]. Green buildings are more habitable and healthy for their residents[4]. Early integration of energy-saving strategies, such as passive design[5], optimal orientation, daylighting, using sustainable building materials[6] and efficient appliances, implementing BIM, can lead to substantial cost savings over time. Innovations like electrochromic windows offer increased window-to-wall ratios without sacrificing energy performance, aligning with the Net Zero Energy Building (NZEB) goal[7]. Furthermore, Computer modeling (e.g. 6D BIM), BIM tools like Revit, and whole-building design, allow us to estimate and minimize consumption in early design stages[8]. The effectiveness of these strategies is evidenced by LEED-certified buildings in North America, which report 25-30% energy savings compared to national averages[9]. There are many green building certifications worldwide such as BREEAM, LEED, HQE, NABERS, CASBEE, Green globe etc.[10]. Thanks to initiatives like "Horizon 2020", nearly €80 billion in funding is available to NZEB (Net-Zero Energy Building) cause in addition to private investments [11].

In this work, a deeper dive has been taken to address this issue and examine numerous aspects such as using sustainable materials, improving building orientation, glazing, and sun-shading to minimize energy demand of buildings while also trying to quantify the effects of various parameters on energy efficiency of buildings using BIM based approach.

2 Research Methodology

A conventional commercial plaza building was designed in Autodesk Revit using architectural drawings, then necessary energy settings were applied to perform its energy analysis in Autodesk Insight, then its energy model was generated in Revit and analysed in Insight. After that, the same process was repeated for another model of the same size, shape and form, and other structural and architectural features but with a more energy efficient wall material CLC (Cellular Lightweight Concrete) with Fiberglass insulation and double-glazed windows. Then the model was analysed with different iterations to come up with the most efficient scenario.

2.1 Model

A 3D Revit model of a Commercial Plaza (Fig. 1, a) assumingly located in Lahore using real architectural drawings was developed, which is 4 storeys high with 212 shops and having approximately 208x90 (ft^2) covered area. 12" First Class Brick Masonry wall with 20mm Cement Sand plaster (U=1.736 W/m^2K) with no insulation material. Single-pane, glass windows with wooden frames were installed as glazing material (U=3.688 W/m^2K). The floor and roof are made of 12", cast-in-place concrete (U=3.4318 W/m^2K). Then a replica of that model was created but with a sustainable approach. For walls, 12" Cellular lightweight Concrete with 20mm cement sand plaster (U=1.0716 W/m^2K) was used and Fiberglass was used as insulation material (U=0.187 W/m^2K). Double-glazed windows were installed (U=1.2 W/m^2K). Floor and roof materials were unchanged. Then energy models for both buildings were generated to analyze and compare them.

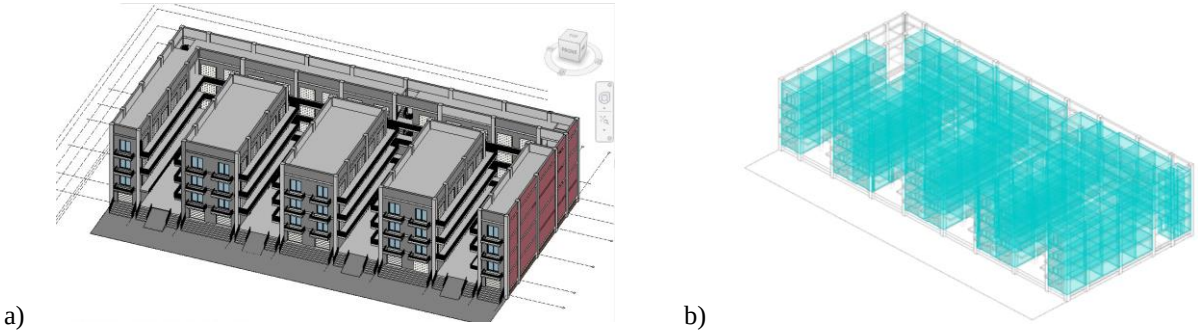

a) b)

Figure 1: a. Revit Building Model, b. Revit-Generated Energy Model

2.2 Analysis

First, energy settings such as thermal properties of all material components of the model and weather data were configured, then both the energy models were analyzed using Autodesk Insight. With the energy analysis model (Fig. 1, b) in place, energy consumption and performance simulations were conducted. Using the specified occupancy schedules, lighting fixtures, HVAC systems, and other energy-related parameters, the building's energy usage and performance was simulated over time. After the energy simulations were completed, the results provided by Autodesk Revit were reviewed and analyzed. Energy consumption data, including energy use intensity (EUI), heating and cooling loads, and energy cost estimates were examined. The performance of different design options, such as varying building orientation, wall-to-window ratios, and glazing types, was compared to identify energy-saving opportunities.

3 Results

3.1 Initial Cost Comparison of Conventional and Green Building

The capital cost for both models was calculated in Revit Schedule of Rates, and rates were taken from MRS-2022 (Market Rate System). The cost comparison is enlisted below. It can be seen in Table 1 that the initial cost of Green building is $125,221 higher than that of conventional building. Which is equivalent to 45.7% increase in initial cost.

Table 1: Initial Cost Comparison of Conventional and Green Building

Building Type	Walls Cost (USD)	Roof & Floor Cost (USD)	Doors Cost (USD)	Windows Cost (USD)	Total Cost (USD)
Conventional	100,009	169,097	3,907	1,067	274,080
Green	224,616	169,097	3,907	1,680	399,301

3.2 Energy Consumption and Performance Simulation

Using specified occupancy schedules, lighting fixtures, HVAC systems, building orientation, window-to-wall ratios etc., annual energy consumption cost per square feet of the energy model was calculated in Autodesk Insight. The energy consumption cost of the Conventional model was calculated to be 2.76 USD/ft^2/yr. (Fig. 2, a). Multiplying this with the floor area of the building, which is 30316 ft^2, the annual consumption cost was found to be 83,672 USD/yr.

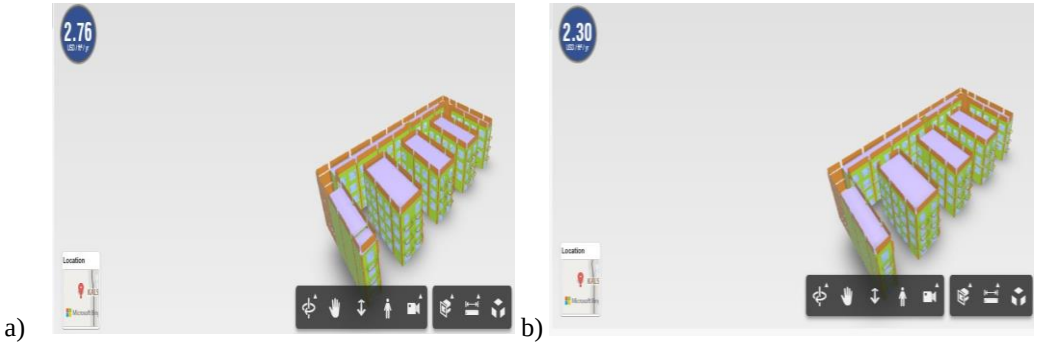

Figure 2: Annual Energy Consumption Cost per sq. ft., a. Conventional Building, and b. Green Building

The energy consumption cost of the Green model was calculated to be 2.30 USD/ft^2/yr. (Fig. 2, b) with only changing wall material, insulation and glazing. Hence, the annual consumption cost of this model was reduced to 69,727 USD/yr. observing a decrease of 16.7%.

3.3 Annual Consumption Cost Variation

The above model was selected as a base model and factors affecting energy consumption such as building orientation, WWR, light and plug load efficiency, and HVAC etc. were varied in multiple iterations to look for the best-case scenarios that will result in minimum energy consumption (Fig. 3). After applying all the optimum parameters, the annual energy cost was reduced to just 0.89 USD/ft^2/yr. Which totals about $27,000 per year. Hence the total annual energy consumption cost was reduced from $83,672 to $27,000; a 67.7% decrease, leading to savings of $56,672 per annum.

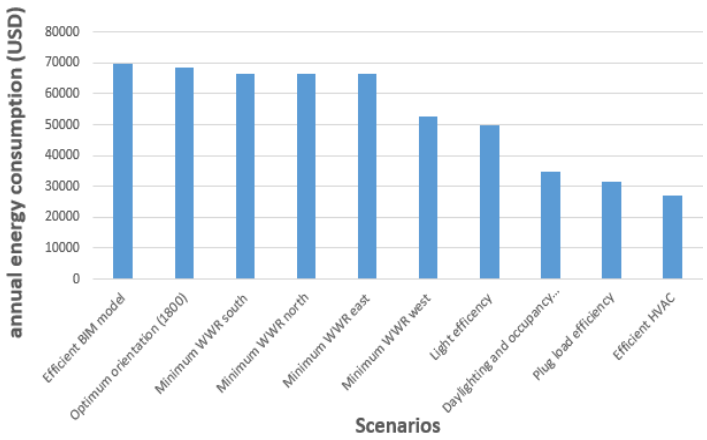

Figure 3: Annual Consumption Cost Variation with Various Factors

4 Practical Implementation

From this experiment, it is evident that there is a formidable margin for energy and consumption cost savings by applying Green building design strategies in early design stages of the project.

5 Conclusion

The following conclusions can be drawn from this work:

1 By implementing sustainable design strategies, the carbon footprint and overall lifecycle cost of buildings can be minimized which will reimburse the initial high cost through savings.
2 Using CLC (Cellular Lightweight Concrete) as wall material increases thermal resistance and minimizes heat loss, which in turn leads to reduced energy consumption required to heat or cool the building.
3 The double-glazed windows have higher initial cost but pay back their initial investment through energy savings because they have lower U-value (thermal transmittance) compared to single-glazed windows, which minimize heat loss and thermal bridging that normally lead to excessive energy consumption.
4 Building orientation also affects energy consumption based on path followed by the sun throughout the year and the heat gain that takes place when sunlight enters the interior spaces of the building.

The above results indicate further opportunities for energy efficiency and reducing carbon footprint of buildings. Next approach should be analyzing the impact of solar photovoltaics on annual energy consumption cost.

Acknowledgment

First and foremost, we want to express our gratitude to Almighty Allah for giving us the ability to finish our research, then to Dr. Qazi Samiullah, our supervisor, for his advice and thorough feedback. We would also like to acknowledge our department and the teachers who taught us well and our parents whose prayers helped us through our journey.

References

[1] N. Huberman and D. Pearlmutter, "A life-cycle energy analysis of building materials in the Negev desert," *Energy Build.*, vol. 40, no. 5, pp. 837–848, 2008.
[2] S. Sarihi, F. Mehdizadeh Saradj, and M. Faizi, "A Critical Review of Façade Retrofit Measures for Minimizing Heating and Cooling Demand in Existing Buildings," *Sustain. Cities Soc.*, vol. 64, p. 102525, Jan. 2021, doi: 10.1016/j.scs.2020.102525.
[3] E. Kusi, I. Boateng, and H. Danso, "Energy consumption and carbon emission of conventional and green buildings using building information modelling (BIM)," *Int. J. Build. Pathol. Adapt.*, vol. ahead-of-print, no. ahead-of-print, Jan. 2024, doi: 10.1108/IJBPA-09-2023-0127.
[4] Y. Xu, D. Luo, Q. K. Qian, and E. H. W. Chan, "Are green buildings more liveable than conventional buildings? An examination from the perspective of occupants," *J. Hous. Built Environ.*, vol. 38, no. 2, pp. 1047–1066, Jun. 2023, doi: 10.1007/s10901-022-09983-9.
[5] M. H. Elnabawi, E. Saber, and L. Bande, "Passive Building Energy Saving: Building Envelope Retrofitting Measures to Reduce Cooling Requirements for a Residential Building in an Arid Climate," *Sustainability*, vol. 16, no. 2, Art. no. 2, Jan. 2024, doi: 10.3390/su16020626.
[6] K. Shahzada and U. Amjad, "Mechanical Properties Evaluation of SIMBRI Fly Ash Bricks".
[7] M. Detsi, I. Atsonios, I. Mandilaras, and M. Founti, "Effect of smart glazing with electrochromic and thermochromic layers on building's energy efficiency and cost," *Energy Build.*, vol. 319, p. 114553, Sep. 2024, doi: 10.1016/j.enbuild.2024.114553.
[8] Liu, L. Jiang, M. Osmani, and P. Demian, "Building Information Management (BIM) and Blockchain (BC) for Sustainable Building Design Information Management Framework," *Electronics*, vol. 8, p. 724, Jun. 2019, doi: 10.3390/electronics8070724.
[9] C. Turner, M. Frankel, and U. G. B. Council, "Energy performance of LEED for new construction buildings," *New Build. Inst.*, vol. 4, no. 4, pp. 1–42, 2008.
[10] S. Vierra and V. Design, "GREEN BUILDING STANDARDS AND CERTIFICATION SYSTEMS".
[11] "From nearly zero energy buildings (NZEB) to positive energy buildings (PEB): The next challenge - The most recent European trends with some notes on the energy analysis of a forerunner PEB example - ScienceDirect." Accessed: Jul. 19, 2023. [Online]. Available: https://www.sciencedirect.com/science/article/pii/S2666165920300156

ASSESSMENT OF ABLUTION WASTE WATER QUALITY FOR VARIOUS MOSQUES IN PESHAWAR CITY

[a] Hamad Khan*, [b] Abdullah Khan Jadoon

a: Department of Civil Engineering, University of Engineering and Technology, Peshawar, Pakistan. 20pwciv5445@uetpeshawar.edu.pk
b: Department of Civil Engineering, University of Engineering and Technology, Peshawar, Pakistan. 20jzciv0405@uetpeshawar.edu.pk
* Corresponding author.

Abstract- Ablution water refers to the water utilized by worshippers for washing (wudhu) before engaging in prayers. Different researchers have described the usage of ablution water for different purposes by channeling it through basic treatment. In this case study, ablution water quality of various mosques for Peshawar city is assessed on the basis of various parameters i.e. biological oxygen demand(BOD), chemical oxygen demand (COD), total dissolved solids(TDS), total suspended solids(TSS), PH and electrical conductivity(E.C) so that it can use in functional purposes without any initial treatment. Water samples were collected from different mosques, and tests were conducted for the mentioned parameters. The results were compared with the National Environmental Quality standards and other international standards for water usage in various applications. The laboratory test comparisons indicated that the ablution water in Peshawar city can be used directly for irrigation after primary treatment to remove suspended particles, industrial use, and concrete mixing without any initial treatment.

Keywords- Ablution Water, Biological Oxygen Demand, Chemical Oxygen Demand, Wudhu.

1 Introduction

The ablution act, which Muslims perform before their five daily prayers, requires a significant amount of clean water. Muslims use approximately 3.9 to 4.42 liters of water per person a day for performing ablution [1]. This means that the Mosque needs the continuous supply of clean water five times a day, source of which is well. The wells are affected by continuous discharge l1 eading to serious problems in dry seasons. The ablution waste water can be reused by treating it by different methods. One of the researcher [2] suggested the reuse of ablution waste water in ablution activities by treating it by electrocoagulation method. A study conducted in Lahore to find the most acceptable space dimensions of ablution units and design for the user's comfort while performing the ablution activity, so that people would face no difficulty in ablution actions[3]. Another researcher [4] in Saudi Arabia proposed the reuse of ablution waste water from the Mosques by treating them from simple sand and carbonic filters along with sterilization method. Our study is actually about the same concept of reuse of ablution waste water from Mosques in Peshawar city so that it can be used for functional purposes without any basic treatment.

The water used for ablution purposes came from the tubewells, that is the freshest water source in Pakistan. Even by treating it by simple methods, it can be used for a lot of purposes. In this study the ablution water in the different Mosques of Peshawar city is assessed, for the direct reuse in essential purposes without any initial treatment. The Primary objective of the study is to Assess the quality of ablution water from various mosques in Peshawar City, compare the water quality parameters with national and international standards and determine the feasibility of reusing ablution water for purposes such as irrigation, industrial use, and concrete mixing without significant treatment. After testing the collected water from different Mosques in Peshawar and comparing them with standards, it was concluded that the ablution water from the Mosques in Peshawar city can be directly used in the Irrigation purposes, mixing water in concrete and industrial use especially for cooling for hot machinery.

2 Research Methodology

2.1 Data Collection From Different Places

Water samples from all main places Mosques in Peshawar city are collected. Sampling places vs pollution level bar graph and their standard deviation are shown in Figure 1. Not any specific method is used to categorize Mosques for sampling purposes on the basis of pollution level rather they are categorized on visual method. Mosques situated in residential areas are classified as less polluted, those in commercial areas as highly polluted, and mosques located between residential and commercial zones are categorized as moderately polluted.

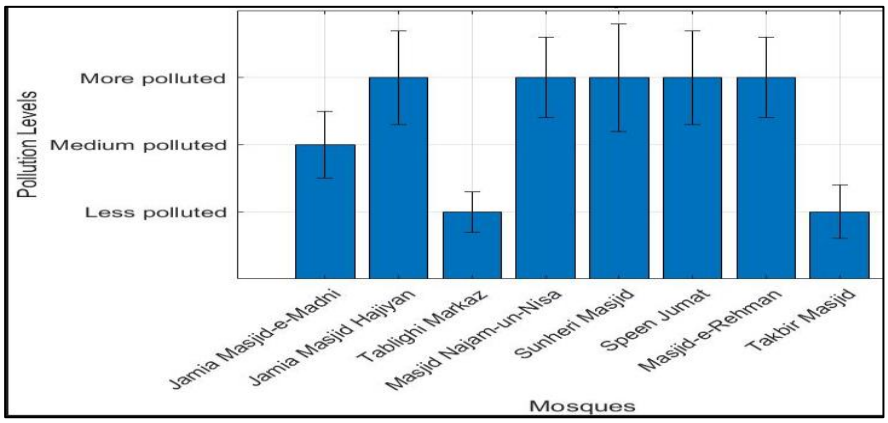

***Figure 1**: Sampling places for ablution water collection along with standard deviation in Peshawar*

Sampling of waste water samples from various sites are taken as per NEQ standards Pakistan. Table 1 presented the sampling Techniques for various parameters, preservation methods, container type, Technique for analysis procedure, special equipment for analysis purpose and make and model name.

2.2 Summary of Sampling

***Table 1** Sampling Techniques according to NEQS(National Environmental Quality Standards Pakistan)*

S. No.	Parameters	Container	Preservation	Technique	Equipment Name (Make and Model)
1	pH	Plastic/Glass	Analyze immediately	Electrode Method	pH Meter (Hanna HI 2211)
2	TDS	Plastic/Glass	Refrigerate	Gravimetric analysis	TDS Meter (Apera Instruments PC60)
3	B.O.D	Plastic/Glass	Refrigerate	Winkler method	BOD Incubator (Labtech LI-126)
4	C.O.D	Plastic/Glass	Analyze as soon as possible or add H_2SO_4 to pH <2 and refrigerate	Dichromate reflux method	COD Reactor (Hach DRB200)
5	TSS	Plastic/Glass	Refrigerate and analyze within 7 days	Filtration and drying method	Analytical Balance (Mettler Toledo ML204)
6	EC	Plastic/Glass	Refrigerate and avoid freezing.	Conductivity method	Conductivity Meter (Hach HQ440d

2.3 Laboratory Testing

Tests were conducted in the laboratory for required parameters i.e. BOD, COD, TSS, TDS, E.C and pH with proper safety and protocol. Sampling was done according to NEQ standards as shown in Table 1.

Table 2: Laboratory test results of ablution water samples collected in Peshawar city

Sample ID	BOD(mg/l)	COD(mg/l)	TSS(mg/l)	TDS(mg/l)	E.C(µS/cm)	PH
Jamia Masjid-e-Madni	35	49.42	1333	154	308	7.03
Jamia Masjid Hajiyan	52	98.85	1666	348.5	697	7.18
Tablighi Markaz	38	49.00	1332	457.5	915	7.11
Masjid e Najm-u-Nisa	58	98.80	1998	415.5	831	7.15
Sunehri Masjid Saddar	63	98.90	666	426.5	853	7.05
Speen Jumat	49	49.48	1333	415.5	831	7.15
Masjid-e-Rehman	55	98.90	1200	382	764	7.03
Takbir Masjid	31	49.00	1250	380	760	7.10

2 Results and Discussions

In Table 2, laboratory test results for various parameters i.e. BOD, COD, TDS and TSS etc. are shown. These parameter results are then compared with different Water quality standards as shown in Table 3,4,5 and 6.

*Table **3:** Comparison with NEQS limits [5]*

S.#	Parameter	NEQS Limit	Data Range	Compliance
1	BOD	80 mg/l	31 - 63 mg/l	Compliant
2	COD	150 mg/l	49.00 - 98.90 mg/l	Compliant
3	TSS	200 mg/l	666 - 1998 mg/l	Non-Compliant
4	TDS	3500 mg/l	154-457.5 mg/l	Compliant
5	EC	1200 µS/cm	308 - 915 µS/cm	Compliant
6	PH	6-9	7.03 - 7.18	Compliant

*Table **4:** Mixing water quality standards for ready mix concrete ASTM C94[9]and[8]*

S.#	Parameters	Unit	Maximum Limits	PH
1	TSS	Mg/l	2000	7.03
2	TDS	Mg/l	2000	7.18
3	COD	Mg/l	500	7.11
4	pH	N/A	98.90	6-8

*Table **5:** Permissible limits of water for Irrigation use [5]*

S.#	Water class	Sodium (Na) %	Electrical Conductivity µS/cm at 25˚C
1	Excellent	<20	<250
2	Good	20-40	250-750
3	Medium	40-60	750-2250
4	Bad	60-80	2250-4000
5	Very bad	>80	>4000

*Table **6:** Permissible limits of water for Industrial useBIS (IS: 10500: 1991)*

S.#	Parameters	Prescribed Limits		Probable Effects
		Desirable	Permissible	
1	pH	6.5	8.2	pH 7.0 is required for most industries, low pH increases corrosion
2	Total dissolved solids, mg/l	50	3000	Foaming occurs in boilers and solids interfere with clearness, taste or colour of products. Low TDS values are required for most industries.

By comparing the results of Table 2 to various standards, i.e. Irrigation water guidelines for Pakistan [5], Indian standards [6], NEQS Pakistan [7]and ASTM concrete standards[8] and[9], ablution water can be used ablution water in the Peshawar city can be directly used in industrial use, concrete mixing and in the irrigation (after primary treatment to remove Total suspended particles), without any initial treatment.

3 Practical Implementation

Study significantly conserves the fresh water resources, especially in regions facing water scarcity. Reusing ablution water can reduce the demand for treated potable water, leading to cost savings for mosques. This research contributes to all of SDGs but specifically, it contributes to SDG 2, 4, 6, 9, 11, 12, 14, 15 and 16.

4 Conclusion

By comparing the results to different standards in table 3,4,5 and 6, ablution water can be used for;

- For concrete mix preparation, without any basic treatment as compared to ready mix standards ASTM [8]and[9].
- For industrial usage, compared to table 6,ablution water can also be used without any treatment.
- Compared to Pakistan's NEQ standards Table 6, ablution water is suitable for various uses, including irrigation (following primary treatment through sedimentation to remove total suspended solids(TSS), concrete mixing, industrial applications (such as cooling and boiler feed water), recreational purposes (like fountains), and aquaculture (suitable for fish).

For future, Exploration of other sources of greywater, such as domestic wastewater from kitchens etc. should be carried out, to compare their quality and reuse potential with ablution water. Also, investigation on its impact on soil health, plant growth, and industrial processes will be carried out to ensure sustainable practices.

References

[1] R. Mafra, K. Kurnia, A. Ardabili, F. Ferdiansyah, H. Handaka, and I. Irawan, "Pengukuran Durasi Waktu Berwudhu dan Volume Penggunaan Air Pada Masjid-Masjid di Kota Palembang," *Arsir*, vol. 2, no. 2, p. 71, Jan. 2019, doi: 10.32502/arsir.v2i2.1299.

[2] M. Mudofir, Moh. Taufik, I. H. Rusdan, W. D. Silviani, and P. Purwono, "Investigation of time impact on electrocoagulation process to treat ablution wastewater," *IOP Conf. Ser.: Earth Environ. Sci.*, vol. 1098, no. 1, p. 012047, Oct. 2022, doi: 10.1088/1755-1315/1098/1/012047.

[3] I. Malik, "Analytical Study of Ablution Spaces: Case Analysis of Mosques in Lahore, Pakistan," *AHSS*, vol. 4, no. I, Mar. 2023, doi: 10.35484/ahss.2023(4-I)11.

[4] M. I. Al, "Simple system for handling and reuse of gray water resulted from ablution in Mosques of Riyadh City, Saudi Arabia".

[5] "W.W.F. Pakistan, 2007. National Surface Water Classification Criteria and Irrigation Water Quality Guidelines for Pakistan. Feb 2007. Waste Water Forum Pakistan."

[6] "Drinking Water Standards of BIS (IS: 10500: 1991)."

[7] "REVISEDNATIONALENVIRONMENTAL QUALITYSTANDARDS (NEQS)." [Online]. Available: https://epd.punjab.gov.pk/system/files/Revised%20NEQS%202000.pdf

[8] A. M. Neville, *Properties of concrete*, vol. 4. Longman London, 1995.

[9] "ASTM C94/C94M-14b. Standard specification for ready mix concrete; 1994."

ENHANCING ASPHALT PAVEMENT PERFORMANCE WITH PHASE CHANGE MATERIALS

[a] ***Muhammad Usman,*** [b]***Affaq Arif Gill****

a: Civil Engineering Department, Army Public College of Management and Sciences, Rawalpindi. rajusman2001@gmail.com
b: Civil Engineering Department, Army Public College of Management and Sciences, Rawalpindi. gillaffaq777@gmail.com
* Corresponding author.

Abstract- This study aims to utilize Phase Change Materials (PCM) technology to protect and maintain asphalt pavement from temperature changes, thereby preventing cracks. PCM assists in temperature regulation by exploiting latent heat characteristics, thereby maintaining the workability of asphalt surfaces. Asphalt pavement, often exposed to temperatures up to 60°C in summer, becomes prone to cracking due to sunlight. The issue can be resolved by using PCM, which will extend the life and performance of asphalt pavement. In this investigation, the asphalt mixture had gravel and sand as fine and coarse particles, respectively, and a bitumen penetration grade of 50/60. To implement PCM in asphalt pavement, we took into account the mechanisms for temperature regulation, road efficiency, and mix design techniques. According to the findings, there was a maximum temperature difference of 4.72°C between the top and the bottom, with peak surface and bottom temperatures of 43.41°C and 46.47°C, respectively. This study demonstrates the potential of PCM technology to effectively mitigate temperature fluctuations within asphalt pavement, thereby improving its durability and performance.

Keywords- Asphalt Pavement, 50/60 Grade Bitumen, Surface and Bottom Temperature, Phase Change Materials.

1 Introduction

Asphalt pavement can reach temperatures up to 60°C due to its high heat absorption from the sun. To optimize this heat retention, a layer can be installed underneath the pavement to store and utilize the thermal energy effectively [1]. Utilizing the stored heat can mitigate the heat effect and prevent the pavement from becoming excessively soft and prone to rutting. When it comes to using solar energy, we need two main parts: a collector to gather the sunlight and a storage unit to hold onto the collected energy. The collector takes in sunlight and turns it into heat or electricity. To store this solar energy in the pavement, we need materials that can absorb and hold onto heat [2]. The use of phase change materials, or PCMs, in concrete pavement was discovered to have a combined effect of lowering surface temperatures and weakening the pavement [3]. To solve this issue, we suggest investigating microencapsulated PCM particles for asphalt pavement that have stronger outer shells. Before the asphalt mix is rolled out, such particles could be added to help stop the mechanical impacts of compaction on the PCMs. Capsules containing the PCM materials will be used, but they won't be loaded with PCM [4]. This prevents excessive pressure from building up and breaking the capsules while allowing the PCM material within to expand and compress. To simulate sun radiation, the PCM-filled capsules will buried in the pavement's top layer and subjected to infrared heat [3]. They will then be allowed to cool naturally. We can investigate the impact of PCMs by timing temperature variations during this procedure [5]. Phase transitions between solids and liquids, solids and solids, liquids and solids, and solids and gases are examples of latent heat storage. These storage compounds come in a variety of forms, from inorganic to organic, including paraffin and non-paraffin. Organic-organic, organic-inorganic, and inorganic-inorganic are the three primary categories of inorganic PCM and eutectic mixes. Since they possess melting points between 115°C and 897°C, inorganic materials are typically chosen in the setting of solar power generation [6].

1.1 Phase Changing Material (PCM)

Pavement is continuously exposed to the elements, which over time may cause deterioration. Temperature is one of the most important variables affecting pavement performance. Significant temperature variations can put a lot of strain on the pavement, which can result in fractures and damage. It might be less expensive to maintain if these temperature swings are smaller. Phase Change Materials, or PCM, can be added to a pavement mixture to accomplish this. PCMs are materials that can expend or absorb heat, which aids in temperature regulation. The range of temperatures at which the change in phase takes place and how heat is absorbed or released during the phase shift are major determining factors in deciding what kind of PCM to utilize in the mixture. When a car's wheels spin vertically on the pavement, it can cause, [7, 8] which causes adjacent pavement portions to move sideways. As seen in Figure 1, this movement causes channels or ripples to appear on the pavement's surface.

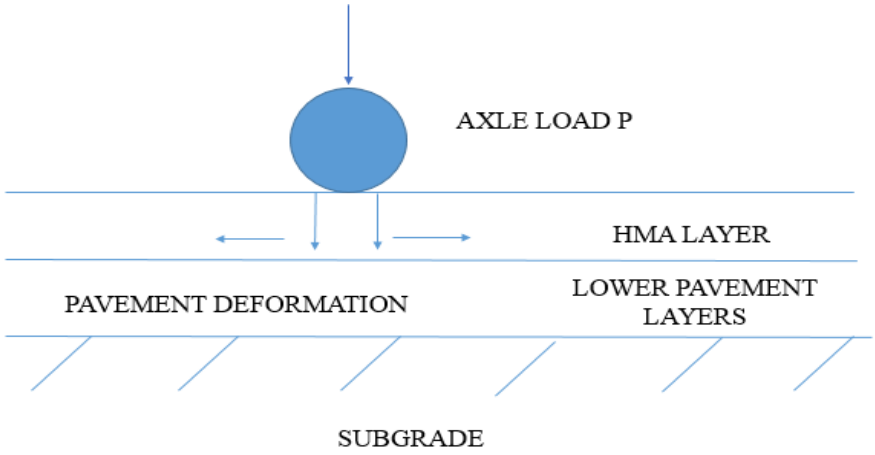

Figure 1: Rutting in hot asphalt mixtures primarily results from the prolonged application of heavy wheel loads

According to the temperature range, different phase-change materials, or PCMs, are employed. Three primary categories are commonly used to classify PCMs: organic, inorganic, and eutectic material (PCM) [9]. There are two primary categories of organic PCM, like paraffin: paraffin hydrocarbons and paraffin waxes. The most popular organic phase change material (PCM) for heat storage among them is paraffin wax. Its volume swells by roughly 10% as it melts. Furthermore, because paraffin is softer, it exerts less force when it expands, making it less likely to cause harm [8]. Because of this, it can be used in applications without phase separation concerns where repeated cycles of melting and solidification are required. The majority of PCMs are classified as non-paraffin compounds, which have a variety of characteristics. These materials are combustible, which presents a major disadvantage that renders them inappropriate for elevated temperature storage purposes. The three main categories of non-paraffin compounds are polyalcohol, fatty acids, and glycols [10]. The challenges posed by temperature-induced strains on asphalt pavement can result in degradation and increased upkeep costs. [11] To tackle this challenge, the study delves into the potential of phase change materials (PCMs) for temperature management in pavement systems. Through the exploration of microencapsulated PCM particles and their incorporation into asphalt mixes, the research seeks to alleviate the negative impacts of temperature variations, thereby enhancing pavement resilience and diminishing maintenance expenditures [12].

2 Research Methodology

In this investigation, bitumen with a penetration grade of 50/60 was kept for use, with its essential properties, such as penetration (65 at 0.1 mm) and softening point (47 degrees Celsius), determined according to the guidelines of ASTM D5 and ASTM D36, respectively as shown in table 1. The composition of the asphalt mixture comprised gravel as the coarse aggregate and sand as the fine aggregate. Introducing Phase Change Material (PCM) into the mixture at a 5% proportion served as a substitute for filler, enhancing its thermal properties.

Table 1: Bitumen Properties

Property	Result	Limits	Standard
Penetration (0.1mm)	64	60-70	ASTM D5
Softening Point (°C)	48	45-55	ASTM D36

To facilitate experimentation, asphalt slabs measuring 30 by 30 cm were meticulously prepared. Continuous exposure to heat radiation over 10 days, maintained for 24 hours each day, simulated real-world conditions,[13] allowing for an in-depth assessment of the asphalt's response to thermal stress. Mechanical evaluations of the asphalt samples were then conducted to gauge their performance under varied conditions. Stiffness, rutting resistance, and fatigue life were among the key parameters assessed, employing standardized testing methodologies such as ASTM D6373, ASTM D6925, and ASTM D7460, respectively. Each test was executed with precision, adhering strictly to the protocols outlined by standards, thereby ensuring the accuracy and reliability of the experimental results. This meticulous approach not only facilitated a comprehensive understanding of the asphalt mixture's behaviour but also provided valuable insights into the efficacy of incorporating PCM as a filler substitute to enhance its thermal characteristics and overall performance. The temperature was measured using embedded thermocouples. The optimal temperature range for preventing and healing asphalt cracks is typically between 50°C and 70°C, as this range supports proper compaction and bonding, reducing the likelihood of cracking.[14]

3 Results

This study's experiment concentrated on pavement elements that are exposed to high surface temperatures. The mixture reached its maximum temperature between three and six o'clock in the evening. Figure 2 shows the mean, highest, and lowest temperatures of PCM over 10 days. 37.15°C is the average degree at the PCM's bottom. The PCM's average bottom temperature ranges from 31.41°C to 45.95°C at its maximum and minimum, respectively. The PCM's surface has an average temperature of 36.55°C. The PCM's average surface temperature is 30.45°C at its lowest and 42.41°C at its highest points. The PCM's bottom and surface have an average temperature differential of 0.45°C. While the average lowest temperature difference is 0.30°C, the mean highest temperature variation of the PCM is 4.85°C.

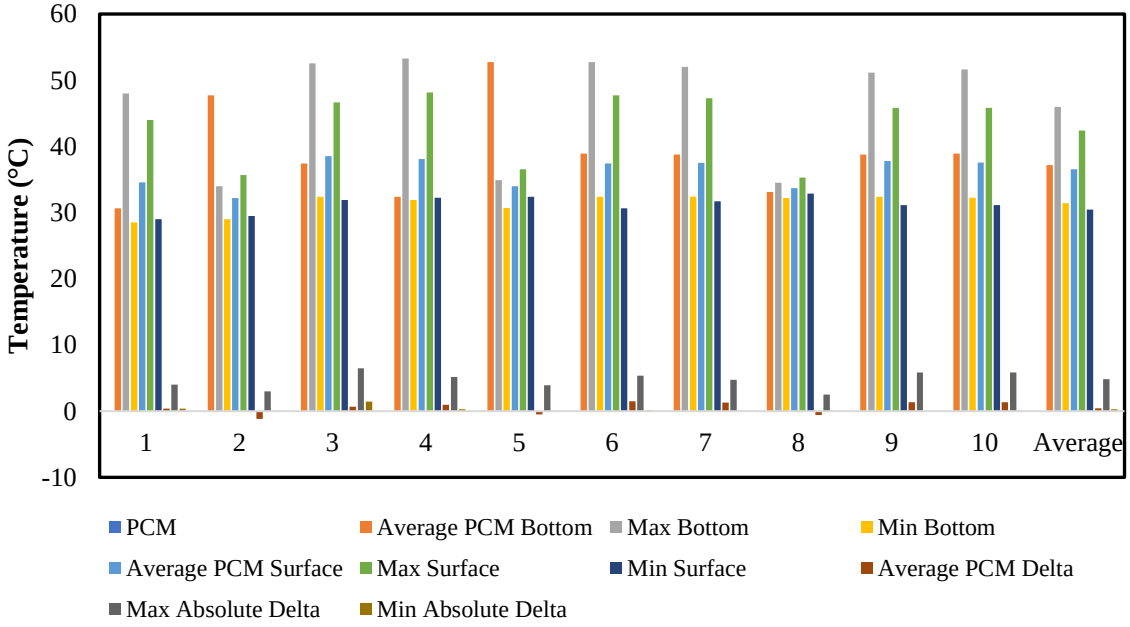

Figure 2: PCM Results

4 Practical Implementation

Observing how the PCM reacts with asphalt and variations in the temperature leads to improving the temperature of the pavement. This research helps in controlling of temperature of the pavement layer and maintaining its span against temperature variations.

5 Conclusion

- In this study, the temperature of the PCM asphalt mixture was measured, and a comparison was made between the temperatures at the top and bottom of the mixture. The highest temperature of the mixture was observed between 3 and 6 p.m. at the bottom layer and between 4 and 7 p.m. at the surface layer.
- The highest temperature measured at the surface was 42.41°C, while the lowest recorded temperature was 45.95°C. Furthermore, we noted that the absolute greatest temperature differential between the bottom and surface was 4.85°C. These encouraging results imply that temperature changes within asphalt pavement can be effectively improved by utilizing organic PCM encapsulated in about 800µm capsules.

Acknowledgment

The authors would like to thank every person/department who helped throughout the research period, particularly the CE department and Engr. Muhammad Waleed for their guidance.

References

1. Li, Y., Liu, L., Xiao, F., & Sun, L, *Effective temperature for predicting permanent deformation of asphalt pavement.* Construction and Building Materials, 2017. **156**: p. 871-879.
2. Ma, T., Li, S., Gu, W., Weng, S., Peng, J., & Xiao, G, *Solar energy harvesting pavements on the road: comparative study and performance assessment.* Sustainable Cities and Society, 2022. **81**: p. 103868.
3. Ryms, M., H. Denda, and P. Jaskuła, *Thermal stabilization and permanent deformation resistance of LWA/PCM-modified asphalt road surfaces.* Construction and Building Materials, 2017. **142**: p. 328-341.
4. Ma, B., S.S. Wang, and J. Li, *Study on application of PCM in asphalt mixture.* Advanced Materials Research, 2011. **168**: p. 2625-2630.
5. Cabeza, L. F., Martínez, F. R., Borri, E., Ushak, S., & Prieto, C, *Thermal Energy Storage Using Phase Change Materials in High-Temperature Industrial Applications: Multi-Criteria Selection of the Adequate Material.* Materials, 2024. **17**(8): p. 1878.
6. Yang, X. H., Tan, S. C., Ding, Y. J., Wang, L., Liu, J., & Zhou, *Experimental and numerical investigation of low melting point metal based PCM heat sink with internal fins.* International Communications in Heat and Mass Transfer, 2017. **87**: p. 118-124.
7. Chilukwa, N. and R. Lungu, *Determination of layers responsible for rutting failure in a pavement structure.* Infrastructures, 2019. **4**(2): p. 29.
8. Feldman, D., M. Khan, and D. Banu, *Energy storage composite with an organic PCM.* Solar energy materials, 1989. **18**(6): p. 333-341.
9. Zastawna-Rumin, A. and K. Nowak, *Experimental research of a partition composed of two layers of different types of PCM.* Energy Procedia, 2016. **91**: p. 259-268.
10. Yan, J., Shamim, T., Chou, S. K., Li, H., Zhang, P., Meng, Z., & Peng, S Zhang, P., *Experimental and numerical study of heat transfer characteristics of a paraffin/metal foam composite PCM.* Energy Procedia, 2015. **75**: p. 3091-3097.
11. Karam, J., *Innovative Modification and Testing of Asphalt Crack Sealants*. 2024, Arizona State University.
12. Yang, Z. L., Walvekar, R., Wong, W. P., Sharma, R. K., Dharaskar, S., & Khalid, M., *Advances in phase change materials, heat transfer enhancement techniques, and their applications in thermal energy storage: A comprehensive review.* Journal of Energy Storage, 2024. **87**: p. 111329.
13. Zhou, L., Zhang, T., & Luo, Y, *Numerical study and in-situ measurement of temperature features of asphalt supporting layer in slab track system.* Construction and Building Materials, 2020. **233**: p. 117343.
14. Piao, R., Kim, G. W., Chun, B., Oh, T., Jeong, J. W., & Yoo, D. Y, *Achieving thermoelectric properties of ultra-high-performance concrete using carbon nanotubes and fibers.* Renewable and Sustainable Energy Reviews, 2024. **199**: p. 114496.

TO ASSESS THE IMPACT OF ORGANOPHILIC NANOCLAY ON MARSHALL PROPERTIES OF ASPHALT MATERIAL

[a] Abu Bakar*, [b] Zimran Nasir,

a: Civil Engineering Department, APCOMS, Rawalpindi, Pakistan. chabubakar2003@gmail.com

b: Civil Engineering Department, APCOMS, Rawalpindi, Pakistan. zimrannasir@gmail.com

*Corresponding author.

Abstract- In recent years, the escalation in traffic volume and loads, alongside fluctuating temperatures, particularly high summer temperatures in winter, pose a significant challenge for pavement construction companies and engineers. This research aims to explore the impact of Organophilic Nano Clay on the Marshall Properties of Asphalt Mixture. The study investigates the Marshall properties of both Nano clay- modified asphalt mixture and conventional asphalt mixture. In the Nano clay-modified asphalt mixture, filler aggregates were substituted with varying percentages of Nano clay, ranging from 3.5% to 5.5%, with an optimum value of binder (OBC) of 4.33%. The OBC value was determined through Marshall Stability testing on the conventional asphalt mixture. Findings reveal that the addition of Nano clay enhances the Marshall Stability of the asphalt mixture, with the maximum stability observed at 4.5% Nanoclay content. Conversely, the Marshall Flow of the asphalt mixture decreases with the inclusion of Nano clay.

Keywords- Marshall Stability Test, Marshall Flow, Modifiers, Nano clay.

1 Introduction

Asphalt mixtures are widely used as a road pavement material across the globe. A durable mixture is required to sustain heavy loads form the anticipated traffic and also to with stand extreme weather conditions[1]. The road pavements are designed to last for a certain period of time, but sometimes premature failure occurs due to different distress types, which the pavement undergoes during its lifespan[2]. One of the major distress among all is moisture damage. These days, flexible pavement is the utmost commonly utilized material for roadways, finding employment in a variety of settings including parking lots, highways, walkways, runways, and harbors. Over 90% of European pavements are thought to be made of bituminous materials[3].

The commendable skid resistance, minimal noise levels, smoothness, safety, and long-lasting nature of asphalt pavements are directly linked to the composition of aggregates, fillers, and asphalt binder employed. Still, the problem of pavement distresses, including fatigue and heat cracking, rutting, and raveling, cannot be overlooked[4]. It's important to note that these distresses have escalated recently due to increased vehicle loads as well as the effects of environmental changes. The behavior of asphalt concrete, in particular, is largely determined by the asphalt, which also affects the pavement's performance and service life[5]. Pavement service life is shortened due to the aging of asphalt, which exacerbates fatigue and low-temperature performance during the service period. Therefore, building high- performance asphalt pavements may benefit from the use of asphalt with improved qualities[6]. Great efforts have been made by researchers and practitioners to accomplish this goal. Many studies have shown that in order to increase the overall performance of asphalt pavements, various additives such as polymers[7].

The application of fibers, one of the most often used additions in asphalt mixtures Using fibers with a high tensile strength could be a workable solution in this situation. When fibers are added to asphalt mixtures, they function as reinforcing elements and improve mix cohesiveness, reducing reflective or fatigue cracking and boosting resilience to

long-term deformations[8]. Additionally, fibers can be added to asphalt mixtures as stabilizers to lessen their drain-down effects. This is particularly useful for porous asphalt mixtures and SMAs (Stone Matrix Asphalts), which are often high in asphalt binders[9]. All things considered, adding fibers can change the visco elasticity of asphalt, raise the dynamic modulus, increase creep compliance, and enhance water stability, cracking resistance, freeze-thaw resistance, rutting performance, and so on. Moreover, fibers added to the asphalt mixtures can be utilized in many ways[10].

2 Research Methodology

The experimental program consisted of preparing asphalt mixtures with different combinations of binder and organophilic Nano clay. The 60/70 bitumen was selected as the binder, and Margalla aggregates were used for mixture preparation. Organophilic Nano clay was incorporated into the asphalt mixtures at varying percentages to determine the optimal dosage for Marshall Stability improvement and to study Marshall Flow of asphalt mixture. Mechanical testing, including Monotonic resistance evaluation using appropriate testing protocols, was conducted on the prepared asphalt specimens. The experimental setup and all samples of Marshall Test are shown in Figure 1.

Figure 1: Marshall Apparatus and Marshall Molds

Conventional Properties of bitumen used in the study are shown in Table1.

Table 1: Conventional Test results of 60/70 binder

Binder Test	Binder (60/70)	Limit
Softening Point	48 ℃	46-54
Penetration	63 mm	60-70
Ductility	119cm	100 (min)
Flash and fire Point	248°C and 252°C	232-450
Specific Gravity	1.02	0.99-1.05

3 Results

3.1 Optimization of Organophilic Nano Clay

Research findings indicate a correlation between the proportion of Nano clay and Marshall Stability, revealing a pattern where stability initially rises with increased Nano clay content, peaking at 4.5% with a maximum value of 14.5 KN. However, beyond this threshold, as the Nano clay percentage continues to escalate, stability diminishes. The effect of Nano clay on Marshall Stability is shown in Figure 2.

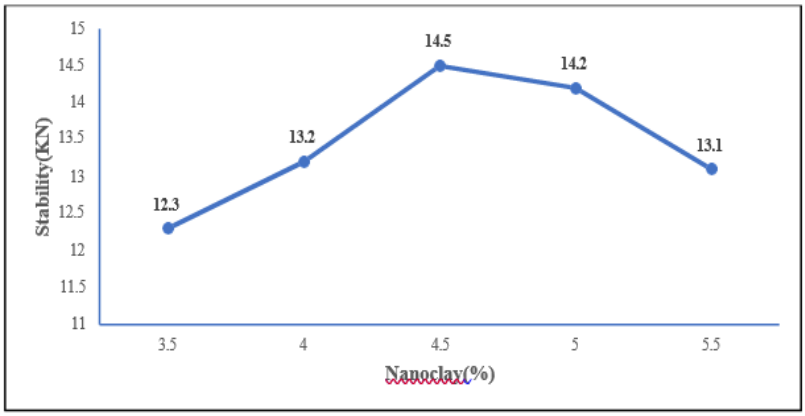

Figure 2: Effect of Nano clay on Marshall Stability of asphalt mixture

3.2 Effect of Nano Clay on Marshall Flow

Incorporating organophilic Nano Clay led to enhanced stiffness of the asphalt cement, as indicated by lower Marshall Flow values. Modifiers like as polymers or fibers can improve the characteristics of an asphalt mix, but they frequently limit flow ability, resulting in lower Marshall flow values. Low Marshall flow values in hot mix asphalt suggest higher stiffness and resistance to deformation. This can be advantageous since it indicates stronger resistance to rutting and deformation under traffic loads, resulting in increased pavement durability and performance. Hot mix asphalt with low Marshall flow values has a higher viscosity. This higher viscosity increases the stiffness of the asphalt mix, which improves resistance to deformation and performance under traffic loads. Figure 3 shows that at an optimum bitumen percentage of 4.5%, the marshall value for modified asphalt binder is 7.01, compared to 7.3 for virgin asphalt with no modifier. The Marshall Flow values with and without modifier are shown in Figure 3.

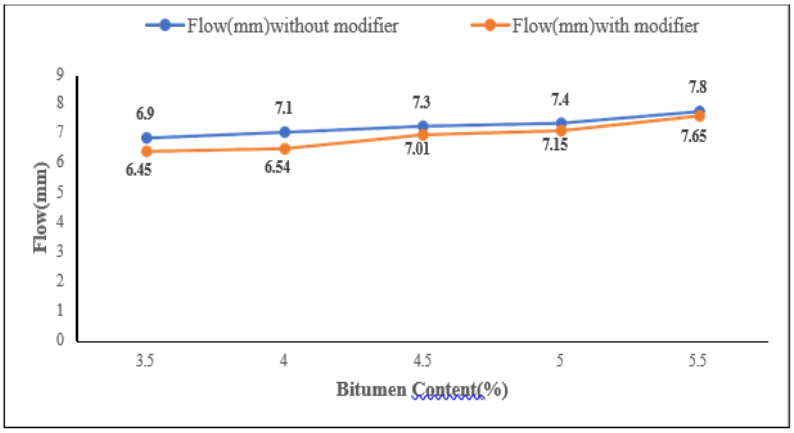

Figure 3: Effect of Nano clay on Marshall Flow of asphalt mixture

4 Practical Implementation

Incorporating Organophilic Nano clay into the asphalt concrete wearing course can prolong the serviceability of pavement. The adaptation of asphalt concrete with organophilic Nano clay enhances pavement design and fatigue life. Introducing Nano Clay into asphalt pavement significantly mitigates rutting and raveling which are the major pavement failures.

5 Conclusion

Following conclusions can be drawn from the conducted study:

- Adding Nano clay increased the Marshall Stability of the asphalt mixture, with the highest value observed at a 4.5% Nano clay concentration.
- Marshall Flow of asphalt mixture decreased with the addition of Nano clay and consequently its stiffness increased.

References

[1] Y. Liu, P. Su, M. Li, Z. You, M. J. J. o. T. Zhao, and T. Engineering, "Review on evolution and evaluation of asphalt pavement structures and materials," vol. 7, no. 5, pp. 573-599, 2020.

[2] N. Sudarsanan, Y. R. J. J. o. T. Kim, and T. Engineering, "A critical review of the fatigue life prediction of asphalt mixtures and pavements," vol. 9, no. 5, pp. 808-835, 2022.

[3] S. P. J. I. J. o. S. R. Singh, "ANALYSIS AND EVALUATION OF FLEXIBLE PAVEMENT DEFECTS," vol. 12, no. 1, pp. 96-106, 2021.

[4] J. Isooba, "Effect of filler and binder contents on air voids in hot-mix asphalt for road pavement construction," Kyambogo University, 2021.

[5] A. Suppasri, E. Maly, M. Kitamura, G. Pescaroli, D. Alexander, and F. J. I. J. o. D. R. R. Imamura, "Cascading disasters triggered by tsunami hazards: A perspective for critical infrastructure resilience and disaster risk reduction," vol. 66, p. 102597, 2021.

[6] S. Sreedhar and E. J. I. J. o. P. E. Coleri, "The effect of long-term aging on fatigue cracking resistance of asphalt mixtures," vol. 23, no. 2, pp. 308-320, 2022.

[7] S. Wu, A. Haji, I. J. R. M. Adkins, and P. Design, "State of art review on the incorporation of fibres in asphalt pavements," vol. 24, no. 6, pp. 1559-1594, 2023.

[8] K. Liu, T. Li, C. Wu, K. Jiang, X. J. C. Shi, and b. materials, "Bamboo fiber has engineering properties and performance suitable as reinforcement for asphalt mixture," vol. 290, p. 123240, 2021.

[9] Y. Guo, P. Tataranni, C. J. C. Sangiorgi, and B. Materials, "The use of fibres in asphalt mixtures: A state of the art review," vol. 390, p. 131754, 2023.

[10] W. Wang, G. Tan, C. Liang, Y. Wang, and Y. J. P. Cheng, "Study on viscoelastic properties of asphalt mixtures incorporating SBS polymer and basalt fiber under freeze–thaw cycles," vol. 12, no. 8, p. 1804, 2020.

ASSESSING THE COMBINED EFFECTS OF STEEL SPEED HUMPS AND ROAD STUDS ON SPEED REDUCTION

[a] Ali Hassan Waraich*, [b] Jamal Ahmed Khan

a: Transportation, University of Engineering and Technology, Taxila, Pakistan. alihassanwaraich050@gmail.com
b: Transportation, University of Engineering and Technology, Taxila, Pakistan. jamal.ahmed@uettaxila.edu.pk
* Corresponding author.

Abstract- The safety and efficiency of roadway design greatly influence traffic flow and accident prevention. In this paper, the effects of road studs and steel speed bumps on vehicle behavior when combined are studied. The study is intended to provide an in-depth understanding of traffic calming devices on vehicle dynamics and road safety. To investigate the effects, selected designs, or a combination of designs of steel speed hump and road studs were used to conduct an extensive field study of two months from Dec-2023 to Feb-2024 in a controlled urban area. The number of vehicles tested were hundred in total which involved 50 Cars, 30 Bikes, and 20 Heavy Traffic vehicles. The test area consisted of steel speed humps and strategically placed road studs. In our study, we analyzed data that profiled a sample of cars based on the speed data readings and the acceleration and deceleration patterns in graphical charts. The findings show that using road studs in combination with a steel speed hump adequately reduces the speed of a vehicle and by extension help in a safer way of driving in areas where illegal speeding is rampant. Road studs enhance the visual perception of the driver and, thus, consistent engagement in the deceleration and speed decline. Moreover, a drastic decrease in the number of cases of sudden braking occurred when both speed bumps and road studs were implemented as cars rolled over the humps rather than braking to drive over them. Although the implementation of the above components dramatically improves traffic safety, our study identifies numerous challenges. Firstly, humps and studs should be designed optimally as cars experience increased wear and tear of the suspensions and wheels, whereas, at high speeds, the drivers may feel uncomfortable. Based on our study outcomes, substantial attention seems appropriate regarding speed bump height and spacing and the number and location of road studs that should be factored into their use to avoid unfavorable effects and maximize safety benefits. In summary, combining steel speed humps and road studs has great potential to improve road safety. More investigations should focus on designing and positioning them to achieve a traffic-calming-vehicle performance tradeoff in a balanced way. This article contributes to the body of knowledge for urban planners, traffic engineers, and policymakers to make roads safer in urban areas.

Keywords- Traffic Calming, Speed Humps, Road Studs, Traffic Engineering.

1 Introduction

One of the primary risk factors for road traffic safety is speed, which affects the likelihood and seriousness of accidents[1]. Ensuring drivers adhere to speed restrictions is one of the primary responsibilities of the organizations in charge of road safety[2]. Traffic engineers use a variety of physical speed control techniques that can be used individually or in combination to lower the speed to a reasonable level[3]. A research report highlights the issue of speeding in Denmark and the use of speed hump to reduce the matter of speeding[4]. It's critical to evaluate the effects of safety measures on road safety after a predetermined amount of time has passed since they were installed. Different studies have been made regarding this topic one of the studies concludes that installing TRS (Transverse Rumble Strips) with road studs effectively reduces speed, which is consistent with the results of the public opinion poll[5]. In this study, we concluded that It's important to ascertain whether road safety precautions placed in specific areas have a beneficial effect. For a traffic planner, who is primarily looking to address the problem and come up with a plan that would satisfy predetermined objectives, it

is crucial to understand the relative impact of different traffic calming mechanisms. From a scientific perspective, in addition to the technical aspect, an economic assessment should be made, including a societal cost-benefit analysis, to assess whether safety benefits justify the cost. Steel speed humps and road studs can be combined to reduce speed and make the road safer[6].

One critical factor resulting from these methods that must be considered is their impact on driver behavior and traffic flow. The various methods, including speed humps, road width narrowing, and blocking, circles, and signage, can affect road behavior and safety[7]. Therefore, traffic control should only be concerned with specific aspects and how others would be overly positive or burdensome and determine that point will minimize the harm to achieve the optimal balance between safety and efficiency. This focus is essential with a long-term view of creating a safe and feasible traffic regulatory regime.

Economic analysis should also be conducted to determine the cost-effectiveness of traffic-calming measures in other locations. Policymakers would be able to balance the conduct-related costs with those related to the installation and maintenance of security measures and compare the benefits of security using the open-cost technique. The most cost-effective types of investments in terms of traffic safety superiority and the decrease in accident frequency are more financially rational using this method.

To conclude, the understanding of the comparative advantages of different ways of traffic calming and economic analysis are important parts of the creation of comprehensive and effective driving control measures. Road studs and steel speed bumps are the two most effective methods of reducing car speeds and improving the safety of roads, which, in turn, will allow an improvement in the transport system for everyone[8].

2 Literature Review

Analyzing the impact of traffic calming devices has always been a topic of study in the field of road safety. To determine their effectiveness, we need to collect data from different types of vehicles passing over different types of traffic calming devices to know the significance of different types of these devices. One of the studies concludes that the installation of TRS with road studs effectively reduces the speeds of vehicles from each category. To determine whether TRS with road studs is effective and how people feel about it, this research is carried out on a section of TRS with road studs[5]. Another study determined the variation in speeds by different categories of vehicles when encountering speed breakers and created a model for determining the appropriate height of bumps that should be implemented on specific roads, by the given safe speed limits for different vehicle types[9]. Several studies have shown that as the class of the vehicle increases, the percentage of speed reduction of vehicles increases at the location of traffic calming devices[9], [10].

Figure 1: Steel speed hump along with Road studs

Figure 2: Study Location on a dual carriageway

3 Research Methodology

The purpose of the investigation was to ascertain how much steel speed hump along with road studs reduced vehicle speed. The investigation was conducted on an urban road with high traffic volume and a track record of speeding incidents. Using speed detection tools, including a radar gun, vehicle speeds were recorded at several points along the route. Before and after the installation of the traffic calming devices, data was gathered. After collecting the information, the average speeds were noted before and after Traffic calming devices. The effect of road studs was determined based on instantaneous speed and the vehicle type. The study site was divided into two points before 150ft and after 150ft. Speeds were noted at both points using a radar gun and speed data was collected for different types of vehicles.

4 Study Location

The study site we chose was at least 3 km away from the main city. It was an industrial area where the movement of different types of vehicles was repeated throughout the day. *Figure 2* shows that the study location was selected away from any traffic signal and any intersection. It was an industrial area and the road was dual carriageway.

5 Results

The results were analyzed to determine how well road studs and steel speed bumps work to slow down moving cars. In-depth tables and charts were used to present the results and show how the average speed and speed distribution changed before and after the traffic calming device. Comprehensive data tables and visual charts are used to show the difference in average speed and speed distribution before and after the steel speed humps. Graphical representations of distinct vehicle speeds before and past the Traffic calming devices are shown in *Figure 3* below.

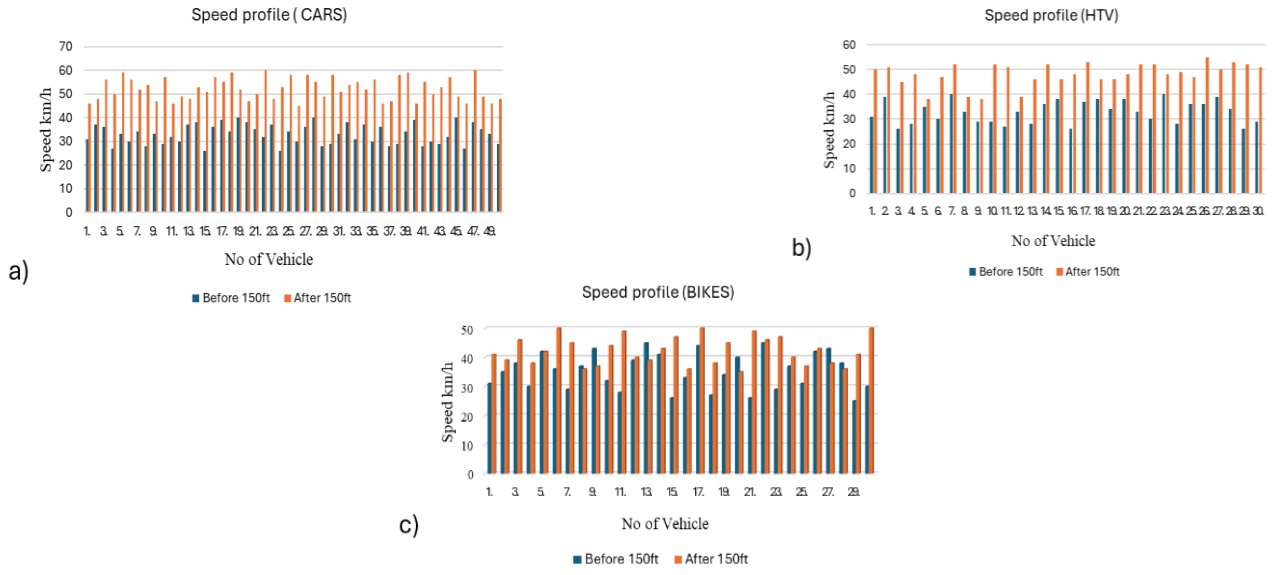

Figure 3: Speed Profile graph for different types of vehicles, a. Speed profile of Cars, b. Speed profile for HTV, c. Speed Profile for Bikes

From empirical studies, it has been determined that steel speed humps along with road studs could not positively impact the reduction of velocities of the vehicular type bike within the proximity of the Road Studs. The reason behind this was the difference in drivers' behavior. Behavior changes depend on the type of vehicle, region to region, etc. The speed of various kinds of vehicles was measured using a radar gun before and after the steel hump along with road studs, as illustrated in *Figure 1*. Vehicle speeds were shown to decelerate/decrease before 150 feet of the traffic calming device. Their average speeds were noted. The study of the obtained speed data demonstrated a considerable decrease in average vehicle speed following the installation of steel speed bumps and road studs, shown in *Table 1*.

Table 1: Average speed before and after steel speed hump

Type of Vehicle	Average speed before hump (150ft)	Average speed after hump (150ft)	Average percentage difference
Car	33.02	52.26	45.12%
Bike	32.86	48.13	37.70%
HTV	35.20	42.23	18.15%

6 Practical Implementation

For anyone working in traffic engineering, urban planning, or policymaking who wants to improve road safety in urban areas, this article offers insightful information. This study opens new doors for finding the impact of different types of road studs on different types of vehicles. The study provides the information that steel speed hump along with road studs have different impact on cars, bikes, and HTV, which shows the difference in drivers' behavior.

7 Conclusion

The study aimed to assess the extent to which road studs and steel speed bumps are effective in reducing the speed of cars in a dual-carriageway urban route. The study provides critical findings on using steel speed bumps given its comprehensive approach in terms of data collection before and after the installation of the road traffic-restraining measures.The obtained results undoubtedly demonstrated that adding road studs and steel speed bumps significantly reduced the speed of cars. Firstly, the mean speed had fallen by 10-15 km/h. This is a powerful speed reduction indicator. Secondly, the percentage of cars going over the limit again dropped, which means that the drivers' behavior improved.

In conclusion, the above study provides robust evidence that road studs and steel speed humps are effective in reducing vehicle speeds and encouraging safe driving behavior on urban roads having a dual carriageway. This work has immense policy implications by emphasizing the urgent need to implement effective traffic calming methods to promote road safety and enhance the overall quality of transport infrastructure. From a practical standpoint, these findings will be invaluable to agencies involved in activities related to urban integration, planning, and traffic management. In the end, more research in this field will help us in the future to improve our knowledge of the connection between traffic calming interventions and road safety, which will lead to the creation of safer environments and more efficient methods for reducing risks associated with traffic. This study also helps in future research, finding the optimal spacing of speed humps in different combinations of road studs, a valuable study tool for field engineers to design traffic calming devices geometry for speed control of vehicles. There is also no comparison between different income and socioeconomic groups, between different developing and underdeveloped countries. In the future, we can give names to different combinations of road studs as there are no such names given to them.

Acknowledgment

The authors would like to thank every person/department who helped throughout the research work, particularly the CE Department, FWO, and Muhammad Bilal Khurshid.

References

[1] J. Gulden and J. De La Garza, "Traffic Calming," in *Traffic Engineering Handbook*, John Wiley & Sons, Ltd, 2015, pp. 501–540. doi: https://doi.org/10.1002/9781119174738.ch14.

[2] P. W. G. RV Ponnaluri, "Operational Effectiveness of Speed Humps in Traffic Calming," vol. 75, no. 7. Institute of Transportation Engineers.

[3] T. M. Pharoah and J. R. E. Russell, "Traffic calming policy and performance: The Netherlands, Denmark and Germany," *Town Planning Review*, vol. 62, p. 79, 1991, [Online]. Available: https://api.semanticscholar.org/CorpusID:148538404

[4] N. Agerholm, L. H. Sørensen, P. R. Gøeg, H. Lahrmann, and A. V. Olesen, "A large-scale study on the speed-calming effect of speed humps," *Transactions on Transport Sciences*, vol. 11, no. 2, pp. 28–38, Sep. 2020, doi: 10.5507/TOTS.2020.006.

[5] M. F. Hazim, N. Mashros, S. A. Hassan, N. A. Hassan, and A. Y. Kurnia, "Effectiveness of and Public Perception about the Installation of Transverse Rumble Strips with Road Studs," in *IOP Conference Series: Earth and Environmental Science*, IOP Publishing Ltd, Feb. 2022. doi: 10.1088/1755-1315/971/1/012008.

[6] K. G. D. Gamlath, N. Amarasingha, and V. Wickramasinghe, "Evaluating the Effectiveness of Speed Humps Related to Speed Profile and Noise Profile," *Journal of Advances in Engineering and Technology*, vol. 1, no. 2, pp. 1–13, Mar. 2023, doi: 10.54389/OPDO9291.

[7] S. N. Densu and P. Damoah-Afari, "Effects of speed hump on vehicle performance in the Sekondi-Takoradi Metropolis, Ghana," *Cogent Eng*, vol. 9, no. 1, 2022, doi: 10.1080/23311916.2022.2143066.

[8] N. Mashros, M. F. Md Nor, A. Y. Kurnia, S. A. Hassan, N. A. Hassan, and N. Z. M. Yunus, "Evaluating the effectiveness of road humps in reducing vehicle speed: Case study of a university campus," *Int J Adv Sci Eng Inf Technol*, vol. 10, no. 2, pp. 814–820, 2020, doi: 10.18517/ijaseit.10.2.5836.

[9] T. Teja and M. Jyothi, "Speed Profile Analysis at Speed Breakers on An Urban Road," *i-manager's Journal on Civil Engineering*, vol. 7, no. 1, p. 25, 2017, doi: 10.26634/jce.7.1.10370.

[10] T. Sayed, P. deLeur, and J. Pump, "Impact of Rumble Strips on Collision Reduction on Highways in British Columbia, Canada: Comprehensive Before-and-After Safety Study," *Transp Res Rec*, vol. 2148, no. 1, pp. 9–15, 2010, doi: 10.3141/2148-02.

6th Conference on Sustainability in Civil Engineering (CSCE'24)
Department of Civil Engineering
Capital University of Science and Technology, Islamabad Pakistan

A CROSS-SECTIONAL ANALYSIS OF SUSTAINABLE MOBILITY FOR FEMALE UNIVERSITY STUDENTS IN KARACHI

[a] Ashar Ahmed*, [b] Bakir Rehman

a: Department of Urban and Infrastructure Engineering, NED UET, Karachi, Pakistan. aahmed@cloud.neduet.edu.pk
b: Department of Urban and Infrastructure Engineering, NED UET, Karachi, Pakistan, rehman4404840@cloud.neduet.edu.pk
* Corresponding author.

Abstract- Limited mobility restricts educational opportunities for female students in Karachi, Pakistan. This study investigates the various factors related to their travel patterns. Safety concerns regarding harassment on public transport and deserted streets are key deterrents. Data was collected through in-person questionnaire survey. It was found that the female students are from diverse backgrounds, which in turn affects their travel pattern and mode choice. This research found that public transport such as bus and chingchi are cost effective as well as sustainable and are also more utilized by female hostel students as compared to car and ride-hailing services. It is recommended that increasing the accessibility and safety of public transport services will not only improve female mobility but also help achieve sustainability.

Keywords- Cost, Gender, Mobility, Public Transport, Student.

1 Introduction

Karachi's mobility pattern is dominated by cars and bikes, leading to traffic congestion. The public bus system, though present, is limited and often overcrowded. Many citizens are forced to rely on informal options like rickshaws due to a lack of better alternatives. Furthermore, the city lacks sufficient infrastructure for pedestrians and cyclists, making commuting difficult and unsafe for a significant portion of the population. This car-centric approach not only creates congestion but also exacerbates social and economic inequality by limiting mobility options for those who cannot afford private vehicles as indicated in a previous study [1].

There are two main categories of transport: active and inactive transport. Active transport uses your own energy to move, like walking, or cycling. Inactive transport relies on an external power source, like cars, bikes, buses, or trains. Active options offer health benefits, cost savings, and environmental advantages, while inactive modes can be convenient but contribute to traffic congestion and pollution as mentioned in the study conducted by Conor C.O. Reynoldsa et al. [2].

The limited mobility faced by female students in Karachi, Pakistan is a critical issue that motivates this research as indicated in the recent study [3]. Our aim is to analyze data to understand the everyday travel patterns of female students within Karachi and in their hometowns. By examining these patterns, we hope to identify the challenges they face, such as safety concerns on public transport, societal limitations, and economic constraints this is in alignment with previous study [4]. This knowledge will then be used to develop solutions that improve safety, affordability, and accessibility of transportation options. Ultimately, this will empower female students in Karachi to pursue their educational goals, similar to Humayun et al. 2017 [5]. This paper consist of Section 2 which details the study area, section 3 presents descriptive statistics, section 4 analyzes trips within the city, examining how trip purpose and cost influence travel choices, as outlined in a previous study [6]. Section 5 focuses on trips outside the city, analyzing cost omparisons for sustainable vs. non-sustainable travel modes. The paper ends with the conclusions and recommendations for future research.

2 Study Area

This study focuses on the travel patterns of female students at NED University, a prominent institution and one of the largest universities in Pakistan, located in Karachi, as shown in Figure 1. The university caters to a substantial number of undergraduate and postgraduate students. Some undergraduate female students are hostel residents out of which we have conducted survey of 28 students, 4 students are from Sri Lanka and 24 students are Pakistan.

Figure 1: Study location, NED University of Engineering and Technology, Karachi, Pakistan
Source: https://www.openstreetmap.org/#map=15/24.9301/67.1114&layers=TNG (accessed 3rd July 2024)

3 Descriptive Statistics

The data was collected across various modal, geographic, and economic parameters to understand travel patterns in Karachi. Modal Parameters refers to the different modes of transportation used. The data includes categories like Car, Bus, Chingchi (likely referring to rickshaws), Ride Hailing Service, Train, Van, and by Air. Geographic Parameters captures information related to travel distances. It includes "Distance to hometown" categorized by nationality (Pakistani/International) and "Travel Time for intercity journey". Economic Parameters focuses on the financial aspects of travel. The data includes "Average intercity mobility Cost/year" and "Average intracity mobility Cost/year". The table 1 provides additional details with: Nationality; Pakistani or International, Participant's age range, and number of participants in each category. It's important to note that some categories lack minimum, maximum, and mean values, likely due to the nature of the parameter (e.g., nationality might not have numerical values), similar to the presentation of such kind of data in a previous study [7].

Table 1: Descriptive statistics of survey data

Parameters	N	Min	Max	Mean
Nationality:				
Pakistani	24	-	-	-
International	4	-	-	-
Age	28	19	25	21
Distance to hometown:				
Pakistani	24	162.4	1412.1	371
International	4	2769	2769	2769
Average intracity mobility Cost/year	28	2000	10000	5660
Average inter-city mobility Cost/year	28	5000	77206.47	13661
Number of intracity trips/month:				
Chingchi	155	-	-	-
Bus	157	-	-	-
Car	5	-	-	-
Ride Hailing Service	83	-	-	-
Number of inter-city trips/month:				
Bus	10	-	-	-
By Air	4	-	-	-
Van	5	-	-	-
Train	1	-	-	-
Car	7	-	-	-
Travel Time for intercity journey	28	1.5	16.75	5.76

4. Trips Within City

4.1 Analysis with Respect to Trip Purpose

A comparative analysis of the overall trips made in a month via each mode for a specific purpose is presented in Figure 2. The data is also categorized with respect to sustainable (e.g., bus, chingchi) and non-sustainable options (e.g., car, ride-hailing). Interestingly, sustainable options seem favored by the students. Bus appears to be the most used mode across various trip purposes (shopping, work, medical, recreation). Chingchi, which are three-wheelers and are similar to rickshaws, is the second most used option especially for shopping and recreation as shown in Figure 2. Options like car and cab-service see minimal usage, suggesting they might not be the preferred choice due to factors such as cost, safety concerns, or limited access. These findings are in alignment with a previous study [8].

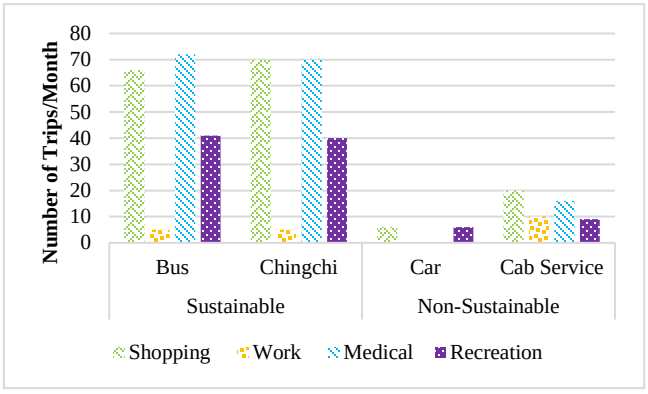

Figure 2: Number of trips produced from different modes

4.2 Analysis with Respect to Trip cost

For the trip made within city analysis was performed with respect to cost as well. The data was collected for the total number of trips made during a month and the total cost incurred thereto. This method of analysis is in alignment with a previous study [9]. The exploratory analysis of the data shows is presented in Figure 3. It can be clearly seen that public transport modes, which are bus and chingchi, are more cost effective as compared to private transport modes such as car and cab service.

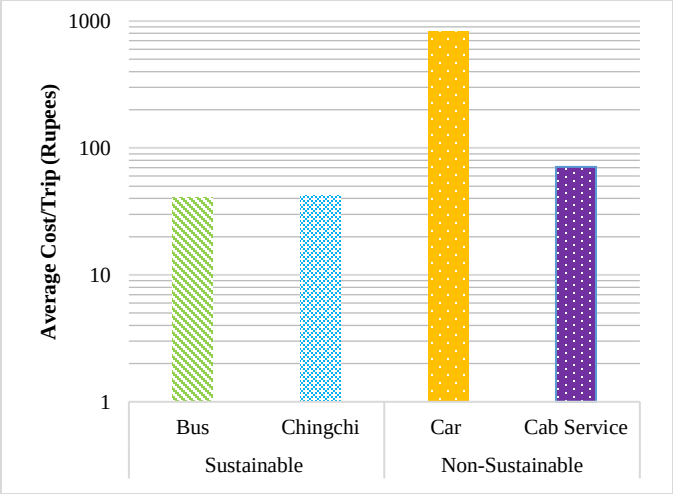

Figure 3: Trip cost with in city travel

5. Trips Outside City

The sole purpose of female hostel students of travelling outside city is to go to their respective hometowns. Therefore, analysis was made with respect to cost only. A comparison of costs for different modes of travel between cities is presented in Figure 4. Trains and vans are the cheapest options for trips within the country based on this information. This makes them a good choice for people who are on a budget. It's important to remember that international students wouldn't be able to use these options and would likely need to travel by air. As indicated in a previous study [9].

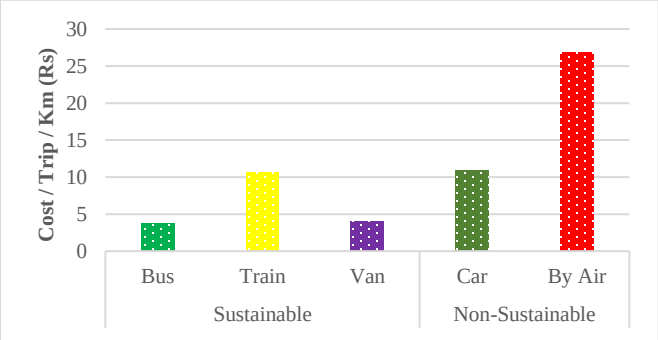

Figure 4: Cost per trip per km for home town travel

6. Conclusion and Recommendation

This study investigates the various mobility patterns of female university hostel students. It was found that transport choices like buses and rickshaws are common since they are accessible and reasonably priced. The usage of rickshaws and ride-hailing services may be restricted due to safety concerns. However, another important factor was cost. It was found that students choose less expensive solutions, such as bus and chingchi, when it comes to mobility. Trains and vans are affordable options for intercity travel. The research concludes that female hostel students mostly prefer public transport for their mobility, which is also a sustainable mode. This is an important finding. The report suggests improving the safety of public transportation, advocating for secure infrastructure like well-lit sidewalks, provision of reasonably priced ride-hailing services or student transportation assistance programs, to enhance accessibility to students belonging to all types of socio-economic background. The ultimate goal is to provide educational opportunities by making the transit network safer and easier to use for everyone.

Reference

[1] F. Anwar, F. Fatima and N. Panjwani, "Urban Mobility in Mexico: Towards Accessible Cities Less Reliant on Cars," *Sustainable Urban Mobility for Karachi,* 2012

[2] C. C. O. Reynoldsa , M. Wintersb , F. J. Riesa and B. Gougea, "Active Transportation in Urban Areas," *National Collaborating Center For Environmental Health,* 2010

[3] S. Nasrin and S. Chowdhury, "Exploring transport mobility issues and adaptive behavior of women in a developing country," *Transportation Research Interdisciplinary Perspectives*, vol. 23 2024

[4] Shabina Faraz, "Poor urban planning blocks dreams of women and girls in Karachi," *Justice,* 2022

[5] A. Humayun, H. Saleem, R. Raza and S. Aziz, "Transportation Difficulties Faced by Female Students of KarachiMedical and Dental College (KMDC) and University of Karachi (UoK)" *Transportation(1).P65*, 2017

[6] Hiba, Shoaib and Z. Imran, "Women Traversing Gendered Public Spaces in Urban Karachi" *Female Mobility,* 2021

[7] K. Mouratidis, J. D. Vos, A. Yiannakou and I. Politis, "Sustainable transport modes, travel satisfaction, and emotions: Evidence from car-dependent compact cities," *Travel Behaviour & Society,* vol. 33, 2023

[8] R. Mehnaj, A. Raida and M.N. Murshed, "Mode Choice Preferences of Female University Students and Impacts of Ride-Sharing Thereon – 2022," *Journal of Engineering Science,* vol. 13(2) pp 43-49, 2022,

[9] M. Schnieder, "Effective Speed: Factors That Influence the Attractiveness of Cost Effective and Sustainable Modes of Transport in Cities," *Sustainability,* vol. 15, 2023

EXAMINATION OF THE EFFECT OF ILLEGAL PARKING ON CAPACITY REDUCTION OF URBAN ROADS

[a] Ashar Ahmed*, [b] Muhammad Shair

a: Department of Urban and Infrastructure Engineering, NED UET, Karachi, Pakistan. aahmed@cloud.neduet.edu.pk
b: Department of Urban and Infrastructure Engineering, NED UET, Karachi, Pakistan shair4304316@cloud.neduet.edu.pk
* Corresponding author.

Abstract- The city of Karachi has more than 20 million residents which face severe traffic congestion due to infrastructure problems and inefficient traffic management. One of the reasons for the congestion is the habit of illegal parking which results in the formation of bottlenecks. This study investigates the impact of illegal parking on traffic congestion, which is a major cause for air pollution and increased emission levels. On-site surveys were conducted to measure vehicle flow, illegal parking extent, and operational lanes during peak hours. Data was collected manually at Allama Shabbir Ahmed Usmani Road, in Gulshan-e-Iqbal Town. It was found that an average of 2.05 lanes are operational which cater a traffic volume of 2575 PC/hr in front of Blue Ribbon Bakery and 1.88 lanes are operational with a traffic volume of 3144 PC/hr in front of Manpasand Foods. The calculated road capacity was found to be 2075.6 PC/hr/lane. This slightly higher peak hour volume, indicates a near saturation condition and that congestion is inevitable. This congestion leads to increased fuel consumption and emissions, adversely affecting commuters' health. The study underscores the need for improved traffic management to mitigate these issues.

Keywords- Sustainability, Illegal Parking, Congestion, Emissions.

1 Introduction

Karachi being a mega city is home to more than 20 million people spread over 3530 square kilometers [1]. This vast population commutes daily through the city for work, education and other purposes. Similar to other metropolitan cities, including developed countries, Karachi also suffers from traffic congestion and subsequently the emissions that occur due to it. These issues become severe due to its problematic infrastructure and highly inefficient traffic management and public transport system. These issues range from illegal parking, badly optimized traffic signals, unreliable public transport system, worn-out roads and deteriorating pavements.

In Karachi, the average total delay of vehicles throughout the city due to congestion is estimated to be 600,000 minutes/day which is nearly 410 days/day [2]. Faiq et al. (2012) found that the primary reasons for these traffic jams in Karachi are encroachments on roads and footpaths, an excess of cars, and insufficient parking facilities [3]. These key factors contribute significantly to severe traffic congestion leading to increased travel time, additional fuel costs, delays, and consequently, higher emissions[3]. Now, these delays not only results in reduced mobility but it has a direct impact on the energy consumption which is mostly fossil fuel for vehicles. The more time a vehicle spend on roads in idling crawling or undergoing acceleration and deceleration, the more fuel it is likely to consume resulting in higher emissions and longer exposure times for commuters in these polluted environments.

These emissions include a variety of air pollutants including Black carbon (BC), Carbon Dioxide (CO_2), carbon monoxide (CO), hydrocarbons (HC), nitrogen oxides (NO_X), nitrogen dioxide (NO_2), PM2.5 and PM10 particulate matter, and particles with a diameter < 0.1 µm also known as ultra fine particles (UFP) [4][5]. Delays in commuting time increase the daily exposure to these pollutants, which in turn raises the risk of skin, eye, and lung-related health issues, as well as

physical and mental health problems due to traffic congestion[6][7]. Traffic-related air pollution constitutes a significant public health crisis. Its impact is substantial and continues to grow as advancements in knowledge and quantification methods emerge [8].

This study focuses on causes and effects of illegal parking on congestion which eventually results in traffic related air pollution and emissions. The first section of study covers the study area, the second details capacity and peak hour volume calculations, the third presents results and discussions, and the final section offers recommendations.

2 Study Area

The study solely focuses on the impact of illegal parking on traffic congestion. To investigate this issue, a survey was conducted on a 100 meter section of Allama Shabbir Ahmed Usmani Road, extending from Maskan Chowrangi, in front of Blue Ribbon Bakery and Manpasand Sweets.

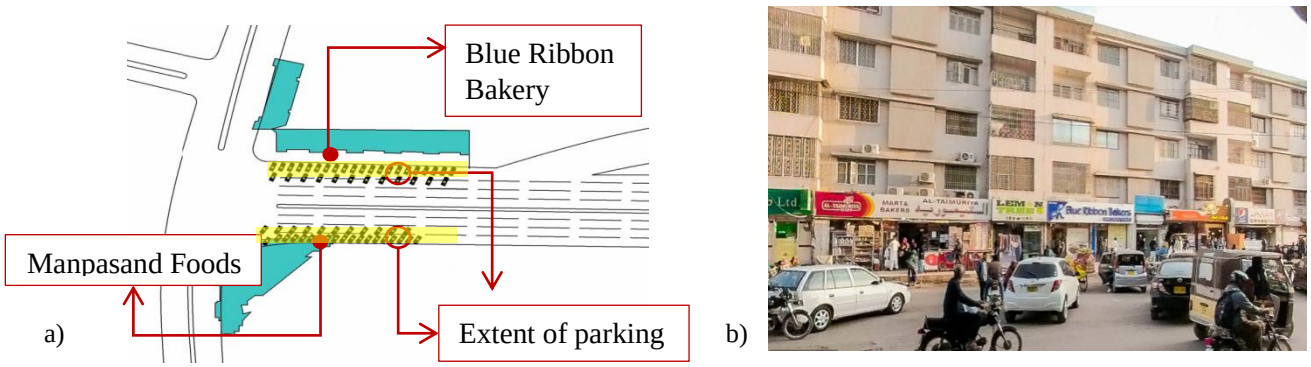

Figure 1: Study Area, a. Geometry of study area, b. Condition of illegal parking in front of Blue Ribbon as of 30 May,2023 at 6:00 pm.

Figure 1 depicts the geometry and current conditions of the study area on Allama Shabbir Ahmed Usmani Road, with the 100-meter section under observation highlighted in yellow (Figure 1a). Figure 1b captures the reality of vehicles illegally parked along this specific section of the road.

2.1 Locations

The location selected for this particular study is the starting point of Allama Shabbir Ahmed Usmani Road, in front of the Manpasand Foods (coordinates: 24.935039N, 67.104908E) and Blue Ribbon Bakery (coordinates: 24.934667N, 67.105108E) (Figure 2).

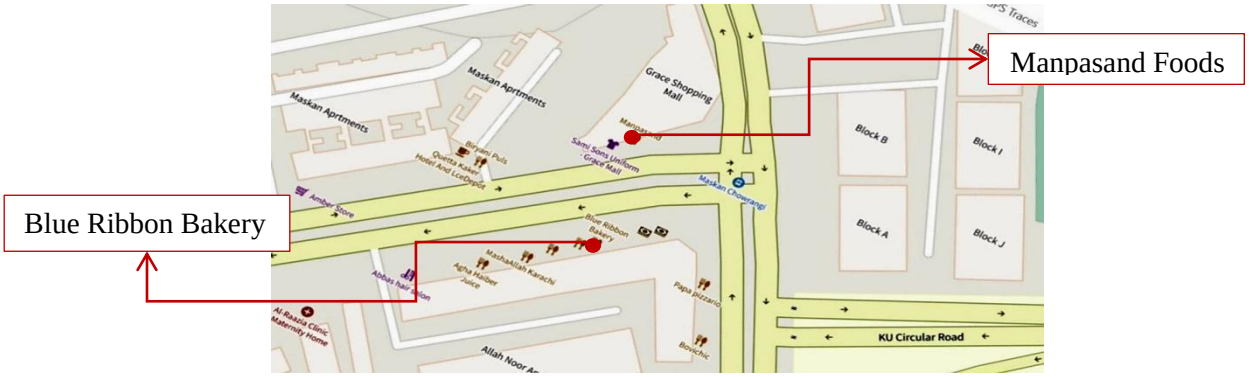

Figure 2: Location of the study area (Source: openstreetmap.org)

2.2 Data Collection

The survey was performed on 30 May, 2023 from 6 pm till 10 pm at the specified location. The data was collected manually in a group of two by stationing at the site to obtain required information. The survey focused on the number of operational lanes on each side of the road during peak hours and the traffic volume. The finding indicate an average of 2 operational lanes in front of Blue Ribbon and 1.88 in front of Manpasand Foods with traffic volumes are 2575 PC/hr and 3144 PC/hr respectively.

3 Capacity Analysis

For capacity analysis we consider a segment of road on level terrain with a length of 180 m and a base free flow speed of 60 kmph. The peak hour volume recorded is 3144 veh/hr. The road features a width of 13 meters with individual lane widths of 3.6 m and lateral clearance of 2.5 meters. Based on these parameters, we proceed with the capacity and Level of Service (LOS) calculations.

3.1 Current Capacity and LOS

The current capacity was calculated considering the adverse conditions, with operational traffic lanes of 1.88 and a volume of 3144 PC/hr, as indicated by the survey. Hence,

FFS= BFFS – F_{LW} – f_{LC}- f_M - f_A [9]

$$FFS = 40 - 0 - 1.44 - 0 - 1 = 37.56 \text{ km/hr}$$

$$FHV = \frac{1}{1+Pt(Et-1)+Pr(Er-1)} = 0.989 \quad [9]$$

When N=1.88,

$$VP = \frac{V}{PHF \times N \times FHV \times FP} = \frac{3144}{0.9 \times 1.88 \times 0.989 \times 1} = \textbf{1878.82 PC/hr/ln} \quad [9]$$

LOS for Vp=1878.82 PC/hr/ln is: **LOS F**

For practical capacity,

$$\text{Capacity} = 2200 + 10 * (V - 50) \quad [9]$$

When V = 37.56 km/hr, Capacity = 2075.6 PC/hr/ln

Capacity = **3902.128 PC/hr/roadway** (*when, no of operational lanes = 1.88*)

3.2 Proposed Capacity and LOS

Proposed capacity will be when all 3 of the lanes will become functional, so the peak hour volume per lane will reduce while the practical capacity per lane will remain same. Hence,

When N=3,

$$Vp = \frac{V}{PHF \times N \times FHV \times FP} = \frac{3144}{0.9 \times 3 \times 0.989 \times 1} = \textbf{1177.39 PC/hr/ln} \quad [9]$$

LOS for Vp=1177.39 PC/hr/ln is: **LOS D**

For practical capacity,

Capacity = **6226.8 PC/hr/roadway** (*when, no of operational lanes = 3*)

3.3 Comparison Between Proposed and Current LOS

A comparative analysis of the LOS at the study location is presented in Table 1. It can be observed that the current and proposed capacity and LOS changes with the change in available number of functional lanes. A noteworthy increase of 37% in the capacity of the road in a particular direction can be achieved if the numbers of functional lanes increase from 1.8 to 3.

Table 1: Comparison table between current and proposed conditions

	Capacity (PC/hr/roadway)	LOS
Current	3902	F
Proposed	6226	D

4 Discussions

The maximum per lane capacity of road is coming out to be 2075.6 PC/hr/lane. This capacity is calculated at a base free flow speed of 40 kph. The value of this capacity is more than the peak hour volume, which is 1878.8 PC/hr/lane. Since, the capacity of the road is greater than the peak hour volume this means that the condition is not saturated and there will not be any further queuing of vehicles and the outflow will be equal to the inflow. But in practical and as per our observation, since the value of Vp is very close to the capacity of the road, the road can become oversaturated when parking maneuvers occurs, therefore congestion will be imminent. This will create delay eventually causing more fuel to burn resulting in emissions and more exposure time to the commuters. Furthermore, the investigation indicates that if all three lanes will remain operational the peak hour volume per lane will reduce improving the level of service (LOS) from F to D. This indicates that restoring the full capacity of the road by eliminating illegal parking could significantly reduce congestion, reduce fuel consumption, and lower emissions.

5 Recommendations

In order to effectively mitigate the issue of illegal parking it is crucial to enforce traffic regulations. Research shows that rigorous enforcement significantly reduces traffic violations by imposing substantial penalties, encouraging compliance and keeping lanes clear. For the successful execution of an optimal enforcement strategy, it is crucial to consider its selection as a fundamental part of the comprehensive transport plan, rather than treating it as an afterthought to be added later [10].

Other effective strategies include congestion pricing, successfully used in Singapore and London to reduce traffic volumes. Incentives like free entry for electric vehicles and public transport into congestion zones have proven even more successful [11]. Implementing similar strategies in Pakistan could lower traffic volumes, carbon emissions, air pollution, and queuing times.

References

[1] S. Qureshi, "The fast growing megacity Karachi as a frontier of environmental challenges: Urbanization and contemporary urbanism issues," Journal of Geography and Regional Planning, vol. 3, no. 11, pp. 306, 2010.
[2] M. S. Ali, M. Adnan, S. M. Noman, and S. F. A. Baqueri, "Estimation of traffic congestion cost—a case study of a major arterial in Karachi," Procedia Engineering, vol. 77, pp. 37-44, 2014.
[3] F. Matin, G. M. Herani, and U. A. Warraich, "Factors affecting traffic jam in Karachi and its impact on performance of economy," KASBIT Business Journal, vol. 5, no. 1, pp. 25-32, 2012.
[4] H. Khreis, M. J. Nieuwenhuijsen, J. Zietsman, and T. Ramani, " Chapter 1 - Traffic-related air pollution: Emissions, human exposures, and health: An introduction". Traffic-Related Air Pollution, pp. 1-21, 2020.
[5] A. Choudhary, and S. Gokhale, "Urban real-world driving traffic emissions during interruption and congestion," Transportation Research Part D: Transport and Environment, vol. 43, pp. 59-70, 2016.
[6] R. Mushtaq and O. Hashmi, "Traffic congestion and prevalence of mental and physical health issues in Karachi," Pakistan Journal of Psychology, vol. 53, no. 2, 2022.
[7] J. Javed, E. Zahir, H. A. Khwaja, M. K. Khan, and S. S. Masood, "Black Carbon Personal Exposure during Commuting in the Metropolis of Karachi". Atmosphere, vol. 13, pp. 1930, 2022.
[8] C.J. Matz, M. Egyed, R. Hocking, S. Seenundun, N. Charman, and N. Edmonds, "Human health effects of traffic-related air pollution (TRAP): a scoping review protocol". Systematic reviews, vol. 8, pp.1-5, 2019.
[9] Highway Capacity Manual 2000. Transportation Research Board, National Research Council, Washington, D.C., 2000.
[10] K. Cullinane, and J. Polak, "Illegal parking and the enforcement of parking regulations: causes, effects and interactions". Transport Reviews, vol. 12, pp.49-75, 1992.
[11] A. Farooq and M. Javid, "Practices of Traffic Congestion Pricing Policies – Implications and Challenges for Cities in Pakistan", TJ, vol. 3, no. ICACEE, pp. 433-440, May 2024.

THE IMPACT OF GYPSUM ON THE STABILIZATION OF PEAT SOIL

[a] Affaq Arif Gill*, [b] Muhammad Waleed

a: Civil Engineering Department, Army Public College of Management and Sciences, Rawalpindi. gillaffaq777@gmail.com
b: Civil Engineering Department, Army Public College of Management and Sciences, Rawalpindi. rajawaleed918@gmail.com
* Corresponding author.

Abstract- Peat soil, characterized by its high organic content, presents significant challenges in construction due to its compressibility and low strength. This study investigates the potential of gypsum as a stabilizing agent for peat soil. Laboratory experiments were conducted by adding varying amounts of gypsum (5–15%) to the soil, and the effects on dry density, optimum moisture content (OMC), Atterberg limits, and California Bearing Ratio (CBR) were evaluated. Results showed a 38.89% reduction in OMC at 15% gypsum, with the maximum dry density decreasing from 0.802 g/cc to 0.715 g/cc. The liquid limit decreased from 49% to 39%, and the plastic limit from 20% to 16%, reducing the plasticity index. Furthermore, unsoaked CBR values increased from 1.802% to 2.94% and soaked CBR values improved from 0.801% to 1.634%. These findings highlight gypsum's effectiveness in enhancing the engineering properties of peat soil.

Keywords- Gypsum, Maximum Dry Density, Optimum Moisture Content, California Bearing Ratio.

1 Introduction

Peat soil comes with a lot of challenges for construction because of its high water and organic content, and the weak load-bearing capacity. To solve these problems, a process is required to make peat soil better for building on. [1] Peat is widespread globally, except in deserts and the Arctic, with the largest areas found in the northern hemisphere. Peatlands cover approximately 4.5% of total land, around 1 billion acres. These soils are composed of 50–60% carbon and have a high water content of 50–110% in a wide range. [2] Chemically, peat soils are high in carbon and water; the normal composition is nitrogen (2-4%), phosphorus, and hydrogen (5-7%). [3] Soil stabilization, a contemporary approach, aims to improve soil properties for specific purposes, notably in construction, rendering it stable and suitable. Traditional methods often proved less cost-effective and environmentally friendly. [4] Gypsum, used in cement, plaster, and fertilizer production, also influences soil properties, especially in construction. Studies show it increases Maximum Dry Density (MDD) while reducing Optimum Moisture Content (OMC) in soil. Various gypsum additives are available for soil improvement.[5] Studies demonstrate gypsum's crucial role in stabilizing various soils, such as enhancing processed soft kaolin clay by combining it with Palm Oil Fuel Ash (POFA). Individual treatment with POFA had limited effectiveness in improving soil properties, suggesting that combining it with gypsum yields greater benefits.[6]

Andi Herius et al., [7] aimed to enhance the properties of peat soils for construction purposes by investigating the effectiveness of stabilizing them with a combination of Petra soil and cement. They evaluated the impact of different cement percentages (ranging from 2.5%, 7.5%, 12.5%, and 17.5%) alongside a constant Petra soil ratio of 1:75. Their findings showed significant improvements in soil density, stability, and bearing capacity. Leong Sing Wong et al., [8] explored kaolin's efficacy in stabilizing peat. Using laboratory tests, they found that a 10% kaolin replacement yielded the highest compressive strength, surpassing the required minimum. Stabilized peat showed significantly reduced permeability compared to untreated samples. Energy Dispersive X-ray (EDX) analysis indicated cement hydrolysis, while Scanning Electron Microscope (SEM) observations revealed pore refinement due to silica sand and kaolin. This study highlights kaolin's potential in enhancing strength and reducing permeability in stabilized peat.

2 Research Methodology

2.1 Materials

In Pakistan, peat soil occurs in natural wetlands near the Northern Mountains and is categorized as fen or bog peat based on plant remains and formation methods.[9] This research examines soil from a Rawalpindi nursery, classified as highly organic PT peat soil according to USCS. Table 1 presents the key physical properties of peat soil.
Gypsum, tested at 5%, 10%, and 15%, is vital for soil stabilization. Recycling gypsum from leftover plasterboard for ground improvement is promising but requires investigation into its environmental effects on soil longevity.[10] Gypsum was added by weight to soil samples, with four trials conducted: one for natural soil and three with varying gypsum percentages.

Table 1: Characteristics of Peat Soil

Characteristics	Values	Guidelines
Color	Blackish Brown	
Organic Content (%)	40	ASTM D2974–00
Moisture Content (%)	54	ASTM D2974–00
Liquid Limit (%)	49	ASTM D4318–17
Plastic Limit (%)	20	ASTM D4318–17
OMC (%)	54	ASTM D698-12
MDD (g/cc)	0.802	ASTM D698–12

2.2 Testing

2.2.1 Atterberg Limits

The Atterberg limits, comprising the liquid limit and plastic limit tests, were conducted following ASTM standards (ASTM D4318-17). The Casagrande apparatus determined the liquid limit, recording the number of blows and the weights of dry and moist soil. For the plastic limit test, the soil sample was rolled out on a glass plate and thinned to fit a steel rod of 1 mm diameter. Gypsum was incrementally added by weight to soil specimens, ranging from 5% to 15%.

2.2.2 Compaction Test

The optimum moisture content and maximum dry density of the soil were determined by the compaction test. ASTM D698-12 was adhered to, and the Standard Proctor test was performed. The compaction test, measured the MDD and OMC of soil at natural bases and after the addition of gypsum to check the parameters of this test in peat soil.

2.2.3 California Bearing Ratio

The CBR test is used to check the strength of soil when used as subgrade, the higher the value of CBR higher the strength of the soil. The experiment was performed under the guidelines of ASTM D-1883-09 and the molds were prepared of natural soil and with gypsum percentages and the samples were produced for soaked test which were placed in water for 96 hours before the test. Both soaked and unsoaked tests were carried out and the results are shown in the next section.

3 Results

3.1 Atterberg Limits

Figure 1 illustrates the relationship between moisture content and the number of blows, indicating the soil's liquid limit. The liquid limit of the natural soil and soil with added gypsum (0%, 5%, 10%, and 15%) was tested. The results showed that the liquid limit decreased from 49% to 39% with 15% gypsum, while the plastic limit decreased from 20% to 16%.

Consequently, the plasticity index (Liquid limit - Plastic limit) dropped from 29% to 23%, indicating reduced clay content. The addition of gypsum caused flocculation, altering soil consistency and improving workability and drainage

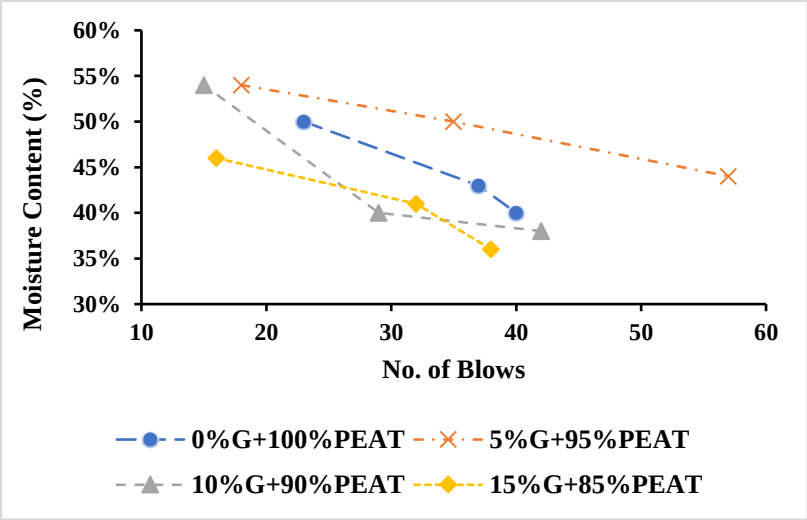

Figure 1: Liquid Limit of Peat Soil with Gypsum

3.2 Compaction Test

Figure 2 shows the compaction characteristics of soil, showing that the Optimum Moisture Content (OMC) decreased with increasing gypsum percentages. At 15% gypsum, the OMC was 33%, compared to about 54% in natural peat, reducing the soil's water retention by 39%. The Maximum Dry Density (MDD) dropped from 0.802 g/cc to 0.715 g/cc. This reduction in density resulted from the high organic content of the soil, which decreased its natural density, and the addition of gypsum, which has a lower density, further reduced the soil's overall density.

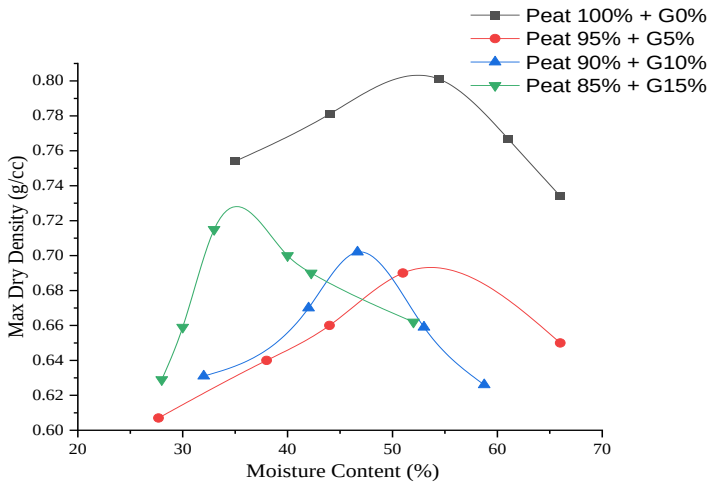

Figure 2: Moisture Density relationship of soil

3.2 California Bearing Ratio

Gypsum enhances soil-bearing strength by filling pores. Figure 3 illustrates the relationship between gypsum content and the California Bearing Ratio (CBR). As gypsum content increased, CBR values rose from 1.805% to 2.94% in unsoaked conditions and from 0.801% to 1.634% in soaked conditions at 15% gypsum. This consistent increase in CBR values, as shown in Figure 3, indicates an improvement from poor to fair soil strength.

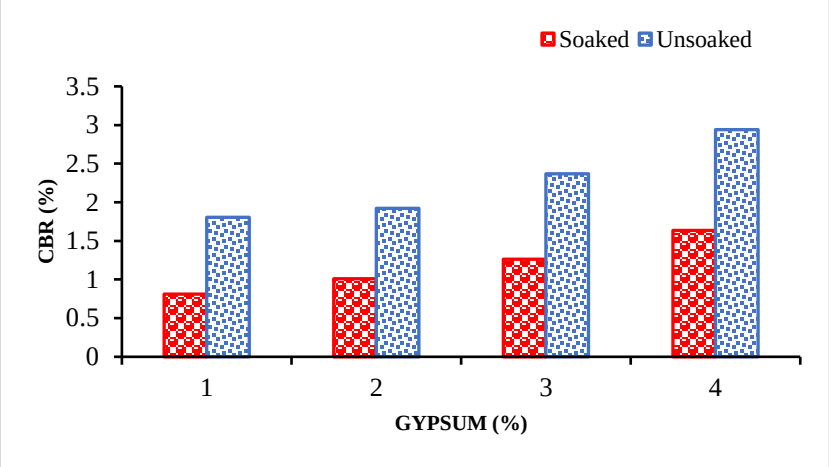

Figure 3: Relationship of CBR with Gypsum

4 Practical Implementation

These experiments studied peat soil with added gypsum to assess its impact on properties like Optimum Moisture Content (OMC), California Bearing Ratio (CBR), and Atterberg limits. Results indicated that gypsum enhances the soil's load-bearing capacity, moisture stability, and plasticity, crucial for construction projects involving peat soil.

5 Conclusion

The tests' results have led to the following conclusions to be drawn:

- The results revealed a 20.5% reduction in the liquid limit of peat soil, from 49% to 39% with 15% gypsum. Similarly, the plastic limit decreased from 20% to 16%, indicating a 20% reduction both with 15% gypsum. These reductions in both limits enhanced soil stability.
- The compaction test revealed that with 15% gypsum, the Optimum Moisture Content decreased to 33%, a 38.89% reduction from the natural peat's 54%.and the Maximum Dry Density also decreased to 0.715g/cc from 0.802g/cc.
- The CBR value of soil improved from 1.802% to 2.94% in unsoaked conditions and from 0.801% to 1.634% in soaked conditions with 15% gypsum addition, indicating enhanced soil strength.

References

[1] Abdel-Salam, A.E., *Stabilization of peat soil using locally admixture.* HBRC journal, 2018. **14**(3): p. 294-299.
[2] Deboucha, S., R. Hashim, and A. Alwi, *Engineering properties of stabilized tropical peat soils.* Electronic Journal of Geotechnical Engineering, 2008. **13**: p. 1-9.
[3] Norazam, P.N.F.I., et al. *Stabilization of peat soil by using envirotac*. in *MATEC web of conferences*. 2017. EDP Sciences.
[4] Khairina, S., et al., *Analysis of Strength and Compressibility on Stabilization of Peat Soil with Industrial Mg-Rich Synthetic Gypsum and Concrete Waste Aggregate.* Available at SSRN 4429085.
[5] Kalantari, B. and B.B. Huat, *Peat soil stabilization, using ordinary portland cement, polypropylene fibers, and air curing technique.* Electron. J. Geotech. Eng, 2008. **13**: p. 1-13.
[6] Al-Hokabi, A., et al., *Improving the early properties of treated soft kaolin clay with palm oil fuel ash and gypsum.* Sustainability, 202[1] **13**(19): p. 10910.
[7] Herius, A., J. Fikri, and M.S. Ramadhinata. *Stabilization of Peat Soils Using Petrasoil with Cement Viewed From CBR Value and Free Compressive Strength Value Of Soils*. in *Journal of Physics: Conference Series*. 2020. IOP Publishing.
[8] Wong, L.S., R. Hashim, and F. Ali, *Improved strength and reduced permeability of stabilized peat: Focus on application of kaolin as a pozzolanic additive.* Construction and Building Materials, 2013. **40**: p. 783-792.
[9] Zainorabidin, A. and D.C. Wijeyesekera, *Geotechnical characteristics of peat.* Proceedings of the AC&T, pp, 2008.
[10] Ahmed, A. and K. Ugai, *Environmental effects on durability of soil stabilized with recycled gypsum.* Cold regions science and technology, 201[1] **66**(2-3): p. 84-92.

EFFECT OF ASPECT RATIO ON BENDING MOMENT AND SHEAR FORCE DISTRIBUTION OF AXIALLY LOADED PILES

[a] Moeez Saqib, [b] Salman Ali Suhail*

a: Department of Civil Engineering, The University of Lahore, Lahore, Pakistan. 70087026@student.uol.edu.pk
b: Department of Civil Engineering, The University of Lahore, Lahore, Pakistan. salman.suhail@ce.uol.edu.pk
* Corresponding author.

Abstract- Piles are categorized as a type of deep foundation and are generally adopted as an appropriate foundation system for high-rise structures, bridges, offshore structures etc. Generally, piles are constructed in a group to enhance their efficiency and capacity to resist loads. The procedure to evaluate the axial load-carrying capacity of piles is well documented in various codes adopted around the globe, however, determination of the variation in moment and shear with pile length is not explicitly incorporated in codes. In this study, an attempt is made to determine the bending moment and shear force distribution along the length of piles constructed in group of 2x2 pile configuration, in layered soil for different aspect ratios. Numerical simulations based on the finite element method were performed by considering three pile diameters to obtain a comprehensive understanding on the effect of aspect ratios on bending moment and shear along pile lengths. The results showed higher moments and shear at the top of the pile. Furthermore, bending moment and shear force decrease with an increased aspect ratio.

Keywords- Aspect Ratio, Layered Soil, Finite Element Method, Bending Moment, Shear Force.

1 Introduction

Piles are defined as slender members, used to transfer load to deeper layers preferably rock or hard soil. In general, piles are always constructed in groups. With an increase in urbanization, the construction of high-rise structures, industrial buildings and bridges is in abundance. These structures withstand higher loads and are required to be supported on deep foundations preferably piles. There are numerous megacities in the world where ground profiles consist of layers of different soil types. One such example is Lahore, the second largest city in Pakistan, where the soil profile is composed of layers of clayey and sandy soil.

The procedure to evaluate the vertical load-carrying capacity is well documented in codes and standards such as NAVFAC DM7.02, AASHTO LRFD Design Specification etc. [1, 2]. Furthermore, many correlations are available based on SPT N values to obtain the vertical load-carrying capacity of the piles. Over the past few decades, many researchers had proposed methods to obtain pile load transfer mechanisms. Vijayvergia proposed T-Z curves for sandy and silty soils [3]. Later Kraft et. al presented a displacement-resistance relationship by considering soil as a continuum material [4]. Another study proposed a set of equations to anticipate the displacement of driven pipe piles by analyzing the results of pile load tests. These earlier studies set the tone for researchers and the subject of soil-pile interaction became a topic of interest in the field of geotechnical engineering. The load-displacement response of bored piles was investigated by considering modulus degradation [5]. A study was published that appraised simplified nonlinear prediction models for pile groups under axial loading, offering insights into the limitations and potential of various analytical methods. Their work contributes to the ongoing efforts to establish well-defined analysis methods considering all influencing parameters [6]. Zhao et al. explored the pile response subjected to repeated axial loads through numerical simulation, provided useful insights on the performance of piles [7]. The load transfer mechanism of single piles embedded in layered soil was investigated and correlations were developed to anticipate pile skin resistance using SPT N values [8].

Very limited number of studies were available that focused on the determination of bending moment and shear force distribution of group piles embedded in layered soil, considering the effect of aspect ratios on the bending moment and shear force distribution. In this study, an effort is made to determine the bending moment and shear force distribution of the pile group constructed in layered soil by varying pile diameters. A configuration of 2x2 pile group along with three

pile diameters such as; (i) 0.76m; (ii) 1m and (iii) 2m with a constant pile length of 55m, that worked aspect ratios of 72.5, 55 and 27.5 respectively were considered for this study.

2 Research Methodology

The research methodology employed for the study is shown in Figure 1.

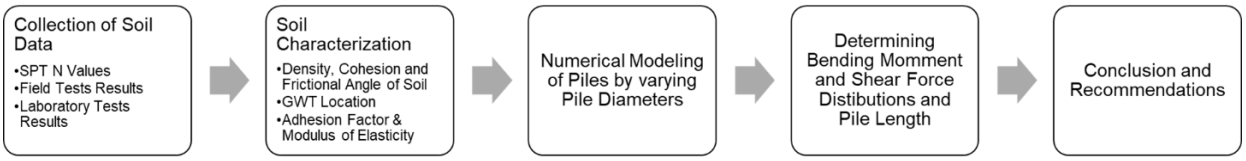

Figure 1: Research Methodology

2.1 Data Collection

The data of sixteen boreholes, drilled up to the depth of 60m, were collected. The collected data included SPT N values and soil index properties such as bulk and dry densities, NMC, OMC and MDD. Soil characterization was then performed on the collected soil data and the generalized layered subsoil profile soil was compiled. The strength properties were then estimated using corrected SPT N values and are presented in Table 1.

2.2 Numerical Modelling

The numerical simulations were performed in PLAXIS 3D connect version employing finite element method. Layered soil was modelled using Mohr-Coulomb failure criteria. Cohesion, friction angle, bulk density, saturated density and soil modulus were used are input parameters to model the soil. Piles were modelled as volume element, using section designer option. Pile cap was modelled using plate element. Medium mesh size was used in accordance with guidelines incorporated in PLAXIS 3D manual. A configuration of 2x2 pile group along with three pile diameters such as; (i) 0.76m; (ii) 1m and (iii) 2m with a constant pile length of 55m that worked aspect ratios of 72.5, 55 and 27.5 respectively were considered for this study. The pile diameters are selected to represent piles having small, medium and large diameter piles. All the three diameters are commonly used in various project in Lahore, Pakistan. The mesh of 2x2 pile configuration is shown in Figure 2. The spacing between the piles are kept at 2.5 times of pile diameter, in line with recommendations proposed by various codes.

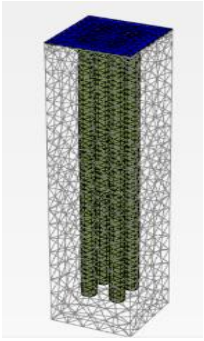

Figure 2: Mesh of Pile Models

Table 1: Soil Properties Used in Numerical Simulation

Layer No.	Soil Type	Thickness (m)	Bulk Density (tons/m^3)	Elastic Modulus (MPa)	Cohesion (tons/m^2)	Friction Angle
01	CL	3	1.84	10	07	-
02	SM	27	1.70	15	-	30
03	CL	5	1.90	20	15	-
04	SC	25	1.95	20	-	33

3 Results

3.1 Bending Moment and Shear Force Variation along the Pile Length

The variation of obtained bending moments and shear forces along pile length is presented in Figure 3(a), (b) and (c) for piles measuring 0.76m, 1.0m and 2.0m in dia. respectively. It can be observed from Figure 3, that the maximum bending moment is obtained at the pile head level. A similar trend is observed for shear forces. There are two primary reasons of the higher values at the pile top. The first reason is the accumulation of axial load at the top of pile. Since axial loading is applied at the pile cap, in which pile is embedded, as a result higher concentration of axial load is at the pile head level.

The second major reason, is because of higher stiffness at the pile head. The stiffness of the structural member governs the load distribution, accumulation and other important dynamic parameters of the structure. Due to the joint of pile and pile cap at the top, the stiffness of the overall system is higher at the top of the pile and decreases along pile length. The decrease in the stiffness along the length leads to decrease in the moment and shear values. Another interesting observation noted from the obtained results is the nominal moment and shear at the pile tip level. This observation endorses the codes recommendation of the pile critical depth concept which ranged between 12D to 18D in mostly adopted codes around the globe. Both the findings as explained above are consistent with the results published by other researchers [9].

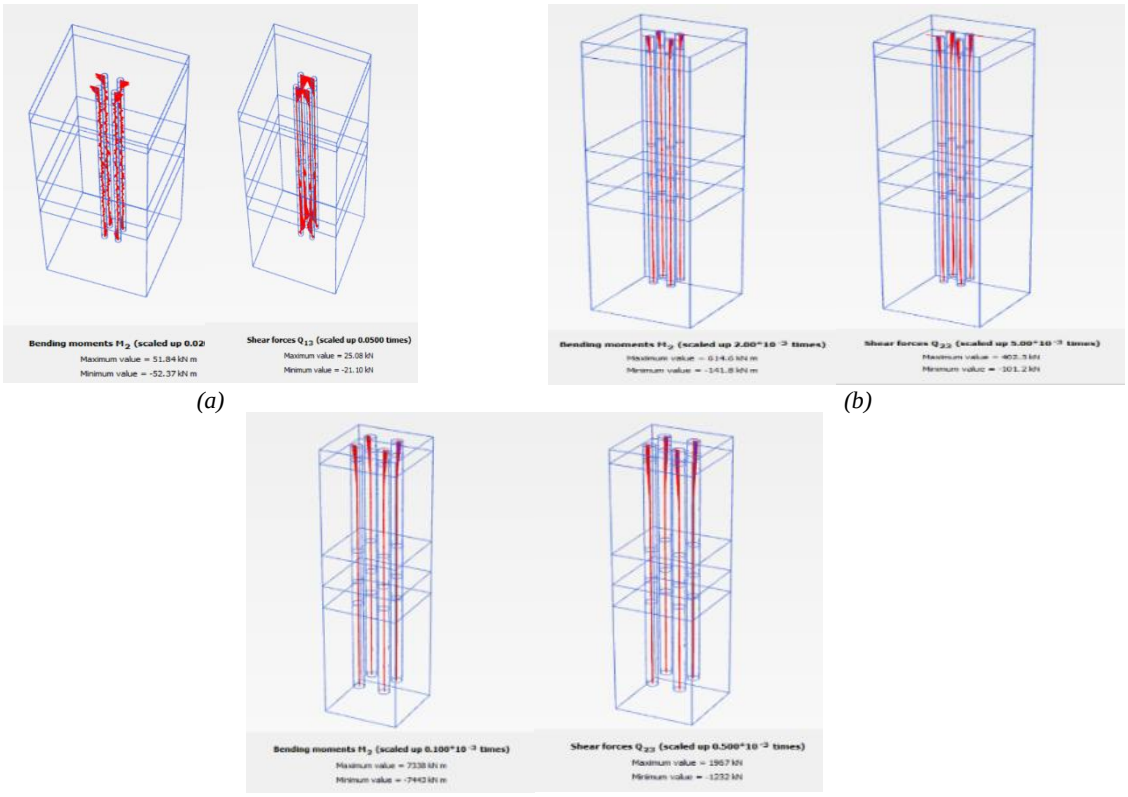

Fig 3: Bending Moment and Shear Force Distribution of Piles (a) Dia. = 0.76m, (b) Dia. = 1.0m, (c) Dia. = 2.0m

3.2 Effect of Pile Diameter on Maximum Bending Moment and Shear Forces

As stated in the introduction of this paper, a total of three (03) pile diameters i.e.; (i) 0.76m; (ii) 1m and; (iii) 2m with a constant pile length of 55m were considered in this study. The corresponding aspect ratios (L/D) are 72.5, 55 and 27.5 respectively. The obtained maximum moment and shear with aspect ratio are shown in Figure 4. Interestingly, the paper posits that the occurrence of higher moment and shear at the minimum aspect ratios of piles i.e. at maximum diameters. Thus, it can be concluded that an increase in diameter leads to increased moment and shear. Furthermore, the relationship between aspect ratio of piles with bending moment and shear is nonlinear in general. The aspect ratio of a pile influences how these internal forces distribute along the pile diameter. The increase in moment and shear with diameter is justified as increase in diameter leads to higher stiffness of the pile. As stated above stiffness plays a major role in accumulating bending moment and shear forces, so higher internal forces will be concentrated with an increase in diameter. Similar results were obtained by Salman and Thammarak in their published research (2021) [9].

The present study provides an overview of pile group response, subjected axial loading, constructed in layered soil. Understanding the accumulation of moment and shear along with relationship between aspect ratio of piles and internal actions (bending moment and shear force) is crucial for optimizing pile design. The outputs of the study will help practice engineers gain insights while dealing with piles installed in layered soil strata. The outcomes of the study can be used for optimizing pile design encountering layered soil, mitigate risks and also enhance significance of soil conditions. For

academicians and researchers, this study provides a detailed methodology to simulate the response of pile groups subjected to axial loading and determine moment and shear distribution along the pile length.

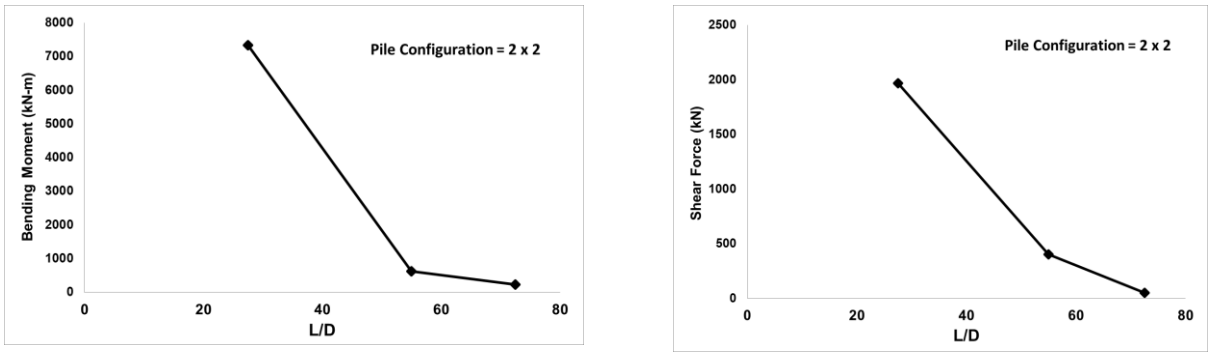

(a) *(b)*

Figure 4: Effect of Pile Diameter (a) Relationship between Bending Moment and L/D ratio (b) Relationship between Shear Force and L/D ratio

4 Conclusion

- The overall stiffness of the soil-pile systems is vital to anticipate the accumulation of moment and shear in the pile-soil systems.
- From the results, it can be concluded that maximum moment and shear will occur at the top of the pile.
- It is further concluded that moment and shear reduced with the length the pile and become negligible at the pile tip level.
- The moment and shear will increase with an increase in dia. of the pile due to increase stiffness.

References

[1] Foundations and Earth Structures: NAVFAC DM 7.02

[2] AASHTO LRFD bridge design specifications. (2019). Washington, D.C. :American Association of State Highway and Transportation Officials.

[3] Vijayvergiya, V. N. (1977). Load Settlement Characteristics of Pile. Proceedings of Port 77 Conference, Loong Beach California, 269-284[4] Kraft, L. M., Kagawa, T., & Ray, R. P. (1981). Theoretical tz curves. Journal of the Geotechnical Engineering Division, 107(11), 1543-1561.

[5] Zhu, H., & Chang, M. F. (2002). Load transfer curves along bored piles considering modulus degradation. Journal of geotechnical and geoenvironmental engineering, 128(9), 764-774

[6] Zhao, M. H., Liu, D. P., Zhang, L., & Jiang, C. (2008). 3D finite element analysis on pile soil interaction of passive pile group. Journal of Central South University of Technology, 15, 75-80

[7] Zhang, Q. Q., Zhang, Z. M., & He, J. Y. (2010). A simplified approach for settlement analysis of single pile and pile groups considering interaction between identical piles in multilayered soils. Computers and Geotechnics,37(7), 969-976

[8] Suhail, S.A (2014). Assessment of subsoil condition and behavior of axially loaded single piles in the subsoil of Lahore

[9] Suhail, S. A., & Thammarak, P. (2021). Evaluation of dynamic behavior of single floating piles embedded in soft clay layer under lateral harmonic and impulse loading. Innovative Infrastructure Solutions, 6(3), 172.

EXAMINING IMPACT OF GROUP CONFIGURATION ON PILE RESPONSE USING NUMERICAL METHOD

[a] Muhammad Awais Yaseen, [b] Salman Ali Suhail*

a: Department of Civil Engineering, The University of Lahore, Lahore, Pakistan. 70109718@student.uol.edu.pk,
b: Department of Civil Engineering, The University of Lahore, Lahore, Pakistan. salman.suhail@ce.uol.edu.pk
* Corresponding author.

Abstract- The anticipation of load transfer mechanism of piles has been topic of interest in the domain of geotechnical engineering. Many researchers have proposed various methods to anticipate load transfer mechanism and effect of pile spacing on the load deformation characteristics of piles. However, understanding the effect of pile configuration on bending moment and shear force distribution, when installed in groups remains area to be further explored, particularly in layered soil conditions. This study aims to investigate how the arrangement of piles in groups affects the bending moment and shear force experienced at the pile heads in layered soil. Numerical simulations using the finite element method were conducted, varying the configurations of pile groups to gain a comprehensive insight into the changes in bending moment and shear force. The findings indicate that both bending moment and shear force increase as the number of piles in a group is increased

Keywords- Pile Configuration, PLAXIS 3D, Bending Moment, Shear Force.

1 Introduction

Piles are slender structural elements designed to transfer loads to deeper layers, ideally to rock or firm soil. Typically, piles are installed in clusters. As urbanization continues to grow, there is a rising demand for constructing tall buildings, industrial facilities, and bridges. These structures must support substantial loads and often necessitate deep foundations, typically using piles. Many megacities around the world feature complex ground profiles comprising layers of various soil types. Lahore, the second largest city in Pakistan, serves as an example, where the soil profile consists of alternating layers of clayey and sandy soils.

The design of piles may be categorized into two groups i.e. (i) Traditional design approaches; and (ii) Load Deformation Analysis using advanced tools. Traditional design approaches involve use of numerical calculations based on SPT N values, closed form solutions and code-based equations such as NAVFAC DM7.02, AASHTO LRFD Design Specification etc. [1, 2]. Many researchers proposed various equations to anticipate the load – settlement and load transfer mechanisms of piles constructed in layered soil [3-8]. Traditional approach of pile design has some obvious limitations mainly (i) Ignore load deformation of bored piles, (ii) Mandatory vertical movement up to 0.5 % of pile diameter and 10 % of pile diameter to invoke skin and base resistance respectively; and (iii) Underestimation of skin resistance [3]. One of the most commonly employed method to understand pile performance is load transfer approach. The aforementioned method provides realistic estimates even considering soil as nonlinear material. In this approach, pile is discretized into nonlinear elements whereas soil is modelled as nonlinear springs. The spring stiffness determines the resistant of the soil. The springs defined and modelled at pile tip level is referred as Q-Z spring whereas spring used to represent soil around pile is termed as T-Z springs. [4-9]. With an advancement in the computation, the researchers shifted to adopt load deformation analysis instead of traditional methods using advanced tools. Among them finite element method had gained significant popularity among researchers. A comprehensive review on use of finite element method to anticipate pile performance subjected to axial and lateral loading is already well documented in literature [10].

The effect of pile configuration and pile spacing on the load deformation characteristics of helical pile group are well understood and documented in the literature [11]. However, very limited number of studies were available that focused effect of pile configuration on the bending moment and shear force of bored pile group embedded in layered soil subjected to axial loading. In this study, an effort was made to determine effect of pile configuration installed in groups on the

bending moment and shear force constructed in layered soil profile of Lahore. The relationship between aspect ratio with bending moment and with shear forces was obtained by varying number of piles in group. A total of three pile group configurations i.e., 2 x 1, 2 x 2 and 3 x 3 with a constant pile diameter and length of 2.0m and 55m respectively, are used for the present study,

2 Research Methodology

The research methodology adopted for the present study is shown in Figure 1. Soil data upto depth of 60 m were collected and analyzed to obtain soil mechanical and strength properties to be used for numerical simulations. The strength properties were collected by using SPT N correlation. The soil properties used in numerical simulations is presented in Table 1.

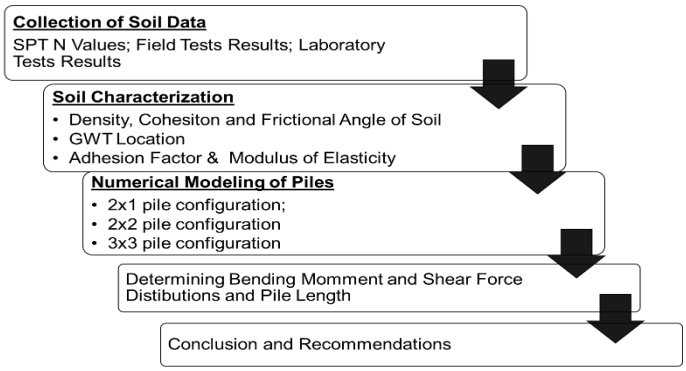

Figure 1: Research Methodology

Table 1: Soil Properties Used in Numerical Simulation

Soil Type	CL	SM	CL	SC
Thickness(m)	3	27	5	25
γ_b (kN/m^3)	1.84	1.70	1.90	1.95
E (MPa)	10	15	20	20
c (tons/m^2)	7	-	15	-
ϕ (deg)	-	30	-	33

Once the required soil properties were evaluated, numerical models were created in PLAXIS 3D connect version. Mohr-Coulomb failure criteria is used to define layered soil mass. A borehole method was used to define soil layers in PLAXIS 3D. Section designer was used to model piles as volume element whereas plate element was used define pile cap. Adequate mesh size was adopted in accordance with the guidelines incorporated in PLAXIS 3D. The models of all three-pile configurations are shown in Figure 2.

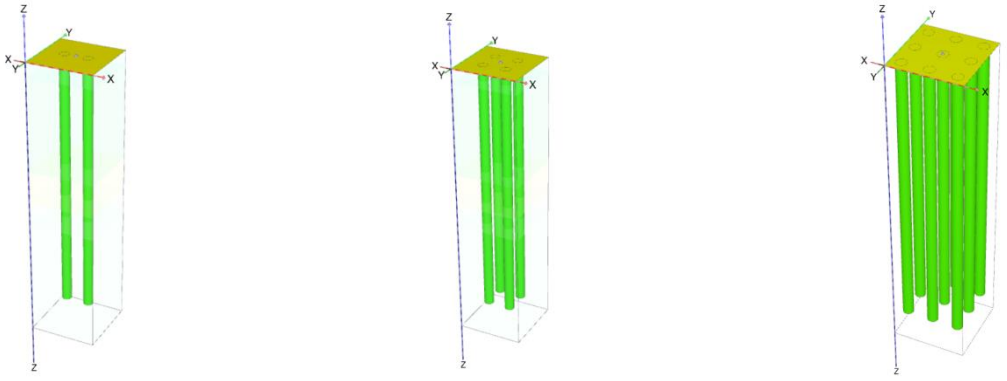

(a) *(b)* *(c)*

Figure 2: FEM Models of Pile (a) 2 x 1 (b) 2 x 2 (c) 3 x 3

3 Results

3.1 Bending Moment and Shear Force Variation along the Pile

The variation of moment and shear along pile length is presented in Figure 3 for all three configurations of piles measuring 2.0m in diameter and length of 55m. It can be observed from Figure 3, that the maximum bending moment are obtained at the pile head level. A similar trend is observed for shear forces as the maximum shear force values are at the pile head level. There are two primary reasons for the higher maximum bending moment and shear forces at the pile head level. The first reason is the accumulation of axial load at the top of the pile. This axial loading originates from the pile cap where the pile is embedded, resulting in a concentrated axial load at the pile head. The second major reason for higher bending

moment and shear forces at the pile head is the higher stiffness at the pile head level due to joint of pile cap and pile. The stiffness of a structural member influences the distribution and accumulation of loads, as well as other dynamic parameters of the structure. Due to the connection between the pile and pile cap at the top, the overall system stiffness is highest at the pile head and diminishes with increasing pile length. This decrease in stiffness along the length reduces the bending moment and shear force along the pile. This also result in decrease in the intensity of moment and shear with embedded depth of the pile, and becoming almost negligible at the pile tip. This observation supports the recommendation in building codes for the critical depth concept of piles, typically ranging between 12D to 18D in widely adopted codes globally. These results of the present study are in agreement with the results published in the literature [11].

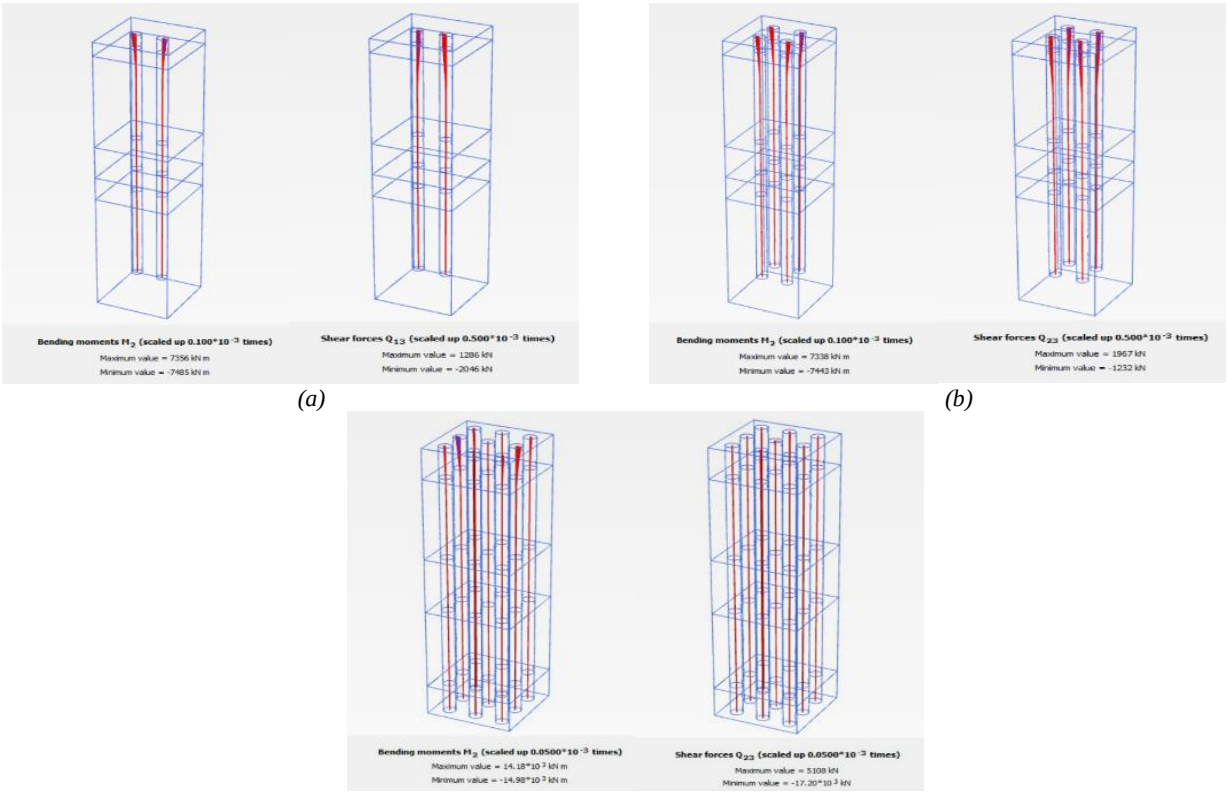

Figure 3: Bending Moment and Shear Force Distribution of Piles having configuration (a) 2 x 1 (b) 2 x 2, (c) 3 x 3

3.2 Effect of Pile Configuration on Maximum Bending Moment and Shear Forces

A total of three (03) pile configurations i.e. 2x1, 2x2 and 3x3 were used in this study. The corresponding number of piles are 2, 4 and 9 respectively. Figure 4 shows the relationship between the obtained maximum bending moment and shear forces with a number of piles in each configuration. From the obtained results, it is observed that bending moment and shear increase with an increase in no, of piles. Thus, it can be concluded that bending moment and shear force will be directly proportional to the number of piles. As the increase in the no. of piles increases the stiffness of the overall system, the higher bending moment and shear forces are resulted. Another reason for increased bending moment and shear forces with an increase in number of piles is attributed to degradation of the soil between the two piles. As more soil in pile group configuration of 3x3 was degraded as compared to pile group configuration of 2x2, due to development of transfer of the load to the surrounding soil and the pile tip level, this load transfer affects the distribution of shear forces and bending moment. These observations are consistent with the other results documented in literature [12].

The present study provides an effect of pile group configuration on the bending moment and shear forces, subjected axial loading, constructed in layered soil. Understanding the accumulation of bending moment and shear forces along with relationship between number of piles in particular configuration and its corresponding internal actions (bending moment and shear force) is vital for design optimization. The outputs of the study will help practice engineers gain insights while dealing with piles installed in layered soil strata. The outcomes of the study can be used for optimizing pile design

encountering layered soil, mitigate risks and also enhance significance of soil conditions. For academicians and researchers, the present study provides a framework to simulate the response of pile groups subjected to axial loading and determine moment and shear force distribution along the pile length.

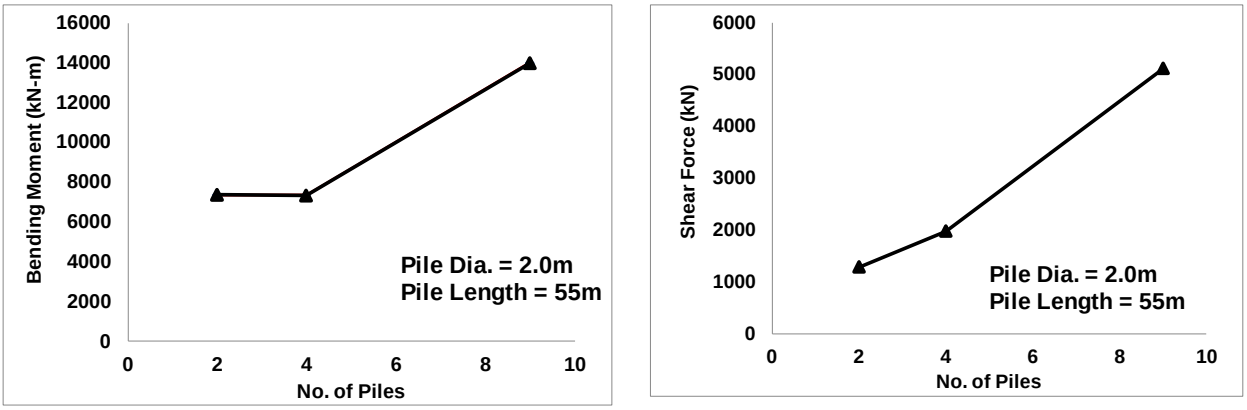

(a) (b)

Figure 4: Effect of Pile Configurations (a) Relationship between Bending Moment and no. of Piles (b) Relationship between Shear Force and no. of Piles

4 Conclusion

The following conclusions can be drawn from the present study:

- The result concludes the bending moment and shear concentrate at the connection between the pile and pile cap due to higher stiffness.
- The bending moment and shear forces will increase with an increase in the number of piles.
- The increase in the number of piles enhances the soil degradation between the piles as higher load will be transferred to the soil in case of higher pile configuration.

References

[1] Foundations and Earth Structures: NAVFAC DM 7.02
[2] AASHTO LRFD bridge design specifications. (2019). Washington, D.C. :American Association of State Highway and Transportation Officials.
[3] Burland, J. B., & Twine, D. (1988, June). The shaft friction of bored piles in terms of effective strength. In Proceeding of 1st international conference on deep foundations, bored and Augered piles (pp. 411-420).
[4] Vijayvergiya, V. N. (1977). Load Settlement Characteristics of Pile. Proceedings of Port 77 Conference, Loong Beach California, 269-284
[5] Kraft, L. M., Kagawa, T., & Ray, R. P. (1981). Theoretical tz curves. Journal of the Geotechnical Engineering Division, 107(11), 1543-1561.
[6] Zhu, H., & Chang, M. F. (2002). Load transfer curves along bored piles considering modulus degradation. Journal of geotechnical and geoenvironmental engineering, 128(9), 764-774
[7] Zhao, M. H., Liu, D. P., Zhang, L., & Jiang, C. (2008). 3D finite element analysis on pile soil interaction of passive pile group. Journal of Central South University of Technology, 15, 75-80
[8] Zhang, Q. Q., Zhang, Z. M., & He, J. Y. (2010). A simplified approach for settlement analysis of single pile and pile groups considering interaction between identical piles in multilayered soils. Computers and Geotechnics,37(7), 969-976
[9] Suhail, S. A., & Thammarak, P. (2021). Evaluation of dynamic behavior of single floating piles embedded in soft clay layer under lateral harmonic and impulse loading. Innovative Infrastructure Solutions, 6(3), 172.
[10] P. E. Kavitha, K. S. Beena, and K. P. Narayanan, "A review on soil–structure interaction analysis of laterally loaded piles," Innov. Infrastruct. Solut., vol. 1, no. 1, pp. 1–15, 2016
[11] Venkatesan, V., Mayakrishnan, M., & Shukla, S. K. (2024). Effect of pile spacing in helical pile groups in soft clays under combined loading. Marine Georesources & Geotechnology, 42(4), 432-452.
[12] Suhail, S. A., & Thammarak, P. (2021). Evaluation of dynamic behavior of single floating piles embedded in soft clay layer under lateral harmonic and impulse loading. Innovative Infrastructure Solutions, 6(3), 172.

INVESTIGATING LOAD TRANSFER BEHAVIOUR OF BORED PILES IN LAYERED SOIL

[a] Muhammad Ammar, [b] Salman Ali Suhail*

a: Department of Civil Engineering, The University of Lahore, Lahore, Pakistan. 70133993@student.uol.edu.pk
b: Department of Civil Engineering, The University of Lahore, Lahore, Pakistan. salman.suhail@ce.uol.edu.pk
* Corresponding author.

Abstract- Piles foundation is considered as an appropriate foundation system for structures subjected to higher axial or lateral loading. In general, piles are constructed in a group to enhance their efficiency and capacity to resist loads. This study investigates the effect of pile configuration and diameter on the pile group efficiency factor, ultimately affecting the overall pile group capacity. Additionally, pile load transfer behavior was also examined to enhance understanding on the pile group response constructed in layered soil. A total of three pile group configurations i.e., 2 x 1, 2 x 2 and 3 x 3 along with three pile diameters of 0.76m, 1.0m and 2.0m with a constant length of 55m, were used for the present study. The results highlight the group efficiency factor reduces with piles. Furthermore, it was observed that major percentage of the load is transfer to the soil around the pile length instead of pile tip in bored piles.

Keywords- Load Transfer Behavior, Bored Piles, Axial Load Capacity.

1 Introduction

Piles are defined as slender members, whose primary function is to resist axial load coming from the superstructure. Pile offered resistance to axial loading in two ways i.e. (i) resistance offered along the length of the pile, termed as skin/shaft/frictional resistance; and (ii) resistance offered at the base of the pile, called as base/tip/end resistance. The pile capacity subjected to axial loading is generally obtained in two ways; (i) by adopting well documented procedures in various codes; and (ii) by performing static pile load [1,2]. In both the aforementioned methods, the axial load carrying capacity of the pile along with its settlement is obtained with precision. However, no information related to resistance offered by a particular soil layer is obtained in either of the aforementioned methods.

Researchers over the past few decades had proposed various equations to anticipate load transfer mechanism of piles. The transfer of compressive loads using helical piles was investigated using 3D FEM by varying diameter [3]. In another study, a correlation was proposed to evaluate behavior of screw piles subjected to compression [4]. The load transfer response of driven piles installed in soft soil was studied and the results were compared with the results of static pile load to enhance the understanding of load transfer response of driven piles [5]. Another study concluded that, load displacement at the pile head is direct outcome of reaction forces and their corresponding displacement around the pile head. Based on this conclusion, a mathematical formulation was proposed to anticipate the load transfer response of piles for various soil conditions [7-9]. Based on various research work, it was noticed that load transfer response correlations provides reasonable accuracy during loading phase of the pile. However, load tests had confirmed that unloading of pile does not result into zero settlement resulting into inaccurate estimation during unloading phase of the pile. A modification in the earlier correlation was then proposed to further enhance accuracy of load transfer mechanism of piles [10].

The subsoil of Lahore, the second largest city of Pakistan mainly composed of layered with alternate layers of clay and sandy soil [11]. Whenever the layered soil is encountered, it is vital to know the contribution of each layer in the overall resistance offered by the pile. This information becomes even more crucial when pile groups are considered as group interaction can affect soil degradation and ultimately the capacity of the piles. In the present study, an effort is made to determine the load transfer mechanism of bored piles constructed in-group. To enhance our understanding various scenarios were created by varying pile diameter and pile configuration. Three configurations i.e. 2x1, 2x2 and 3x3 of pile group were considered in the present study. Furthermore, three pile diameters of 0.76m, 1m and 2m with a constant pile

length of 55m that worked aspect ratios of 72.5, 55 and 27.5 respectively were considered for the present study. Pile capacity and load transfer behavior is obtained from numerical modeling in PLAXIS 3D.

2 Research Methodology

The research methodology adopted for the present study is shown in Figure 1.

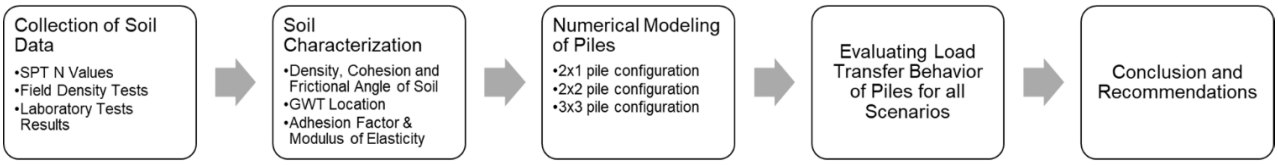

Figure 1: Research Methodology

2.1 Data Collection

The data of sixteen boreholes, drilled up to the depth of 60m, were collected. The collected data included corrected SPT N values and soil index properties such as bulk and dry densities, NMC, OMC and MDD. Soil characterization was performed based on the collected soil data, the generalized profile of layered soil, composed of layers of alternate layers of clay and sand, was compiled. The strength properties, (cohesion, frictional angle and elastic modulus) were estimated on the basis corrected SPT N values and presented in Table 1.

Table 1: Soil Properties Used in Numerical Simulation

Layer No.	Soil Type	Thickness (m)	Bulk Density (tons/m^3)	Elastic Modulus (MPa)	Cohesion (tons/m^2)	Friction Angle
01	Silty Clay (ML)	3	1.84	10	07	-
02	Silty Sand (SM)	27	1.70	15	-	30
03	Lean Clay (CL)	5	1.90	20	15	-
04	Clayey Sand (SC)	25	1.95	20	-	33

2.2 Numerical Modelling

The numerical simulations were performed in PLAXIS 3D connect version using finite element method. Layered soil is modelled using Mohr-Coulomb failure criteria. Cohesion, friction angle, bulk density, saturated density and soil modulus are used are input parameters to model the soil. Piles are modelled as volume element, using section designer option. Pile cap is modelled using plate element. Medium mesh size was used in accordance with guidelines incorporated in PLAXIS 3D manual. The mesh models of three pile configurations are shown in Figure 2.

(a) *(b)* *(c)*

Figure 2: Mesh of Pile Models (a) 2 x 1 (b) 2 x 2 (c) 3 x 3

3 Results

3.1 Capacity of Pile Group

The capacity of piles group obtained from numerical simulation is presented in Figure 3. The pile group efficiency factor was calculated using Converse-Labarre equation. The capacity of pile group configuration of 2x1, having diameter of 0.76m, 1.0m and 2.0m were found to be 216 tons, 713 tons and 5805 tons respectively. Whereas the capacity of pile group configuration of 2x2, having diameter of 0.76m, 1.0m and 2.0m were found to be 205.5 tons, 665 tons and 5000 tons

respectively. Furthermore, the capacity of pile group configuration of 3x3, having diameter of 0.76m, 1.0m and 2.0m were found to be 198 tons, 633 tons and 4472 tons respectively. From Figure 3, it can be observed that axial load carrying capacity of piles increase with an increase in diameter and number of piles This is primarily to increase stiffness of overall soil pile system due to increase in pile size and numbers. Stiffness of the structure is major factor that governs the overall capacity of the structure. This observation is consistent with the results and recommendations published by another researcher [11].

From Figure 4, it can be noticed that attained group efficiency decrease with an increase in piles. The obtained values of pile group efficiency factor for 2x1 pile group were found to be 0.95, 0.94 and 0.88 for pile measuring dia. of 0.76m, 1.0m and 2.0m respectively. The pile group efficiency factor for 2x2 pile group were found to be 0.90, 0.88 and 0.76 for pile measuring dia. of 0.76m, 1.0m and 2.0m respectively. Whereas group efficiency factor for 3x3 pile group were found to be 0.88, 0.83and 0.67 for pile measuring dia. of 0.76m, 1.0m and 2.0m respectively. It is important to note that spacing between the two piles were kept at 2.5 of pile diameter. Due to this close spacing, the increase in the number of piles resulted into block failure which leads to reduction into overall pile group efficiency factor. Another reason for reduction in the pile group efficiency factor is the formation of pressure bulb. Due to the close spacing, the pressure bulb of the pile overlaps, leading to soil degradation, ultimately affecting pile group capacity. These observations are in agreement with the already published research study [12].

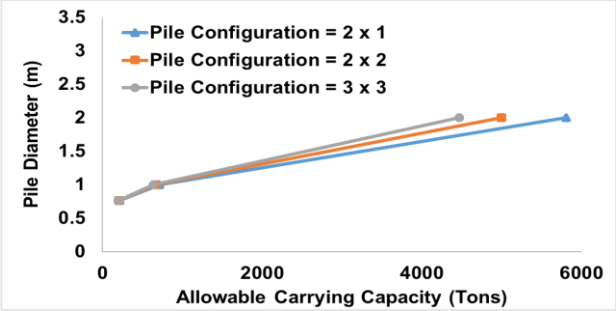

Figure 3: Allowable Load Carrying Capacity

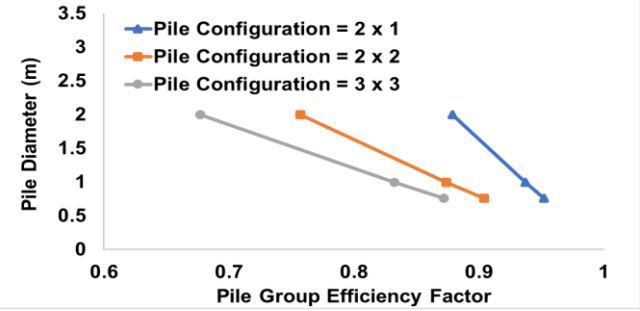

Figure 4: Pile Group Efficiency Factor

3.2 Load Transfer Behaviour of Piles Groups

The load transfer performance of the pile is presented in Fig 5 for all the three pile group configurations and pile diameters. It can be observed. The load transfer behavior is primarily governed by two important parameters i.e., strength characteristics of the soil and the pile construction method. In case of bored piles that pile resistance is mainly composed of shaft resistance. This can be seen in the Figure 5, that major portion of the load is transfer to the soil around the pile shaft and minor portion of the overall load is resisted at the pile tip for all three pile configurations and pile diameter. In the present study the obtained percentage of load transfer through shaft resistance for piles measuring diameter of 0.76m, 1.0m and 2.0m were found to be 85%, 80% and 65% respectively. The trend will be entirely opposite in case of driven piles where load is primarily transferred to the soil at the pile tip level instead of pile shaft. It is noteworthy that with an increase in the diameter of the pile, the contribution of base resistance is increasing in the overall resistance of piles.

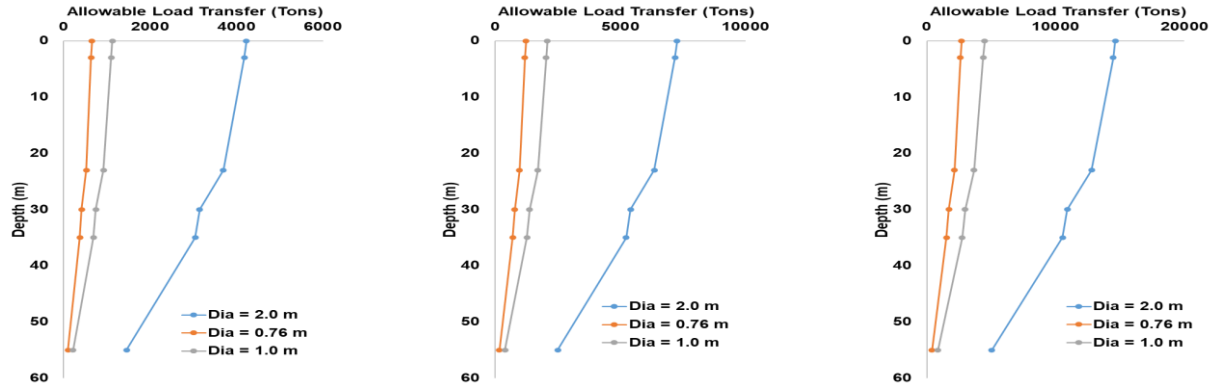

Figure 5: Load Transfer Mechanism of Piles (a) Pile Configuration 2x1 (b) Pile Configuration 2x2 (c) Pile Configuration 3x3

4 Conclusion

The following conclusions can be drawn from the present study:

- It can be concluded from the obtained results that pile configuration have significant impact on the axial load carrying capacity and load transfer response of piles groups due to variation of pile-soil system's stiffness .
- From the results, it can be concluded that group efficiency factor reduces with more piles due to overlapping of pressure bulb and formation of block failure.
- The load transfer performance of the pile obtained in this study substantiate that major portion of load in bored piles will be resisted through shaft resistant.
- From the results of load transfer behavior of piles, it is concluded that contribution of pile end bearing in the overall resistance of piles to axial load enhances with an increase in the pile diameter.

References

[1] Foundations and Earth Structures: NAVFAC DM 7.02
[2] AASHTO LRFD bridge design specifications. (2019). Washington, D.C. :American Association of State Highway and Transportation Officials.
[3] Sprince, A., & Pakrastinsh, L. (2010). Helical pile behaviour and load transfer mechanism in different soils. In Modern Building Materials, Structures and Techniques. Proceedings of the International Conference (Vol. 10, p. 1174). Vilnius Gediminas Technical University, Department of Construction Economics & Property.
[4] Soltani-Jigheh, H., & Zahedi, P. (2020). Load transfer mechanism of screw piles in sandy soils. Indian Geotechnical Journal, 50, 871-879.
[5] Palmer, Andrew L., "Load Transfer Mechanisms for Piles in Soft Soils" (1994). All Graduate Theses and Dissertations, Spring 1920 to Summer 2023. 4603.
[6] Coyle, H. M., and Reese, L. C. (1966). "Load transfer for axially loaded piles in clay." J. Soil Mech. Found. Eng. Div., 92(2), 1–26
[7] Fleming, K., Weltman, A., Randolph, M. F., and Elson, K. (2008). Piling engineering, 2nd Ed., Blackie and Son, Glasgow, U.K
[8] Poulos, H. G., and Davis, E. H. (1980). Pile foundation analysis and design, Rainbow-Bridge Book Company, Taipei, Taiwan
[9] Randolph, M. F. (2003). "Science and empiricism in pile foundation design." Géotechnique, 53(10), 847–875.
[10] Dias, T. G. S., & Bezuijen, A. (2018). Load-transfer method for piles under axial loading and unloading. Journal of Geotechnical and Geoenvironmental Engineering, 144(1), 04017096.
[11] Suhail, S.A (2014). Assessment of subsoil condition and behavior of axially loaded single piles in the subsoil of Lahore
[12] Pratama, I. T., Widjaja, B., & Budianto, K. A. (2023). Numerical study on pile group efficiency for piles embedded in cohesive and cohesionless soils. In E3S Web of Conferences (Vol. 429, p. 04003). EDP Sciences.

OPTIMIZED PREDICTION MODELING FOR TiO_2-CATALYZED PHOTO-DEGRADATION RATE CONSTANTS OF WATER CONTAMINANTS USING MACHINE LEARNING

[a] Ayesha Noreen, [b] Majid Khan*

a: Departement of Civil Engineering, University of Engineering and Technology, Peshawar, Pakistan.18pwciv5186@uetpeshawar.edu.pk
b: Departement of Civil Engineering, COMSATS University, Abbottabad, Pakistan. 18pwciv4988@uetpeshawar.edu.pk
* Corresponding author.

Abstract- Titanium dioxide (TiO_2) is widely recognized as a photocatalyst in water contaminant treatment applications. Generally, obtaining the kinetics of photo-degradation rates requires extensive experimentation, involving significant labor and experimental resources. This study presents a unique approach to employing multi-expression programming (MEP) and artificial neural networks (ANN) to forecast the photo-degradation of water contaminants using TiO_2. The collected dataset for model development consists of 446 data points with six input variables. The MEP model exhibited higher prediction accuracy for the TiO_2-photocatalytic degradation of organic water contaminants. The MEP model exhibited predictions with R values of 0.946, 0.862, and 0.869 for training, testing, and validation, respectively. While the ANN model exhibited good accuracy during the training phase, its performance in testing and validation was poor, with the R-value significantly lower than the recommended threshold of 0.80. Among both developed models, MEP is a better choice to forecast the degradation of organic water contaminants using the TiO_2-photocatalytic process.

Keywords- Machine Learning, Titanium Dioxide, Photo-degradation of Water Contaminants, Water Treatment.

1 Introduction

Recognizing the significance of environmental preservation, researchers are diligently pursuing eco-conscious alternative technologies across various aspects of daily living. Variations in water quality worldwide due to industrial and geographical factors, mean that a single solution cannot address all water contamination issues. Consequently, nanotechnology will always be essential in developing effective water treatment technologies [1]. In this context, photocatalysis using TiO_2 is a widely used technique for wastewater treatment. Titanium dioxide stands out among semiconductor photocatalysts due to its remarkable chemical and biological inertness, resistance to photoanodic corrosion, and cost-effective production. The use of TiO_2 in photocatalytic water and air purification is widely preferred for its efficacy and environmentally friendly nature, making it a favored advanced oxidation process [2]. Similarly, the photo-Fenton approach is also an effective advanced oxidation process for oxidizing water pollutants. Moreover, the non-selective nature of the photocatalytic process enables TiO_2 to degrade contaminants [4]. Over recent decades, extensive research has focused on experimentally examining the photo-catalytic degradation of various water pollutants using TiO_2. The recent research has also delved into exploring the underlying principles and theoretical aspects of TiO_2 performance. However, experimental testing requires significant time and financial investment, demanding considerable resources in terms of labor and equipment. To address the challenges associated with experimental testing, machine learning (ML) approaches have recently been widely utilized to predict outcomes, optimizing both time and resources. By leveraging ML, researchers can efficiently model complex systems and identify key variables, significantly reducing the need for extensive and costly experimentation. This integration of ML into water treatment technology development, particularly in the context of nanotechnology, offers a promising pathway to tailor solutions for better wastewater treatment [5,6]. This study introduces two predictive models utilizing MEP and ANN to estimate the photo-degradation rate constants of contaminants exposed to TiO_2 and ultraviolet irradiation in aqueous solutions. The database for

these predictive models comprises 446 data points gathered from published experimental reports. Six input variables are considered for the model development. Different statistical performance metrics were utilized to assess the efficacy of the developed models.

2 Research Methodology

2.1. Data collection

The database for model development was collected from 26 published experimental studies, acquired by Jiang et al. [7]. The dataset consists of 446 data points. Six experimental variables were considered which include, experimental temperature (T), type of organic contaminant (OC), TiO_2 dosage (D), ultraviolet light intensity (I), initial water contaminant concentration (IC), and solution pH (pH). The response parameter is the photo-degradation rate constant (k), which is converted to its base 10 logarithm -log(k) for better understanding. In a typical experimental procedure, a specified content of Degussa TiO_2 was mixed with polluted water with a modified pH for about 45 minutes to achieve adsorption-desorption equilibrium before UV light irradiation. The statistical description of the input variables is given in Table 1. The suspension was exposed to UV light. At specified intervals, small samples were extracted and filtered to remove the TiO_2. The first order of k was determined using Eq. 1.

$$\frac{dC}{dt}=kC \qquad (1)$$

Table 1: Statistical analysis of the collected dataset

Statistics	I ($mW\ cm^{-2}$)	T (^oC)	D ($g\ L^{-1}$)	IC ($mg\ L^{-1}$)	pH	K (min^{-1})
Mean	3.90	27.78	1.12	43.29	5.24	1.21
Kurtosis	6.01	1.67	8.33	4.71	0.56	1.90
Skewness	2.16	1.33	2.03	1.85	1.01	0.70
Mode	0.18	25.00	1.00	10.00	3.60	1.30
Standard Deviation	12.34	7.54	1.01	50.99	1.96	0.55
Minimum	0.18	20.00	0.00	0.13	2.00	0.02
Range	74.82	40.00	7.50	342.34	9.00	3.98

2.2. Model Development

The ANN model was implemented in MATLAB 2021a. The hyperparameters of the ANN model were optimized using random search, where the parameters of the model are selected arbitrarily from a predefined space. This method enables extensive exploration of the parameter range. Different random combinations of hyperparameters are evaluated based on a predetermined metric to assess model performance. The goal is to find the combination that yields the best results. For optimizing the ANN model, the number of neurons is adjusted to improve accuracy. The Levenberg-Marquardt was utilized for the training process. The optimized parameters of the ANN model are given in Table 2. Certain parameters for the MEP approach need to be adjusted to build a good predictive model. These parameters are selected based on an iterative process. The population size defines the established programs; a larger population can result in a more intricate and reliable model but takes longer to converge and risks overfitting if too large. Table 2 details the setup variables used in this work. The function set includes basic mathematical operations (-, ×, ÷, +, sqr, exp) to establish a simple model. The number of generations affects the method's precision, with more generations leading to fewer errors. Various variable combinations were tested to hyper-tune the model. The optimized prediction model with the lowest error was selected as presented in Table 2.

Table 2: Hyperparameters optimization of the suggested models

MEP		ANN	
Parameter	**Optimized value**	**Parameter**	**Optimized value**
Sub-population size	50	Number of epochs	100
Mutation probability	0.01	Activation function	purelin, logsig, tansig
Generations	250	Learning rate	0.26
Operators	sqr, exp, ×, ÷, +, −	Momentum rate	0.9

MEP		ANN	
Parameter	**Optimized value**	**Parameter**	**Optimized value**
Tournament size	2	Hidden neurons	40
Length of code	0.5		
Fitness function	MAE		
Crossover prob.	0.9		

3 Results

3.1 ANN Model Performance

The performance of the ANN is depicted in Figures 1-3, demonstrating a consistent decrease in error, indicative of improved model accuracy with more training cycles. Figure 1 highlights the MSE across validation, training, and testing stages, showing a significant optimization after seven epochs. This trend is corroborated by Figures 2 and 3, underscoring the model's effectiveness in reducing error throughout various stages. This hyper-tuning process provides a better understanding of the ANN performance and convergence. The training of the ANN utilized R and MSE as an ultimate termination approach. Specifically, adjustments to the neural network architecture were made when the accuracy metric (R) showed no significant improvement over several epochs, or when the R-value on the validation set plateaued and the MSE stopped decreasing. The ANN model with a 40-neuron architecture demonstrated good prediction records. To further provide a performance assessment of the ANN model, regression plots of the ANN approach are illustrated in Figure 4. The ANN model showed excellent precision with an R-value of 0.843 in training and an MSE value of 0.156. Moreover, while the model exhibited good accuracy during the training phase, its performance in testing and validation was poor, with the R-value significantly lower than the recommended threshold of 0.80. This disparity suggests that the model may be overfitting to the training data, failing to generalize well to unseen data.

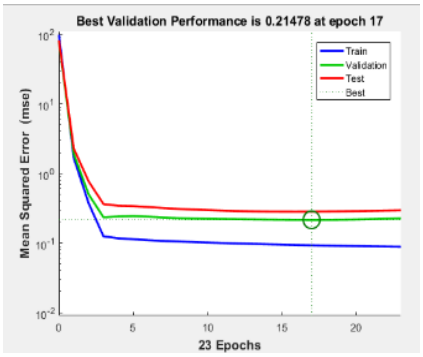

Figure 1: ANN model Performance

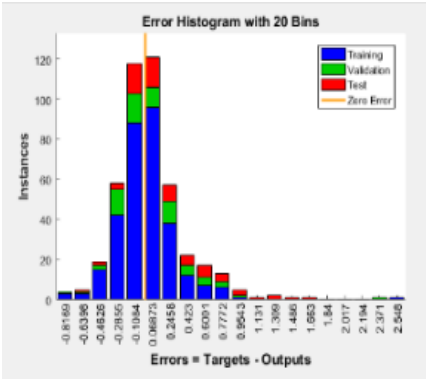

Figure 2: ANN model. Training state

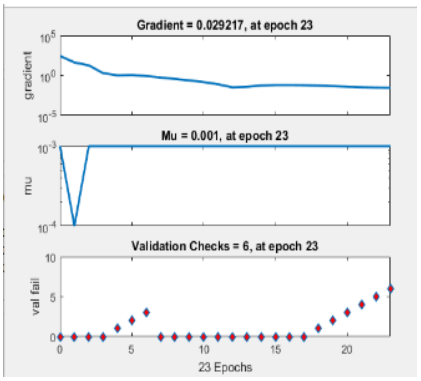

Figure 3: ANN model Error Limits

3.2 MEP Model Performance

The performance of the established MEP model is illustrated in Figure 5**.** It is generally recommended that the regression slope should be higher than 0.80 for an accurate prediction model. The MEP approach showed good predictions with a regression slope value of 0.996 for training, 0.901 for testing, and 0.856 for validation. These values are significantly higher than the recommended criteria of 0.80, suggesting a good alignment between the model and experimental data. Furthermore, the fitting lines for all three subsets are well-aligned with the ideal fit line, indicating that the MEP model provided comparable performance for all three subsets, thereby overcoming the issue of overfitting. Moreover, the MEP model demonstrated good accuracy in predicting the output, with R and MSE values of 0.946 and 0.064 for training, 0.862 and 0.184 for testing, and 0.869 and 0.083 for validation. The R-values for the three subsets are higher than 0.80 and close to 1, indicating the MEP model's potential to provide high prediction accuracy. The MEP model exhibited superior efficacy compared to the developed ANN model, making it the best choice for estimating TiO2-catalyzed photo-degradation. Additionally, the lower MSE values across training, testing, and validation further reinforce the reliability and robustness

of the MEP model in practical applications. In addition, the MEP model provides better accuracy than the ML-based prediction model developed by Jiang et al. [7].

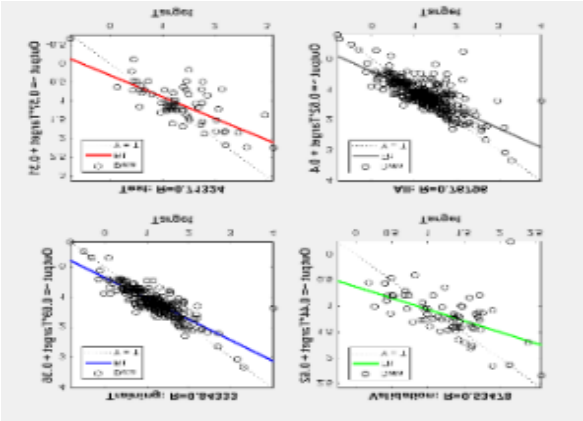

Figure 4: ANN model Regression analysis

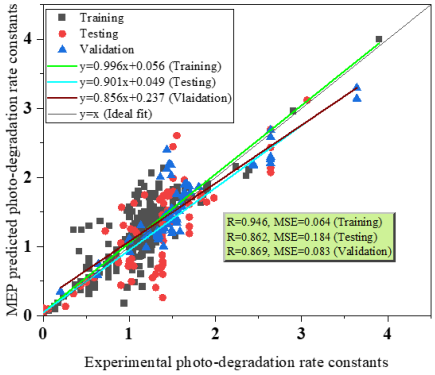

Figure 5: Performance of the developed MEP model

4 Conclusion

In the present study, ANN and MEP models were developed to predict the TiO_2-assisted photo-degradation efficiency for the removal of water contaminants. The models incorporated data from extensive studies with six input features and considered 78 organic contaminants, covering most experimental setups for the photocatalytic degradation process. SHAP interpretations were provided to enhance model interpretability. The major findings of the study are summarized herein:

1. The MEP model exhibited higher prediction accuracy for the TiO_2- photocatalytic degradation of organic water contaminants. The MEP model exhibited predictions with R values of 0.946, 0.862, and 0.869 for training, testing, and validation, respectively.
2. ANN model showed excellent accuracy with an R-value of 0.843 in training and an MSE value of 0.156. Moreover, while the model exhibited good accuracy during the training phase, its performance in testing and validation was poor, with the R-value significantly lower than the recommended threshold of 0.80.
3. Among both developed models, MEP is a better choice to forecast the TiO_2- photocatalytic degradation of organic water contaminants.

Reference

[1] M.M. Mahlambi, C.J. Ngila, B.B. Mamba, Recent Developments in Environmental Photocatalytic Degradation of Organic Pollutants: The Case of Titanium Dioxide Nanoparticles—A Review, J. Nanomater. 2015 (2015) 1–29. https://doi.org/10.1155/2015/790173.

[2] Z. Guo, X. Zhang, X. Li, C. Cui, Z. Zhang, H. Li, D. Zhang, J. Li, X. Xu, J. Zhang, Enhanced charge separation by incomplete calcination modified co-doped TiO2 nanoparticle for isothiazolinone photocatalytic degradation, Nano Res. 17 (2024) 4834–4843. https://doi.org/10.1007/s12274-024-6453-4.

[3] V.J.P. Vilar, L.X. Pinho, A.M.A. Pintor, R.A.R. Boaventura, Treatment of textile wastewaters by solar-driven advanced oxidation processes, Sol. Energy. 85 (2011) 1927–1934. https://doi.org/10.1016/j.solener.2011.04.033.

[4] A.J. Haider, Z.N. Jameel, I.H.M. Al-Hussaini, Review on: Titanium Dioxide Applications, Energy Procedia. 157 (2019) 17–29. https://doi.org/10.1016/j.egypro.2018.11.159.

[5] J.C. Serna-Carrizales, A.I. Zárate-Guzmán, R. Flores-Ramírez, L. Díaz de León-Martínez, A. Aguilar-Aguilar, W.M. Warren- Vega, E. Bailón-García, R. Ocampo-Pérez, Application of artificial intelligence for the optimization of advanced oxidation processes to improve the water quality polluted with pharmaceutical compounds, Chemosphere. 351 (2024) 141216. https://doi.org/10.1016/j.chemosphere.2024.141216.

[6] I. Salahshoori, M. Namayandeh Jorabchi, A. Baghban, H.A. Khonakdar, Integrative analysis of multi machine learning models for tetracycline photocatalytic degradation with MOFs in wastewater treatment, Chemosphere. 350 (2024) 141010. https://doi.org/10.1016/j.chemosphere.2023.141010.

[7] Z. Jiang, J. Hu, X. Zhang, Y. Zhao, X. Fan, S. Zhong, H. Zhang, X. Yu, A generalized predictive model for TiO2–Catalyzed photo-degradation rate constants of water contaminants through artificial neural network, Environ. Res. 187 (2020) 109697. https://doi.org/10.1016/j.envres.2020.109697.

EVALUATION OF ENERGY CONTENT IN MUNICIPAL SOLID WASTE OF LOW-INCOME AREA TEHKAL AND HIGH-INCOME AREA HAYATABAD OF PESHAWAR K.P.K PAKISTAN

[a] Muhammad Shahid Khan*, [b] Saeed Hijab

a: Civil Engineering Department, University of Engineering and Technology, Peshawar, Pakistan.20pwciv5439@uetpeshawar.edu.pk
b: Civil Engineering Department, University of Engineering and Technology, Peshawar, Pakistan.20pwciv5402@uetpeshawar.edu.pk
* Corresponding author.

Abstract- In developing countries like India and Pakistan, municipal waste creation is increasing rapidly because of ongoing population, urbanization, and industry growth. In addition to having a detrimental impact on the environment. Managing MSW effectively and producing sustainable non-fossil fuel, energy can both be accomplished by converting trash to energy. This study aims to provide a thorough assessment of the energy content of municipal solid waste (MSW) from high-income area Hayatabad and low-income area Tehkal of Peshawar city KPK Pakistan. First, selected the solid waste sample in plastic bags from the dumpsite in the low-income area Tehkal and high-income area Hayatabad of Peshawar city K.P.K Pakistan. Each sample was 100 kg from both the areas. The collected waste is separated to different component of solid waste. Then find the moisture content of each component in MSW. It almost took 3 to 4 weeks to collect this data. After finding the dry weight, find the energy content of high-income zone, which was found out to be 28026.7292kJ/100 kg, and for low-income zone, it was 14794.7395kJ/100kg.

Keywords- Energy Content, Municipal Solid Waste, Moisture Content, Waste Composition.

1 Introduction

Developed nations generate a greater amount of waste than developing nations. Nonetheless, because they have strong management systems, they produce significant amounts of energy from these wastes. Due to the high cost of MSW management and producing energy from it, it is a significant issue in developing nations like Pakistan. The handling of MSW is not merely a technical problem; a number of legal, political, ecological, and financial variables influence it [1]. Approximately 60% of solid garbage is collected, while the remainder is left at collecting places or in streets, emitting toxins and rendering the environment unfit for human interactions [2].

Municipal solid waste includes degradable, partially degradable, and non-biodegradable items such paper, textiles, food waste, straw, yard trash, leather, plastics, rubbers, metals, glass, ash, dust, and electronics [3]. The findings imply that total worldwide trash generation would be roughly 20 billion tons in 2017. This equates to 2.63 tons of total garbage per person (cap) each year. Under the current business-as-usual scenario, worldwide trash production is predicted to reach 46 billion tons by 2050 [4].

MSW recuperation can be in many ways, such as composting, which is the process of recycling biodegradable parts of MSW through a number of technological processes and thermochemical therapy, which comprises of pyrolysis, gasification, and incineration [5]. From the above, it is clear that there is potential to produce energy from MSW by incineration which involves burning garbage at high temperatures in order to produce heat that can be used to produce power and heat buildings. Biodegradable are those that decompose spontaneously in the environment, such as vegetable

peels and natural textiles. These are used to produce energy manure, compost and biogas. Non-biodegradable substances are those that cannot naturally decompose in the environment, such as plastic and metals. These can be separated and recycled but it may be very costly.

The purpose of this research work is to assess the potential power that can be generated from municipal solid trash in two diverse areas of Peshawar, K.P.K Pakistan, specifically the low-income area Tehkal and the high-income area Hayatabad of Peshawar city KPK Pakistan. The results of this study will provide helpful information regarding the capability of producing energy via MSW in the region under study, as well as help alleviate the region's energy shortfall and waste management concerns. This study paper will contribute to the current collection of literature on how to handle MSW and provide the groundwork for long-term waste to energy conversion practices in Peshawar's low-income area Tehkal and high-income area Hayatabad.

2 Research Methodology

2.1 Sample Collection

We collected 100 kg sample of solid municipal waste from the largest MSW disposal place, located in high and low-income areas of Peshawar city KPK Pakistan. The 100 kg sample was collected in one week. In every day of the week 14.38 kg was collected. The dumpsites are shown in Figure 1 respectively.

a)  b) 

Figure 1: Dumpsites a) Tehkal Low-Income Area Dumpsite and b) Hayatabad High-Income Area Dumpsite

2.2 Characterization and Physical Analysis of MSW

The municipal waste (MSW) specimen was characterized by manually separating and classifying it into various components. The components in MSW were separated manually. The mass of each element in the total MSW specimen was measured using a device known as a digital balance

2.3 Moisture Percentage

To determine the amount of moisture of individual components, everyone was freshly weighed via an electronic balance and dried inside an oven at 100°C for 3 hours.

3 Results

In Tehkal, a low-income neighborhood, garbage is primarily composed of biodegradable products, with a minimum proportion of recyclables. Tehkal's trash is largely biodegradable with few recyclables, demonstrating the complex interplay of economic, cultural, infrastructural, and behavioral elements in waste management in low-income communities. In contrast, the high-income region of Hayatabad, non-biodegradable products have a higher percentage, reflecting a more consumer-oriented lifestyle.

Table 1 shows the waste components, percentage composition, moisture content, dry unit weight, and total energy based on a 100 kg sample from the high-income area Hayatabad. The outcome of the table 1 is the energy calculated present in 100 kg of sample which is collected from high-income area Hayatabad.

Table 1: Total energy based on 100 kg of sample of high-income area Hayatabad

S. No	Components	Composition % by weight (total 100kg)	Moisture Content (%)	% Dry Weight (kg)	Default energy values (KJ/Kg)	Total energy (KJ/Kg)
1	Plastic	14.1	2	13.818	32600	600466.8
2	Paper	8.5	6	7.99	16750	133832.5
3	Cardboard	7.6	5	7.22	16300	117686
4	Food waste	10.5	70	3.15	4650	20647.5
5	Yard waste	11.2	60	4.48	6500	29120
6	Textiles	3.9	10	3.51	25400	159154
7	Glass	5.8	2	5.684	1650	9378.6
8	Tin Cans	2.8	3	2.716	700	1901.2
9	Tetra Pack	5.6	11	4.984	12000	59808
10	PET Bottles	9.3	4	8.928	29400	392483.2
11	Ash/ Sand	3.3	26	2.442	250	610.5
12	Polythene	7.2	18	5.904	15690	92633.76
13	Wood	8.6	36	5.504	18600	152374.4
14	Rubber	1.6	2	1.568	23750	40240
15	Total	100	-	77.898	-	2802672.92

Energy Value = 2802672.92kJ/100kg

Energy Value in kJ/kg for high-income area Hayatabad = 28026.7292kJ/kg

The component of waste, its percentage composition in 100 kg sample, moisture content and dry unit weight of MSW and Total energy based on 100 kg of sample of low-income area Tehkal is calculated given below in the table 2.

Table 2: Total energy based on 100 kg of sample of low-income area Tehkal

S. No	Components	Composition % by weight (total 100kg)	Moisture Content (%)	% Dry Weight (kg)	Default energy values (KJ/Kg)	Total energy (KJ/Kg)
1	Plastic	16.1	6	15.134	32600	493368.4
2	Paper	6.5	8	5.98	16750	100165
3	Cardboard	5.6	10	5.04	16300	82152
4	Food waste	8.2	60	3.28	4650	15252
5	Yard waste	3.5	40	2.1	6500	13650
6	Textiles	5.6	8	5.152	25400	130860.8
7	Glass	4.9	3	4.753	1650	7842.45
8	Tin Cans	2.7	2	2.646	700	1852.2
9	Tetra Pack	6.3	10	5.67	12000	68040
10	PET Bottles	12.4	5	11.78	29400	346332
11	Ash/ Sand	9.5	25	7.125	250	1781.25
12	Polythene	5.7	35	3.705	15690	58131.45
13	Wood	10.6	46	5.724	18600	106466.4
14	Rubber	2.4	6	2.256	23750	53580
15	Total	100	-	80.345	-	1479473.95

Energy Value = 1479473.95kJ/100kg

Energy Value in kJ/kg for low-income area Tehkal = 14794.7395kJ/100kg

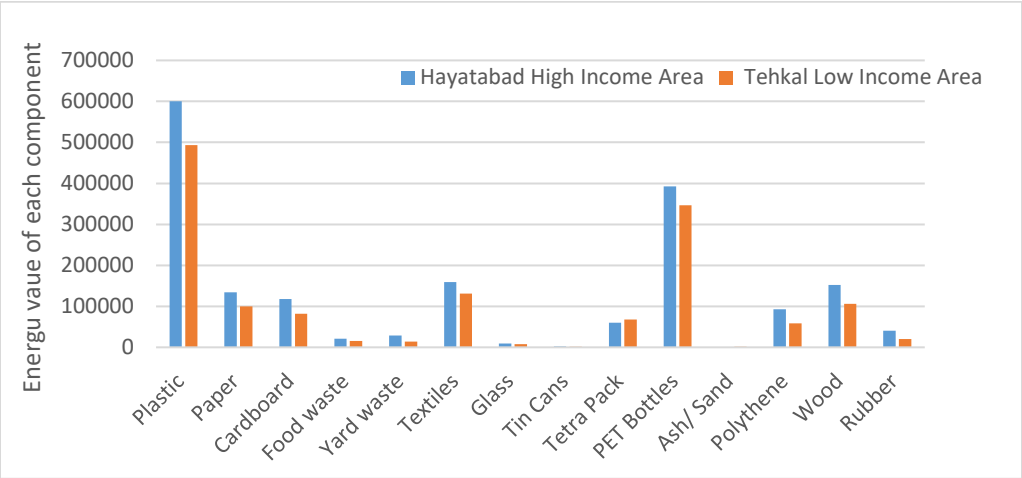

Figure 2: Comparison of energy values of MSW components in Hayatabad and Tehkal

The MSW in high-income area Hayatabad exhibited a higher calorific value, attributed to the increased presence of non-biodegradable materials, which have a higher energy content when incinerated. Low-income area Tehkal produces the lowest calorific value because MSW has the possibility for energy recovery via organic waste digestion and biogas production. It is observed from the energy values if in the future we have to install the energy generation plant in these regions then high-income area Hayatabad is preferred over low-income area Tehkal. The research highlights the importance of efficient waste management, including tailored methods, optimal collection schedules, improved segregation and recycling, and Waste-to-Energy facilities, which can reduce landfill dependence and achieve renewable energy targets.

4 Conclusion

The energy content disparities between Tehkal and Hayatabad highlight the need for waste-to-energy solutions in every city, especially in areas with higher energy content. Specialized solutions are needed in Peshawar City for sustainable development and maximum energy recovery. The study suggests developing effective waste management strategies to enhance resource utilization and minimize environmental harm, requiring careful planning, regulation, and public engagement for waste-to-energy adoption. This study highlights the importance of localized initiatives in waste management and renewable energy, emphasizing the need for stakeholder engagement to develop sustainable, equitable solutions.

References

[1] Veasna Kum, Alice Sharp, Napat Harnpornchai, Improving the solid waste management in Phnom Penh city: a strategic approach, Waste Management, Volume 25, Issue 1, 2005, Pages 101-109, ISSN 0956-053X, https://doi.org/10.1016/j.

[2] Ahmad, Waqas & Hassan, Muhammad & Nawaz, Tahir & Ashfaq, Muhammad & Khan, Muhammad. (2020). Status of Solid Waste Management in Peshawar, Pakistan.

[3] Arvind K. Jha, C. Sharma, Nahar Singh, R. Ramesh, R. Purvaja, Prabhat K. Gupta, Greenhouse gas emissions from municipal solid waste management in Indian mega-cities: A case study of Chennai landfill sites, Chemosphere, Volume 71, Issue 4, 2008, Pages 750-758, ISSN 0045-6535, https://doi.org/10.1016/j.chemosphere.2007.10.024.

[4] Maalouf, Amani & Mavropoulos, Antonis. (2022). Re-assessing global municipal solid waste generation. Waste Management & Research: The Journal for a Sustainable Circular Economy. 41. 0734242X2210741. 10.1177/0734242X221074116.

[5] M. U. Farooqi and M. Ali, "Effect of pre-treatment and content of wheat straw on energy absorption capability of concrete," *Construction and Building Materials*, vol. 224, pp. 572-583, 2023.

Annexure A

Photo Gallery













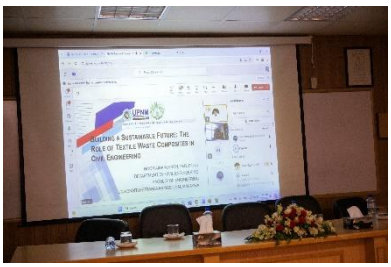
Building a Sustainable Future: The Role of Textile Waste Composites in Civil Engineering

		
		
		
		
		

		
		
		
		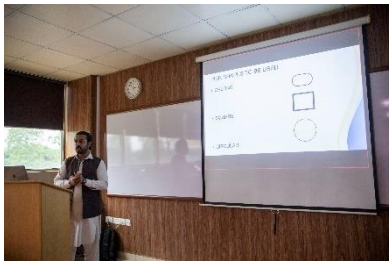
		

		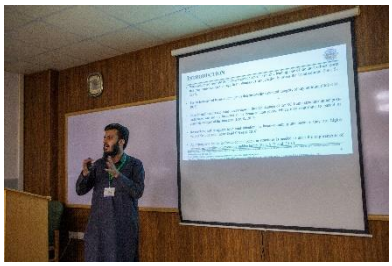
	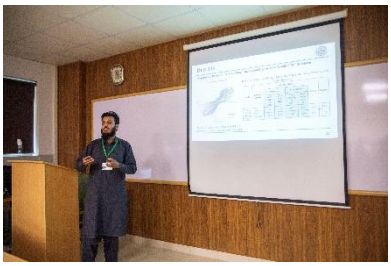	
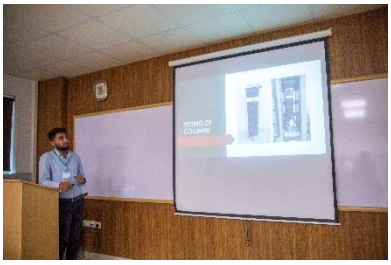		
		
		

Authors Index

A
Ahmad, Z. **(58)**
Ahmed, A. **(194)**
Ahmed, A. **(198)**
Ajwad, A. **(106)**
Ajwad. A. **(110)**
Akram, W. **(154)**
Ali, M. **(26)**
Ali, M. **(166)**
Ali, M. D. **(94)**
Ammar, M. **(214)**
Anjum, S. U. **(38)**
Anwar, G. A. **(134)**
Arif, M. **(86)**
Ashfaq, F. **(82)**
Ashraf, M. **(114)**
Aslam, F. **(162)**
Ahmed, Z. **(50)**
Azad, M. **(142)**
Azeem, M. **(102)**

B
Bakar, A. **(186)**
Bilal, M. **(122)**

E
Elahi, A. **(30)**
Ejaz, A. **(94)**

F
Fahad, M. **(158)**
Fahim, M. **(102)**
Faraz, A. **(34)**

G
Grill, A. A. **(182)**
Grill, A. A. **(202)**
Gul, F. A. **(98)**

H
Haseebullah, S. **(162)**
Hijab, S. **(222)**
Hussain, M. **(30)**

I
Ilyas, U. **(82)**
Iqbal, M. A. **(126)**

J
Jadoon, A. K. **(178)**
Jamshaid, H. A. **(158)**
Javaid, F. **(122)**
Javed, M. U. **(42)**

K
Kabir, M. H. **(150)**
Khairuddin, F. H. **(66)**
Khan, A. **(90)**
Khan, H. A. **(5)**
Khan, H. **(178)**
Khan, J. A. **(190)**
Khan, M. **(8)**
Khan, M. **(74)**
Khan, M. **(218)**
Khan, R. B. N. **(78)**
Khan, M. S. **(222)**
Khan, S. S. **(170)**
Khan, Y. **(134)**
Khan, Z. J. **(22)**
Khitab, A. **(34)**
Khitab, A. **(78)**
Khitab, A. **(150)**

L
Latour, M. **(106)**
Latour, M. **(110)**
Liu, J. C. **(11)**
Luqman, M. **(74)**
Luqman, M. **(86)**

M
Malik, M. A. **(42)**
Mehwish, J. **(154)**
Misnon, N. A. **(17)**
Misnon, N. A. **(66)**

N
Nadeem, H. **(70)**
Noreen, A. **(218)**
Numan, M. **(54)**
Numan, M. **(130)**
Nasir, Z. **(186)**

Q
Qadeer, A. **(166)**
Qamar, F. **(138)**
Qazi, S. **(118)**

R
Raza, A. **(46)**
Raza, A. **(126)**
Rehman, B. **(194)**
Rehman, S. U. **(38)**
Rehman, S. U. **(114)**

S
Sami, M. A. **(50)**
Saqib, M. **(206)**
Shabbir, F. **(62)**
Shair, M. **(198)**
Shahzada, K. **(19)**
Shakeel, M. **(14)**
Shaukat, H. **(46)**
Sial, A. A. **(62)**
Sohaib, M. **(174)**
Subhan, M. **(70)**
Subhani, M. B. **(142)**
Suboor, A. **(118)**
Suhail, S. A. **(206)**
Suhail, S. A. **(210)**
Suhail, S. A. **(214)**

T
Tahir, H. **(54)**
Tahir, H. **(130)**
Tahir, H. **(146)**
Tahir, M.F. **(26)**
Tariq, K. A. **(58)**

U
Usman, M. **(182)**
Ullah, A. **(98)**
Ullah, Q. S **(90)**
Umair, M. **(146)**

W
Waleed, M. **(202)**
Waraich, A. H. **(190)**
Wardeh, G. **(2)**

Y
Yaseen, M. A. **(210)**

Z
Zwain, M. **(138)**